PAUL DARIO TOASA CAIZA

Consideration of runouts by the evaluation of fatigue experiments

KIT Scientific Publishing

Paul Dario Toasa Caiza

Consideration of runouts by the evaluation of fatigue experiments

BAND 8

Versuchsanstalt für Stahl, Holz und Steine
Berichte zum Stahl- und Leichtbau

Consideration of runouts by the evaluation of fatigue experiments

by
Paul Dario Toasa Caiza

KIT Scientific Publishing

Karlsruher Institut für Technologie
Versuchsanstalt für Stahl, Holz und Steine

Consideration of runouts by the evaluation of fatigue experiments

Zur Erlangung des akademischen Grades eines Doktor-Ingenieurs
von der KIT-Fakultät für Bauingenieur-, Geo- und Umweltwissenschaften
des Karlsruher Instituts für Technologie (KIT) genehmigte Dissertation

von M.Sc. Dipl.-Math. Paul Dario Toasa Caiza aus Quito, Ecuador

Tag der mündlichen Prüfung: 30. November 2018
Referent: Prof. Dr.-Ing. Thomas Ummenhofer
Koreferent: Prof. Dr.-Ing. Alain Nussbaumer (EPFL)

Impressum

KIT Scientific Publishing

Karlsruher Institut für Technologie (KIT)
KIT Scientific Publishing
Straße am Forum 2
D-76131 Karlsruhe

www.ksp.kit.edu

Print on Demand 2019 – Gedruckt auf FSC-zertifiziertem Papier

ISSN 2198-7912
ISBN 978-3-7315-0900-4
DOI 10.5445/KSP/1000091208

A Heike, por lo positivo de su cariño y por soportar mis errores, debilidades y excentricidades.
A mis hijos Raquel Lucrecia Sol y Bernardo Paolo Luciano por recordarme que alguna vez fui niño y que apesar de mis enormes limitaciones me idolatran.

Acknowledgements

A mis padres José Ismael y María Lucrecia les agradezco la confianza incondicional y el permanente apoyo a mis causas y a mi rebeldía personal. A mis hermanos Peto y Diegin les debo la compañía, su cariño y comprensión. Mis luchas hubiesen sido tan solitarias sin ustedes.

A los agrios de la Facultad de Ciencias de la Escuela Politécnica Nacional (EPN) del Ecuador y a los rastas del Departamento de Cultura de la EPN les debo el haberme mantenido con los pies en la tierra para no volverme un completo orate.

A la asociación Amarun por darme la oportunidad de compensar en algo lo recibido por la EPN. Quid pro quo.

To Jennifer Hrabowski and Stefan Herion from the Research Center for Steel, Timber & Masonry[1] from the Karlsruhe Institute of Technology (KIT) who gave me the opportunity to work at our institute.
To Prof. Thomas Ummenhofer for giving me a place in his team to make research and to understand better what applied mathematics mean.

Nada hubiese podido ser tan grato sin el placer que me ha brindado el heavy metal y la salsa. La magia de sus ritmos han tranquilizado mi espíritu y mi cuerpo respectivamente.

Alea jacta est.

[1] Versuchsanstalt für Stahl, Holz und Steine

Kurzfassung

Seit der industriellen Revolution ist die Erforschung der Ermüdung und ihre Modellierung eine Herausforderung für Ingenieure und Forscher. In Anerkennung des Pioniers August Wöhler werden die Abbildung der Ermüdungsversuchsdaten und ihre statistische Bewertung als Wöhlerkurven bezeichnet. Die Beschreibung der Wöhlerkurven stellt aufgrund der stochastischen Natur des Ermüdungsvorgangs ein komplexes mathematisches Problem dar.

Im Bereich des Stahlbaus erfolgt die Voraussage der Lebensdauer einer zyklisch beanspruchten Schweißverbindung zumeist mit Kerbfallkatalogen, die auf experimentell ermittelten Wöhlerkurven basieren. Die derzeit angewendete Methodik zur Ermittlung von Wöhlerkurven basiert auf der Durchführung von Ermüdungsversuchen im Zeitfestigkeitsbereich und der anschließenden Auswertung der Ermüdungsdaten unter Anwendung des linearen Basquin-Modells. Dieses Modell ermöglicht jedoch aus statistischer Sicht weder eine Extrapolation der Wöhlerkurven in den High Cycle Fatigue Bereich (HCF) noch eine Berücksichtigung von Durchläufern, d.h. die aufwändigsten und teuersten Versuche können bei der Datenauswertung nicht berücksichtigt werden.
Dies beeinflusst sowohl die Prognose der Dauerfestigkeit als auch die Bemessung von Kerbfällen für hohe Lastspielzahlen.

Das auf der Weibull-Verteilung basierende Modell von Castillo und Fernández-Canteli erlaubt eine umfassendere Beschreibung der Wöhlerkurven vom Zeitfestigkeits- bis in den HCF-Bereich.
Es bietet bei der Analyse von Ermüdungsversuchsdaten zudem die Möglichkeit der Berücksichtigung von Durchläufern und ihrer Wiederversuche mit einer höheren Spannungsschwingbreite.
Die Gleichung

$$p = 1 - \exp\left\{ - \left[\frac{(\log N - B)(\log \Delta\sigma - C) - a}{b} \right]^c \right\}$$

weist zwei geometrischen Parameter B, C und drei Weibull Parameter a, b, c auf und beschreibt die Versagenswahrscheinlichkeit p als Funktion der Lastwechselzahl N sowie der zugehörigen Spannungsschwingbreite $\Delta\sigma$. Die Parameter B und C sind durch die Lösung eines nichtlinearen Optimierungsproblems bestimmt und die Weibull-Parameter a, b, c werden durch die Anwendung der Probability Weighted Moments (PWM) und der Maximum Likelihood Estimation Methode (MLE) abgeschätzt. Die Effizienz der PWM und MLE Methode wird anhand simulierter und experimenteller Daten überprüft
Die entsprechenden Algorithmen und Berechnungen wurden in Matlab implementiert und angewendet. Die Verwaltung der Daten wird mit einer MySQL Datenbank durchgeführt.

Die Anwendung und Bewertung des erarbeiteten Weibull-Modells erfolgt an Ermüdungsversuchen an sechs Reihen von Versuchskörpern:

- Querstumpfstöße aus S690QL
- Probekörper mit Längsrippe aus S355J2
- Hauptträger der Stahringer Brücke, gebaut 1895
- Probekörper aus Stahl 49MnVS3
- Probekörper mit Längsrippe aus S690QL. Schweißnahtdetail kugelgestrahlt
- Probekörper aus S355J2+N

Die Ergebnisse zeigen, dass die Weibull-Methode eine geeignete Alternative ist, um die Ermüdungsdaten zu analysieren und die Wöhlerkurven zu beschreiben.
Die Quantilen der Spannungsschwingbreite sind eindeutig höher und ihre entsprechenden Vertrauensintervalle schmaler im Vergleich zu den Quantilen und Vertrauensintervallen des Basquin-Modells, welches derzeit im Eurocode 3 und anderen Regelwerken Anwendung findet.

In fachlicher Hinsicht zeigen die Resultate, dass die Anwendung der Methode von Castillo und Fernández-Canteli zu einer genaueren und zuverlässigeren statistischen Schätzung der Lebensdauer im HCF- bzw. Dauerfestigkeitsbereich führt und eine verbesserte Abbildung der Wöhlerkurve ermöglicht.

Diese Dissertation wurde im Rahmen des Forschungsvorhabens "Berücksichtigung von Durchläufern bei der Auswertung von Ermüdungsversuchen", das von der Deutsche Forschungsgemeinschaft (DFG) gefördert wurde, erstellt.

Abstract

Since the heyday of the Industrial Revolution, the research of fatigue and its modeling has been a challenge for scientists and engineers. Because of the stochastic characteristics from the fatigue of steel, the description of the Wöhler curves is a complex mathematical problem.

According to the Eurocode EC3, the estimation of the fatigue life from a welded structure subjected to a cyclic load is determined by considering its corresponding detail category. The details categories have been made from Wöhler curves which have been obtained from experimental fatigue data. Currently, the determination of the Wöhler curves is made by applying the Basquin model in order to evaluate the fatigue experiments.

Unfortunately, from the statistical point of view this model does not allow to extrapolate the Wöhler curves in the High Cycle Fatigue (HCF) region. Moreover, the runouts which are the most expensive experimental tests are not considered into the evaluation of fatigue data. These deficiencies affect the estimation from the fatigue life and the design of a steel structure subjected to a high amount of cyclic loads.

In order to overcome these deficiencies, a new methodology has been proposed by Castillo and Fernández-Canteli. Based on a Weibull distribution, this methodology allows estimating the fatigue life of a steel structure in the HCF region. Moreover, it allows considering the runouts and their subsequent retests under a higher load into the modeling of the Wöhler curves.

The equation

$$p = 1 - \exp\left\{ - \left[\frac{(\log N - B)(\log \Delta\sigma - C) - a}{b} \right]^c \right\}$$

depends on two geometrical parameters B and C, and on three Weibull parameters a, b, and c. It describes the probability of failure p as function of the number of load cycles N and of the stress range $\Delta\sigma$.

The parameters B and C are determinate by solving a nonlinear optimization problem and the Weibull parameters are estimated by applying the Probability Weighted Moments (PWM) and the Maximum Likelihood Method (MLE).

The application and evaluation from the proposed Weibull model is performed by considering the experimental fatigue data from six different steel specimens:

- Welded specimens made from steel S690QL
- Welded specimens made from steel S355J2
- Main girders from the Stahringer bridge, built in 1895
- Specimens made from steel 49MnVS3
- Welded specimens made from steel S690QL which received an ultrasonic impact treatment (UIT)
- Specimens made from steel S355J2+N

The obtained results show that the Weibull model represents a suitable alternative to evaluate the fatigue data and to model the Wöhler curves. The quantiles obtained by applying the Weibull model are higher than the quantiles obtained by applying the Basquin model. Moreover, the corresponding intervals of confidence obtained by applying the Weibull model are tighter than those obtained by applying the Basquin model.

From the technical point of view, the results show that the application of the method from Castillo and Fernández-Canteli offers a reliable alternative to estimate the lifetime or fatigue limit from a steel structure and to depict the Wöhler curves.

This dissertation is part of the research project "Berücksichtigung von Durchläufern bei der Auswertung von Ermüdungsversuchen" supported by the German Research Foundation (DFG).

Table of contents

List of figures

List of tables

Glossary

Acronyms / Abbreviations

ALT Accelerated Life Tests; these tests are performed to reduce the time to failure by applying a higher level of stress on the test specimens, so that they will fail earlier than under normal operation conditions

CDF Cumulative Distribution Function; it describes the probability that a random variable X takes a value less than or equal to x according to a given probability distribution

CI Confidence Interval; interval which encloses a target parameter with certain probability. The probability identifies the fraction of the time, in repeated sampling, that the interval will contain the target parameter

F Failure. It identifies a test specimen which fails under a fatigue test. The failure occurs before reaching the censoring criterion

HCF High Cycle Fatigue; the fatigue which is obtained under low stress ranges and it usually considers a number of cycles between $5 \cdot 10^6$ and $1 \cdot 10^8$. Within this range the elastic behavior is present

LCF Low Cycle Fatigue; the fatigue which is obtained under high stress ranges and it allows to reach a number of cycles between $1 \cdot 10^2$ and $1 \cdot 10^4$. Within this range the plastic behavior is present

MLE Maximum Likelihood Estimation; it is a method based on the likelihood function of a random variable used to estimate the parameters of a determined statistical distribution

PDF Probability Density Function; it describes the probability that a random variable X takes a given value x. It is a theoretical model for the frequency distribution of a population of measurements. It is defined as the derivative of the cumulative distribution function CDF

PWM Probabiliy Weighted Moments; they are quantities given by integrals which are used to estimate the parameters of a determined statistical distribution

RO Runout. It identifies a specimen which does not fail under a fatigue test until the censoring criterion is reached. This criterion depends on the available ressources or the maximum time to perform a fatigue test. It is assumed that a fatigue failure could occur if the test had not been stopped

RT Retested. It identifies a specimen corresponding to a runout which fails under a subsequent fatigue test. The failure may occur after one or more subsequent tests. The subsequent tests may have their own censoring criterion

S-N Alternative name for the Wöhler curves. They depict the number of cycles during a fatigue test as function of the applied stress range

VAS Versuchsanstalt für Stahl, Holz und Steine. Karlsruher Institut für Technologie

VHCF Very High Cycle Fatigue; the fatigue which is obtained under low stress ranges and usually considers a number of cycles larger than $1 \cdot 10^8$

VLCF Very Low Cycle Fatigue; the fatigue which is obtained under very high stress ranges and usually considers a number of cycles smaller than $1 \cdot 10^2$

Chapter 1

Introduction

> The stability of a building is inversely proportional to the science of the builder.
>
> *Thomas Tredgold*

Modelling the fatigue of materials has been a technical challenge for engineers, phyisicians and mathematicians since the late 19th century. The interest on this research topic increased during the Industrial Revolution[1]. Fatigue failures of mechanical parts in cars, railways, automobiles, airplanes, structures and machines occured often and their causes demanded a reasonable and scientific explanation to improve their design and manufacturing.

1.1 Background and motivation

Fatigue of materials is a very complex phenomen, which has been studied for decades by enginners and scientists. The advances in material sciences, physics, mathematics and optical technology allowed to understand much better tha nature of fatigue. One of the fields which became relevant in the study of fatigue was the mathematical statistics, which allows to describe its random behaviour. The automotive industry and the aircraft industry have already considered several concepts from mathematical statistics in their fatigue research. However, in civil engineering the statistical considerations applied to evaluate fatigue data have not changed too much

[1] The period of time covered by the Industrial Revolution varies with different historians. Eric Hobsbawm held that it 'broke out' in Britain in 1789 and was not fully felt until 1848, while T. S. Ashton held that it occurred roughly between 1760 and 1830.

since Basquin proposed a linear model to describe the Wöhler curves.
The main target of this dissertation has been proposing a statistical method to evaluate fatigue data of structures in civil engineering.
This work started in chapter one with a historical summary of fatigue and the proposed models to describe it. In chapter two and three, the Weibull distribution and its application to model the Wöhler curves are shown. The chapter four includes six applications on experimental fatigue data which are evaluated by applying the Weibull model shown in chapter three. Finally in chapter five, conclusions of this work, recommendations to apply the Weibull model and an overview of the subsequent research are presented.

This dissertation is part of the research project "Berücksichtigung von Durchläufern bei der Auswertung von Ermüdungsversuchen" supported by the German Research Foundation (DFG).

1.2 Objective and scope

As it was mentioned before, the main goal of this dissertation is proposing a statistical method to evaluate fatigue data of structures in civil engineering. Since fatigue is a very complex phenomen, the proposed method does not pretend to be a general model and it has limitations and strengths. On the one hand, the main limitation of the Weibull model is that the evaluation of the fatigue data and the modelling of the corresponding Wöhler curves cannot be performed in the ULCF and LCF regions. On the other hand, the Weibull model offers the opportunity of considering runouts and their subsequent retests into the statistical evaluation of fatigue data. In comparison with the method applied in Eurocode 3 this fact makes the difference.

The scope of this work concerns to civil engineers who are interested in applying an alternative method to evaluate experimental fatigue data and to estimate the fatigue strength of a structure but based on a solid mathematical background.

1.3 A short history of fatigue

Since begining of the Industrial Revolution, research on fatigue has been linked to reliability problems of mechanical components in machines. Engineers and scientists have tried to develop a general theory which describes this phenomenom, and this task has not been yet completely done.

Maybe the first technical mention about the relevance of the fatigue in iron structures was done by Thomas Tredgold[2] (Figure 1.1) in 1822 [1], who wrote:

"But, in a great number of substances, we seem to have an instinctive knowledge of this property of the matter: a bent wire retains its curvature; and it may be broken by repeated flexure, with much less force than would break it at once: indeed, when we attempt to break any flexible body, it is usually by bending and unbending it serveral times, and its strenght is only beyond the effort applied to break it when we have not power to give it a permanent set at each bending. A permanent alteration is a pertial fracture, and hence it is the proper limit of strenght."

Figure 1.1: Thomas Tredgold - Pioneer in the research of load bearing capacity of timber and iron structures

The first known fatigue test results were published by Wilhelm August Julius Albert[3] (Figure 1.2) in 1837 in Clausthal, Germany, see Figure 1.3 [2]. Albert constructed a test machine for the conveyor chains which failed while used in the Clausthal mines. Nevertheless, his most important contribution was the wire rope which was used as a replacement of the expensive hemp ropes [3], see Figure 1.4.

In 1842 William John Macquorn Rankine[4] discussed about fatigue strenght of rail axles, and recognised that fatigue failures were caused by the initiation and growth of brittle cracks. Also in 1842, John O. York[5] conducted some experiments with rail axles and published the results in 1843 [5]. York described the causes of fracture

[2]Brandon, County Durham 22.08.1788 – London, 28.01.1829. English civil engineer, known for his early work on railroad construction.

[3]Hannover, 24.01.1787 - Clausthal, 04.07.1846. Royal Hannoverian german mining administrator, civil servant "Oberbergrat".

[4]Edinburgh, 05.07.1820 - Glasgow, 24.12.1872. Scotish mathematician, famous for his works in thermodynamics.

[5]Birmingham, 09.03.1811 - 28.05.1887. English civil engineer, specialist on railways contruction.

Figure 1.2: Wilhelm A.J. Albert - The inventor of the wire rope [4].

VII.

Ueber Treibseile am Harz.

Von

Herrn Ober-Bergrath Albert
zu Clausthal.

Als ich im Jahre 1806 meine Dienstlaufbahn auf dem Harze antrat, waren von den 35 Hauptschächten des oberharzischen Silbergruben-Berghaues nur zwei — Dorothea und Herzog Georg Wilhelm — mit hanfenen Treibseilen belegt. Die übrigen Treibwerke waren mit Kettenseilen aus Eisendraht mit abnehmender Stärke der Glieder versehen. Seit dieser Zeit fand ein fast ununterbrochener Kampf der Ansichten in Beziehung auf die bei den Haupt-Treibwerken anzuwendenden Treibseile Statt. Das geringere Gewicht, eine grössere Sicherheit bei dem Gebrauch, selbst in Rücksicht auf Leben und Gesundheit der Arbeiter, und die Möglichkeit, bei gespannten Treibwerken durch grössere Tonnen mehr leisten zu können, — diese

Figure 1.3: Albert's fatigue report - First page taken from the original report from 1837 [2].

Figure 1.4: Wire rope - Original sample of the wire rope invented by Albert. It had 18 mm of diameter and consisted of three strands with four wires. Its calculated breaking load was 6000 kgf and it was tested for first time on 23.07.1834 on a depth of 484 m.

in railway axles, which he attributed to the sudden strains and injury produced by strokes and vibrations. Back then, the occurence of many railroad accidents, such as the Versailles train crash on 5th October 1842, motivated the researchers to study their causes. This accident was caused when a locomotive axle broke by fatigue and sixty people died.

The research of August Wöhler[6] (Figure 1.5) on railway axles, stablished the fundaments of fatigue tests whose results currently are represented as *S-N* curves. To carry out these experiments Wöhler designed a rotating-bending machine, which ran at a very low frequency. Wöhler also designed machines which performed axial-bending and torsion tests on different notched and unnotched specimens. In 1870 Wöhler published his results, which contained the following conclusions [6], and often are called “Wöhler’s laws".

Der Bruch des Materials läßt sich auch durch vielfach wiederholte Schwingungen, von denen keine die absolute Bruchgrenze erreicht, herbeiführen.	*Material cracking can be caused through multiple repeated oscillations, whereas none of them reaches the absolute ultimate strength.*
Die Differenzen der Spannungen, welche die Schwingungen eingrenzen, sind dabei für die Zerstörung des Zusammenhangs maßgebend.	*The stress ranges limiting the oscillations are decisive for the destruction of the cohesion of the material.*
Die absolute Größe der Grenz-Spannungen ist nur insoweit von Einfluß, als mit wachsender Spannung die Differenzen, welche den Bruch herbeiführen, sich verringern.	*The absolute value of the stress levels has only an influence while with increasing stresses the stress ranges, which are causing the crack, are decreasing.*

[6] Soltau, 22.06.1819 - Hannover, 21.03.1914. German engineer, Royal “Obermaschinenmeister” of the "Niederschlesisch-Mährische" Railways in Frankfurt an der Oder.

Wöhler therefore stated that the stress amplitudes are the most important parameters for fatigue life, even though the tensile mean stress also have a detrimental influence.

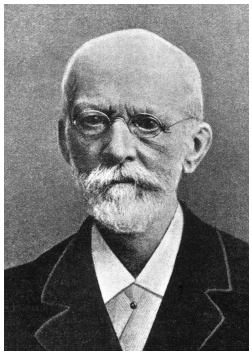

Figure 1.5: August Wöhler - Pioneer in the fatigue research [7].

Wöhler presented the results in tables and in 1874 his sucessor L. Spangenberg presented the results as *S-N* curves plotted in a system whose axis were linear [8]. Nevertheless, 62 years later, in 1936 Kloth and Stroppel called these curves “Wöhler curves" [9], [10].

In 1876 Wöhler proposed to the technical comittee of the German Railways, to stablish requierments for the tensile and yield strengths of steels and irons. In 1881 this initiative was rejected violently by the german and austrian steel makers. This initiative can be considered as the reason for the foundation of the “Royal Prussian Materials Testing Institute", which today is known as the “Bundesanstalt für Materialforschung und -prüfung (BAM)" in Berlin.

Not until 1910 the US researcher O.H. Basquin [11] represented fatigue results in the finite life region of the Wöhler curves with the logarithmic axes $\log \Delta\sigma$, $\log N$. Basquin’s model is given by

$$\log N = A - B \log \Delta\sigma; \qquad \Delta\sigma \geq \Delta\sigma_\infty, \tag{1.1}$$

and it is still applied in official standards such as Eurocode 3, ISO 12107, IIW [12], [13], [14], [15], [16].

In opinion of W. Schütz in [3], fatigue research between 1920 and 1925 was domained by British and US scientists. During this period, motivated by the first World War, the first full-scale fatigue tests with large aircraft components and experiments to improve their fatigue strength were carried out at the Royal Aircraft Establishment in the UK.

Figure 1.6: Nils Arvid Palmgren - Pioneer in the field of rolling technology.

In 1924 the article of Nils Arvid Palmgren[7] (Figure 1.6) regarding the approach for bearing life prediction[8] laid down the basis of the research on damage accumulation [17], [18]. The linear damage rule given by

$$D = \sum_{i=1}^{k} \frac{m_i}{n_i} = 1, \tag{1.2}$$

where

D: Damage

m_i: Number of applied cycles of type i

n_i: Total cycles to failure

calculates the effect of different types of loads that change over time. This concept was incorporated in the ISO-ANSI/ABMA standards, and Equation (1.2) is the basis for most variable-load fatigue analysis and it is still used in bearing life prediction and nonbearing aerospace design. Palmgren is perhaps the first person to advocate a probabilistic approach to engineering design and reliability, and maybe he is the most relevant person concerning to the rolling bearing technology in the first half of the 20th century [19]. Based on the paper of Palmgren and with the support of Professor Gustav Lundberg from Chalmers University in Göteborg, the first theory for calculation of bearing life was developed in 1947. The statistical considerations of this theory were determined in cooperation with W. Weibull, whose research on

[7] Falun, 30.04.1890 - Lerum, 14.11.1971. Swedish engineer and pioneer in the research of bearing technology. In 1918 he invented the spherical roller bearing, a strong and self-aligning bearing intended for railway equipment.

[8] Research performed in the SKF (Aktiebolaget Svenska Kullagerfabriken) company.

probability was very relevant to determine the equations regarding life prediction of ball bearings [20].

Twenty one years after Palmgren in 1945, A.M. Miner at the Douglas Aircraft Company proposed independently the same equation to quantify the damage [21]. Since then, Equation (1.2) has been known as the Palmgren-Miner rule.

The foundations for most of the fatigue knowledge were established between 1920 and 1945. In this period research and publications made by german institutions was considerably bigger in comparison with the work done in U.S.A. and U.K. [3], [22], see Figure 1.7. The german dominance during this period can be attributed primarily to the work of A. Thum[9], Föppl, Graf, E. Gaßner[10] (Figure 1.8) at the DVL[11] in Berlin and Göttingen.

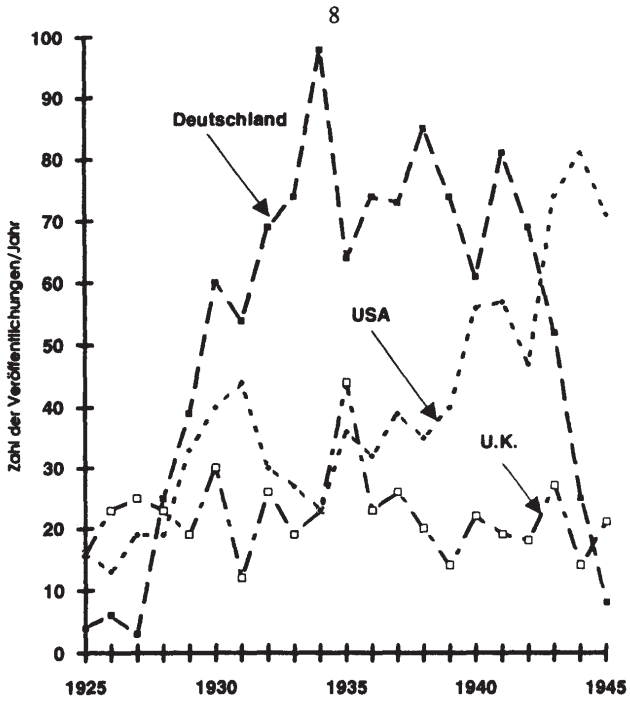

Figure 1.7: Number of publications on fatigue research - Comparison of the work performed in U.S.A., U.K. and Germany [3].

[9] A. Thum was co-author of 524 papers in several topics related with the fatigue from 1922 to 1956.

[10] Bingen, 22.05.1908 - Darmstadt, 25.11.1988. German engineer co-founder from the LBF (Fraunhofer-Institut für Betriebsfestigkeit und Systemzuverlässigkeit) in Darmstadt.

[11] Deutsche Versuchsanstalt für Luftfahrt.

Figure 1.8: Ernst Gaßner - Father ot the term “Betriefsfestigkeit" (operational fatigue strength) [23].

Particulary in Germany the research on aircraft components was motivated by the fatigue failure of the left wing strut which caused the devastating crash of a Lufthansa Dornier “Merkur" D-585 in 23.09.1927 on the route Berlin-Munich [24], [25]. As a consequence of these studies, the fundamental ideas of the variable amplitude fatigue tests were described by Gaßner in 1939 in the technical report [26] and translated by the NACA[12] from the original german article [27].

Based on the scatter of fatigue lives, Gaßner also considered the probability of survival P_s, where the value of P_s depends on the component in question. This idea made it possible to represent the fatigue life in different units of time and distance such as flying hours or kilometers. For his contributions in the fatigue research, Gaßner is considered a great engineer like Wöhler and Thum.

After the end of the second World War (WW II) the scene of fatigue research changed considerably. On the one hand, all of the industrial countries started to research fatigue of materials, so that the amount of tests, papers, books and meetings increased substantially. This interest was based on the occurence of failures on all types of fatigue-loaded structures, vehicles, aircrafts, trains and machines.

The cold war provided the adequate motivation to invest on fatigue research of aircraft components, so that full-scale fatigue tests were performed in U.K. and U.S.A. The United States Air Force suffered many accidents due to fatigue, such as the crash of two nuclear bombers Boeing B-47 on 13.03.1958. This situation was dangerous for the national safety of the U.S.A. and its allies because at that time, the B-47 was the only aircraft capable to reach the U.S.S.R.

On the other hand, the defeat of Germany in the WW II and the subsequent prohibition of building aircrafts stablished on the Postdam Conference in 1945, made

[12] Predecesor of the National Aeronautics and Space Administration NASA

almost dissapear the global leading position of Germany on fatigue research. As a consequence, the automobile industry was the only one where the fatigue research continued. This situation was also possible due to Gaßner, who together with Svenson in 1946 founded the “Physikalisch-Technisches Laboratorium" at Kempten, Bavaria. In subsequent years, most german automobile manufacturers built up large fatigue laboratories. This allowed Germay to become a leader in fatigue research in the automobile industry over its competitors in Europe and U.S.A.

In the 50s and 60s the scatter of the data corresponding to the number of cycles to failure and the fatigue limit became very important into the fatigue analysis. This fact motivated the use of mathematical statistics in order to estimate or model the fatigue behaviour in regions out of the experimental frame, such as the HCF region. At this point, the research performed by Ernst Hjalmar Waloddi Weibull[13] is essential. Weibull perfomed thousands of fatigue tests in order to prove his statistical distribution. The Weibull distribution is by far the world’s most popular statistical model for lifetime data. It is also used in many other applications such as reliability, survival analysis, weather forecasting and extreme value theory.

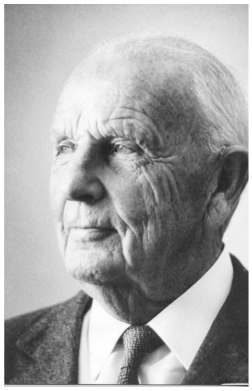

Figure 1.9: Waloddi Weibull - Pioneer in reliability analysis [28].

In 1951, Fredrick J. Plantema from the NLL (today NLR[14]) in The Netherlands led the creation of the International Committee on Aeronautical Fatigue (ICAF[15]) with the objectives of forming closer cooperation with various institutes carrying out non-classified work. As a result, the first ICAF conference took place in Amsterdam in 1952 and since then, it has become the place of meeting for fatigue experts.

[13] Vittskövle (Sweden), 18.06.1887 - Annecy (France), 12.10.1979. Swedish engineer and mathematician.

[14] Nationaal Lucht- en Ruimtevaartlaboratorium - National Aerospace Laboratory

[15] The original 5 member nations were: The Netherlands, Sweden, United Kingdom, Belgium and Switzerland

Since 1954 a new field of research started and grew fastly; the low cycle fatigue (LCF), which considers mechanical components loaded in service by relatively few cycles at elevated temperatures such as discs of gas, steam turbines and pressure vessels. Such is the case of the aircraft industrie wich made high demands of turbine discs: low weight, high fuel efficiency (i.e. high temperatures), structural integrity and a long fatigue life [3]. In 1958 G.R. Irwin[16] of the US Navy realized that the stress intensity factor given by

$$K = S \cdot \sqrt{\pi \cdot a}, \tag{1.3}$$

was the determining factor for static strength in the cracked state. If K reaches a certain critical value depending on the “fracture toughness" of the material, instant fracture occurs. This represented the born of the linear elastic fracture mechanics (LEFM).

In 1962 P.C. Paris showed that the fatigue crack propagation or crack growth rate can be described by

$$\frac{\mathrm{d}a}{\mathrm{d}N} = C \cdot \Delta K^n, \tag{1.4}$$

where

a: Crack length

N: Number of cycles

ΔK: Range of the stress intensity factor K

This equation motivated the rapid development of fracture mechanics. Particulary, Paris fixed the value of the slope in his equation to $n = 4.0$ for all metallic materials.

In 1974 the US Air Force introduced the “Damage Tolerance Requirements". These requirements assume that crack-like defects are present in all critical points of the structure even from the manufacturing process. Therefore, an aircraft manufacturer had to prove that for this condition sufficient life and static strength were available.

Since 1974, the automotive and aircraft industry have been working on the fatigue research in order to satisfy the most demanding requests regarding durability, speed and reduction of weight.

Fatigue research is also present in the construction industry. The standards to build steel bridges established in Great Britain in 1951 are an example of the

[16] 26.02.1907 - 09.10.1998. US scientist internationally known for his study on fracture of materials.

first studies in this field. In the 60s, researchers started to consider mathematical statistics, experimental design and data analysis on the fatigue research of metallic constructions, and mainly in welded structures. The inclusion of these topics helped to stablish the regulations and codes in the construction industry [29], [30]. Currently, the rules for the design of steel structures given by Eurocode 3 are based on the fatigue model of Basquin (1910). These norms consider the fatigue failures in the design specifications [16] and embrance such components or structures which have not been yet investigated, for example, oil rigs, offshore structures, cranes or oil pipes.

Despite of all the results on fatigue research, there are still some questions and unsolved problems including:

- Prediction of fatigue life under variable amplitudes.
- The optimal transference of fatigue results from test components to real components.
- Modelling of corrosion fatigue
- Fatigue at high temperatures
- A general fatigue model for stress-based, strain-based and the fracture mechanics approaches.
- Development of mathematical or statistical methods in order to model the fatigue in the VLCF region.

1.4 Phases of fatigue as a material phenomenon

In a specimen subjected to a cyclic load, a fatigue crack nucleus can be initiated on a microscopically small scale, followed by crack grows to a macroscopic size, and finally to specimen failure in the last cycle of fatigue life.
In order to perform a dependable fatigue analysis of a steel structure it is mandatory to understand the fatigue mechanism, i.e. the factors which influence the fatigue life and crack growth such as the material surface quality, residual stress, notch effect, size, temperature, corrosion and environmental conditions. Fatigue prediction methods can only be evaluated if the fatigue is understood as a crack initiation process followed by a crack growth period or propagation until rupture of the remaining section [15], [31], see Figure 1.10.

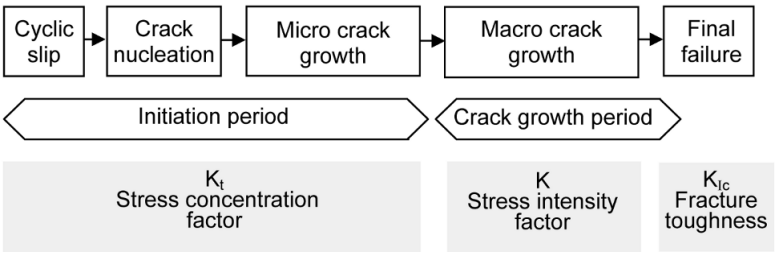

Figure 1.10: Fatigue Phases - Crack initiation and crack growth period [15].

The crack initiation period is a phenomenon which occurs in most cases on the surface of the material, and it begins with a cyclic slip which leads to a crack nucleation represented by invisible microcracks and implies cyclic plastic deformation. In other words, the crack initiation period is the consequence of agglomeration of dislocations in the crystal lattice forming inner voids or surface intrusions and extrusions. The crack nucleation occurs below the fatigue limit, which is the lowest stress amplitude for which crack nucleation is followed by crack growth until failure. Therefore, the fatigue limit is the threshold for the growth of small cracks, and not the threshold for crack nucleation [15].
In welded joints under cyclic load, the stage of crack initiation is very short in relation to the whole life of the joint [31].
Thanks to the advances in the optical technology, nowadays it is possible to obtain valuable microscopic information and images from the microcracks, such as the Figure 1.11 known as the "Microcanyon"[17]. Thereby it has been determined that the nucleation of microcracks generally occurs during the early stages of the fatigue life. For instance, the nucleation on low carbon steel starts between the 10% and 20% of its fatigue life and then the microcracks continue growing until failure of the specimen [32]. In fact, some results suggest that nucleation may take place almost immediately if a cyclic load above the fatigue limit is applied.

In the crack growth period, the fracture mechanics considerations prevail, the crack is growing regularly until complete failure and it is no longer a surface phenomenon. The mechanism is dominated by the energy release of the elastic field at crack increment. This energy release is governed by the elasticity modulus of the material [31]. Once this stage is reached the remaining fatigue life of a laboratory specimen is very small compared with the total life, although in the case of real structures this time may be longer.

[17] Winner of the grand prize in the 2011 FEI Owner Image Contest

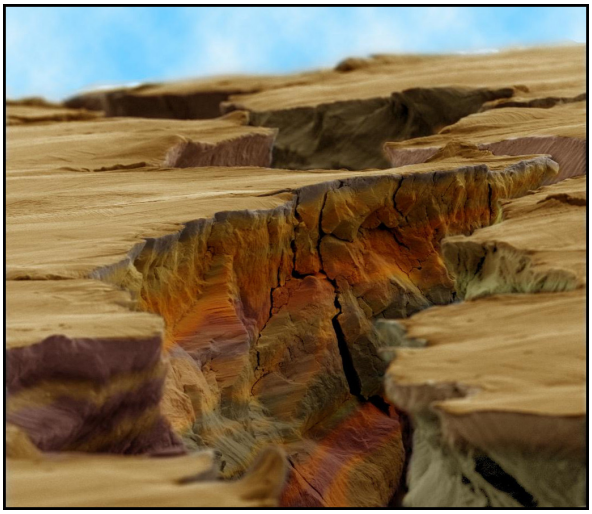

Figure 1.11: Micro-crack in Steel - Image taken with an electron microscope after a bending test failure. Institute for Electron Microscopy and Fine Structure Research (FELMI) at the Graz University of Technology [33].

From the technical point of view, it is appropriate considering the crack initiation and the crack growth as two separated phenomenons.

1.5 Common models for the Wöhler curves

As it has been seen in the previous sections, fatigue failures in steel structures are a common technical problem, which has been studied since the 19th century. August Wöhler recognized that applying a single load, which is much lower than the static strength of the material, does not damage it, but if this load is applied several times, it could induce a complete failure of the structure.

Modelling the fatigue is a complex mathematical problem, because of its random behaviour and the different mechanical phenomena involved in every fatigue phase. Fatigue models can be built from two main different points of view. The first approach, known as the fracture mechanics approach, consists in analyzing cracks and modelling how they grow in terms of the applied repetitive loads. The second one, the engineering approach, consists in modelling the experimental results according to a selected function, wich express the fatigue lifetime N in terms of the applied loads or stress range $\Delta\sigma$. The selected function has parameters which should be estimated, based on engineering and statistical considerations. For example, laboratory tests show that the fatigue lifetime N increases while decreasing stress range $\Delta\sigma$, and

becomes very large, maybe infinite [34], for loads below the endurance limit[18] $\Delta\sigma_\infty$, see Figure 1.12. The experimental data also suggest that the standard deviation of the fatigue lifetime N increases with decreasing the stress range $\Delta\sigma$.

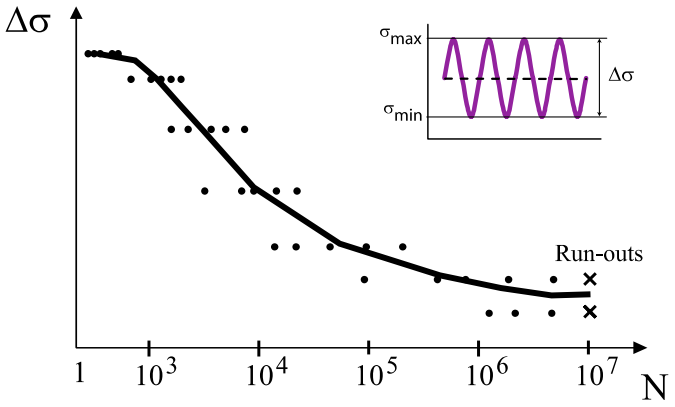

Figure 1.12: Fatigue data - Typical example of a Wöhler curve of constant stress range [35].

Currently, the following linear fatigue model based on the Basquin function (1910) is used in the Eurocode 3 [16], [36] to depict the Wöhler curves [15] on the finite life fatigue zone, see Figure 1.13.

$$\log N = A - B \log \Delta\sigma; \qquad \Delta\sigma \geq \Delta\sigma_\infty; \qquad B \geq 0. \tag{1.5}$$

The curves obtained from Equation 1.5 describe the mean lifetime N as a function of the stress range $\Delta\sigma$ for a constant stress level (σ_M or σ_m). Moreover, based on experimental data from the finite life fatigue zone, this model has been applied in the Eurocode 3 in order to estimate the stress range $\Delta\sigma$ and its confidence intervals in the HCF zone, see Figure 1.13.

[18] Stress below which failure never occurs, even for an indefinitely large number of loading cycles

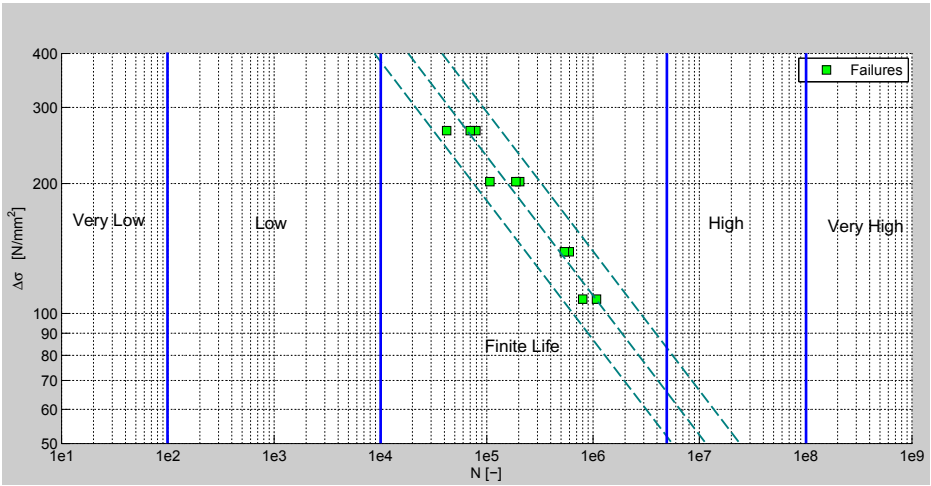

Figure 1.13: Fatigue zones - Classification according to the number of cycles from fatigue experiments [37].

The estimation of the parameters A and B from Equation (1.5) can be done by applying standard least square methods [38], [39]. Additionally, it is assumed that the lifetime N_i and the stress range $\Delta\sigma_i$ follow a normal or t-student distribution [40]. This assumption allows to estimate the confidence intervals of the stress range [41].

The following model is an extension of the traditional linear model from Basquin and it considers the HCF region [42].

$$\log N = A - B \log\left(\Delta\sigma - \Delta\sigma_\infty\right) \qquad \Delta\sigma \geq \Delta\sigma_\infty; \qquad B \geq 0. \tag{1.6}$$

Equation (1.6) is called Stromeyer function (1914), where $\Delta\sigma_\infty$ is the endurance fatigue limit. Although, it is a nonlinear model, if $\Delta\sigma_\infty$ is assumed to be known, the estimation of the parameters and confidence intervals of the stress range can be done as in the previous linear case from Basquin, otherwise the estimation can be more complex.

The model of Bastenaire [43] given by

$$N = \frac{A}{\Delta\sigma - \Delta\sigma_\infty} \exp[-C(\Delta\sigma - \Delta\sigma_\infty)] - B, \tag{1.7}$$

where the coefficients A, B, C have to be estimated, is an additional nonlinear alternative to represent the fatigue data. From the geometrical point of view, this model

offers good diagrams of the Wöhler curves and allows the extrapolation of the curves into the LCF and the HCF regions.

The model of Stüssi [44] given by

$$\Delta\sigma = \frac{R_m + \Delta\sigma_\infty \cdot cN^p}{1 + cN^p} \tag{1.8}$$

gives a good geometrical approach of the Wöhler curves. However, in order to estimate the parameters c and p, it requires that the ultimate strenght R_m and the fatigue limit $\Delta\sigma_\infty$ are already known.

Recently, new models have been proposed to describe the fatigue with more accuracy such as the model from Kohout and Věchet [45] given by Equation (1.9). This model is a general extension of the Basquin function and considers the LCF and the HCF regions as it is shown in Figure 1.14.

$$\log\left(\frac{\Delta\sigma}{\Delta\sigma_\infty}\right) = \log\left(\frac{N + N_1}{N + N_2}\right)^b. \tag{1.9}$$

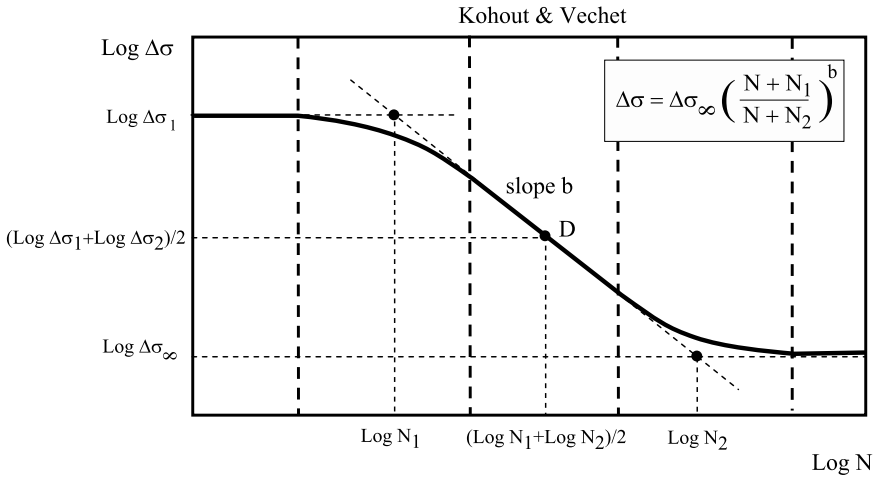

Figure 1.14: Kohout and Věchet model - Wöhler curve according to Equation (1.9) [45].

The approach of this model is quite good from the geometrical point of view, unfortunately, the authors do not provide any suggestion about the statistical distribution

of the lifetime N. So, the estimation of the confidence intervals of the stress range $\Delta\sigma$ is not possible.

The model of Pascual und Meeker [46] is built from the model of Stromeyer given by Equation (1.6), and it suggests a statistical distribution for N and $\Delta\sigma_\infty$. The authors assume that the random variable $V = \log(\gamma) = \log(\Delta\sigma_\infty)$ has the following probability density function

$$f(v) = \frac{1}{\sigma_\gamma}\phi(v) = \frac{1}{\sigma_\gamma}\phi\left(\frac{v-\mu_\gamma}{\sigma_\gamma}\right), \tag{1.10}$$

where $\phi(v)$ is the normal density function, μ_γ is the location parameter and σ_γ is the scale parameter [47], [48] and [49].
Afterwards, the authors assumed for a fixed value $V < x$ that the random variable $Y = \log(N)$ has the following probability density function

$$f(y|v) = \frac{1}{\sigma}\phi(y|v) = \frac{1}{\sigma}\phi\left(\frac{y-[A+B\log(e^x-e^v)]}{\sigma}\right), \tag{1.11}$$

where $X = \log(\Delta\sigma)$, $\phi(y|v)$ is the normal density funtion, $Z = A + B\log(e^x - e^v)$ is the location parameter and σ is the scale parameter.
Based on the Equations (1.10) and (1.11) the authors suggest the following marginal distribution for the lifetime

$$\begin{aligned} P(Y \leq y) &= \int_{-\infty}^{x} \frac{1}{\sigma_\gamma}\Phi(y|v)\phi(v) \\ &= \int_{-\infty}^{x} \frac{1}{\sigma_\gamma}\Phi\left(\frac{y-[A+B\log(e^x-e^v)]}{\sigma}\right)\phi\left(\frac{v-\mu_\gamma}{\sigma_\gamma}\right)\,\mathrm{d}v, \end{aligned} \tag{1.12}$$

where $\Phi(y|v)$ is the marginal distribution of $(Y|V)$. Subsequently the parameters $A, B, \sigma, \mu_\gamma, \sigma_\gamma$ should be estimated.

As a matter of fact, the models presented above have several limitations [34], [35], which should be overcome in order to obtain reliable results and predictions. The main deficiencies of the mentioned fatigue models are:

- Because of their assumed linearity the models of Basquin and Stromeyer given by Equations (1.5) and (1.6) respectively are not suitable to extrapolate the Wöhler curves from the finite life region into the HCF region and neither are to

provide an estimation of the fatigue life. In order to overcome this limitation, the existence of a knee point on the linear regression has been suggested [12], [31], [36]. This point represents the classical transition from the endurance line to the fatigue limit, and its existence is based on empirical knowledge [31]. However, until now the location of this knee point is a topic of debate in the scientific community.

- From the statistical point of view, the arbitrary assumption of a normal or log-normal distribution in the models given by Equations (1.5) and (1.6) is not suitable to model fatigue data [31].

- The model of Kohout and Věchet given by Equation (1.9) does not suggest a suitable statistical distribution of the data. This fact does not allow to estimate confidence intervals for the stress range $\Delta\sigma$.

- The models of Basquin, Stromeyer , Stüssi and Kohout and Věchet given by Equations (1.5), (1.6), (1.8) and (1.9) do not consider the fatigue data from runouts, i.e. specimens which do not present fatigue failures at the moment that the test was interrupted due to economical or time reasons.

- The model from Bastenaire given by Equation (1.7) depicts an arbitrary family of curves which only provide a geometrical fitting of the data [35]. Moreover, the author assume a normal distribution of the data without neither statistical nor physical arguments.

• For the model from Bastenaire given by Equation (1.7) even a small value of stress will induce a fatigue failure with certain small probability, i.e. it is assumed that no fatigue limit exists. The parameter $\Delta\sigma_\infty$ does not remain constant, in fact it changes for every probability curve, so that an estimation of this parameter must be done every time.

- The iterative method to estimate the coefficients of the model of Bastenaire given by Equation (1.7) assumes that initial near values are known, otherwise there is no convergence. Moreover, the parameters A, C, $\Delta\sigma_\infty$ are not dimensionless.

- In the model of Pascual and Meeker, the assumption regarding the density functions given by Equations (1.10) and (1.11) is not justified. Additionally, the model is not dimensionless.

- The models above offer an elementary approach or a simple geometrical description of the Wöhler curves. For this reason, with their application it is possible to perform only a limited evaluation of the fatigue data.

In order to overcome the deficiencies mentioned above, a new methodology to model the fatige has been proposed by Castillo and Fernández-Canteli [35]. This methodology considers the fatigue phenomem as a stochastic process and applies functional equations [50], probability theory, and practical knowledge [51].
First of all, a dimensional analysis of all variables involved on the fatigue phenomenon is performed, this step is based on the application of Buckingham's theorem and ensures obtaining a dimensionless model [52].

Then, based on the Weibull distribution function [53], [54], the authors propose the following dimensionless model to depict the Wöhler curves.

Weibull distribution model

$$p = 1 - \exp\left\{ - \left[\frac{(\log N - B)(\log \Delta\sigma - C) - a}{b} \right]^c \right\}; \qquad (\log N - B)(\log \Delta\sigma - C) \geq a, \tag{1.13}$$

where

p : Probability of failure

Geometrical parameters:

B : Threshold value of lifetime N

C : Endurance limit $\Delta\sigma_\infty$

Weibull parameters:

a : Location parameter

b : Scale parameter

c : Shape parameter or slope of the CDF from the Weibull distribution

This model describes the probability p of a failure as a function of the stress range $\Delta\sigma$ and the number of load cycles up to failure N, and it overcomes the defficiencies of the fatigue models mentioned above.
The parameters estimation of the model of Castillo and Fernández-Canteli given by Equation (1.13) depends on the experimental data and can be divided in two stages:

1. Estimation of the geometrical parameters B and C
2. Estimation of the Weibull parameters a, b and c.

The application of the Weibull distribution for modelling the fatigue life of steel structures has been already considered by some researchers who emphasize the feasibility and the advantages of this distribution [55] or suggest its application on this engineering field because of the possibility to study the influence of the runouts [56], [57], [58].
In research concerning to VHCF, the Weibull distribution has been applied to model the *S-N* curves by considering different failures modes [59] or types of fracture initialization [60]. It has also been applied to model the scatter in fatigue life by considering the influence of crack initiation life, crack propagation life, fatigue life and small crack growth [61], [62], [63]. In these applications a particular Weibull distribution has to be defined for each physical phenomen.

As a matter of fact, it has been also determined that the fatigue data is a heterogeneous population, which does not follow a Gaussian normal or log-normal distribution. Therefore, simple statistical methods or arbitrary assumptions are not applicable to evaluate fatigue data [31].

Chapter 2

The Weibull distribution

> There are two quite different lines of attacking fatigue problems: the phenomenological and the metallographical.
>
> *Waloddi Weibull*

Since its official presentation in 1951 the Weibull distribution has been applied in several engineering fields. The Weibull distribution belongs to the family of extreme value distributions which are the limit distributions of the smallest or the greatest value from a sample of size $n \to \infty$. The origins of this distribution date back to 1920s, and its research increased because of the study of different industrial and technological phenomens. Nowadays, the Weibull distribution is the most used one for modelling process related to reliabilty, weather forecasting, survival analysis, tensile strength of materials, and lifetime expectation.

2.1 Origins and deductions

In 1951 Waloddi Weibull presented a distribution which described several phenomens such as yield strength of steel, fiber strength of cotton or size distribution of fly ash [64]. Afterwards, Weibull used the fatigue tests he had performed with bolts and aluminum specimens in order to show the application of his distribution. The distribution proposed by Weibull in [64] did not have a theoretical basis when the article was published but the corresponding analysis was based on the empirical experience of the author. This distribution was widely accepted and became a powerful statistical tool in engineering, in part due the advertising of their applications made by Weibull

himself. Despite the fact that other scientists have found this distribution before, it was maybe unfairly named as Weibull distribution [65].

The origins of this distribution are back in the 1920s and were established when the distribution of the sample minimum or sample maximum were studied. As a matter of fact, in 1927 a theoretical approach was performed by Maurice Frechet[1] who found an asymptotic distribution for the largest value of a random variable [66]. Besides Weibull's practice research, a group of scientists from the "Bergakademie Freiberg" known as RRSB[2] made earlier an independent approach while modeling the size of particles of coal dust between 1932 and 1936, which gave as result the two-parameter Weibull distribution as it is known today [67], [68]. Actually, due to the scientific isolation of the German Democratic Republic (DDR) where the leader of the RRSB Erich Rammler[3] (Figure 2.1) lived, only in 1976 he got to know about the Weibull distribution, and he was astonished. For this reason Rammler suggested, that it is perhaps not a good idea giving personal names to scientific discoveries, since the fortune sometimes is involved [69].

Figure 2.1: Erich Rammler - Leader of the "unknown" RRSB group which deduced earlier the Weibull distribution [68].

2.1.1 Approach from Rosin, Rammler, Sperling, Bennet - RRSB

Based on empirical knowledge and on the results of Rammler and Rosin; Sperling and Mayer [68] arrived to the conclusion that the PDF of the size of coal particles x can be written as follows

[1] Maligny, 02.09.1878 - Paris, 04.06.1973. French mathematician.

[2] It comes from the surnames of the german engineers Paul Rosin, Erich Rammler, Karl Sperling and the english engineer John Godolphin Bennet

[3] Tirpersdorf, 09.07.1901 - Freiberg, 06.11.1986. German engineer, pioneer in the study of particle technology.

$$f(x) = px^r \exp(-qx^c); \qquad x \geq 0; \quad p, q, c > 0; \quad r > -1. \tag{2.1}$$

However, it is complicated to integrate this function in order to obtain the CDF of x. Sperling then assumed that $r = c - 1$ and obtained

$$f(x) = px^{c-1} \exp(-qx^c); \qquad x \geq 0; \quad p, q, c > 0. \tag{2.2}$$

Then by definition, the CDF can be written as follows

$$F(x) = \int_0^x pt^{c-1} \exp(-qt^c)\, \mathrm{d}t = \frac{p}{qc}\left[1 - \exp(-qx^c)\right]. \tag{2.3}$$

Afterwards, considering the property that $\lim_{x\to\infty} F(x) = 1$ leads to $p = qc$, and later on the following equations are obtained:

$$f(x) = qcx^{c-1} \exp(-qx^c), \tag{2.4}$$

$$F(x) = 1 - \exp(-qx^c). \tag{2.5}$$

Finally, Bennett suggested to write $q = \frac{1}{b^c}$ in order to obtain the following equations

$$f(x) = \frac{c}{b}\left(\frac{x}{b}\right)^{c-1} \exp\left[-\left(\frac{x}{b}\right)^c\right] \tag{2.6}$$

and

$$F(x) = 1 - \exp\left[-\left(\frac{x}{b}\right)^c\right]. \tag{2.7}$$

The Equations (2.6) and (2.7) are not more than the PDF and CDF of the today known two-parameter Weibull distribution respectively.

2.1.2 Approach from Weibull

The model proposed by Weibull in order to model several phenomens, such as the strength of materials and the distribution of the size of ash particles was published on his most famous paper *"A statistical Distribution Function of Wide Applicability"* in 1951 [64]. The empirical knowledge and the practical experience of Weibull played a crucial role in his assumptions and show how helpful the technical intution can be.

Consider now the case of a chain made of n links, and let P be the probability that a simple link fails under a load x. Then, the obvious question is: what is the probability P_n of failure of the whole chain? It is clear that a chain fails when its

weakest link fails, in other words, a chain is as strong as its weakest link. This situation is known as the weakest link principle and it is considered below.

Let $\varphi(x)$ be an arbitrary positive non-decreasing function, and let $F(x)$ be the CDF of the random variable X defined as

$$F(x) = P(X \leq x) = 1 - \exp\Big[- \varphi(x)\Big]. \tag{2.8}$$

From Equation (2.8) it is easy to obtain the following relationship

$$(1 - P)^n = \exp\Big[- n\varphi(x)\Big]. \tag{2.9}$$

Then, according to the definition of probability, it can be assumed that the probability of nonfailure of the whole chain $(1 - P_n)$ is equal to the probability of the simultaneous nonfailures of all the links; in other words

$$(1 - P_n) = (1 - P)^n. \tag{2.10}$$

Manipulating the Equations (2.9) and (2.10) leads to the mathematical expression of the weakest link principle in the chain, or more generally, for the size effect on failures in solids.

$$P_n = 1 - \exp\Big[- n\varphi(x)\Big]. \tag{2.11}$$

In the next assumption Weibull applied his practice and empirical knowledge to suggest the form of the function $\varphi(x)$ from Equation (2.8). Hereafter, he proposed the following positive non-decreasing function

$$\varphi(x) = \left(\frac{x - a}{b}\right)^c, \qquad x \geq a; \quad b, c > 0. \tag{2.12}$$

There were some objections to the definition of $\varphi(x)$, mainly regarding the absense of a theoretical basis. To these criticisms, Weibull wrote that the only practicable way of progressing is choosing a simple function, test it empirically, and stick to it as long as none better has been found.

Finally, by substitution of Equations (2.11) for $n = 1$ and (2.12) on Equation (2.8), the three-parameter Weibull distribution as it is known today is obtained

$$F(x) = 1 - \exp\left[- \left(\frac{x - a}{b}\right)^c\right], \qquad x \geq a; \quad b, c > 0. \tag{2.13}$$

2.2 Definitions and properties

According to Wöhler's theory, a steel structure subject to a continuos cyclic load can resist a finite time before it fails. This time span known as lifetime is measured in number of cycles and can not be fixed or predetermined; in fact the lifetime is a continuos and non-negative random variable. Within this dissertation, it is considered that the lifetime follows a three-parameter Weibull distribution $W(a, b, c)$.

As every random variable, the lifetime X can be described by the following functions:

2.2.1 Probability density function - PDF

It is also called failure density, and it allows to obtain the probability of having a life span between two fixed values.

By definition a PDF $f(x)$ satisfies the following properties:

$$f(x) \geq 0 \qquad \text{and} \qquad \int_{-\infty}^{\infty} f(x)\,\mathrm{d}x = 1.$$

Definition 1 (Weibull PDF)**.** *Let X be a random variable which follows a three-parameter Weibull distribution $W(a, b, c)$. The probability density function PDF of X is given by*

$$f(x \mid a, b, c) = \frac{c}{b}\left(\frac{x-a}{b}\right)^{c-1} \exp\left[-\left(\frac{x-a}{b}\right)^{c}\right], \qquad x \geq a, \tag{2.14}$$

where

$a \in \mathbb{R}$: *Location or translation parameter, also known as threshold.*

$b > 0$: *Scale or statistical dispersion parameter.*

$c > 0$: *Shape parameter.*

The variation of the parameters a, b, c leads the following effects:

- Increasing (decreasing) the value of a while b, c held constant will result in a translation of the PDF to the right (left) over the abscissa. See Figure 2.2.
- Increasing (decreasing) the value of b while a, c held constant leads to an increment (reduction) of the variation interval of x. See Figure 2.3.

- Changing the value of c affects the geometry or the appearance of the PDF. See Figure 2.4.

Particularly if the random variable X represents the lifetime, the Weibull parameters have the following properties:

Location parameter a: It is measured in the same units of time like X and it represents the minimum life, guarantee time, save life or shelf age. Its domain is reduced to be positive, i.e. $a \in [0, \infty[$.

Scale parameter b: It is measured in the same units of time like X and it represents the range of the distribution. In other words, it determines the statistical dispersion of the probability distribution.

It is also known as characteristic life if the location parameter $a = 0$, otherwise the characteristic life is equal to $a + b$. Precisely the 63.2% of all values fall below the characteristic life regardless of the value of the shape parameter c. See Figure 2.5

Shape parameter c: It does not have dimension and gives the slope of the CDF $F(x \mid a, b, c)$ when graphed on Weibull probability paper.

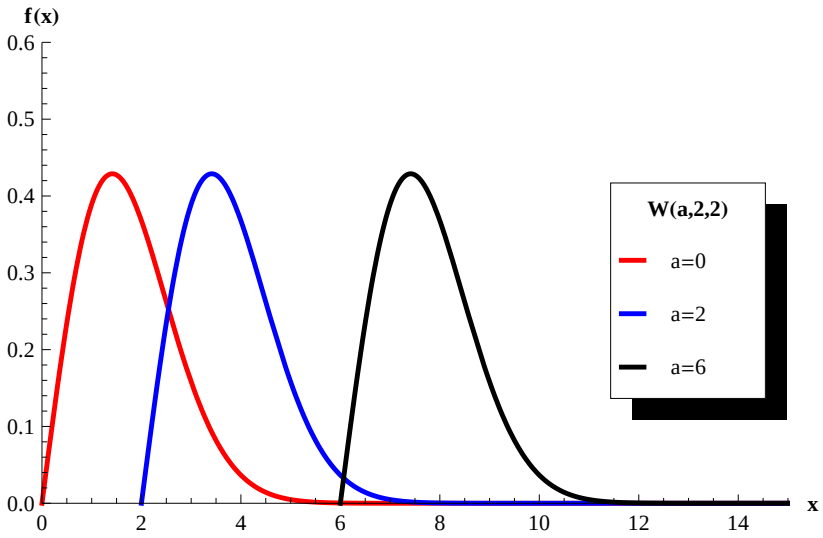

Figure 2.2: Probability density function of $W(a, 2, 2)$ - Variation of the location parameter a.

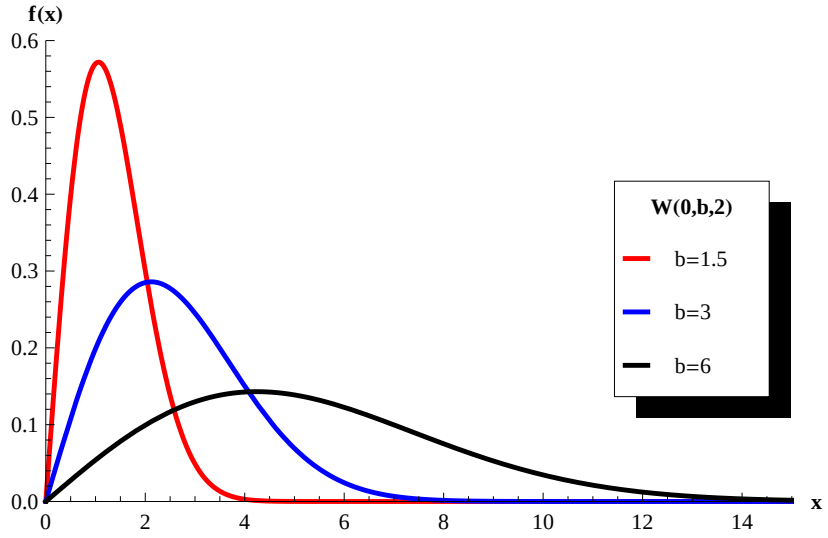

Figure 2.3: Probability density function of $W(0, b, 2)$ - Variation of the scale parameter b.

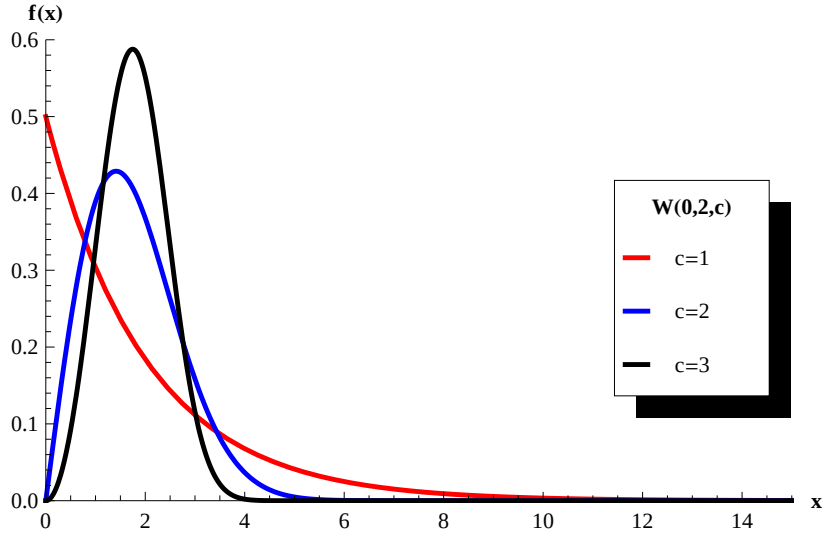

Figure 2.4: Probability density function of $W(0, 2, c)$ - Variation of the shape parameter c.

2.2.2 Cumulative distribution function - CDF

This function is also known as life distribution or failure distribution. It gives the probability of failing up to time x or having a life span of at most x.

Definition 2 (Weibull CDF)**.** *Let X be a random variable which follows a three-parameter Weibull distribution $W(a, b, c)$. The cumulative distribution function CDF of X, denoted by $F(x)$ is given by*

$$F(x \mid a, b, c) = 1 - \exp\left[- \left(\frac{x - a}{b} \right)^c \right] = P(X \leq x). \tag{2.15}$$

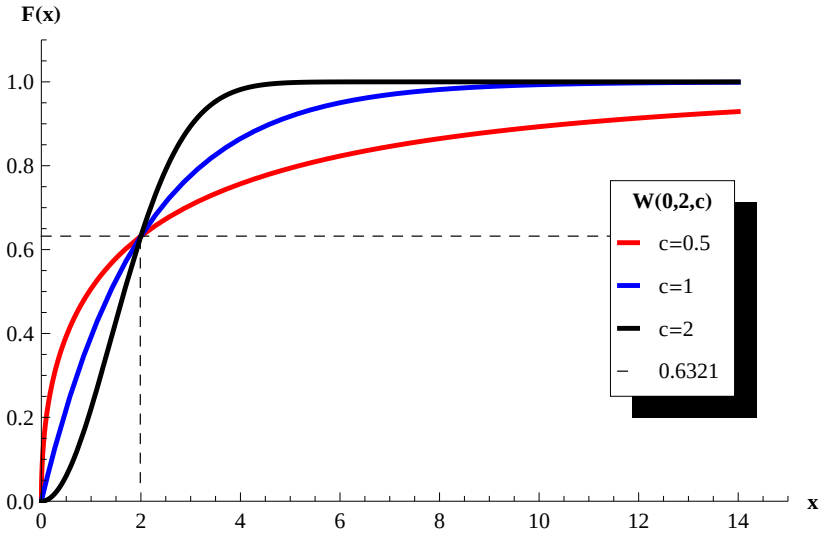

Figure 2.5: Cumulative distribution function of $W(0, 2, c)$ - Variation of the shape parameter c. The value of the scale parameter $b = 2$ corresponds to the probability $p = 0,6321$.

2.2.3 Statistical measures

The mean, variance and standard deviation are the most relevant parameters which describe a random variable that follows a three-parameter Weibull distribution $W(a, b, c)$.

Definition 3. *Let X be a random variable which follows a three-parameter Weibull distribution $W(a, b, c)$. The mean and variance of X are given by*

$$\textit{Mean:} \quad \mu(x) \quad = a + b\Gamma\left(1 + \frac{1}{c}\right), \tag{2.16}$$

$$\textit{Variance:} \quad \sigma^2(x) \quad = b^2\left[\Gamma\left(1 + \frac{2}{c}\right) - \Gamma^2\left(1 + \frac{1}{c}\right)\right], \tag{2.17}$$

where Γ is the Gamma function.

Definition 4 (Gamma function)**.** *If the real part of the complex number z is positive $(Re(z) > 0)$, then the integral*

$$\Gamma(z) = \int_0^\infty t^{z-1}e^{-t}\,\mathrm{d}t,$$

converges absolutely and it is known as Gamma function.

2.2.4 Location and scale transformation

The Weibull distribution is stable with respect to location and scale tranformations. This property will be applied in order to normalize the fatigue data coming from different stress ranges and to define a damage measure, see Subsection 3.6.2.

Theorem 1 (Location and scale stability)**.** *Let X be a random variable which follows a three-parameter Weibull distribution $W(a, b, c)$. Then the random variable given by*

$$U = \frac{X - r}{s}, \tag{2.18}$$

follows also a three-parameter Weibull distribution $W\left(\frac{a-r}{s}, \frac{b}{s}, c\right)$.

Proof. The CDF of U can be determined using the PDF of $X = Us + r$ as follows.

$$
\begin{aligned}
F_U(u) &= P(U \leq u) \\
&= P\left(\frac{X-r}{s} \leq u\right) \\
&= P(X \leq us + r) \\
&= \int_a^{us+r} \frac{c}{b}\left(\frac{x-a}{b}\right)^{c-1} \exp\left[-\left(\frac{x-a}{b}\right)^c\right] \mathrm{d}x \\
&= 1 - \exp\left[-\left(\frac{x-a}{b}\right)^c\right]\Bigg|_a^{us+r} \\
&= 1 - \exp\left[-\left(\frac{u - \frac{a-r}{s}}{\frac{b}{s}}\right)^c\right]. \qquad (2.19)
\end{aligned}
$$

The CDF given by Equation (2.19) is the CDF of a Weibull distribution as it was proposed. □

2.3 Parameter estimation methods

The challenge of every scientist is obtaining as far as possible good inferences about the reality; these inferences are based on experimental data which are assumed to be obtained in an unbiased way. In statistics, this goal means choosing a suitable method to estimate the parameters which describe the distribution in use.

There are several methods to estimate the Weibull parameters a, b, c such as those proposed in [70], [71], [72], [73], [74], [75], [76], [77], [78], [79]. Within this research two methods will be applied: the general probability weigthed moments (PWM) method and the maximum likelihood estimation (MLE) method.

2.3.1 The probability weighted moments - PWM

Consider that n experimental data points of the random variable lifetime X are given as follows

$$x_i = x_1, x_2, \ldots x_n.$$

The PWMs were introduced by Greenwood et all in [80] and applied by Hosking to the Extreme Value Distribution in [74]. Particularly for the three-parameter Weibull

distribution $W(a, b, c)$, a general formulation for its PWMs was deduced by Toasa and Ummenhofer in [78], see Theorem 2.

The primary use of PWMs is in the estimation of parameters of a probability distribution. These estimations are often considered to be superior to those based on standard moments and are used when the maximum likelihood estimations are unavailable or difficult to compute. They may also be used as initial values for maximum likelihood methods.

Definition 5. *The PWMs of a random variable X with CDF F are the quantities*

$$M_{p,r,s} = \int_0^1 \big[x(F)\big]^p F^r (1-F)^s \,\mathrm{d}F, \tag{2.20}$$

where $p, r, s \in \mathbb{N}$.

For the three-parameter Weibull distribution $W(a, b, c)$ its PWMs are defined as follows [78].

Theorem 2. *The general PWMs of a three-parameter Weibull distribution $W(a, b, c)$ are given by*

$$M_{p,r,s} = \sum_{i=0}^{p} \binom{p}{i} a^{p-i} b^i \sum_{k=0}^{r} \binom{r}{k} (-1)^k \frac{\Gamma\big(1+\frac{i}{c}\big)}{(s+k+1)^{1+\frac{i}{c}}}, \quad c > 0. \tag{2.21}$$

Proof. The inverse function of Equation (2.15) is given by

$$x(F) = a + b\big[-\log(1-F)\big]^{\frac{1}{c}}. \tag{2.22}$$

Replacing Equation (2.22) into Equation (2.20) gives a general equation of the PWMs.

$$M_{p,r,s} = \int_0^1 \Big\{a + b\big[-\log(1-F)\big]^{\frac{1}{c}}\Big\}^p F^r (1-F)^s \,\mathrm{d}F. \tag{2.23}$$

Making the substitution $u = -\log(1-F)$ into Equation (2.23) results in

$$M_{p,r,s} = \int_0^\infty \big[a + b u^{\frac{1}{c}}\big]^p (1-e^{-u})^r e^{-(s+1)u} \,\mathrm{d}u. \tag{2.24}$$

Considering the binomial theorem given by

$$(x+y)^n = \sum_{k=0}^{n} \binom{n}{k} x^{n-k} y^k, \tag{2.25}$$

it can be proved that

$$(a + bu^{\frac{1}{c}})^p = \sum_{i=0}^{p} \binom{p}{i} a^{p-i} b^i u^{\frac{i}{c}}. \tag{2.26}$$

Then, replacing Equation (2.26) in the first term of the integral of Equation (2.24) leads to

$$M_{p,r,s} = \sum_{i=0}^{p} \binom{p}{i} a^{p-i} b^i \int_0^{\infty} u^{\frac{i}{c}} (1-e^{-u})^r e^{-(s+1)u} \, \mathrm{d}u. \tag{2.27}$$

Then, applying again the binomial theorem and the Definition 4, the integral of Equation (2.27) becomes

$$\int_0^{\infty} u^{\frac{i}{c}} e^{-(s+1)u} \sum_{k=0}^{r} \binom{r}{k} e^{-ku} (-1)^k = \sum_{k=0}^{r} \binom{r}{k} (-1)^k \int_0^{\infty} u^{\frac{i}{c}} e^{-(k+s+1)u} \, \mathrm{d}u$$

$$= \sum_{k=0}^{r} \binom{r}{k} (-1)^k \frac{\Gamma\left(1+\frac{i}{c}\right)}{(s+k+1)^{1+\frac{i}{c}}}. \tag{2.28}$$

Finally, the general PWM $M_{p,r,s}$ for the three-parameter Weibull Distribution are determined by

$$M_{p,r,s} = \sum_{i=0}^{p} \binom{p}{i} a^{p-i} b^i \sum_{k=0}^{r} \binom{r}{k} (-1)^k \frac{\Gamma\left(1+\frac{i}{c}\right)}{(s+k+1)^{1+\frac{i}{c}}}, \quad c > 0.$$

□

Let $M_{1,0,s}$ be the particular PWMs given by

$$M_{1,0,s} = \frac{a}{s+1} + \frac{b}{(s+1)^{1+\frac{1}{c}}} \Gamma\left(1+\frac{1}{c}\right), \qquad c > 0. \tag{2.29}$$

Afterwards, the first three PWMs according to the subscript s will be considered in order to estimate the Weibull parameters a, b and c.

Denoting $M_s = M_{1,0,s}$, where $s = 0,\ 1,\ 2$ and $\Gamma_c = \Gamma(1 + \frac{1}{c})$ in Equation (2.29), the following system of equations is obtained

$$M_0 = a + b\Gamma_c, \tag{2.30}$$

$$M_1 = \frac{a}{2} + \frac{b}{2^{1+\frac{1}{c}}}\Gamma_c, \tag{2.31}$$

$$M_2 = \frac{a}{3} + \frac{b}{3^{1+\frac{1}{c}}}\Gamma_c. \tag{2.32}$$

Combining Equations (2.30) and (2.31) gives

$$2M_1 - M_0 = b\Gamma_c\Big(2^{\frac{-1}{c}} - 1\Big). \tag{2.33}$$

Combining Equations (2.30) and (2.32) gives

$$3M_2 - M_0 = b\Gamma_c\Big(3^{\frac{-1}{c}} - 1\Big). \tag{2.34}$$

Then dividing Equation (2.34) by Equation (2.33), leads to the following equation that determines the parameter c.

$$\frac{3M_2 - M_0}{2M_1 - M_0} = \frac{3^{\frac{-1}{c}} - 1}{2^{\frac{-1}{c}} - 1}. \tag{2.35}$$

The non linear Equation (2.35) should be solved by numerical methods in order to continue with the estimation of the parameters a, b.

From Equation (2.33), the value of the parameter b is given by

$$b = \frac{2M_1 - M_0}{(2^{\frac{-1}{c}} - 1)\Gamma_c}. \tag{2.36}$$

From Equation (2.30), the value of the parameter a is given by

$$a = M_0 - b\Gamma_c. \tag{2.37}$$

It is also necessary to know the value of the PWMs $M_0,\ M_1,\ M_2$ to solve the equations (2.35)-(2.37). For this reason, their estimators which depend on the ordered experimental data are used.

Let $x_1 < x_2 < \ldots < x_n$ be the order sample of the experimental data points. Then the estimators of the first three PWMs M_s [70], [77], [81] are given by

$$\widehat{M_0} = \frac{1}{n}\sum_{i=1}^{n} x_i, \tag{2.38}$$

$$\widehat{M_1} = \frac{1}{n(n-1)}\sum_{i=1}^{n-1}(n-i)x_i, \tag{2.39}$$

$$\widehat{M_2} = \frac{1}{n(n-1)(n-2)}\sum_{i=1}^{n-2}(n-i)(n-i-1)x_i. \tag{2.40}$$

By replacing the estimators given by Equations (2.38) to (2.40) in the Equations (2.35) to (2.37) the value of the Weibull parameters a, b, c are determined.

The PWM method suggested above has been already applied in order to model the tensile strength of concrete, as it can be seen in [82]. The results in this field have been remarkable, so that the authors suggest to apply this method to estimate the Weibull parameters.

Aplication of the PWM method on simulated fatigue data

In order to prove the efficiency of an estimation method, it is necessary to test its application on simulated data. In this case, simulated fatigue data given by

$$x_i = (\log N_i - B)(\log \Delta\sigma_i - C), \qquad i = 1, 2, \cdots, n \tag{2.41}$$

are generated. In Chapter 3 is demonstrated that in fact, the random variable x_i follows a Weibull distribution $W(a, b, c)$.

A general simulation is performed as follows. Let z_i be random numbers uniformly distributed in the interval $[0, 1]$, and replacing them in the CDF of the Weibull distribution given on Definition 2 leads to

$$z_i = 1 - \exp\left[-\left(\frac{x_i - a}{b}\right)^c\right]. \tag{2.42}$$

Taking into account the inverse function of the CDF given by Equation (2.22) leads to

$$x_i = a + b\big[-\log(1 - z_i)\big]^{\frac{1}{c}}, \tag{2.43}$$

which represents the equation to generate random numbers of a three-parameter Weibull distribution $W(a, b, c)$ based on the random numbers z_i. Moreover, these numbers x_i are the same of those x_i in Equation (2.41).

Then the random number of cycles N_i are determined by manipulating Equations (2.41) and (2.43) as follows.

$$N_i = \exp\left[\frac{x_i}{\log \Delta\sigma_i - C} + B\right]$$

$$= \exp\left\{\frac{a + b\big[-\log(1 - z_i)\big]^{\frac{1}{c}}}{\log \Delta\sigma_i - C} + B\right\}. \tag{2.44}$$

Since the fatigue is the random variable of interest, random fatigue data should be simulated. The simulation is based on the information provided by the fatigue experiments which were performed on specimens of steel S355 from the REFRESH project [83]. The main properties of the specimens are described on Table 2.1 and their geometry and measurements are showed in Figure 2.6.

S1-16-S355J2-AW Properties	
Project	REFRESH
Material	S355J2
Minimum yield strength R_{eH}	355 MPa
Treatment	As welded
Thickness	16 mm
Geometry	see Figure 2.6
Nr. of samples	14

Table 2.1: REFRESH S1-16-S355J2-AW. Properties - Corresponding to the specimens tested in the fatigue experiments.

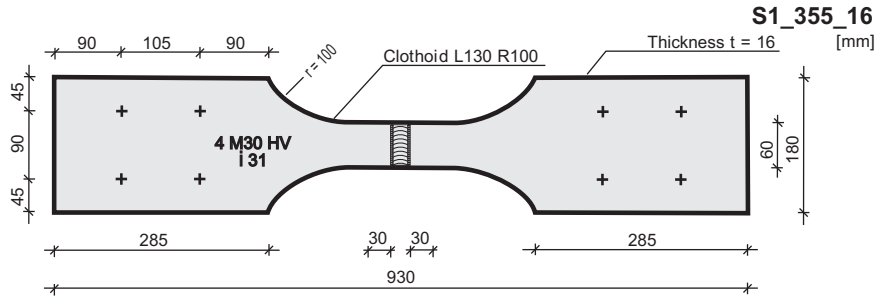

Figure 2.6: REFRESH S1-16-S355J2-AW. Specimens - Geometry and measurements.

During the performance of the fatigue experiments six different stress range values $\Delta\sigma_i$ were applied until the crack initiation of the specimens. Their corresponding stress ratio R and number of cycles N are presented in the Table 2.2.

S1-16-S355J2-AW $\mathbf{R = 0,1}$			
$\mathbf{\Delta\sigma}$ [MPa]		$\mathbf{N}$ [-]	
288	241 038	268 300	116 530
263	373 714	–	–
244	327 424	708 841	443 152
225	549 023	503 468	–
206	695 951	1 670 384	601 024
188	1 700 000	567 089	–

Table 2.2: REFRESH S1-16-S355J2-AW. Fatigue data - Experimental results.

The random variable x_i is defined by the geometrical parameters $B = -5,717$ and $C = 4,826$, while the corresponding Weibull distribution is $W(10,932; 3,725; 4,826)$. The determination of these parameters is explained in Section 3.4
Based on these five given parameters, two samples were simulated. Each sample contains 300 fatigue data, fifty data for each stress range.
The estimators of the Weibull parameters do not differ significantly from the default values. This fact shows how reliable the PWM method is. The results of the estimation are shown in Table 2.3.

Estimated Weibull Parameters - PWM			
Parameter	Real value	1^{st} simulation	2^{nd} simulation
a	10,93	11,02	10,89
b	3,72	3,57	3,78
c	4,83	4,81	5,02

Table 2.3: Estimated Weibull parameters of simulated fatigue data - Results based on the application of the PWM method [78].

In both cases the Wöhler curves based on the Weibull parameters estimated by the PWM method have a quite similar geometry to those curves based on the predetermined Weibull parameters, see Figures 2.7 and 2.8. This fact justifies the application and reliability of the PWM method.

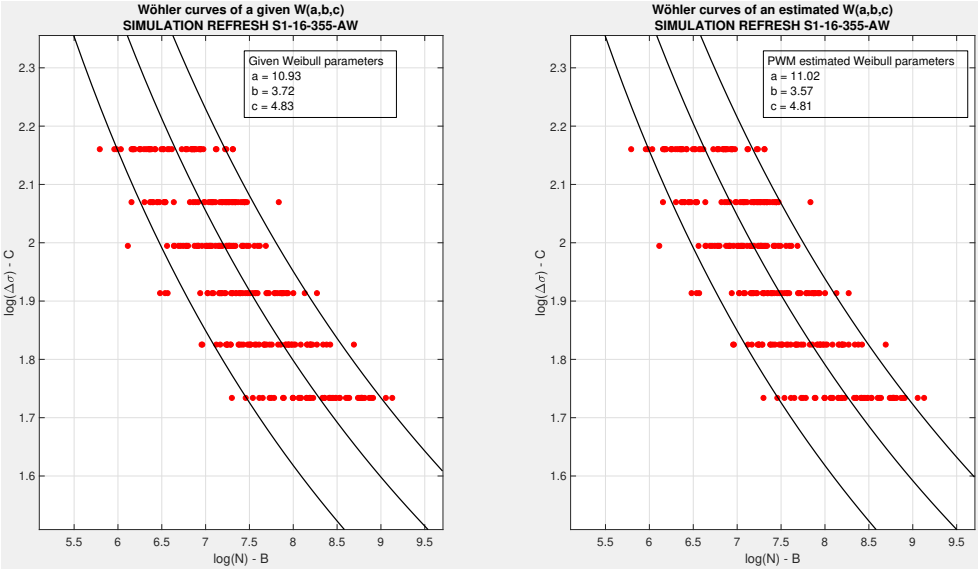

Figure 2.7: Wöhler curves of simulated fatigue data, PWM method - 1^{st} simulation from the REFRESH project. The curves corresponding to the given Weibull parameters are on the left and the curves corresponding to the estimated parameters are on the right.

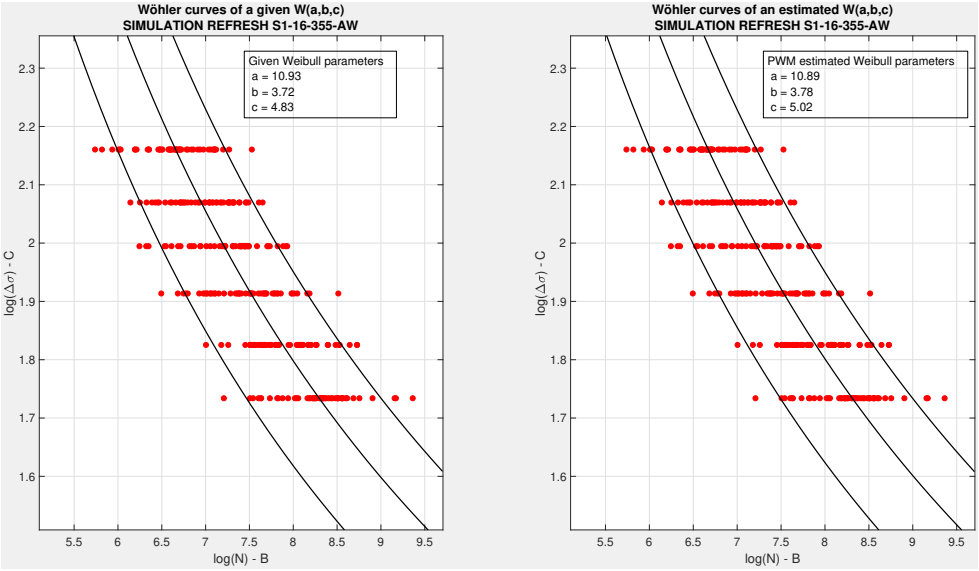

Figure 2.8: Wöhler curves of simulated fatigue data, PWM method - 2^{nd} simulation from the REFRESH project. The curves corresponding to the given Weibull parameters are on the left and the curves corresponding to the estimated parameters are on the right.

2.3.2 Maximum likelihood function method - MLE

The maximum-likelihood estimation is one of the most common methods to estimate the parameters of a statistical model and it is based on finding the maximun of the likelihood function. Some advantages of this method are that the estimated parameters are unbiased and have minimal variance [40].

Definition 6 (Likelihood function)**.** *Let $x_1, x_2, \ldots, x_n$ be n sample observations taken on corresponding random variables $X_1, X_2, \ldots, X_n$ whose distribution depends on a unknown parameter θ. The likelihood function $L(\theta) = L(x_1, x_2, \ldots, x_n \mid \theta)$ is the joint probability density function evaluated in $x_1, x_2, \ldots, x_n$ and it is given by*

$$L(\theta) = L(x_1, x_2, \ldots, x_n \mid \theta) = \prod_{i=1}^{n} f(x_i \mid \theta). \tag{2.45}$$

In some cases, it is more convenient to consider the logarithm of the likelihood function, noted by $\mathcal{L}$ and given by

$$\mathcal{L}(x_1, x_2, \ldots, x_n \mid \theta) = \log L(x_1, x_2, \ldots, x_n \mid \theta) = \sum_{i=1}^{n} \log f(x_i \mid \theta). \tag{2.46}$$

Definition 7 (Maximum likelihood estimate)**.** *Let $x_1, x_2, \ldots, x_n$ be a random sample from $f_X(x \mid \theta)$ and let $L(\theta)$ be the corresponding likelihood function. Suppose that $L(\hat{\theta}) \geq L(\theta)$ for all possible values of θ. Then $\hat{\theta}$ is called the maximum likelihood estimate for θ.*

According to Definition 7 an unbiased estimation $\hat{\theta}$ of a parameter θ is the value which maximizes the likelihood or the log-likelihood functions given by Equations (2.45) and (2.46) respectively.

In particular, the likelihood functions for the three-parameter Weibull distribution $W(a, b, c)$ are defined as follows.

Definition 8. *Let $x_1, x_2, \ldots, x_n$ be n data points corresponding to a three-parameter Weibull distribution $W(a, b, c)$. The likelihood and log-likelihood functions are given by*

$$L(a, b, c) = \frac{c}{b} \sum_{i=1}^{n} \left(\frac{x_i - a}{b} \right)^{c-1} \exp\left[- \left(\frac{x_i - a}{b} \right)^{c} \right], \tag{2.47}$$

$$\mathcal{L}(a,b,c) = n\big[\log c - c\log b\big] + (c-1)\sum_{i=1}^{n}\log(x_i - a) - \sum_{i=1}^{n}\left(\frac{x_i - a}{b}\right)^c \tag{2.48}$$

respectively.

The goal is estimating the Weibull parameters a, b, c and their estimators will be the values $\hat{a}, \hat{b}, \hat{c}$ which maximize the log-likelihood function given by Equation (2.48). The corresponding estimation is an unconstrained problem of nonlinear optimization with three variables. The estimators can be calculated by solving the following system of nonlinear equations, which is defined by taking the partial derivatives of Equation (2.48).

$$\frac{\partial\mathcal{L}(a,b,c)}{\partial a} = -(c-1)\sum_{i=1}^{n}\frac{1}{x_i - a} + \frac{c}{b}\sum_{i=1}^{n}\left(\frac{x_i - a}{b}\right)^{c-1} = 0, \tag{2.49}$$

$$\frac{\partial\mathcal{L}(a,b,c)}{\partial b} = -\frac{nc}{b} + \frac{c}{b}\sum_{i=1}^{n}\left(\frac{x_i - a}{b}\right)^{c} = 0, \tag{2.50}$$

$$\begin{aligned}\frac{\partial\mathcal{L}(a,b,c)}{\partial c} &= \frac{n}{c} - n\log b + \sum_{i=1}^{n}\log(x_i - a) - \sum_{i=1}^{n}\left(\frac{x_i - a}{b}\right)^{c}\log\left(\frac{x_i - a}{b}\right)^{c-1} \\ &= 0.\end{aligned} \tag{2.51}$$

The system given by Equations (2.49) to (2.51) can not be solved in an explicit way. As a matter of fact, it is possible to reduce the system so that only two equations have to be solved, however for this purpose a feasible numerical method should be applied.
The value of b can be obtained from Equation (2.50) as follows

$$b = \left[\frac{1}{n}\sum_{i=1}^{n}(x_i - a)^c\right]^{\frac{1}{c}}. \tag{2.52}$$

Then replacing b on Equations (2.49) and (2.51) leads to the nonlinear equations

$$\frac{c-1}{c}\sum_{i=1}^{n}\frac{1}{x_i-a}-n\frac{\sum_{i=1}^{n}(x_i-a)^{c-1}}{\sum_{i=1}^{n}(x_i-a)^{c}}=0, \tag{2.53}$$

$$\frac{1}{c}+\frac{1}{n}\sum_{i=1}^{n}\log(x_i-a)-\frac{\sum_{i=1}^{n}(x_i-a)^{c}\log(x_i-a)}{\sum_{i=1}^{n}(x_i-a)^{c}}=0. \tag{2.54}$$

The method suggested by Gupta and Panchang in [72] defines a discrete domain which contains the parameter a and it uses every discrete value a_j in this domain to find a value c_j from Equation (2.54). Afterwards, the values a_j, c_j are replaced into Equation (2.52) to obtain a value b_j. Obviously, the values a_j, b_j, c_j are vectors, whose components then are replaced in the log-likelihood function $\mathcal{L}$ given by Equation (2.48) in order to chose as estimators those which maximize $\mathcal{L}$.

Looking at the Definition 1, the units of the parameter a should be the same as the random variable x, moreover in terms of lifetime it has sense to assume that a is positive because there is no negative minimum life. For these reasons in this method it is considered that $0 \leq a \leq x$.

Definition 9. *Considering again the ordered sample of experimental data points $x_1 < x_2 < \ldots < x_n$ and in order to avoid logarithms of zero the domain of a is defined by*

$$Da = \left\{ a \middle/ 0 \leq a \leq x_1 - \varepsilon, \textit{ where } \varepsilon \textit{ is a small positive number} \right\}$$

Definition 10. *Let k be the number of intervals in which the domain of a should be discretized. The size of every interval and the values of the nodes are given by*

$$\Delta a = \frac{x_1 - \varepsilon}{k}, \tag{2.55}$$

$$a_j = (j-1)\Delta a \qquad \textit{for } j = 1, 2, \ldots, k+1 \tag{2.56}$$

respectively.

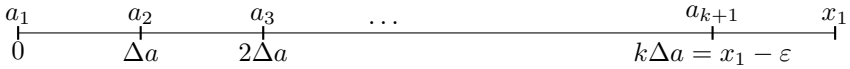

Figure 2.9: Discretization of the domain Da for the MLE method - In order to avoid convergence problems the value of ε is considered very small.

Replacing every a_j into Equation (2.54) allows to obtain its associated value c_j if the following nonlinear equation is solved

$$f(c_j) = \frac{1}{c_j} + \frac{1}{n}\sum_{i=1}^{n}\log\left(x_i - a_j\right) - \frac{\sum_{i=1}^{n}(x_i - a_j)^{c_j}\log\left(x_i - a_j\right)}{\sum_{i=1}^{n}(x_i - a_j)^{c_j}}. \tag{2.57}$$

For the numerical solution the initial value is given by

$$c_o = \frac{n}{n\log(x_n) - \sum_{i=1}^{n}\log(x_i)}, \tag{2.58}$$

where x_n is the maximum value in the ordered data sample.

Afterwards, replacing the values a_j, c_j in Equation (2.52) it is possible to determine their corresponding value b_j as follows

$$b_j = \left[\frac{1}{n}\sum_{i=1}^{n}(x_i - a_j)^{c_j}\right]^{\frac{1}{c_j}}. \tag{2.59}$$

Finally, in order to obtain the corresponding log-likelihood vector $\mathcal{L}_j$, the vectors a_j, b_j, c_j should be replaced into the Equation (2.48). The corresponding components $\hat{a}, \hat{b}, \hat{c}$ from the vectors a_j, b_j, c_j which give the greatest component from the vector $\mathcal{L}_j$ are the MLE estimators of the Weibull parameters a, b, c.

Aplication of the MLE method on simulated fatigue data

Similar to the application of the PWM method, in this case two simulations of the data from the REFRESH project were also performed.

The results of the estimation of the Weibull parameters by applying the MLE method are shown in Table 2.4.

Estimated Weibull Parameters - MLE			
Parameter	Real value	1^{st} simulation	2^{nd} simulation
a	10,93	10,91	10,92
b	3,72	3,72	3,79
c	4,83	4,75	4,55

Table 2.4: Estimated Weibull parameters of simulated fatigue data - Results based on the application of the MLE method [72].

In this case the Wöhler curves based on the Weibull parameters estimated by the MLE method have also a quite similar geometry to those curves based on the predetermined Weibull parameters, see Figures 2.10 and 2.11.

Based on the good results obtained by the PWM and MLE methods, it is reasonable to suggest these two techniques in order to estimate the parameters of a Weibull distribution $W(a, b, c)$. The model for the Wöhler curves, based on the Weibull distribution is presented and detailed in Chapter 3.

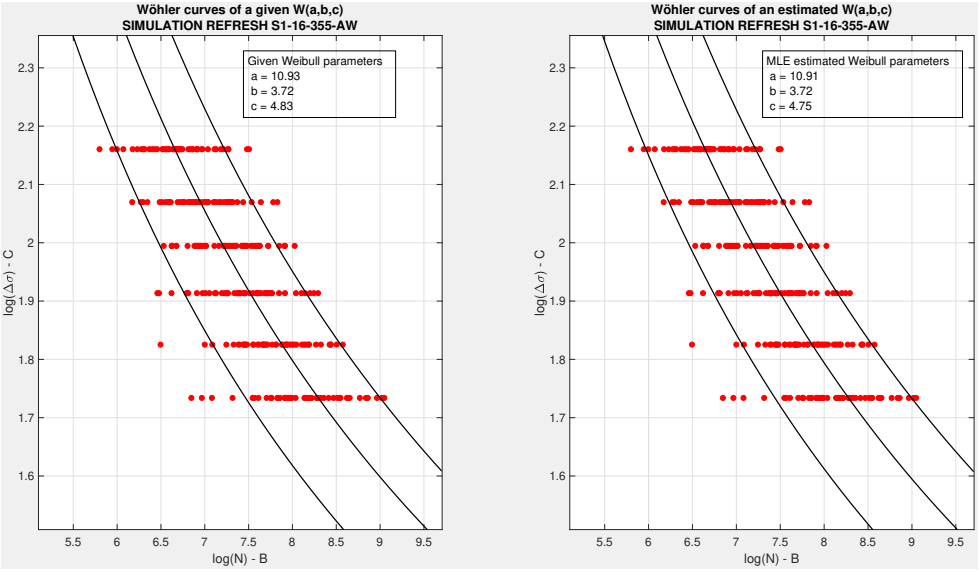

Figure 2.10: Wöhler curves of simulated fatigue data, MLE method - 1^{st} simulation from the REFRESH project. The curves corresponding to the given Weibull parameters are on the left and the curves corresponding to the estimated parameters are on the right.

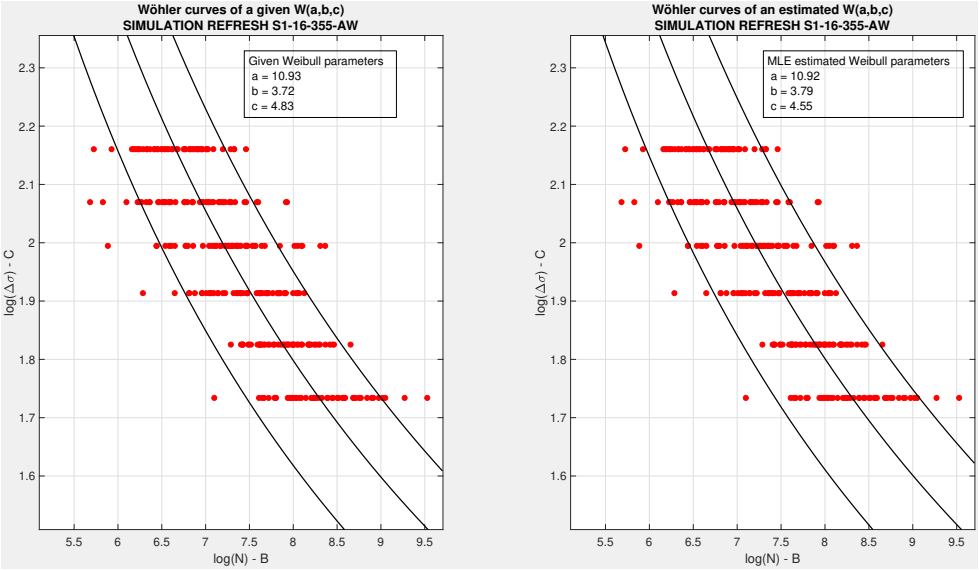

Figure 2.11: Wöhler curves of simulated fatigue data, MLE method - 2^{nd} simulation from the REFRESH project. The curves corresponding to the given Weibull parameters are on the left and the curves corresponding to the estimated parameters are on the right.

Chapter 3

The Weibull model for the *S-N* or Wöhler curves

> Empirical evidence can never
> establish mathematical existence.
>
> *Richard Courant*

Modelling the fatigue lifetime is a complex engineering problem which has not been yet completely solved. Mathematical, statistical and physical considerations have to be taken into account in order to build a suitable fatigue model to be applied in engineering design, structural reliability and risk analysis. A suitable fatigue model should allow making failure prediction with certain probability. Several factors, such as stress range, stress level, size effect are involved in building a fatigue model, as well as the estimation method of the corresponding statistical parameters.

The most common fatigue models and their deficiencies were presented in Section 1.5, however it is necessary to remember that their main weakness are given by:

- Inability to extrapolate the fatigue test results from the experimental area into the HCF or the VHCF region.
- Absence of a suitable statistical distribution or arbitrary assumption that the data follow a Gaussian normal or log-normal distribution
- Absence of a method to include the runouts and their influence in the statistical data analysis

- Not a dimensionless model
- Inability to reuse the runouts in subsequent experiments

3.1 Derivation of the model

In this section an alternative method to model the Wöhler curves for a constant stress ratio and different constant stress ranges is presented. This method has been proposed by Castillo and Fernández-Canteli [35] and it is a stress-based approach which overcomes the deficiencies mentioned above. This method considers the fatigue phenomena as a stochastic process and it applies functional equations [50], probability theory, and practical knowledge [51].

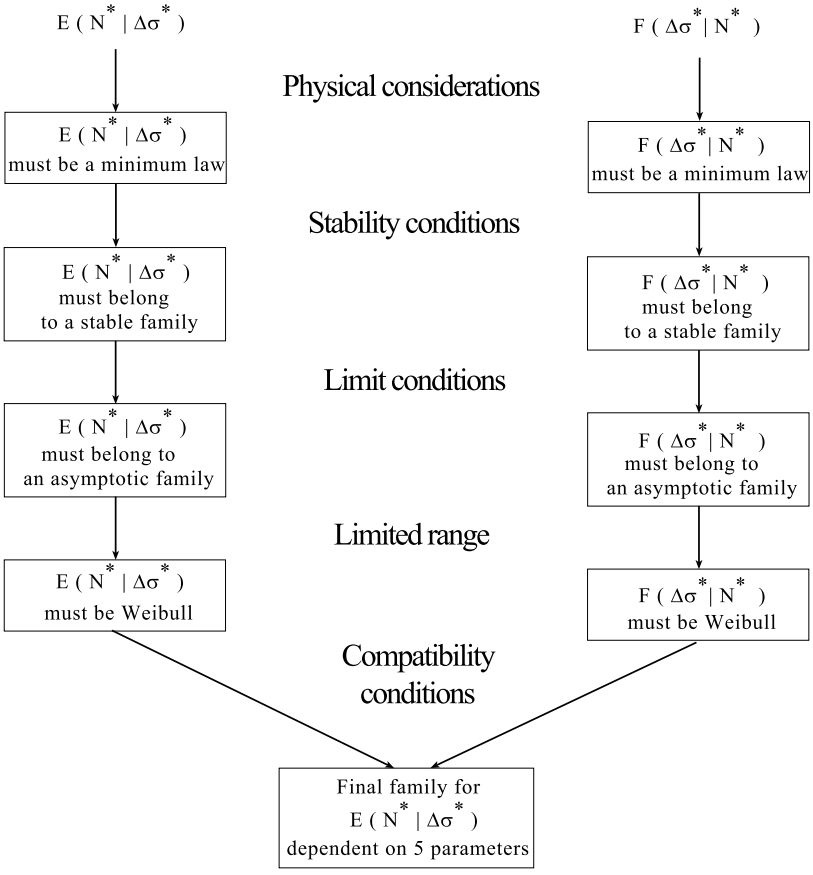

Figure 3.1: Procedure for the derivation of the Weibull model - Considerations made to determine a CDF of the lifetime [35].

First of all, a dimensional analysis of all variables involved on the fatigue phenomenon is mandatory in order to avoid obtaining either complex models or even worse, physically invalid models. This step is based on the application of Buckingham's theorem and it ensures obtaining a dimensionless model [52]. Then, based on a three-parameter Weibull distribution $W(a, b, c)$ [53], [54], the authors propose a dimensionless method to model the Wöhler curves.

The mathematical and physical considerations made by Castillo and Fernández-Canteli during the derivation of the proposed model are shown in the Figure 3.1. In order to understand the theoretical background and the assumptions behind this model, the subsequent subsections present an enhanced explanation of these considerations made by the author of this dissertation.

3.1.1 Dimensional analysis

In order to build a valid mathematical model which describes an engineering problem, it is necessary to perform a dimensional analysis; otherwise there is the possibility to obtain a wrong model which is not consistent from the physical point of view.
The π-theorem of Buckingham [52] is an essential tool which allows to obtain a dimensionless model.

Theorem 3 (Buckingham's π-Theorem)**.** *If there exists a unique relation*

$$\mathcal{B}(A_1, A_2, \ldots, A_n) = 0$$

among n physical quantities which involves k basic or fundamental physical dimensions[1]*, then there also exists a relation*

$$\Phi(\pi_1, \pi_2, \ldots, \pi_{n-k}) = 0$$

among $(n-k)$ dimensionless products made up of the quantities A_i.

Proof. A simple geometrical proof of this theorem can be found in [84].

□

In the case of modelling the Wöhler curves, applying the Buckingham's π-theorem allows to find a relationship between the number of cycles N and the stress range $\Delta\sigma$.

[1] The fundamental physical magnitudes are mass (M), length (L), time (T), electric current (I), temperature (Θ), amount of substance (μ), and luminous intensity (lv).

The five relevant variables or physical quantities in the fatigue model from Castillo and Fernández-Canteli are:

p: Probability

N: Number of cycles

N_0: Threshold value for N or minimum lifetime

$\Delta\sigma$: Stress range

$\Delta\sigma_\infty$: Fatigue or endurance limit

Then the unique relation $\mathcal{B}$ according to Theorem 3 is given by

$$\mathcal{B}(p, N, N_0, \Delta\sigma, \Delta\sigma_\infty) = 0, \tag{3.1}$$

and the involved fundamental physical magnitudes are M, L and T, as it is shown in Table 3.1.

Magnitude	$\mathbf{N}$	$\mathbf{N_0}$	$\mathbf{\Delta\sigma}$	$\mathbf{\Delta\sigma_\infty}$	$\mathbf{p}$
M	0	0	1	1	0
L	0	0	-1	-1	0
T	1	1	-2	-2	0

Table 3.1: Fundamental physical magnitudes and physical quantities of the Weibull fatigue model - Magnitudes and quantities according to Theorem 3 and Equation (3.1).

Hence, the relation Φ can be written as $\Phi(\pi_1, \pi_2) = 0$, and considering N and $\Delta\sigma$ as *independent* variables leads to

$$\pi_1 = N(N_0)^a(\Delta\sigma_\infty)^b(p)^c, \tag{3.2a}$$

$$\pi_2 = \Delta\sigma(N_0)^{\hat{a}}(\Delta\sigma_\infty)^{\hat{b}}(p)^{\hat{c}}. \tag{3.2b}$$

The parameters a, b, c, and $\hat{a}, \hat{b}, \hat{c}$ are those which make the dimension of π_1 and π_2 zero respectively. The value of the parameters can be determined by solving the following system of equations which depends of the fundamental physical quantities of the variables given in Table 3.1.

$$M^0L^0T^0 = T \quad [T]^a \quad [ML^{-1}T^{-2}]^b \quad [0]^c, \tag{3.3a}$$

$$M^0L^0T^0 = [ML^{-1}T^{-2}] \quad [T]^{\hat{a}} \quad [ML^{-1}T^{-2}]^{\hat{b}} \quad [0]^{\hat{c}}. \tag{3.3b}$$

A particular solution of the system is given by

$$\begin{pmatrix} a \\ b \\ c \end{pmatrix} = \begin{pmatrix} -1 \\ 0 \\ 1 \end{pmatrix}, \text{ and } \begin{pmatrix} \hat{a} \\ \hat{b} \\ \hat{c} \end{pmatrix} = \begin{pmatrix} 0 \\ -1 \\ 1 \end{pmatrix}.$$

Actually, the system has infinite solutions, because of the parameters c and $\hat{c}$ can take any real value. However, it has sense to consider 1 as the exponent of the probability p. Then the relation Φ from Theorem 3 can be written as

$$\Phi(\pi_1, \pi_2) = \Phi\left(\frac{N}{N_0}, \frac{\Delta\sigma}{\Delta\sigma_\infty}, p\right) = 0. \tag{3.4}$$

From the statistical point of view it is important to determine a CFD which describes the model, so that it has sense to consider the probability p as dependent variable in Equation (3.4) as follows

$$p = \hat{F}\left(\frac{N}{N_0}, \frac{\Delta\sigma}{\Delta\sigma_\infty}\right). \tag{3.5}$$

The function $\hat{F}$ indicates that the probability p depends on the dimensionless quotients $\frac{N}{N_0}$, $\frac{\Delta\sigma}{\Delta\sigma_\infty}$ or some monotone functions like $h\left(\frac{N}{N_0}\right)$, $g\left(\frac{\Delta\sigma}{\Delta\sigma_\infty}\right)$.

In particular, the Wöhler curves are displayed in a logarithmic scale for both axes, so that the functions h and g can be logarithmic and the probability p from Equation (3.5) becomes

$$p = F\left[\log\left(\frac{N}{N_0}\right), \log\left(\frac{\Delta\sigma}{\Delta\sigma_\infty}\right)\right]. \tag{3.6}$$

And it is precisely the CDF F which has to be determined.
According to Theorem 3 and in order to simplify the notation, making the changes of variable given by

$$N^* = \log\left(\frac{N}{N_0}\right) \tag{3.7}$$

and

$$\Delta\sigma^* = \log\left(\frac{\Delta\sigma}{\Delta\sigma_\infty}\right), \tag{3.8}$$

leads to work with dimensionless variables.

The selection of a CDF $F(N^*, \Delta\sigma^*)$ for the proposed model must be based on physical considerations together with stability, limit and compatibility conditions [51], [85], [35].
Two conditional CDFs will be considered simultaneously:

a). The CDF of the number of cycles N^* for a given stress range $\Delta\sigma^*$ denoted by $F(N^*|\Delta\sigma^*)$

b). The CDF of the stress range $\Delta\sigma^*$ for a given number of cycles N^* denoted by $G(\Delta\sigma^*|N^*)$

3.1.2 Physical considerations

These considerations are related with the weakest link principle which establishes that the fatigue lifetime of an element of length L is the minimum fatigue lifetime of its n constituting pieces of length l, see Figure 3.2. Sometimes, the "weakest link" of the specimen is a terminology to name the location of crack nucleation site [15].
Hence, a minimum value distribution is what properly describes this principle. This kind of distribution is the limit distribution of the smallest value of a random variable X in a sample of size $n \to \infty$.

From the Equation (2.10) it follows

$$P_n = 1 - (1 - P)^n. \tag{3.9}$$

As the probabilities P and P_n are defined by the CDFs, the Equation (3.9) can be written as

$$F_{min}(x) = 1 - \Big[1 - F(x)\Big]^n, \tag{3.10}$$

where $F_{min}(x)$ and $F(x)$ are the probabilities of failure under a load x of the whole element and of a single piece respectively.

These kind of considerations are known as weakest link principle and they have been already applied in order to model strength of long fibers [86], failure time of fibrous materials [87], failure time of systems [88] and size effect on fatigue of steel [89].

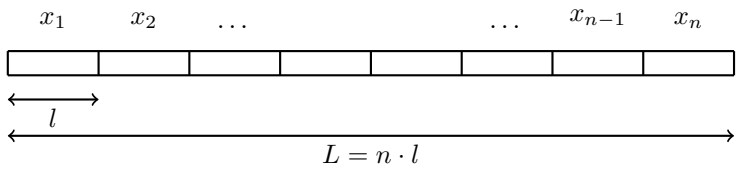

Figure 3.2: Longitudinal element - Discretization in n single pieces of length l.

3.1.3 Stability with respect to minimum

The stability of a CDF F can be ensured if $F_{min}(x)$ and $F(X)$ belong to the same stable familiy of distributions. In the particular case of fatigue, it means that the lifetime of a single component and of the whole element follow the same kind of distribution. The Weibull distribution satisfies this requirement as it is shown in the following theorem.

Theorem 4 (Stability of the Weibull distribution)**.** *Let X_i, $i = 1, 2, \ldots, n$ be independent random variables which follow a three-parameter Weibull distribution $W(a, b, c)$. Then, their minimum follows also a three-paremeter Weibull distribution $W(a, bn^{\frac{-1}{c}}, c)$, whose CDF is given by*

$$F_{min}(x) = 1 - \exp\left[- \left(\frac{x-a}{bn^{\frac{-1}{c}}} \right)^c \right]. \tag{3.11}$$

Proof. From Equation (3.10) it follows

$$\begin{aligned} F_{min}(x) &= 1 - \Big[1 - F(x)\Big]^n \\ &= 1 - \left\{ 1 - \left[1 - \exp\left[- \left(\frac{x-a}{b} \right)^c \right] \right] \right\}^n \\ &= 1 - \left\{ \exp\left[- n \left(\frac{x-a}{b} \right)^c \right] \right\} \\ &= 1 - \exp\left[- \left(\frac{x-a}{bn^{\frac{-1}{c}}} \right)^c \right] \end{aligned}$$

□

3.1.4 Limit behavior

If the length of a single component tends to zero, i.e. $l \to 0$, the amount of components tends to infinity, therefore the conditional distributions $F(N^*|\Delta\sigma^*)$ and $G(\Delta\sigma^*|N^*)$ should be asymptotic. Actually, the only asymptotic families of distributions are the Weibull, Frechet and Gumbel. However, N and $\Delta\sigma$ are positive and the Weibull distribution is the only one which satisfies this requirement [51], [90], [85], [35].

Consider the conditional Weibull distributions of the number of cycles N for a simple component and for the whole component as follows

$$P = F(N^*|\Delta\sigma^*, l) = 1 - \exp\left[- \left(\frac{N^* - a_1(\Delta\sigma^*, l)}{b_1(\Delta\sigma^*, l)} \right)^{c_1(\Delta\sigma^*, l)} \right], \tag{3.12}$$

$$P_n = F(N^*|\Delta\sigma^*, L) = 1 - \exp\left[- \left(\frac{N^* - a_1(\Delta\sigma^*, L)}{b_1(\Delta\sigma^*, L)} \right)^{c_1(\Delta\sigma^*, L)} \right]. \tag{3.13}$$

Applying the Theorem 4 in Equation (3.13) leads to

$$P_n = 1 - \exp\left[- \left(\frac{N^* - a_1(\Delta\sigma^*, l)}{b_1(\Delta\sigma^*, l) \cdot n^{\frac{-1}{c_1(\Delta\sigma^*, l)}}} \right)^{c_1(\Delta\sigma^*, l)} \right], \tag{3.14}$$

where the funtions $a_1(\Delta\sigma^*, L)$, $b_1(\Delta\sigma^*, L)$ and $c_1(\Delta\sigma^*, L)$, have to be determined.

The Equation (3.14) shows that the Weibulll distribution is "closed under minima" [77]. In reliability terms it means that $\min(N^*)$ is the life time for a serial system with n similar components [91].

Afterwards, comparing Equation (3.13) and Equation (3.14) leads to

$$\left(\frac{N^* - a_1(\Delta\sigma^*, L)}{b_1(\Delta\sigma^*, L)} \right)^{c_1(\Delta\sigma^*, L)} = \left(\frac{N^* - a_1(\Delta\sigma^*, l)}{b_1(\Delta\sigma^*, l) \cdot n^{\frac{-1}{c_1(\Delta\sigma^*, l)}}} \right)^{c_1(\Delta\sigma^*, l)}.$$

And in order to satisfy this equality it is necessary that

$$a_1(\Delta\sigma^*, L) = a_1(\Delta\sigma^*, l) = a_1(\Delta\sigma^*), \tag{3.15}$$

$$c_1(\Delta\sigma^*, L) = c_1(\Delta\sigma^*, l) = c_1(\Delta\sigma^*), \tag{3.16}$$

$$b_1(\Delta\sigma^*, L) = b_1(\Delta\sigma^*, l) \cdot n^{-\frac{1}{c_1(\Delta\sigma^*)}}. \tag{3.17}$$

The expressions given by Equations (3.15) and (3.16) prove that the parameters a_1 and c_1 do not depend on the total length L. Moreover, if $n \to \infty$ it also satisfies for b_1 in Equation (3.17).

Similarly, considering the conditional Weibull distribution of the stress range $\Delta\sigma^*$ from a single and a whole component given by

$$P = G(\Delta\sigma^*|N^*, l) = 1 - \exp\left[-\left(\frac{\Delta\sigma^* - a_2(N^*, l)}{b_2(N^*, l)}\right)^{c_2(N^*, l)}\right] \tag{3.18}$$

and

$$P_n = G(\Delta\sigma^*|N^*, L) = 1 - \exp\left[-\left(\frac{\Delta\sigma^* - a_2(N^*, L)}{b_2(N^*, L)}\right)^{c_2(N^*, L)}\right] \tag{3.19}$$

leads to the following expressions

$$a_2(N^*, L) = a_2(N^*, l) = a_2(N^*), \tag{3.20}$$

$$c_2(N^*, L) = c_2(N^*, l) = c_2(N^*), \tag{3.21}$$

$$b_2(N^*, L) = b_2(N^*, l) \cdot n^{-\frac{1}{c_2(N^*)}}. \tag{3.22}$$

In this case the functions $a_2(N^*, L)$, $b_2(N^*, L)$ and $c_2(N^*, L)$ have to be determined.

The expressions given by Equations (3.20) and (3.21) prove that the parameters a_2 and c_2 do not depend either on the total length L. Similarly, if $n \to \infty$ it also satisfies for b_2 in Equation (3.22).

3.1.5 Limited range

The limited range condition implies that the random variables $\Delta\sigma^*$ and N^* are non negative and moreover they have a finite lower end. The lower end must coincide

with the theoretical end of the selected CDF, and the Weibull distribution is the only one which satisfies this requirement.

Additionaly, this condition also means that it is asummed that the fatigue limit $\Delta\sigma_\infty$ considered in the dimensional analysis from Subsection 3.1.1 exists. Eventhough, there is no an agreement regarding the existence of a fatigue limit [34], [92], [93]. For this reason, this assumption may generate a debate and has to be kept in mind when the results given by this model are analysed.

Since $N \geq N_0$ and $\Delta\sigma \geq \Delta\sigma_\infty$ leads to $\log\left(\frac{N}{N_0}\right) \geq 0$ and $\log\left(\frac{\Delta\sigma}{\Delta\sigma_\infty}\right) \geq 0$, the selection of the logarithmic representation is justified, because it leads to a limited random variable in the lower tail. In fact, the Weibull distribution is the only suitable extreme value distribution for minimums.

3.1.6 Compatibility condition

Considering that both conditional Weibull distributions $F(N^*|\Delta\sigma^*)$ and $G(\Delta\sigma^*|N^*)$ correspond to the same percentil curve, they are not independent and have to satisfy a compatibility condition. This compatibility condition can be written as a functional equation given by

$$F(N^*|\Delta\sigma^*) = G(\Delta\sigma^*|N^*) = F_{min}(N^*, \Delta\sigma^*), \tag{3.23}$$

where $F_{min}(N^*, \Delta\sigma^*)$ is the CDF of a minimum law related with the weakest link principle presented in Subsection 3.1.2. According to the results given in Subsection 3.1.4 the functional Equation (3.23) can be written as

$$\left[\frac{N^* - a_1(\Delta\sigma^*)}{b_1(\Delta\sigma^*)}\right]^{c_1(\Delta\sigma^*)} = \left[\frac{\Delta\sigma^* - a_2(N^*)}{b_2(N^*)}\right]^{c_2(N^*)}. \tag{3.24}$$

The expression (3.24) is a particular case of the following functional equation

$$1 - \exp\left\{-\left[a(x)y + b(x)\right]^{c(x)}\right\} = 1 - \exp\left\{-\left[d(y)x + e(y)\right]^{f(y)}\right\}. \tag{3.25}$$

Two general solutions for the functional Equation (3.25) are possible and they are determined in [50]. In the particular case of the Equation (3.24), the following solutions given in [51] agree the practical knowledge obtained from experimental results.

$$a_1(\Delta\sigma^*) = \frac{K_{21}\Delta\sigma^* + K_{22}}{K_{11}\Delta\sigma^* + K_{12}}; \qquad a_2(N^*) = \frac{-K_{12}N^* + K_{22}}{K_{11}N^* - K_{21}};$$

$$b_1(\Delta\sigma^*) = \frac{1}{K_{11}\Delta\sigma^* + K_{12}}; \qquad b_2(N^*) = \frac{1}{K_{11}N^* - K_{21}};$$

$$c_1(\Delta\sigma^*) = c^*; \qquad c_2(N^*) = c^*.$$

Replacing these solutions on Equation (3.23) leads to

$$F_{min}(N^*, \Delta\sigma^*) = 1 - \exp\left\{ - \left[\frac{\left(N^* - \frac{K_{21}}{K_{11}}\right)\left(\Delta\sigma^* + \frac{K_{12}}{K_{11}}\right) - \left(\frac{K_{22}}{K_{11}} - \frac{K_{12}K_{21}}{K_{11}^2}\right)}{\frac{1}{K_{11}}} \right]^{c^*} \right\}. \tag{3.26}$$

Considering the following substitutions

$$B^* = \frac{K_{21}}{K_{11}}$$

$$C^* = -\frac{K_{12}}{K_{11}}$$

$$a^* = \frac{K_{22}}{K_{11}} - \frac{K_{12}K_{21}}{K_{11}^2}$$

$$b^* = \frac{1}{K_{11}}$$

leads to the following dimensionless Weibull model.

$$F_{min}(N^*, \Delta\sigma^*) = 1 - \exp\left\{ - \left[\frac{(N^* - B^*)(\Delta\sigma^* - C^*) - a^*}{b^*} \right]^{c^*} \right\}. \tag{3.27}$$

Afterwards considering the change of variables given by Equation (3.7) and (3.8) leads to

$$F(N|\Delta\sigma) = 1 - \exp\left\{ - \left[\frac{(\log N - \log N_0 - B^*)(\log \Delta\sigma - \log \Delta\sigma_\infty - C^*) - a^*}{b^*} \right]^{c^*} \right\}, \tag{3.28}$$

$$G(\Delta\sigma|N) = 1 - \exp\left\{ - \left[\frac{(\log N - \log N_0 - B^*)(\log \Delta\sigma - \log \Delta\sigma_\infty - C^*) - a^*}{b^*} \right]^{c^*} \right\}. \tag{3.29}$$

Emerging the thresholds $\log N_0$, $\log \Delta\sigma_\infty$ into the constants B^*, C^* respectively leads to the following dimensional Weibull model

$$F_{min}(N, \Delta\sigma) = 1 - \exp\left\{ - \left[\frac{(\log N - B)(\log \Delta\sigma - C) - a}{b} \right]^{c} \right\}; \tag{3.30}$$

with $(\log N - B)(\log \Delta\sigma - C) \geq a$, where the random variable $(\log N - B)(\log \Delta\sigma - C)$ follows a three-parameter Weibull distribution $W(a, b, c)$.
Additionally B, C, a, b, c are the non-dimensional parameters of the model to be estimated and their physical meanings given in [51], [85], [35] are the following:

$F_{min}(N, \Delta\sigma) = p$: Probability of failure

Geometrical parameters:

B : Threshold value of the lifetime N

C : Endurance limit for $\Delta\sigma$

Weibull parameters:

a : Weibull location parameter

b : Weibull scale parameter

c : Weibull shape parameter

3.2 Plot of the Wöhler curves and influence of their parameters

Based on Equation (3.30) it is possible to plot a Wöhler curve which is defined by six parameters as follows

$$\Delta\sigma(p, B, C, a, b, c) = \exp\left\{\frac{\left[-\log(1-p)\right]^{\frac{1}{c}} b + a}{\log N - B} + C\right\}, \quad N \geq 1. \tag{3.31}$$

The Figure 3.3 shows three Wöhler curves corresponding to three different probabilities.

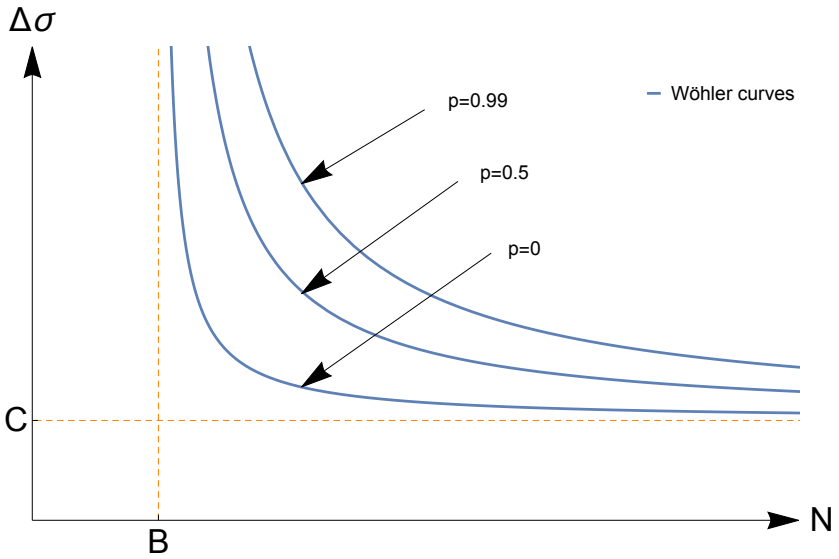

Figure 3.3: Wöhler curves for different values of p - They represent the relationship between lifetime N and stress range $\Delta\sigma$.

Since a Wöhler curve depends on the probability and five parameters, it is necessary to depict the effects of their variation on the geometry of the curves. To do this, a predetermined curve $\Delta\sigma(0,5; 1; 4,7; 11; 1; 1,5)$ is considered. The Figures 3.4 to 3.8 show the influence of the geometrical and Weibull parameters on the geometry of the given Wöhler curve which is plotted in green.

The variation of the geometrical parameters B, C affects considerably how the Wöhler curves are depicted, see Figures 3.4 and 3.5.

The variation of the Weibull parameters a, b affects also considerably how the Wöhler curves are depicted, see Figures 3.6 and 3.7. However, the infuence of the Weibull parameter c is weak, see Figure 3.8.

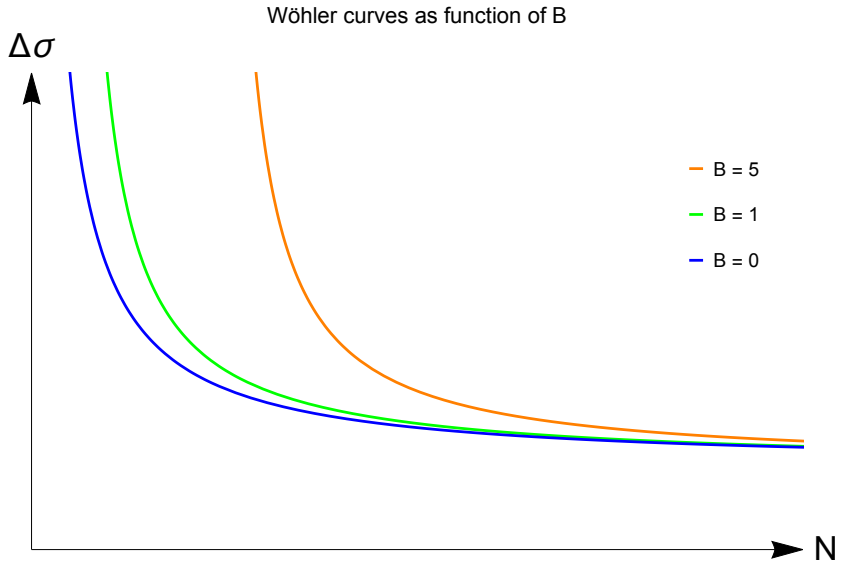

Figure 3.4: Wöhler curves for different values of B - The parameter B represents the threshold of the lifetime.

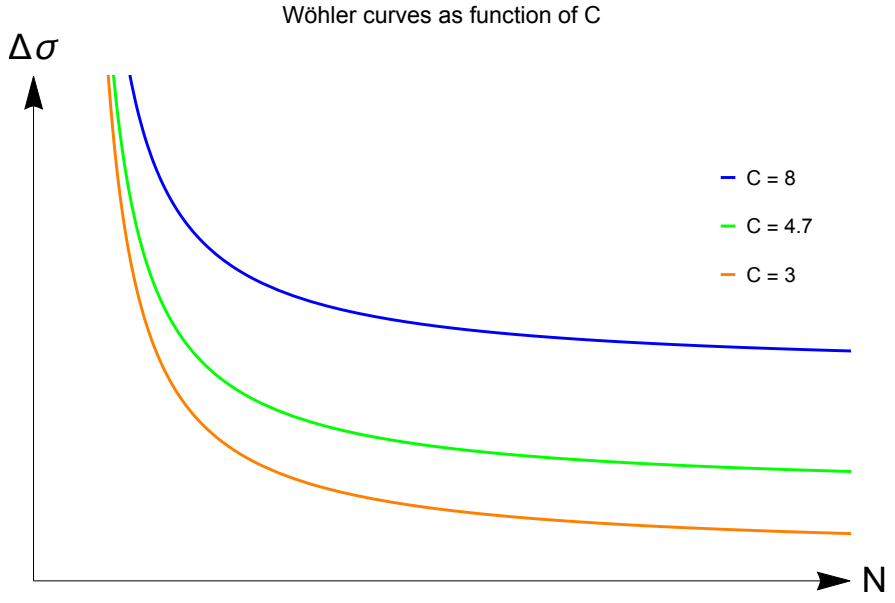

Figure 3.5: Wöhler curves for different values of C - The parameter C represents the endurance limit.

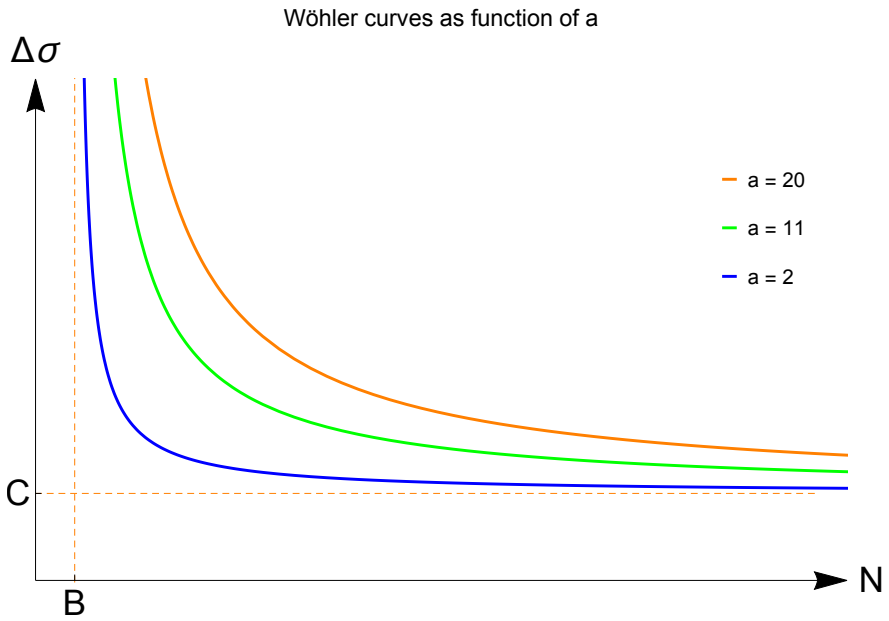

Figure 3.6: Wöhler curves for different values of a - The parameter a is the location of the density function of $W(a, b, c)$.

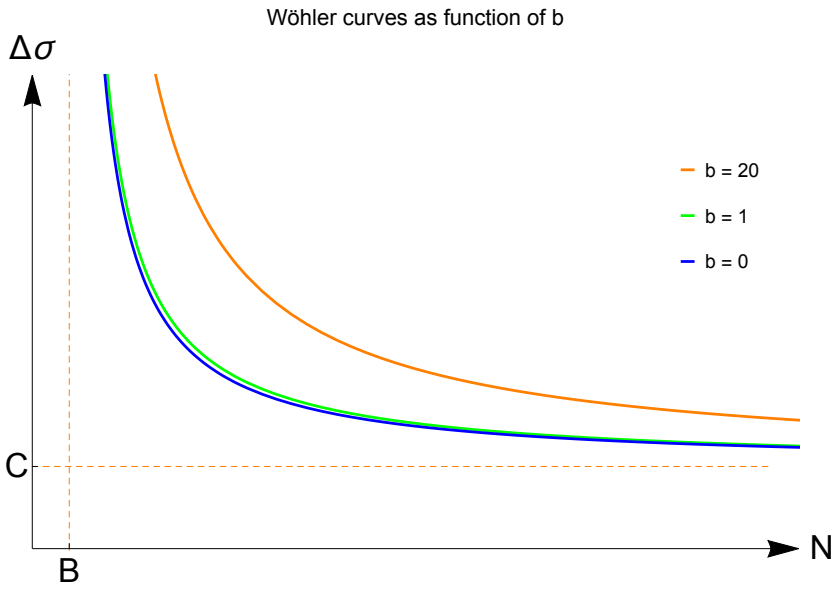

Figure 3.7: Wöhler curves for different values of b - The parameter b is the scale of the density function of $W(a, b, c)$.

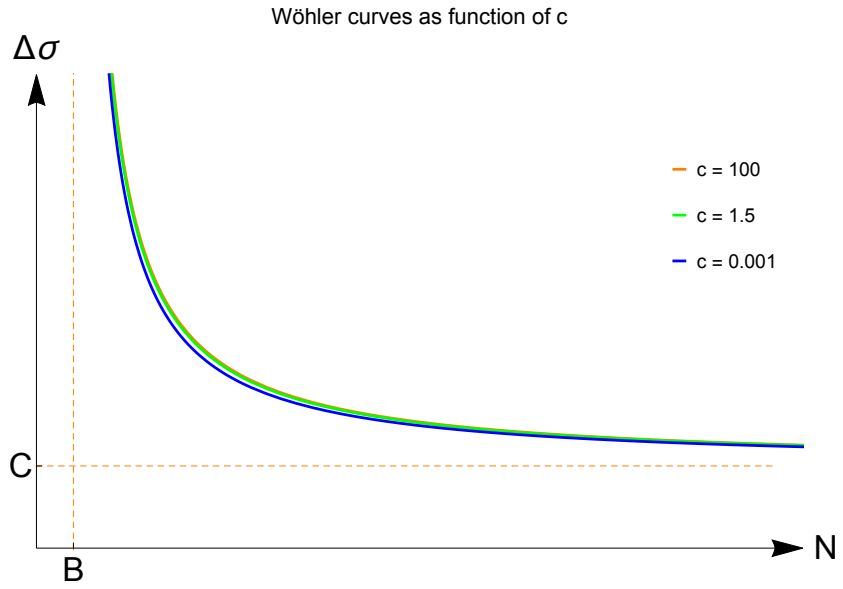

Figure 3.8: Wöhler curves for different values of c - The parameter c is the shape of the density function of $W(a, b, c)$.

From the geometrical point of view, the location parameter a defines the position of the corresponding zero-percentile hyperbola. This hyperbola represents the minimum possible number of cycles to fatigue failure for different values of $\Delta\sigma$, and it can be interpreted as the end of the crack initiation phase and the beginning of the crack propagation process [35].

The Figure 3.9 shows how the Wöhler curves change depending of the probability and the Weibull parameter a. The geometry of a curve is more affected by the variation of the Weibull parameter a than by the variation of the probability p.

3.3 Limitations of the Weibull fatigue model

Eventhough the Weibull fatigue model of Castillo and Canteli overcomes the deficiencies of the traditional fatigue models, the considerations made on Section 3.1 in order to derivate the model can be questioned or at least give rise to a debate [35]. For this reason it is necessary to make the following remarks regarding these considerations.

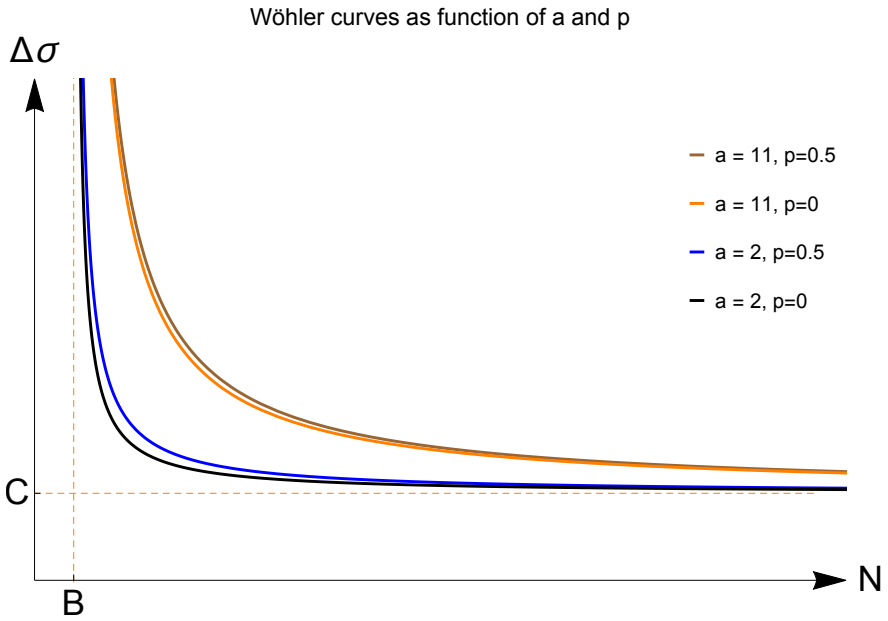

Figure 3.9: Wöhler curves for different values of a and p - The parameter a defines the position of the zero percentile.

1. The assumption of weakest link done in Subsection 3.1.2 implies that the lifetimes of single pieces of a component are independent. This can hold approximately for components of long sizes, but can be not true for small sizes.

2. According to some researchers the assumption made in Subsection 3.1.4 concerning to the limit behavior is not necessary, even though it is a convenient property to model the fatigue. In fact, other models can be determined if some properties, such as random defects, micromechanical stress redistribution, catastrophic or abrupt crack growth, which do not follow a Weibull distribution are considered.

3. The limited range assumptions made in Subsection 3.1.5 imply that the fatigue limit $\Delta\sigma_\infty$ exists, that is the reason because $\Delta\sigma_\infty$ was taken into account in the dimensional analysis. Nevertheless, as it was mentioned in Subsection 3.1.5, its existence has been on the one hand assumed and on the other hand unaccepted.
   Moreover, the geometrical parameters B and C can be viewed as non negative scale constants.

4. Due to plasticity effects, the Wöhler curves should show a change in the curvature in the upper part corresponding to the VLCF region. This fact is related with the crack initiation period or the crack growth period where the work dissipated by plastic straining prevails [94]. In this region, besides the statistical considerations, a continuum mechanics model based on the strain may be more suitable to model the Wöhler curves in this region.
   For these reasons, the Weibull model considered in this dissertation cannnot be applied to model the fatigue in the VLCF region.

5. There is no definition or formulation to describe the transition from the crack initiation period to the crack growth period. It must be admitted that a rigorously and physically satisfactory solution of the fatigue problem is not yet available.

3.4 Parameter estimation

The Weibull model given by Equation (3.30) describes the probability of a failure as a function of the stress range $\Delta\sigma$ and the lifetime N, and overcome the deficiencies mentioned in Section 1.5.
The parameter estimation of this model depends on the experimental fatigue data and can be divided in two stages:

3.4.1 Estimation of the geometrical parameters

Consider that n experimental data points of stress ranges and load cycles corresponding to failures are given as follows.

$$\Delta\sigma_i = \Delta\sigma_1, \Delta\sigma_2, \dots \Delta\sigma_n,$$
$$N_i = N_1, N_2, \dots N_n.$$

According to the deduced model given by Equation (3.30), it is known that $(\log N - B)(\log \Delta\sigma - C)$ follows a three-parameter Weibull distribution $W(a, b, c)$. Then taking into account the scale stability of the Weibull distribution given by Theorem 1 leads to asseverate that

$$\big(\log N - B\big) \rightsquigarrow W\left(\frac{a}{\log \Delta\sigma - C}, \frac{b}{\log \Delta\sigma - C}, c\right), \tag{3.32}$$

whose conditional expected value or mean is given by

$$E\big(\log N - B|\log\Delta\sigma - C\big) = \frac{\mu}{\log\Delta\sigma - C} \quad , \tag{3.33}$$

where μ is the mean of a three-parameter Weibull distribution $W(a, b, c)$.

The Equation (3.33) is equivalent to

$$E\big(\log N|\log\Delta\sigma - C\big) = B + \frac{\mu}{\log\Delta\sigma - C} \quad , \tag{3.34}$$

which is a regression equation for the number of cycles N as a function of the stress range $\Delta\sigma$ [85], [95]. Therefore the thresholds or geometrical parameters B and C and the mean μ are obtained by solving the following non-linear optimization problem [96], [97], [98], [99], [100].

$$\min_{B,C,\mu\in\mathbb{R}} \quad \sum_{i=1}^{n}\left(\log N_i - B - \frac{\mu}{\log\Delta\sigma_i - C}\right)^2. \tag{3.35}$$

Initial values

Since the Equation (3.34) is non-linear, Castillo et al. suggest in [35] obtaining initial values to avoid convergence problems. One possibility consists of using three different stress ranges $\Delta\sigma_i, i = 1, 2, 3$ whose corresponding amount of data is l_i and the number of cycles of each stress range can be denoted as $N_{i,j}$ for $i = 1, 2, 3$ and $j = 1, 2\ldots, l_i$, see Table 3.2.

$\mathbf{\Delta\sigma_i}$	$\mathbf{N_{i,j}}$	**Size**
$\Delta\sigma_1$	$N_{1,1}, N_{1,2}, \ldots, N_{1,l_1}$	l_1
$\Delta\sigma_2$	$N_{2,1}, N_{2,2}, \ldots, N_{2,l_2}$	l_2
$\Delta\sigma_3$	$N_{3,1}, N_{3,2}, \ldots, N_{3,l_3}$	l_3

Table 3.2: Data considered to calculate the initial values of the geometrical parameters - Partition and notation of the experimental data based on the selected three stress levels.

If the means of the $\log N_{i,j}$ from Table 3.2 coincides with the regression curve given by Equation (3.34), the initial values for B, C and μ can be calculated by solving the following sytem of equations.

$$\mu_i = \frac{1}{l_i}\sum_{j=1}^{l_i}\log N_{i,j} = B + \frac{\mu}{\log\Delta\sigma_i - C}, \quad i = 1, 2, 3. \tag{3.36}$$

Fortunately, the system (3.36) has an explicit solution given by

$$B = \frac{\mu_1\Big[\mu_2(-S_1+S_2)+\mu_3(S_1-S_3)\Big]+\mu_2\mu_3(-S_2+S_3)}{\mu_3(S_1-S_2)+\mu_1(S_2-S_3)+\mu_2(-S_1+S_3)}, \tag{3.37}$$

$$C = \frac{\mu_1 S_1(S_2-S_3)+\mu_3(S_1-S_2)S_3+\mu_2 S_2(-S_1+S_3)}{\mu_3(S_1-S_2)+\mu_1(S_2-S_3)+\mu_2(-S_1+S_3)}, \tag{3.38}$$

$$\mu = -\frac{(\mu_1-\mu_2)(\mu_1-\mu_3)(\mu_2-\mu_3)(S_1-S_2)(S_1-S_3)(S_2-S_3)}{\Big[\mu_3(-S_1+S_2)+\mu_2(S_1-S_3)+\mu_1(-S_2+S_3)\Big]^2}, \tag{3.39}$$

where $S_i = \log \Delta\sigma_i$.

3.4.2 Estimation of the Weibull parameters

Once the geometrical parameters have been estimated, it is possible to define the Weibull random variable by $x_i = (\log N_i - B)(\log \Delta\sigma_i - C)$. Within this dissertation, two methods are applied in order to estimate the Weibull parameters a, b, c corresponding to the sample x_i, see Section 2.3. The PWM introduced by Greenwood et al. [74], [80] and completely formulated for the three-parameter Weibull distribution $W(a, b, c)$ by Toasa and Ummenhofer in [78]. The MLE method suggested by Gupta and Panchang in [72].

3.5 Consideration of the runouts

From the statistical point of view, including the runouts into the fatigue data analysis can provide valuable information regarding the quantiles of the Wöhler curves. Samples which cointain failures and runouts are called censored or truncated, and they are widely used in life testing. There exists several parameters which determine the type of censoring to apply in a lifetime experiment. Basically, in a typical lifetime test, n specimens are tested and as each failure occurs, the corresponding time is noted. Additionally, at some preestablished time T or after some pre-determined fixed number of failures m, the fatigue test ends. In both cases, the registered information is obtained from two types of data: those which come from the m specimens that have failed before the time T and those from the $n - m$ specimens that survived

beyond the time T. On the one hand, when the time T is fixed, m is a random variable and the censoring is said to be of Type-I. On the other hand, when m is fixed and the time of termination is random, the censoring is said to be of Type-II.

Under this kind of considerations, several methods have been proposed to include censored data in lifetime testing analysis. Among these proposed methods are the works of A. Cohen done for the normal and exponential distributions [101] and for multi-censored sampling in a Weibull distribution [102], the quasilinearization of the Weibull equations of Wingo [103], the MLE method for the Weibull distribution of Balakrishnan and Kateri [104], the censoring plans of Type-II for the Weibull distribution of Balakrishnan et al [105], the identification of different causes of failure in life tests of Balasooriya and Low [106], the estimation for censoring Type-II in a Weibull distribution of Wu and Kus [107]. A detailed description of the most relevants characteristics of the censoring Type-I and Type-II is presented in the Subsection 4.2.

3.5.1 Likelihood function of the Weibull distribution for censored samples

During the fatigue testing of steel structures it is usual to establish as censoring criterion a predetermined number of cycles N_l, and the specimens that endure without failing until N_l, are classified as runouts. Since the number of cycles N_l can be also considered as the preestablished censoring time T, in the case of fatigue experiments the censoring criterion is of Type-I.

In Type-I censoring, the likelihood functions for any statistical distribution and particularly for the Weibull distribution are given in the following definitions [108], [109].

Definition 11 (Likelihood function for censored samples)**.** *Let $x_1, x_2, \ldots, x_n$ be n data points corresponding to the random variables $X_1, X_2, \ldots, X_n$. Let m be the number of points corresponding to failures and x_l the point corresponding to the preestablished time of termination. The likelihood function L is the joint probability density function evaluated in $x_1, x_2, \ldots, x_n$ and it is given by*

$$L = \frac{n!}{(n-m)!}\left[\prod_{i=1}^{m} f(x_i)\right] \cdot \left[1 - F(x_l)\right]^{n-m}. \tag{3.40}$$

Definition 12 (Likelihood function of the Weibull distribution for censored samples)**.** *Let $x_1, x_2, \ldots, x_n$ be n data points corresponding to a three-parameter Weibull distribution $W(a, b, c)$. Let m be the number of points corresponding to failures and x_l the point corresponding to the preestablished time of termination. The likelihood function*

is given by

$$L = \frac{n!}{(n-m)!}\left[\prod_{i=1}^{m}\frac{c}{b}\Big(\frac{x_i-a}{b}\Big)^{c-1}\exp\Big[-\Big(\frac{x_i-a}{b}\Big)^{c}\Big]\right]\cdot\Big[1-F(x_l)\Big]^{n-m}. \quad (3.41)$$

As in the Definition 8 in order to estimate the Weibull parameters it is more convenient to consider the logarithm of the likelihood function.

Corollary 1 (Log-Likelihood function of the Weibull distribution for censored samples)**.** *Let $x_1, x_2, \ldots, x_n$ be n data points corresponding to a three-parameter Weibull distribution $W(a,b,c)$. Let m be the number points corresponding to failures and x_l the point corresponding to the preestablished time of termination. The log-likelihood function is given by*

$$\begin{aligned}\mathcal{L} &= \log(K) + (n-m)\log\big[1-F(x_l)\big] + \sum_{i=1}^{m}\log\left(\frac{c}{b}\right)\\ &\quad +(c-1)\sum_{i=1}^{m}\log\left(\frac{x_i-a}{b}\right) - \sum_{i=1}^{m}\left(\frac{x_i-a}{b}\right)^{c}, \end{aligned} \quad (3.42)$$

where K is a constant given by $K = \frac{n!}{(n-m)!}$.

Proof. Applying logarithmus on Equation (3.40) leads to

$$
\begin{aligned}
\mathcal{L} &= \log(K) + \log\left[\prod_{i=1}^{m} f(x_i)\right] + \log\left[1 - F(x_l)\right]^{n-m} \\
&= \log(K) + \sum_{i=1}^{m} \log\left[f(x_i)\right] + (n-m)\log\left[1 - F(x_l)\right] \\
&= \log(K) + (n-m)\log\left\{\exp\left[-\left(\frac{x_l - a}{b}\right)^c\right]\right\} \\
&\quad + \sum_{i=1}^{m} \log\left\{\frac{c}{b}\left(\frac{x_i - a}{b}\right)^{c-1} \exp\left[-\left(\frac{x_i - a}{b}\right)^c\right]\right\} \\
&= \log(K) - (n-m)\left(\frac{x_l - a}{b}\right)^c \\
&\quad + \sum_{i=1}^{m}\left[\log\left(\frac{c}{b}\right) + (c-1)\log\left(\frac{x_i - a}{b}\right) - \left(\frac{x_i - a}{b}\right)^c\right] \\
&= \log(K) - (n-m)\left(\frac{x_l - a}{b}\right)^c \\
&\quad + \sum_{i=1}^{m} \log\left(\frac{c}{b}\right) + (c-1)\sum_{i=1}^{m} \log\left(\frac{x_i - a}{b}\right) - \sum_{i=1}^{m}\left(\frac{x_i - a}{b}\right)^c. \qquad (3.43)
\end{aligned}
$$

□

Considering in Equation (3.43) that

$$
-(n-m)\left(\frac{x_l - a}{b}\right)^c = -\sum_{i=m+1}^{n}\left(\frac{x_l - a}{b}\right),
$$

for the runouts, it leads to

$$
\mathcal{L} = \log(K) + \underbrace{\sum_{i=1}^{m} \log\left(\frac{c}{b}\right) + (c-1)\sum_{i=1}^{m} \log\left(\frac{x_i - a}{b}\right)}_{\text{Failures}} - \underbrace{\sum_{i=1}^{n}\left(\frac{x_i - a}{b}\right)^c}_{\text{Failures} \cup \text{Runouts}}, \qquad (3.44)
$$

which is the log-likelihood equation proposed in [35] and [77]. Particularly for the

runouts, in the third sum of Equation (3.44) the variable x_i takes the value corresponding to the preestablished censoring time x_l.

Similarly to the Section 2.3.2, the log-likelihood given by Equation (3.44) can be maximized by applying the method of Gupta and Pachang [72] in order to determine the Weibull parameters a, b, c.

3.5.2 Left censored or truncated Weibull distribution

A truncated distribution is not but a conditional distribution, where the random variable X remains in a restricted range of values. Usually, truncated distributions occur when the random variable is lifetime or durability. In the particular case of fatigue data, the runouts belong to a censored sample. Censored samples are those whose data lie in a restricted sample space, these data can be identified but can not be measured.

A fatigue runout is a pair of the type $(N_l, \Delta\sigma)$, where the value N_l is precisely the value in which the test stops but the value N in which the sample would fail was not measured, but it can be estimated. Therefore, its estimator $E(N) = N_{ro}$ lies in the interval $]N_l, \infty[$.

Denoting the censoring criterion corresponding to the limit number of cycles as N_l, the normalized random variable of the left truncated Weibull model will be:

$$x_l = (\log N_l - B)(\log \Delta\sigma - C). \tag{3.45}$$

Now, let the left truncated density function of x_l be

$$f_{LT}(x \mid X > x_l) = \frac{f(x)}{1 - F(x_l)}, \tag{3.46}$$

where $F(x)$ is the CDF of x. By definition, the CDF of a left truncated density function is the result of integrating Equation (3.46) as follows

$$F_{LT}(x) = \int_{x_l}^{x} \frac{f(t)}{1 - F(t)}\,\mathrm{d}t = P(X \geq x_l). \tag{3.47}$$

In this particular case the CDF of a left truncated three-parameter Weibull distribution $W(a, b, c)$ is given by

$$F_{LT}(x \mid a, b, c, x_l, \infty) = 1 - \exp\left[-\left(\frac{x_l - a}{b}\right)^c - \left(\frac{x - a}{b}\right)^c\right], \qquad a \leq x_l \leq x < \infty \tag{3.48}$$

and the expected value of the rth order statistic of a sample of size q from an uniform distribution $U(0,1)$ is given by $r/(q+1)$.

Then, the censored value x_l from Equation (3.45) can be replaced by the solution of the equation

$$1 - \exp\left[-\left(\frac{x_l - a}{b}\right)^c - \left(\frac{x - a}{b}\right)^c\right] = \frac{r}{q+1}, \tag{3.49}$$

where q is the number of runouts which have identical values of stress range $\Delta\sigma$ and limit number of cycles N_l. Thus, the estimated values of x are given by

$$x = a + b\left[\left(\frac{x_l - a}{b}\right)^c - \log\left(1 - \frac{r}{q+1}\right)\right]^{\frac{1}{c}}, \qquad r = 1, 2, \ldots, q. \tag{3.50}$$

Since $x = (\log N - B)(\log \Delta\sigma - C)$, the estimation of the fatigue lifetime from a runout can be expressed by

$$E(N) = N_{ro} = \exp\left[\frac{x}{\log \Delta\sigma - C} + B\right], \tag{3.51}$$

where x is given by Eq. (3.50).

3.5.3 Censored or truncated fatigue data

The runouts are a kind of truncated fatigue data which can provide useful information to improve the representation of the Wöhler curves. Hereafter, the steps to include the runouts in the modelling of the Wöhler curves based on a three-parameter Weibull distribution $W(a, b, c)$ are presented.

1. Estimate the geometric parameters B and C by solving the Equation (3.35). Consider only the experimental data corresponding to failures.
2. Estimate the Weibull parameters a, b, c by applying the PWM method or the MLE method. Consider only the experimental data corresponding to failures.
3. Estimate the fatigue lifetime from the runouts by applying Equation (3.51).
4. Estimate the model parameters as in steps 1 and 2 considering jointly the data from failures and the expected values obtained from step 3.
5. Repeat steps 3 and 4 until convergence of the process.

3.6 Damage measures

3.6.1 State of the art

The evaluation of fatigue damage is crucial in engineering because fatigue is becoming determinant in design and it is frequently the cause of failure of structural components. Fatigue failure is the culmination of a progressive process that occurs when a certain damage level has been attained. The speed of this process depends on the microstructural characteristics of the material and increases with the number of cycles N, the stress range $\Delta\sigma$ and the stress level in every cycle [35]. Additionally, in the models based on fracture mechanics other factors, such as the load sequence, type of loading, crack closure, overloads, local plastification and type of material are also considered. Within this dissertation the damage measure based on the fracture mechanics principles and on the multiaxial fatigue is not considered. However, the damage measures for which the probabilities of failure can be calculated are taken into account.

As it has been shown in Section 1.5 there are several approaches to model the Wöhler curves and there are even more alternatives to model and measure the damage accumulation [110].

According to the model of Palmgren-Miner [17], [18], which is known as linear cummulative damage hypothesis [22], a structure presents a failure if

$$D = \sum_{i=1}^{n} \frac{n_i}{N_i} = 1, \tag{3.52}$$

where

D: Damage

n_i: Load cycles of type i

N_i: Number of cycles to failure

This linear model measures the damage in a simple way, which assumes a constant work absorption per cycle and a characteristic amount of work absorved at failure. In other words, applying n_i times one cycle with stress amplitude $S_{a,i}$ and a corresponding fatigue life N_i is equivalent to consuming a portion n_i/N_i of the fatigue life, and the failure occurs when the 100% of the fatigue life is consumed.
Therefore, the energy accumulation leads to the linear summation of cycle ratio or damage given by Equation (3.52). Palmgren did not give a physical derivation

of the model but he adopted the most simple assumption for the fatigue damage accumulation [22].

The Palmgren-Miner model and the models derivated from it are still used in most standards related to fatigue design of structures. Unfortunatelly, they do not allow any statistical evaluation of the damage. Since the material is not homogeneous, which means that it has random imperfections, it may be considered that exists an initial random damage state. Therefore, after loading, the subsequent damage state will be also a random variable, which has to be analysed with statistical methods [35].

Because of its inherent deficiencies, life prediction based on Palmgren-Miner rule is often unsatisfactory. In fact, some experimental results have shown values of $D > 1$ for low-to-high loading sequence and $D < 1$ for high-to-low loading sequence [110]. Moreover, it has been shown that statistically similar variable amplitude load histories can give significantly different fatigue lives, whereas the Miner rule predicts the same life [22].

Some of the alternative models to measure the fatigue damage are briefly described below.

The two-stage linear damage approach proposed by Grover [111] and based on the work of Langer [112] has the same formulation. However, it improves the linear damage rules, since it considers two separate stages in the fatigue damage process of constant amplitude stressing:

Damage due to crack initiation, $N_1 = \alpha N_f$

Damage due to crack propagation, $N_2 = (1 - \alpha) N_f$

In each stage the linear damage rule is applied.

The cummulative fatigue damage model proposed by Shanley [113], which is based on the crack growth concept, considers that the crack growth rate varies with the applied stress level in either a linear or an exponential manner. The formulation of this model is based on the dislocation theory and the macroscopic elasto-plastic theory, and it is given by

$$\frac{\mathrm{d}a}{\mathrm{d}N} = C f(\sigma) a, \tag{3.53}$$

where

a: Crack length

C: Material constant

$f(\sigma)$: Function which depends on the material and loading configuration

Other models based on the crack growth concept are those proposed by Valluri [114], [115], Scharton and Crandall [116].

The damage curve approach proposed by Manson and Halford is based on the phenomenological recognition and describes an effective crack growth [117]. This model is represented by

$$a = a_o + (a_f - a_o)r^q, \tag{3.54}$$

where

a_o: Initial crack length ($r = 0$)

a: Actual crack length

a_f: Final crack length ($r = 1$)

q: Function of the load cycles N and given by $q = BN^\beta$, where B and β are material constants.

Damage is then defined as

$$D = \frac{a}{a_f}.$$

The hybrid theory proposed by Bui-Quoc et al. [118] unifies two theories regarding the cummulative fatigue damage: the theory for stress-controlled fatigue and the theory for strain-controlled fatigue.

There are also theories based on the crack growth concept, these theories were accepted since it was recognized that cracks are directly related to damage, and since it was possible to measure small cracks under $1\mu m$. One of these theories was proposed by Wheeler [119], and it assumes that the crack growth rate is related to the interaction of crack-tip plastic zones under the residual compressive stresses created by overloads. These theories overcome the limitations of the Palmgren-Miner rule, but they require more complicated mathematical considerations.

The relationship between the hysteresis energy and the fatigue behavior proposed by Inglis in 1927 is the base of some damage theories [120]. One of the main contribution has been determining that a damage parameter based on energy can unify the damage caused by different types of loading such as thermal cycling, creep, and fatigue. Afterwards, in conjunction with Glinka's rule it is possible to analyze the damage accumulation of notched specimens. The energy based damage models can consider mean stress and multiaxial loads as well.

The most actual approaches to model fatigue damage are based on continuum mechanics. These theories consider the mechanical behavior of a deteriorating medium at the continuum scale and they are based on the orginal concepts of Kachanov [121] and Rabotnov [122] which deal with creep damage problems.

More than fifty fatigue damage models are described in the paper of A. Fatemi and L. Yang [110].

Within this dissertation the fatigue has been considered as a random variable which is an ongoing state damage process that depends on the relationship of the load cycles and the applied stress ranges. At the beginning, it is asummed that the initial damage of the specimens is zero, despite the imperfections from the fabrication of the material. Aferwards, this state damage is affected by the applied loading and it becomes one at the fatigue failure. Between the begining of the fatigue test and the failure of the specimen, the damage condition is considered as a random variable which is dealt in a probabilistic way through the normalization.

3.6.2 Normalization

Statistical normalization is a method used to deal with the errors of experimental data. Particularly, in the case of fatigue tests data, this method allows to reduce data coming from different stress levels and ranges to the same stress level and range. In other words, grouping the data into the same statistical distribution.
The estimation process of the parameters and the understanding of the random behavior of the fatigue are perfomed in a better way after normalization.

Theorem 5 (Normalization or standard score)**.** *Let X be a normal random variable with mean μ and variance σ^2. Then the random variable defined by*

$$U = \frac{X - \mu}{\sigma}, \tag{3.55}$$

follows a dimensionless standard normalized distribution with mean $\mu_U = 0$ and variance $\sigma_U = 1$.

Proof. The expected value of U is given by

$$\begin{aligned} E(U) &= E\left[\frac{X-\mu}{\sigma}\right] \\ &= \frac{1}{\sigma}E\Big[E(X) - \mu\Big] \\ &= 0. \end{aligned}$$

Considering that $V(a+bX) = b^2 V(X)$, the variance of U is given by

$$\begin{aligned} V(U) &= V\left(\frac{X-\mu}{\sigma}\right) \\ &= V\left(-\frac{\mu}{\sigma} + \frac{1}{\sigma}X\right) \\ &= \frac{1}{\sigma^2}V(X) \\ &= 1. \end{aligned}$$

□

Based on Theorem 1 the following corollary is obtained.

Corollary 2. *Let X be a random variable which follows a three-parameter Weibull distribution $W(a,b,c)$ with mean μ and variance σ^2.*
Then the random variable defined by

$$U = \frac{X-\mu}{\sigma}, \tag{3.56}$$

follows a dimensionless three-parameter Weibull distribution $W(\widehat{a},\widehat{b},\widehat{c})$, whose parameters depend on the shape parameter c and are given by

$$\begin{aligned} \widehat{a} &= \frac{a-\mu}{\sigma} \\ &= -\frac{\Gamma\left(1+\frac{1}{c}\right)}{\left[\Gamma\left(1+\frac{2}{c}\right) - \Gamma^2\left(1+\frac{1}{c}\right)\right]^{\frac{1}{2}}}, \end{aligned}$$

$$\begin{aligned} \widehat{b} &= \frac{b}{\sigma} \\ &= \frac{1}{\left[\Gamma\left(1+\frac{2}{c}\right) - \Gamma^2\left(1+\frac{1}{c}\right)\right]^{\frac{1}{2}}}, \end{aligned}$$

$$\widehat{c} = c.$$

The relevance of the Corollary 2 is given by the fact that all of the Weibull distributions which have the same shape parameter c can be transformed into the same distribution by applying the transformation (3.56). From the fatigue's point of view it means that two specimens subject to two different stress ranges and with two different lifetimes can be compared if their fatigue data $(\Delta\sigma, N)$ belong to the same distribution.

Once, the Weibull parameters a, b and c are estimated, the normalization can be made by applying the normalizing variable

$$U = \frac{(\log N - B)(\log \Delta\sigma - C) - a}{b}, \tag{3.57}$$

which follows a three-parameter Weibull distribution $W(0, 1, c)$ in Equation (3.30).

Definition 13 (Damage equivalence)**.** *Two specimens, one subject to $\Delta\sigma_1$ during N_1 cycles, and another one subject to $\Delta\sigma_2$ during N_2 have suffered the same damage if their corresponding normalized values U are identical. It means if the equality*

$$U_1 = \frac{(\log N_1 - B)(\log \Delta\sigma_1 - C) - a}{b} = \frac{(\log N_2 - B)(\log \Delta\sigma_2 - C) - a}{b} = U_2 \tag{3.58}$$

is fulfilled.

Note that the normalization U is valid only for load histories having the same stress level. In case of consideration of experimental data obtained from different stress levels, another normalization should be defined [35].

The damage of a structural component can be measured based on different criteria such as its maximum crack size, number of cycles to failure or probability of failure. A damage measure is an indicator of the deterioration that a structural component has suffered during its service life including its fabrication (random initial damage)[35].
Thus, there are different alternatives and different concepts which can be applied to define a damage measure. However, there are some requirements that a damage measure has to satisfy in order to be suitable.

1. **Increasing with damage:** The damage measure has to be directly proportional to the damage; it means a larger damage corresponds to a higher measure.
2. **Interpretability:** The measure should give clear and usefull information about how far the specimen is from failure.
3. **Dimensionless:** A damage measure must be dimensionless.

4. **Fixed a determined range:** The domain of the damage measure has to be previously defined, independently of the loading.

5. **Statistical distribution:** A damage measure is more valuable if it has a related statistical distribution. So that, it is possible to determine the corresponding probability of failure at the actual stage.

Considering these properties, it seems convenient to propose as a damage measure the random variable U presented in Definition 13. It is not complicated to realize that the variable U satisfies the properties mentioned above and it can be used for any stress level and load history.
An important additional property of the damage measure U can be described as follows:

"If two specimens have the same accumulated damage, then they have the same probablity of failure."

And this property is the basis of the damage accumulation assessment applied in this research. This holds, because U follows a Weibull distribution which depends only of the shape parameter c, see Corollary 2.

3.7 Damage accumulation based on the Weibull distribution

The estimation of the fatigue life of a structural component is a very complex problem. In the real service period, a civil engineering structure is subject to cyclic loads while the stress range and the stress level change continuosly and randomly. The fatigue life depends on the accumulated damage that the structure already has. Therefore, it is necessary to have a damage accumulation model which allows to estimate the risk or probability of failure. This model has to be reliable but not too complex in order to be applied on regulations and design.

In this section an alternative damage accumulation model is presented, and it is based on Wöhler curves and the damage equivalence measure defined in the Subsection 3.6.2. On the one hand, this alternative is a mathematical simplification of the reality, which assumes that the stress range $\Delta\sigma$ and the stress level are kept constant. On the other hand, it does not consider the plasticity influence, overloads or additional interaction process.

The basic concept or tool is the normalization which defines the equivalence in terms of damage or probability of failure between two fatigue states. These fatigue states depend on different stress ranges but on the same stress ratio. The damage equivalence applied in this research has been already defined and given in Equation (3.58). Additionally, according to the Equation (3.30) the Wöhler curves based on the Weibull model describe the number of cycles N to fail under a given stress range $\Delta\sigma$ with the same probability p. These facts allow to consider the Wöhler curves obtained by applying the Weibull model also as a probabilistic representation of the damage state of a specimen as it is shown in Figure 3.10.

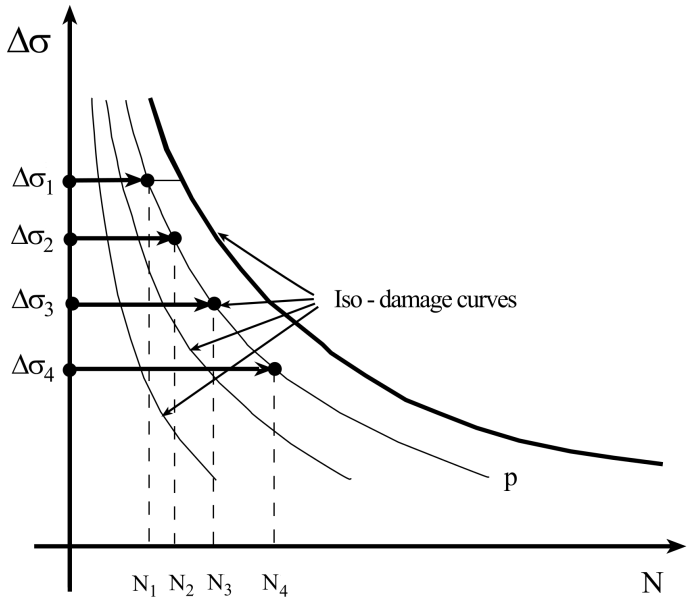

Figure 3.10: Iso-damage Wöhler curves - Curves describing damage states. Representation of four different load histories at constant stress levels which lead to the same damage [35].

3.7.1 Accumulated damage after a constant stress range test

Applying again the concept of normalization, the case of multiple steps loading can be considered as an extension of the single loading test under a constant stress range. In fact, the damage obtained from a single step loading can be also obtained by an equivalent multiple steps loading. Generally, a specimen can bear the same damage through different loading trajectories, which can be determined by one step fatigue test or by multiple tests at different constant stress ranges, see Figure 3.11.

Definition 14 (Steps loading equivalence)**.** *Consider the two following fatigue tests performed under constant stress level.*

1. *A constant load $\Delta\sigma_r$ is applied during N_r cycles.*
2. *A serie of constant loads $\Delta\sigma_1, \Delta\sigma_2, \ldots \Delta\sigma_j$ such that $\Delta\sigma_i \leq \Delta\sigma_{i+1}$ are applied consecutively during $N_1, N_2, \ldots, N_j$ respectively.*

The accumulated damage or the probability of failure of the test specimen is the same under both of the fatigue tests if the pairs $(\Delta\sigma_r, N_r)$ and $(\Delta\sigma_j, N_j)$ belong to the same quantil on the S-N field. See Figure 3.11.

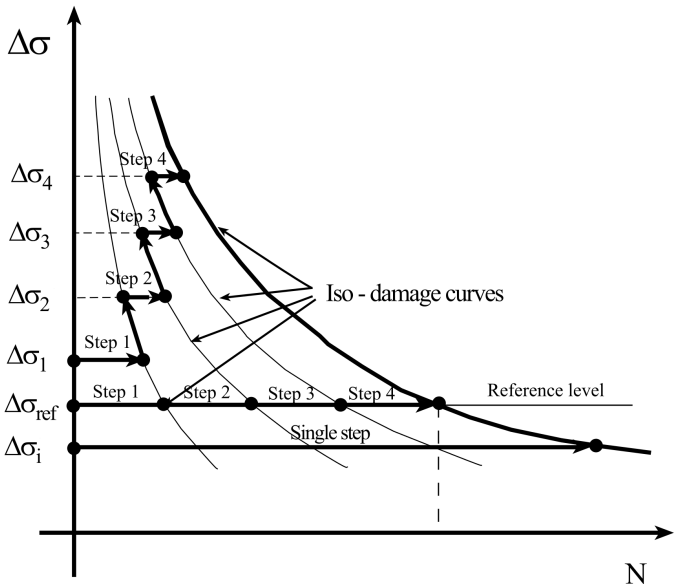

Figure 3.11: Iso-damage Wöhler curves of multiple step loading - Curves describing damage states. Representation of four load histories at constant stress levels leading to the same damage [35].

3.8 Subsequent fatigue tests of the runouts

The presence of runouts from fatigue experiments is a common situation in most of fatigue testing programs. The influence of runouts in the statistical data analysis of fatigue experiments has been already considered by some researchers. In [57] the authors consider the fatigue life as a normal distributed random variable and asumme the existence of the fatigue limit. In [58], the fatigue life is assumed to

follow a two parameter Weibull distribution, however the relationship between the stress range $\Delta\sigma$ and the load cycles N is kept linear. In [56], the authors mentioned that for simplicity they consider a log normal distribution for the fatigue life, but they suggested also to consider the Weibull distribution for this task. Recently, new models have been proposed to consider the runouts. In [123], the authors proposed a six-parameter model which is related to the Forman-Mettu fatigue crack growth rate. This model depicts a curvature which describes a smooth transition between the finite life and the infinite life regions and the existence of the fatigue limit is assumed. The corresponding parameters are estimated by applying the MLE method. In [124], a bilinear model based on the Monte Carlo simulation and on the MLE method is suggested. In this model, the transition between the finite life and the infinite life regions is given by a knee point which is established in advance. This model asummes that the fatigue limit is a random variable as well. Moreover, considering constant or variable amplitude loadings is possible by applying this model. Additional references related to censored sampling are mentioned in Section 3.5.

Nevertheless, as it has been seen in Section 1.5, the model of Basquin given by Equation (1.5), which is applied in most fatigue design standards does not consider the influence of the runouts in the estimation of the fatigue strength curves. These curves are used to design structures which do not present a fatigue failure during their lifetime. Fortunately, the shortcoming of no using the information from the runouts can be overcomed by applying the methodology explained in the Section 3.5. The next question addressed in this research is the following:

Is it possible to re-test the runouts under a different stress range and consider the obtained results in order to improve the modeling of the Wöhler curves?

Based on the Weibull model presented in this chapter the answer is yes.
In addition to allow evaluation of runouts, the Weibull model also permits to quantify the damage accumulation of a runout after a fatigue test. This quantification is fundamental and should be done in order to perform subsequent fatigue tests with runouts, see the Equation (3.57).

In order to include the subsequent fatigue tests from runouts the steps described below must performed.

3.8.1 Estimation of the hypothetical number of cycles

This step shows a good application of the damage equivalence given by Definition 13. Consider that a runout was obtained from a fatigue test performed under a

stress range $\Delta\sigma_1$ during a number of cycles N_1. Afterwards the next test will be performed under a higher stress range $\Delta\sigma_2$. Then, based on the Equation (3.58) the hypothetical number of cycles denoted by $\widehat{N_2}$ or N_{acc} can be defined by

$$\widehat{N}_2 = \exp\left[\frac{(\log N_1 - B)(\log \Delta\sigma_1 - C)}{\log \Delta\sigma_2 - C} + B\right]. \tag{3.59}$$

The value $\widehat{N}_2$ represents an estimation of the number of cycles that the specimen corresponding to the runout could have endured without failing during a fatigue test performed under a stress range $\Delta\sigma_2$. The damage accumulation of the runouts $(\Delta\sigma_1, N_1)$ and $(\Delta\sigma_2, \widehat{N_2})$ are identical, see Figure 3.12.

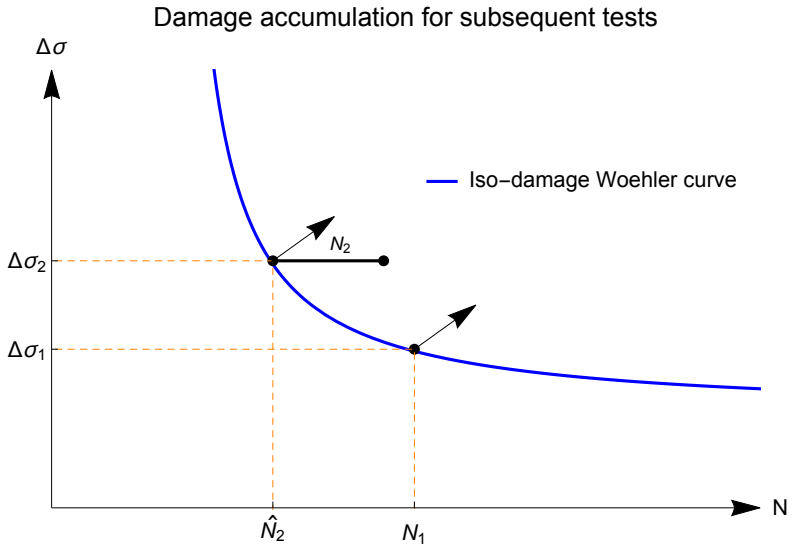

Figure 3.12: Damage accumulation for a retest of a runout under a higher loading - Both runouts have the same probability of failure.

By and large, if n subsequent fatigue tests are performed as it was described in the Definition 14, it is possible to determine the hypothetical number of cycles for every stress range $\Delta\sigma_i$ by using the recursive formula given by

$$\widehat{N}_{i+1} = \exp\left[\frac{(\log N_i - B)(\log \Delta\sigma_i - C)}{\log \Delta\sigma_{i+1} - C} + B\right], \qquad i = 1, 2, \ldots, n-1. \tag{3.60}$$

3.8.2 Second fatigue test on a runout

After performing a fatigue test under a stress range $\Delta\sigma_1$, a subsequent fatigue test can be performed through the application of a higher stress range $\Delta\sigma_2$. By applying the Equation (3.59) an estimation of the number of cycles $\widehat{N}_2$ that the runout could have endured without failing during a fatigue test under $\Delta\sigma_2$ can be calculated. If the specimen fails after the second test, the number of cycles N_2 is obtained.
Therefore, in the modelling of the Wöhler curves, the new pair of data corresponding to a failure from a re-tested runout given by

$$(\Delta\sigma_2, \widehat{N}_2 + N_2), \tag{3.61}$$

can be considered.

3.9 Wöhler curves modelling based on the experimental data classification

Based on fatigue experiments it has been seen that it is possible to obtain two kinds of experimental data: failures and runouts. Moreover, these data can be obtained from the first test or from a subsequent test. This situation demands to stablish a suitable methodology to classify the experimental fatigue data that will be used for modelling the Wöhler curves. As a matter of fact, according to the available fatigue data, it is possible to obtain three types of data groups:

F: Only failures are available

F-RO: Failures and runouts are available

F-RO-RT: Failures, runouts and suqsequent retests are available

Afterwards, the obtained results from each clasification should be evaluated and compared. For applications on experimental fatigue data see the Chapter 4.

3.9.1 Modelling based only on fatigue failures

This is the most simple case which takes into account only the fatigue failures from the first test in order to model the Wöhler curves. Actually, the official norms or standards consider only this case.

In the case of the model based on the Weibull distribution given by Equation (3.30), the Wöhler curves can be determinated when the parameters of the model

are estimated as it has been shown in Section 3.4. In other words, there are two steps to be performed in order to model the Wöhler curves based on fatigue failures.

1. Estimation of the geometrical parameters B and C as explained in Subsection 3.4.1
2. Estimation of the Weibull parameters a, b, c by applying the PWM or the MLE method given in the Section 2.3

3.9.2 Modelling based on fatigue failures and runouts

This is the first advantage of the model based on the Weibull distribution. As it has been seen in Section 3.5, the runouts are a kind of truncated fatigue data which can provide useful information to improve the representation of the Wöhler curves. Hereafter, the steps to include the runouts influence can be described as follows.

1. Estimate the geometrical parameters B and C by solving the Equation (3.35). Consider only the experimental data corresponding to fatigue failures.
2. Estimate the Weibull parameters a, b, c by applying the PWM or the MLE method given in Subsections 2.3.1 and 2.3.2 respectively. Consider only the experimental data corresponding to fatigue failures.
3. Estimate the expected lifetime N_{ro} corresponding to runouts by applying the method described on Subsection 3.5.2
4. Estimate the model parameters as in steps 1 and 2 considering jointly the data from fatigue failures and the expected values obtained from step 3.
5. Repeat steps 3 and 4 until convergence of the process.

3.9.3 Modelling based on fatigue failures, runouts and retested specimens

This case represents the biggest benefit of applying the model based on the Weibull distribution. Considering all the experimental data together: fatigue failures, runouts and retested specimens, allows to have more accuracy and confidence in the estimated results. Moreover, the characteristics of the subsequent tests depend on the results obtained from the runouts of the previous tests.

The following steps should be performed in order to include the data from fatigue failures, runouts and subsequent tests of runouts.

1. Estimate the geometrical parameters B and C by solving the Equation (3.35). Consider only the experimental data corresponding to fatigue failures
2. Estimate the Weibull parameters a, b, c by applying the PWM or the MLE method given in Subsections 2.3.1 and 2.3.2 respectively. Consider only the experimental data corresponding to fatigue failures
3. Determine the expected lifetime N_{ro} of the runouts from the first test by applying the method described on Subsection 3.5.2
4. Estimate the geometrical parameters B and C. Consider the experimental data corresponding to fatigue failures and to runouts whit their expected lifetime determined in the point 3.
5. Estimate the Weibull parameters a, b, c. Consider the experimental data corresponding to fatigue failures and to runouts
6. If there are runouts which were re-tested. Calculate the equivalent number of cycles $\widehat{N}_2$ corresponding to the subsequent fatigue test by applying Equation (3.59). Then the relative number of cycles is given by $N_2^* = \widehat{N}_2 + N_2$ where the second term is the number of cycles registered during the subsequent test perfomed under a stress range $\Delta\sigma_2$
7. Estimate the geometrical parameters B and C. Consider all of the experimental data from fatigue failures, runouts and retested runouts.
8. Estimate the Weibull parameters a, b, c. Consider all of the experimental data as in step 7 as well.
9. Repeat from step 3 until convergence of the process.

3.10 General procedure and flowchart for the analysis of fatigue data

Considering the three cases described in the previous section it is mandatory to determine a procedure or an algorithm which describes the main steps to be done in order to model the Wöhler curves based on any kind of fatigue data [125].

Applying the following notation allows to identify individually every pair $(\Delta\sigma, N)$ obtained from the fatigue tests.

$$(\Delta\sigma, N)_{s,t,f}$$

where

s: Number which individually identifies one specimen,

t: Number of the performed fatigue experiment on the specimen s,

f: Binary variable which describes the fatigue failure occurence. 1 means that the specimen has failed and 0 means that a runout has been obtained.

Based on the considerations made above, a general procedure to model the Wöhler curves can be described as it can been seen in the flowchart on Figure 3.13.

The methodology presented and proposed in this chapter to model the Wöhler curves is consistent from the statistical and physical points of view. Additionally, the innovative characteristic of the model is, that more data are available for the statistical analysis, since the run-outs and their retests are also considered. Hence, this methodology represents a general alternative for analysing and evaluating fatigue data.

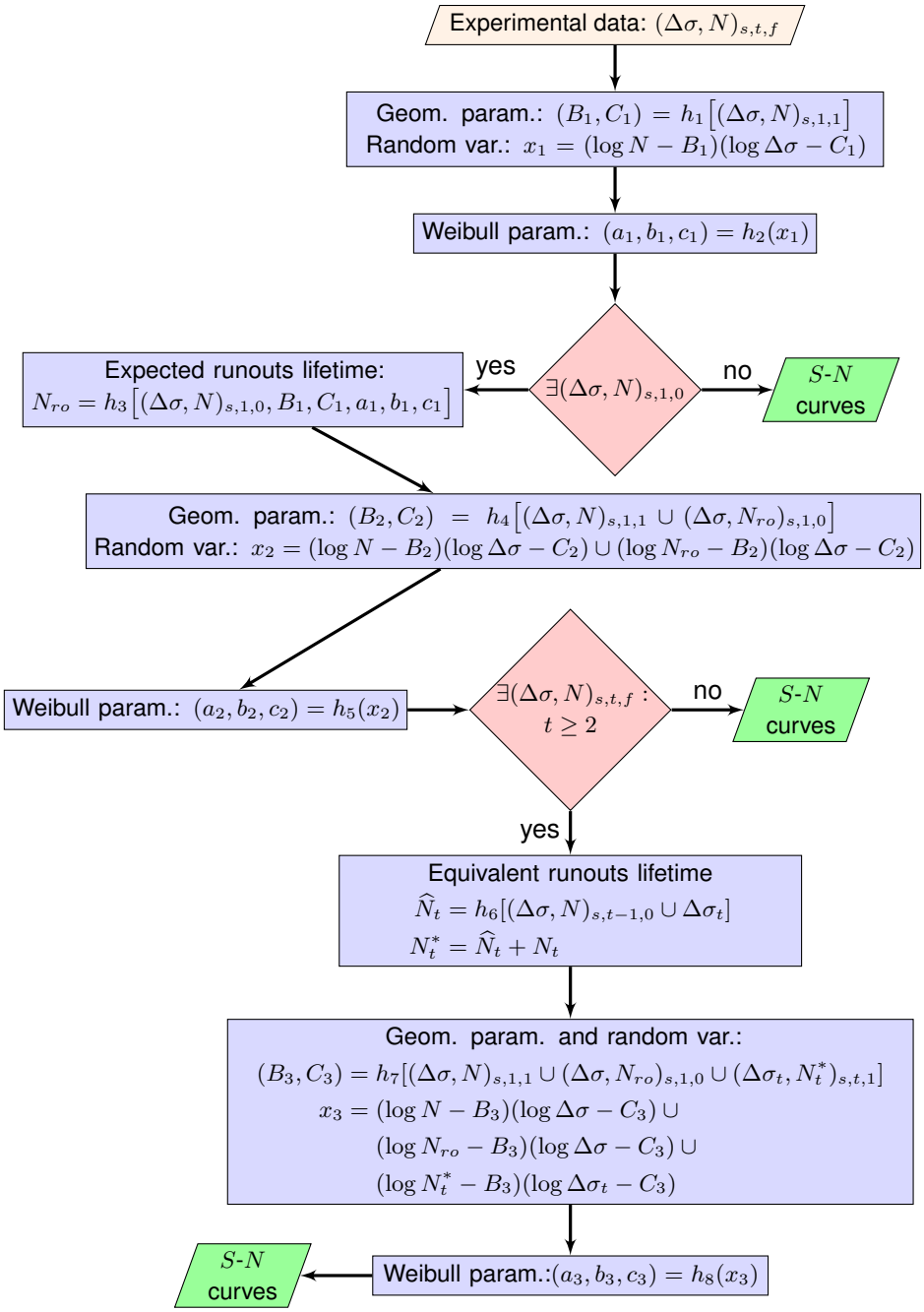

Figure 3.13: Flowchart for the analysis of fatigue data - Procedure for modelling the Wöhler curves.

Chapter 4

Fatigue tests and the application of the Weibull model

> La curiosidad lleva a la experimentación, y ésta a los resultados. Pobre del hombre sin curiosidad.
>
> *Mr. Lasky*

Every proposed mathematical model that pretends to describe a physical law has to be verified by experimental data and simulations. For this purpose, the first step is performing an experimental design which describes all of the characteristics or properties of the fatigue experiment to be considered. These characteristics can be quantitave or qualitative. The inferencial process from lifetime data depends on how these experimental data have been compiled.

In most of cases, the fatigue tests on steel welded structures are performed under constant amplitude loadings, eventhough the real laodings are variable. The main goal of these tests is estimating the fatigue strenght of a structure. This fact helps engineers to establish design stress levels below which failure is unlikely to occur during the design life of the structure. For this purpose, fatigue tests are performed on representative specimens subjected to a representative level(s) of cyclic loads. The especimens are characterized by specific details which usually are defined in the standards or by a particular geometry given by the engineers. Afterwards, based on the fatigue data it is possible to make inferences about a real structure. These inferences should consider the influence of several factors such as amplitude of the constant loading, type of spectrum, mean stress, tensile strength,

specimen size, material, or production parameters. By simplifying and idealizing the test conditions it is possible to vary one or few factors and state their effects [126]. From the statistical point of view, the suitable way to analyse or evaluate the influence of the independent factors mentioned above is performing an analysis of variance ANOVA. In the particular case of fatigue of steel structures, the ANOVA could evaluate the variation of the lifetime of the structure and assign a portion of this variation to each one of these factors. Into the ANOVA, the factors are considered independent and can be quantitative or qualitative.

Unfortunately, there exist some factors which can not be determined or controlled and they produce a large scatter in the fatigue life results, even though the test specimens and conditions are considered to be indentical. In fact, scatter is an inherent characteristic of mechanical properties of structures and materials [15]. For this reason, in order to acquire reasonable results it is advisable to use a large number of specimens as much as possible despite of the cost it represents.

4.1 Statistical parameters of a life test plan

The entirety of rules and specifications according to which a life test has to be run is called a life test plan [77]. Among these rules there are some of purely technical contents while other specifications are of statistical relevance. Based on these statistical rules some specific parameters are defined, which are necessary to design the fatigue testing plan.

4.1.1 Replacement policy R

In lifetime experiments the most relevant parameter for the statistician or the engineer is the number n of specimens to be tested at the beginning. Generally speaking, the item which fails during the test should be replaced and in this case the total number of used specimens denoted by n^* is bigger than n.
The replacement policy can be determined by the parameter R as follows:

$$R = \begin{cases} 0 & \text{no replacement,} \quad n^* = n, \\ 1 & \text{replacement,} \quad n^* \geq n. \end{cases} \tag{4.1}$$

In the case of the fatigue experiments on steel structures which are considered within this research, there is no replacement of the specimens.
Moreover, the random moments of failure given by the number of load cycles $N_{i:n}$;

$i = 1, \ldots, n$ are considered as the lifetimes, and subsequently they can be reordered in ascending way, so that they become order statistics [127].

Definition 15 (Order Statistics)**.** *Let Y be a continuos random variable for which $y_1, y_2, \ldots, y_n$ are the values of a random sample of size n. Reordering the y_i's from smallest to largest as follows*

$$y_1' \leq y_2' \leq \ldots y_n',$$

defines a new random variable Y_i' whith values y_i'. The Y_i' is called the ith order statistic. Sometimes Y_n' and Y_1' are denoted Y_{max} and Y_{min} respectively.

Particularly, fatigue experiments in HCF or VHCF are very expensive and time consuming. Therefore, determining the amount of specimens to be tested is an important task. Based on the Weibull distribution and on Monte Carlo simulations of fatigue life, Vlcek et al. suggest in [128] a method to establish the minimum amount of test samples.

4.1.2 Failure time registration G

From the statistical point of view, for the lifetime test plans it is very important to define the way the failure times are recorded, either exactly or approximately. If during the test there is a continuosly monitoring, either by personnel or by some device, the registration of the failure time is precise and do not present any measurement errors. Then it is said that the data are non grouped. Otherwise, if the inspection of the lifetime tests is made during certain intervals of time, generally periodically, the data are called grouped. Inferences based on grouped data are less reliable than those using exact data registration [77].

The parameter G describes the way how the lifetime data are recorded.

$$G = \begin{cases} 0 & \text{no grouping,} \\ 1 & \text{grouping.} \end{cases} \tag{4.2}$$

In the case of $G = 1$ it is necessary to know how the grouping of the data is perfomed.

4.1.3 Accelerated life tests - ALT and induced stress S

Since the beginning of fatigue research in the late 1800's, the problems associated with the long fatigue or HCF have produced an obvious need to generate data at very

high numbers of cycles [129]. Bridges carrying thousands of moving axle loads every day, railroad wheels making contact with the rails on every revolution over hundreds of thousands of kilometers, off-shore towers under constant loading from the ocean currents are just some of the examples in which the materials can be subjected to large numbers of cycles. These large numbers of cycles may take many years to accumulate in service whereas in design, data are needed in a much shorter period of time.

Historically, engineers and statisticians have devoted considerable effort to develop both equipment that can operate at high frequencies and test procedures to accelerate the manner in which the fatigue limit can be determined. In other words, they have proposed to reduce the time to failure by exercising some level of stress on the test specimens so that they will fail earlier than under normal operating conditions [77]. These approaches are called accelerated life tests (ALT) and the parameter S defined below describes the presence of some type of induced stress.

$$S = \begin{cases} 0 & \text{no stress,} \\ 1 & \text{stress.} \end{cases} \tag{4.3}$$

In the case of $S = 1$, the information regarding how the ALT is performed has to be available.

There are some common alternatives known as types of acceleration for life tests. If these alternatives are applied on lifetime experiments, the experiments are known as ALT. As it is shown below, in most of cases, some parameters are modified in order to reduce the lifetime of the specimens during a fatigue test [77].

1. **High usage rate -** Its target is reducing considerably the testing time and the two common ways are:
   - **Higher velocity or loading frequency-** The speed of the test is higher than the loading frequency of the specimens under normal working conditions, e.g. tests on rolling bearings.
   - **Reduced off time -** Products which have short and specific working times are kept working continuosly for longer periods of time, e.g. washers, dryers, floodlight bulbs.
2. **Specimen design** Lifetime of some products can be accelerated by modifying the size, geometry and finish of test specimens. Generally large test specimens fail sooner than small ones, e.g., cables, steel profiles, chains, fibers.

3. **Overstress loading** Consists of testing the specimens at higher stress levels than those under normal working conditions [130]. Typical examples of high stresses are temperature, pressure, voltage, mechanical load, humidity, salt, sulphur, ozone or radiation, see Figure 4.1.

   – **Constant stress** Each specimen is tested under constant stress until it fails or it achieves the runout criterion.

   – **Step stress** The specimen is subjected to successively higher level of stress. First the specimen is tested under a constant stress during a predetermined interval of time and if it does not fail the specimen is retested under a higher stress. In this way the stress is increased step by step until the specimen fails or the runout criterion is achieved.

   – **Progressive stress** The specimen is tested under a continuos increment of stress. Usually this increment is linear[1], so that the stress at time t is given by $s(t) = at$.

   – **Cyclic stress** The induced stress is applied in a cyclic way such as mechanical load in metal components or alternating current voltages in electronic components.

   – **Random stress** Some products such as airplanes structures are tested under random changes of stress levels.

4.1.4 Censoring criterion D

Censored sampling arises in a lifetime experiment whenever the experimenter does not observe (either intentionally or uintentionally) the failure times of all units placed in the experiment. Very roughly, a sample is said to be censored if out of n specimens placed on a lifetime test, only m ($m \leq n$) of them are actually observed to fail and the others are lost or removed from experimentation before failure [131]. In most of cases the removal of units from experimentation is pre-planned and intentional, and it is done in order to free up testing facilities for other experimentation, to save time and costs, or to exploit the straightforward analysis that often results.

Usually engineers reduce the testing time by applying some of the ideas considered in Subsection 4.1.3, whereas statisticians limit the test duration D by defining some type of censoring.

[1] Such type of stress loading often are called ramp-test.

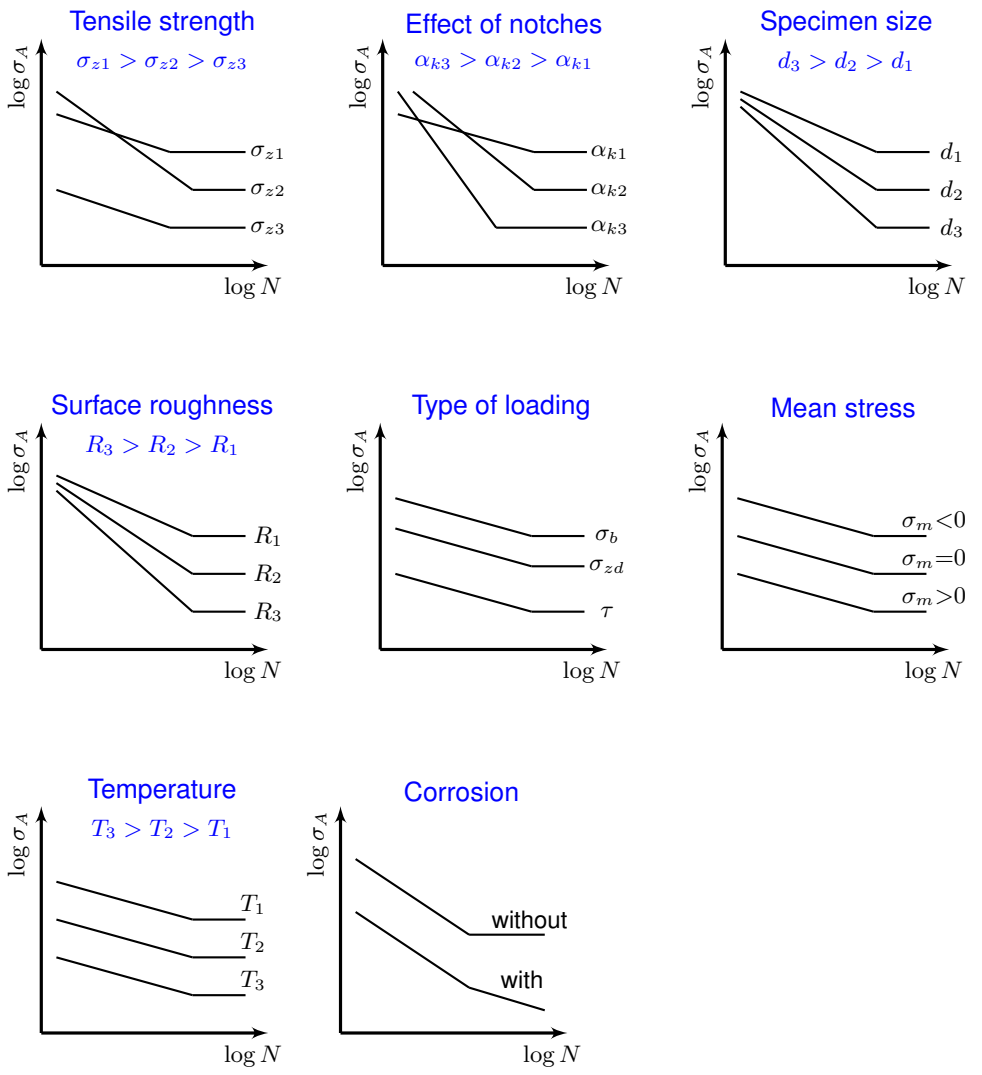

Figure 4.1: Influence factors on the Wöhler curves - Effects on their geometry [130].

4.2 Statistical types of life test plans

Considering the parameters defined in the previous section, a lifetime test plan can be described by the quintuple $\{n, R, G, S, D\}$, and the parameter D is defined depending of which type of censoring is applied [77]. In order to define the types of censoring that can be applied, it is necessary to understand the meaning of censoring.
Let t be the time elapsed since the beginning of the life test and let $A(t)$ be the sum of the random amount of failed specimens in the interval $[0, t]$. $A(t)$ is a discrete function of a continuous variable.
In a specific lifetime test a particular trajectory $a_1(t)$ can be represented in a plane $t - a(t)$. The lifetime tests will be stopped at very moment when the trajectory $a_1(t)$ enters into the region P of this plane. The region P depends on the censoring criterion, see Figures 4.2 and 4.3. As it has been shown in Section 3.5 the estimation of the Weibull parameters depends on the availability or not of censored data.

4.2.1 Type-I censoring

Consider a sample on n specimens placed on a lifetime test at time 0. In conventional Type-I censoring, a time T, independent of the failure times, is pre-fixed such that beyond this time no failures will be observed, that is, the experimentation terminates at time T, see Figure 4.2. Thus, the number of all lifetimes is a random variable which follows a binomial distribution with n as the number of trials and $p = F(T)$ as the probability of success, where F is the CDF of the underlying lifetime distribution [131].

In the case of fatigue experiments performed on steel structures the time is measured in number of cycles, so that, a particular number of cycles N_f is preestablished as limit or end of the fatigue test. Actually, based on the proposed notation a common fatigue test on steel structures can be described as the quintuple

$$\{n, R, G, S, D\} = \{n, 0, 0, 1, N_f\},$$

where there is no replacement of items failing before N_f, see Figure 4.2.

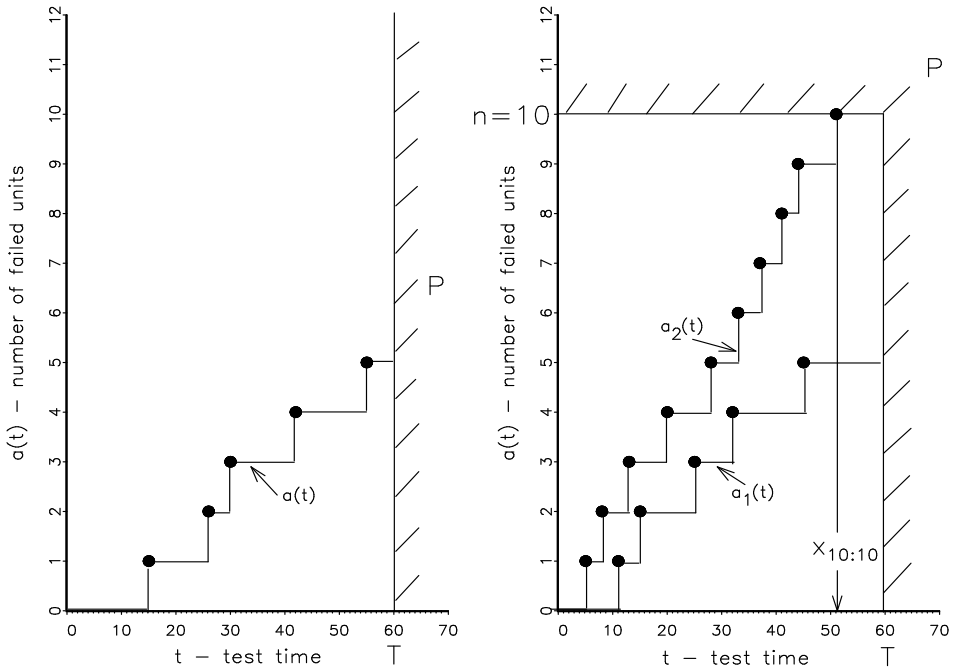

Figure 4.2: Censoring Type-I - Trajectories of a life test plan with replacement $\{n, 1, G, S, T\}$ and a life test plan without replacement $\{10, 0, G, S, T\}$. The trajectory $a_1(t)$ on the right shows that 5 specimens failed before T and 5 specimens are runouts [77].

4.2.2 Type-II censoring

In the case of Type-II censoring, the amount of observed failures $m(m \leq n)$ is pre-established, so that at the time of the mth failure, the experimentation is finished. It leaves the failure times of $n - m$ specimens partially observed [131], see the trajectory $a(t)$ in Figure 4.3. In this case, the time of termination of the experiment is random. In fact, its distribution will be no more than the distribution of the mth order statistic from a sample of size n drawn from a CDF $F(t)$, see Definition 15.

As it has been seen, the loss of specimens at point other than the final termination of the experimentation can be planified by censoring criterions or may also happens unintentionally, as in the case of accidental breakage of the specimens or technical problems of the test equipment.

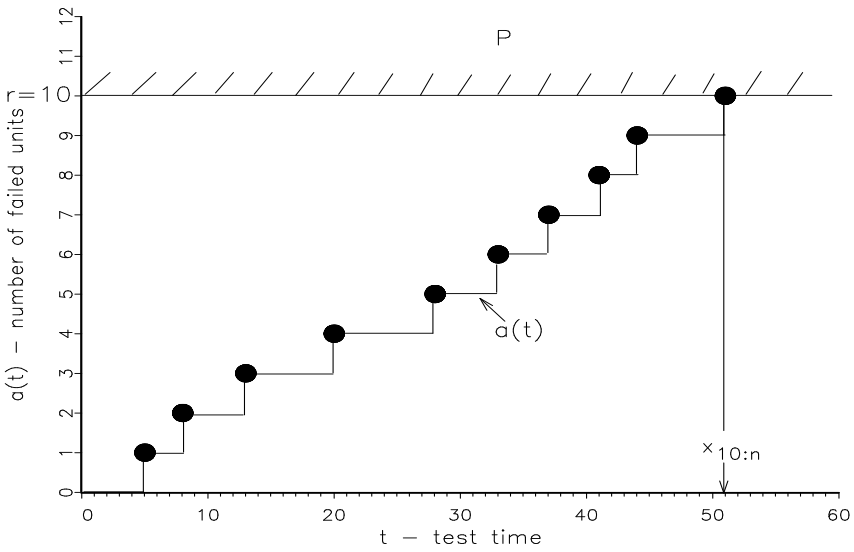

Figure 4.3: Censoring Type-II - Trajectory of a life test plan which shows that the experiment finishes when 10 specimens fail [77].

4.3 Constant amplitude fatigue tests

Usually, in steel structures, constant amplitude fatigue tests are performed at different stress levels, in order to determine the behaviour of the structure under certain stress range and to estimate the fatigue limit of a material.
Experience shows that for unnotched specimens the life until failure is only slightly larger than the crack initiation life; in fact, almost the same. Then, it becomes more difficult for microcracks to grow until failure if the stress level goes down to the fatigue limit [15].
In most cases, in order to save time and costs these fatigue tests are performed at a higher frequency than the normal operative conditions and executing some kind of overstress loading as it was explained in Subsection 4.1.3.

4.3.1 Cyclic loading parameters

Performing a constant stress amplitude test implies, inducing the specimens to fail through a cyclic (repetitive) loading between minimum and maximum constant stress levels. The execution, description and configuration of this kind of tests can be defined by the parameters shown in Figure 4.4 and described below.

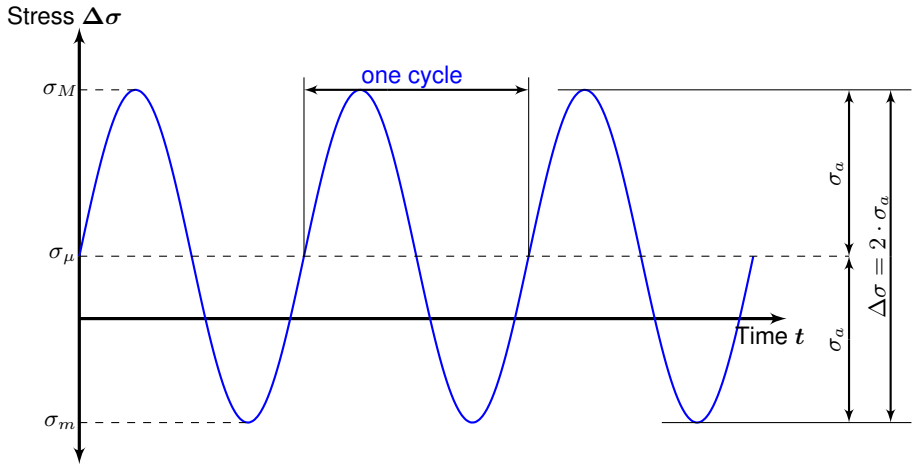

Figure 4.4: Constant stress amplitude fatigue test - Description of the characteristics values for a fatigue lifetime test.

1. **Stress levels σ_M, σ_m -** They are the stress values at which the loading direction is reversed.
   From a mechanistic point of view these values are the best option to configurate or define a fatigue test[15] . The crack extension in one cycle stops at σ_M.

2. **Stress range $\Delta\sigma$ -** It is the difference between the maximum and minimum stress values, graphically it is the peak to peak stress.

$$\Delta\sigma = \sigma_M - \sigma_m.$$

3. **Stress ratio R -** It describes the proportion between the maximum and minimum stress values.

$$R = \frac{\sigma_m}{\sigma_M}.$$

   Consider the situation in which the designer wants to increase the fatigue life by reducing the design stress level, e.g. by increasing the cross section of the fatigue critical area. In this case, all stress levels are then reduced by multiplying them by the same factor. Therefore, the stress ratio R remains constant but the stress range $\Delta\sigma$ is reduced in the same proportion as the stress levels, see Theorem 6.

4. **Mean stress σ_μ-** It is the average of the maximum and minimum stress values.

$$\sigma_\mu = \frac{\sigma_M + \sigma_m}{2}.$$

Concerning to the Wöhler curves, and based on the equations for constant life diagrams, it has been determined that tensile mean stresses lead to a lower curve and compressive mean stresses lead to a higher curve [129]. In fact, fatigue diagrams generally suggest that the effect of the mean stress is not large, especially if the number of cycles N is high.
Moreover, if a negative σ_μ is present, the crack opening, which is necessary for crack extension, requires a larger σ_a. In practice, it implies that fatigue is rarely a problem for a negative mean stress. As a consequence, fatigue diagrams are usually given for positive mean stresses only.
Under a cyclic compressive fatigue load, the microcracks are not effectively opened at σ_a. As a result, the microcracks will be non-propagating [15].

5. **Stress amplitude (alternating stress) $\boldsymbol{\sigma_a}$ -** It is the half value of the stress range, in other words it is the amount the stress deviates from the mean. The stress amplitude is sometimes also called the alternating stress.

$$\sigma_a = \frac{\Delta\sigma}{2} = \frac{\sigma_M - \sigma_m}{2}.$$

The stress amplitude has a much larger effect on fatigue than the mean stress [15]. The trend reflects that fatigue is primarily a consequence of cyclic loads. In service a structure is subjected to a stationary load[2] which is the result of the weight of the structure or the cargo, and simultaneously under a superimposed cyclic loads. The stationary load accounts for the mean stress σ_μ, whereas loads in service induce cycles with certain stress amplitudes σ_a.
If the severety of the cyclic load spectrum can be reduced according to the Theorem 7, the stress amplitude becomes smaller but the mean stress remains the same. Additionally, if σ_μ is increased and σ_a remains constant, then σ_M becomes larger, see Theorem 8.

6. **Amplitude ratio $\boldsymbol{A}$ -** It describes the proportion between the stress amplitude and the mean stress.

$$A = \frac{\sigma_a}{\sigma_\mu}.$$

[2] Load which does not vary as a function of time.

Theorem 6 (Reduction of the stress range)**.** *Consider a constant amplitude fatigue test based on cyclic loads. If the stress levels σ_M, σ_m are reduced in the same proportion. Then, the stress range $\Delta\sigma$, and the mean stress σ_μ are reduced but the stress ratio R remains constant.*

Proof. Let σ_M, σ_m be the initial stress levels. A proportional reduction of these levels can be given by the new stress levels given by $\widehat{\sigma}_M = \delta \cdot \sigma_M$ and $\widehat{\sigma}_m = \delta \cdot \sigma_m$, where $\delta \in]0, 1[$. Then, it follows that

$$\begin{aligned}\Delta\widehat{\sigma} &= \delta \cdot \sigma_M - \delta \cdot \sigma_m \\ &= \delta \cdot (\sigma_M - \sigma_m) \\ &= \delta \cdot \Delta\sigma \\ &< \Delta\sigma.\end{aligned}$$

It occurs similarly for the mean stress σ_μ.
Additionally, it also follows that

$$\begin{aligned}\widehat{R} &= \frac{\widehat{\sigma_m}}{\widehat{\sigma}_M} \\ &= \frac{\delta \cdot \sigma_m}{\delta \cdot \sigma_M} \\ &= R.\end{aligned}$$

□

Theorem 7 (Reduction of the stress amplitude)**.** *Consider a constant amplitude fatigue test based on cyclic loads. If the stress levels σ_M, σ_m are displaced symmetrically closer to the mean stress σ_μ. Then, the stress amplitude σ_a is reduced but the mean stress remains constant*

Proof. Let σ_M, σ_m be the initial stress levels. An internal displacement of these levels can be given by the new stress levels given by $\widehat{\sigma}_M = \sigma_M - \delta$ and $\widehat{\sigma}_m = \sigma_m + \delta$, where $\sigma_a > \delta \geq 0$.

Then, it follows that

$$\begin{aligned}\widehat{\sigma}_M - \widehat{\sigma}_m &= (\sigma_M - \delta) - (\sigma_m + \delta) \\ &= \sigma_M - \sigma_m - 2\delta \\ &\leq \sigma_M - \sigma_m,\end{aligned}$$

which leads to $\widehat{\sigma}_a \leq \sigma_a$.

It also follows that

$$\begin{aligned}\widehat{\sigma}_M + \widehat{\sigma}_m &= (\sigma_M - \delta) + (\sigma_m + \delta) \\ &= \sigma_M + \sigma_m,\end{aligned}$$

which leads to $\widehat{\sigma}_\mu = \sigma_\mu$. □

Theorem 8 (Increment of the stress levels)**.** *Consider a constant amplitude fatigue test based on cyclic loads. If the mean stress σ_μ is increased and the stress amplitude σ_a is kept constant. Then, the stress levels σ_M and σ_m become larger.*

Proof. Let σ_μ, $\widehat{\sigma}_\mu$ be the initial and final mean stresses. An increment of the mean stress means that

$$\begin{aligned}\widehat{\sigma}_\mu &> \sigma_\mu \\ \frac{\widehat{\sigma}_M + \widehat{\sigma}_m}{2} &> \frac{\sigma_M + \sigma_m}{2},\end{aligned}$$

and considering that the stress amplitude remains constant means that

$$\frac{\widehat{\sigma}_M - \widehat{\sigma}_m}{2} = \frac{\sigma_M - \sigma_m}{2}.$$

Then, adding this constraint to the previous inequality leads to

$$\begin{aligned}\frac{\widehat{\sigma}_M + \widehat{\sigma}_m}{2} + \frac{\widehat{\sigma}_M - \widehat{\sigma}_m}{2} &\geq \frac{\sigma_M + \sigma_m}{2} + \frac{\sigma_M - \sigma_m}{2} \\ \widehat{\sigma}_M &\geq \sigma_M.\end{aligned}$$

In a similar way the increment of σ_m can be demonstrated. □

A summary of the mathematical relationships between the cyclic loading parameters, which were proved in Theorems 6 to 8 is described in the Table 4.1.

4.3.2 Classification

According to W. Weibull in [126] the constant amplitude fatigue tests may be classified in three categories, depending on how many load cycles are registered until failure.

Load cycle parameters							
σ_M	σ_m	$\Delta\sigma$	R	σ_μ	σ_a	**Consequence**	**Theorem**
$\Downarrow$	$\Downarrow$	$\downarrow$	$\rightarrow$	$\downarrow$	$\downarrow$	Increment of the fatigue life	6
$\Downarrow$	$\Uparrow$	$\downarrow$	-	$\rightarrow$	$\downarrow$	Reduction of the stress range	7
$\uparrow$	$\uparrow$	$\Longrightarrow$	-	$\Uparrow$	$\Longrightarrow$	Increment of the stress levels Shorter fatigue life Lower fatigue limit	8

Table 4.1: Relationships between the load cycle parameters - The blue arrows represent the behavior of a parameter induced by the behavior of the parameters represented by a black arrow.

a. Short-life tests

In this case the stress levels are situated above the yield stress and some specimens are expected to fail statically at the application of the load. In modern terms, these tests are located in the ULCF region, see Figure 1.13.

b. Routine tests

The applied stresses are choosen in such a way that the number of load cycles to failure $N_i \in [10^4, 10^7]$; in other words these tests belong to the finite life and HCF regions. Usually, the purpose of these tests is estimating the relation between load and fatigue life, with the chief aim of determining with certain probability the fatigue limit by an extrapolation of the Wöhler curve. The presence of runouts may be allowed. These tests are classified in two categories as well.

All-failed tests

They are performed in order to determine the relation between the fatigue life and the amplitude stress for the specimen, keeping the mean stress σ_μ or the stress radio R constant. The efficiency of these tests depends upon the selected stress levels and the corresponding factors which may produce scatter.
The choice of stress levels depends upon the purpose for which the data are required. If the main interest is estimating the long-life range of the Wöhler curve, low stress levels should be choosen. On the other hand, if a complete representation of the Wöhler curve is expected, the stress levels should be distributed among high and low values.

In order to obtain realistic results, it is strongly recommended to perform some static tests in order to obtain an experimental static tensile strength which can be used as a normalization parameter for the choosen stress levels. The influence of the stress levels on the efficiency of the all-failed tests may be enunciated as: the greater difference between the highest and the lowest stress levels, the greater the accuracy. Moreover, it is recommended using equal number of specimens in every stress level.

Fraction-failed tests

The purpose of these tests is the same as in the all-failed tests. Nevertheless, in this case because of time or cost reasons the tests can be stopped when a predefined fraction of the specimens have failed. This stopping represents nothing but a censoring criterion of type II, which has been already explained in Subsection 4.2.2.
From the practical point of view, an engineer is not interested in the fatigue life of the best specimens, but of the weakest ones; for this reason the calculations are based on the worse scenario i.e. the shorter fatigue life. In design matters, it is enough having knowledge about the lower part or minimum extreme value from the fatigue life or from the strength distribution.

c. Long-life tests

The stress levels are situated near to the fatigue limit, and a fraction of the specimens does not fail after a predetermined number of load cycles, which usually is $N \in [10^6, 10^7]$ and represents a censoring criterion of type I, which has been already explained in Subsection 4.2.1. According to the Figure 1.13 these tests are located between the finite life region and the HCF region.
The goal of these tests is determining a percentage points of the distribution of the fatigue strength at a preassigned lifetime given by a number of load cycles. The long-life tests may be classified into two categories: constant amplitude tests known also as response tests and increasing amplitude tests which are described in the next subsection. The methods which belong to the first category can be performed by the following two methods.

The probit method

In this method the stress levels and their corresponding number of specimens are previously determined. The main goal is determinig the complete distribution function of the fatigue strength.

The common procedure is to divide the available specimens in several groups corresponding to each choosen stress level.

The staircase method

This method known also as up and down method is based on sequencial tests, where the choice of the stress level depends on the result from the preceding fatigue test. This method considers the fatigue data as sensitivity data and it is suitable when the specimen can be failed only one time [132]
This method may be applied if the purpose is estimating the median value of the fatigue strength. However, it is not a good method to estimate extreme values since it would imply that the fatigue strength follows a normal distribution and in this work has been proved that it follows a Weibull distribution.
The first step of the procedure is estimating the mean value of the fatigue strength and then performing a test under this estimated stress level. If a failure occurs before the predetermined censoring criterion the next test is performed at a lower stress level; if the specimen survives the next test is performed at a higher stress level.

4.4 Non-constant amplitude fatigue tests

These tests are performed because of time and economical reasons. During their performance the stress level is increased if the specimen has survived a preassigned number of cycles. This increment is known as step increment and every step means the existence of a runout.
In order to evaluate all of fatigue data together i.e. failures and runouts, it is mandatory to define an accumulated damage measure for every stress level, and as it has been seen in Section 3.6 several measures habe been proposed; but particularly in this research the damage accumulation method presented in Section 3.7 is applied.
Another alternative is increasing the stress level continuosly, this method was proposed by Prot in 1947 [133]; nevertheless most of the times it works only in rotating bending machines and it demands much more specimens than the step increment method. Usually, rotating bending machines are used to test small mechanical parts at high frequency.

4.5 Additional properties of importance in fatigue

Besides the parameters and situations mentioned in the previous subsections, there are some environmental characteristics, such as the corrosion level, the wave shape,

and the number of cycles which should be taken into account when a fatigue test is performed.

The presence of pitting corrosion represents a significant reduction of the fatigue limit $\Delta\sigma_\infty$. In general, pitting corrosion leads to acceleration of the crack initiation and crack growth under the effect of cyclic loads or fatigue. Moreover, since corrosion is a time dependent phenomenon, a frequency effect has to be expected. As a matter of fact, this effect is disturbing if the structures are operating in a marine environments, for instance, offshore stuctures, or ships, where load frequencies can be very low [15].

Regarding to the wave shape, in fatigue tests the wave is usually sinusoidal, but in service conditions it can be highly different, see Figure 4.5. Even if the load frequency for the different wave shapes is the same in terms of number of cycles, fatigue does not necessarily occur at the same rate.

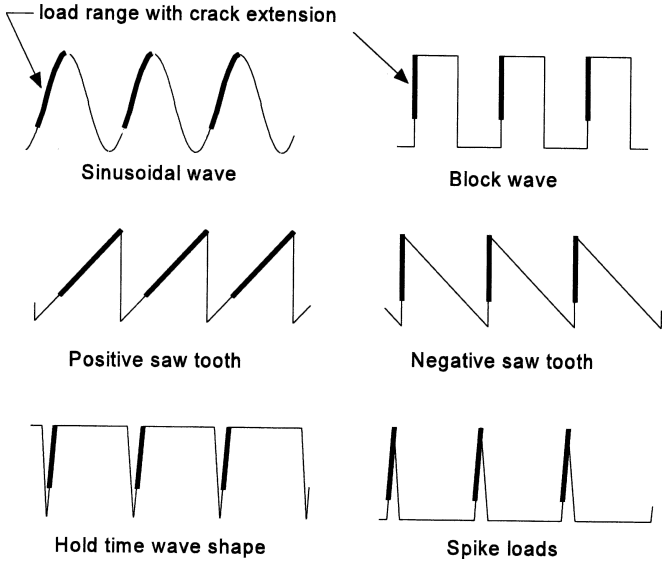

Figure 4.5: Basic wave shapes - Geometries of waves during a cyclic load [15].

In the case of the number of cycles, the differences between low-cycle and high-cycle fatigue are very relevant. The low-cycle fatigue is associated with macroplastic deformation in every cycle. On the other hand, high-cycle fatigue is more related to an elastic behavior on a macro scale of the material. Actually, high-cycle fatigue is the more common case in practice, whereas low-cycle fatigue is associated with specific structures and load spectra [15].

Fatigue properties of unnotched specimens, such as the Wöhler curves or the fatigue limit $\Delta\sigma_\infty$ are generally supposed to be material properties. Particularly, the fatigue limit is defined as the horizontal asymptote of the Wöhler curve. This information is obtained from fatigue tests performed until failure or until satisfying a certain censoring criterion. Based on these information, it has been determined that the fatigue live covers two phases: a) Micro crack initiation period and micro crack growth and b) Crack and macro crack growth period, see Figure 1.10.

Taking into consideration the Weibull model proposed by Castillo and Fernández-Canteli presented in Chapter 3, the methods to estimate the Weibull parameters proposed in the Section 2.3, the fatigue data classification stated in Section 3.9 and the procedure to analyze fatigue data showed in Section 3.10, six applications are presented.

According to the procedure to evaluate the experimental fatigue data given by the flowchart from Figure 3.13, the first step is to estimate the thresholds or geometrical parameters B and C of the Weibull model by solving the non-linear optimization problem given by Equation (3.35). Only then, the Weibull random variable $x = (\log N - B)(\log \Delta\sigma - C)$ can be defined, see Equation (3.30). Afterwards, based on the random variable x, the Weibull parameters a, b and c can be estimated by applying the PWM and the MLE methods which are described in Subsections 2.3.1 and 2.3.2 respectively.

After introducing a specific description of the specimens and the corresponding fatigue data, the six applications and their corresponding results are presented, according to two main aspects:

- The statistical method applied on the estimation of the Weibull parameters, either PWM or MLE.
- The kind of available or considered fatigue data, which are divided in three categories:
  - Only failures (F)
  - Failures and runouts (F-RO)
  - Failures, runouts and retested runouts (F-RO-RT).

Combining the statistical methods and the categories of available data leads to six possible configurations for the evaluation of the fatigue data. Subsequently, the results are presented in the following order:

- Parameter estimation. According to the selected statistical method, the estimations of the Geometrical and Weibull parameters are presented in tables.

- Wöhler curves. These curves are plotted according to both models Weibull and Basquin, which are given by hyperbolas and straight lines respectively. These plots given in a logarithmic scale allow to make a visual comparison between their corresponding quantiles and confidence intervals.
- Quantiles estimation for a specific number of cycles. These results given in tables show the estimation of the 5%, 50% and 95% quantiles given by Weibull and Basquin, and the size of their corresponding 90% confidence intervals.
- Comparison of quantiles and confidence intervals for a specific number of cycles. The absolute difference and the percentage difference between the quantiles and confidence intervals are presented in tables.

Definition 16 (Absolute difference)**.** *Let W and B be the quantiles of Weibull and Basquin. Their absolute difference is given by*

$$d_a(W,B) = \mid W - B \mid . \tag{4.4}$$

Definition 17 (Percentage difference)**.** *Let W and B be the quantiles of Weibull and Basquin. Their percentage difference is given by*

$$d_p(W,B) = \frac{\mid W - B \mid}{\mid B \mid} \cdot 100. \tag{4.5}$$

4.6 Fatigue tests containing only failures

The applications considered in this section belong to the research project REFRESH. This project was focused on the increment of the fatigue life of new and already in service welded steel structures.

The objectives were

- verifying the efficiency of high-frequency post weld treatments for increasing the fatigue strength of existing and freshly welded steel constructions
- Developing a holistic concept for the optimum use of these treatments
- Supervision and the consideration of these treatments in design

These goals were achieved by the inclusion of suppliers and operators as well as accredited test centers [83].

4.6.1 Specimens of S690QL

In this application 30 welded specimens from steel S690QL, which did not receive any post weld treatment are considered. The main properties of the specimens are described in Table 4.2 and their geometry and measurements are showed in Figure 4.6.

S1-30-S690QL-AW Properties	
Project	REFRESH
Material	S690QL
Minimum yield strength R_{eH}	690 MPa
Treatment	As welded
Thickness	30 mm
Geometry	see Figure 4.6
Nr. of samples	30

Table 4.2: Steel S690QL. Properties - Corresponding to the tested specimens.

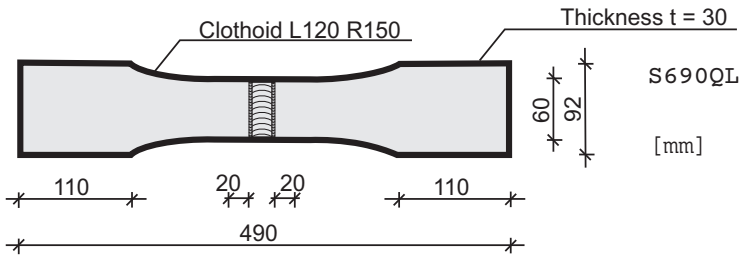

Figure 4.6: Steel S690QL. Specimens - Geometry and measurements.

During the performance of the fatigue experiments five different stress ranges $\Delta\sigma_i$ were applied. As fatigue failure criterion a variation in the test frequency of more than 5% was set in the testing machine. This criterion was related to the presence of large cracks up to the brake-through of the specimens. Their corresponding stress ratio R and number of load cycles N are presented in Table 4.3.

S1-30-S690QL-AW $\mathbf{R = 0,1}$					
$\mathbf{\Delta\sigma}$ [MPa]			$\mathbf{N}$ [-]		
300	82 755	83 640	147 456	–	–
263	92 335	117 468	185 074	188 399	213 459
	254 043	293 389	405 748	–	–
244	177 457	203 986	231 709	287 544	290 839
	561 794	587 410	–	–	–
225	306 397	395 771	810 959	1 348 256	1 596 105
206	646 116	958 599	965 373	1 108 585	1 137 130
	1 408 242	1 655 823	–	–	–

Table 4.3: Steel S690QL. Fatigue data - Experimental results. All specimens failed.

Results and analysis

The results in Table 4.4 show that both the PWM and the MLE methods give almost the same values for the estimation of the Weibull parameters a, b and c.

S1-30-S690QL-AW Parameter estimation		
Geometrical parameters		
B	2,94	
C	4,03	
N_{min} [-]	19	
$\Delta\sigma_\infty$ [MPa]	56,21	
m	6,77	
Weibull parameters		
	PWM	**MLE**
a	12,83	12,84
b	1,68	1,67
c	2,30	2,41

Table 4.4: Steel S690QL. Parameter estimation - Geometrical and Weibull parameters. The corresponding Wöhler curves are shown in Figures 4.7 and 4.8.

The Wöhler curves corresponding to this application are shown in Figures 4.7 and 4.8. Both models, Weibull and Basquin show similar results into the region delimited by $[200, 300]$ MPa and by $[2 \cdot 10^5, 8 \cdot 10^5]$ load cycles. Nevertheless, the main difference between both models is the behaviour of their corresponding curves beyond the 2 millions of load cycles and particularly in the HCF region.

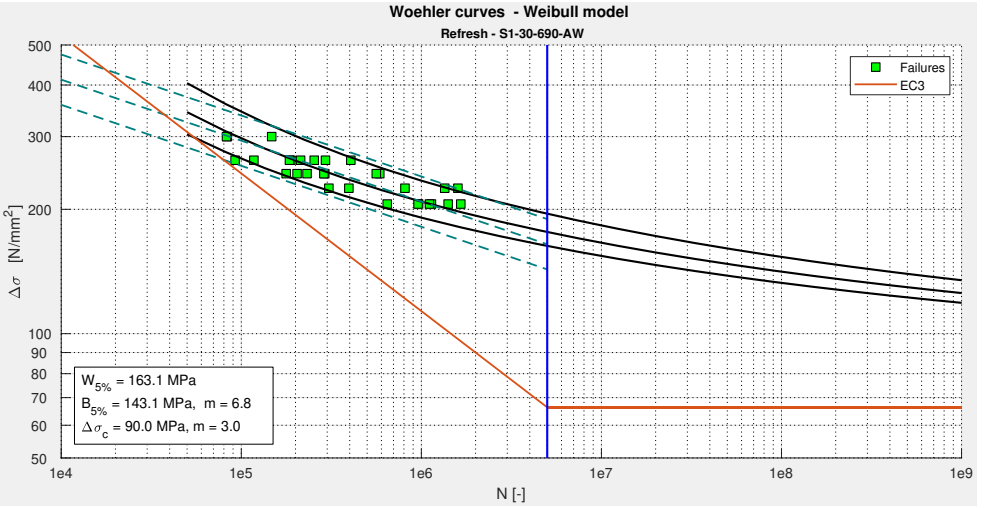

Figure 4.7: Steel S690QL. PWM-Wöhler curves - The curves represent the quantiles corresponding to a failure probability of 5, 50 and 95 percent.

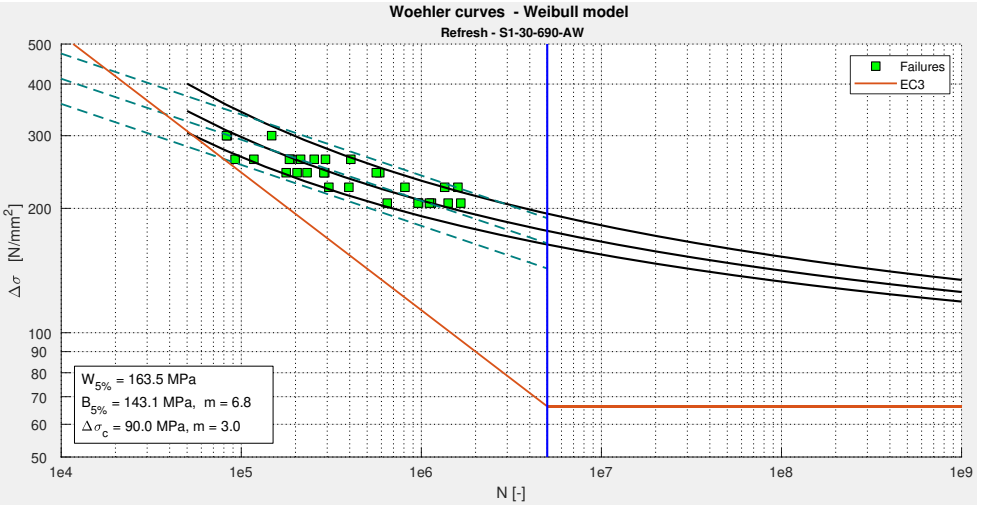

Figure 4.8: Steel S690QL. MLE-Wöhler curves - The curves represent the quantiles corresponding to a failure probability of 5, 50 and 95 percent.

The quantiles corresponding to the Weibull model become higher than those from the Basquin model, and the confidence intervals according to Weibull are significantly tighter than those from Basquin, see Tables 4.5 and 4.6. From the design engineering point of view, these differences represent the main advantage of applying the Weibull model to evaluate fatigue data and to extrapolate the results into the HCF region.

As it is known, according to the Eurocode 3, the 5% quantile is considered in order to estimate the fatigue limit of a structure. In this example the estimation of the 5% quantile increases considerably if the Weibull model is applied. Particularly, at 2 millions load cycles the estimation increases 7,15% by applying the PWM and 7,44% by applying the MLE. At 5 millions load cycles the increment is even more significant, 14% with the PWM method and 14,29% with the MLE method. Moreover, by applying the PWM method, the 90% confidence interval is reduced by 30,76%. By applying the MLE method, the same interval is reduced by 33,74%, see Tables 4.5 and 4.6.

Comparing the Wöhler curves given by applying the Weibull model with those used as reference in Eurocode 3 shows that the reference curve of Eurocode 3 is more conservative. At 5 million load cycles the difference is 73,1 MPa with the PWM method and 73,5 MPa with the MLE method, see Figures 4.7 and 4.8. Moreover, the constant slope $m = 3$ proposed in Eurocode 3 does not describe the behaviour shown by the experimental data.

S1-30-S690QL-AW				
PWM - Quantiles and CIs				
Prob.	$\mathbf{W}$	$\mathbf{B}$	$\mathbf{d_a}(\mathbf{W},\mathbf{B})$	$\mathbf{d_p}(\mathbf{W},\mathbf{B})$
[%]	[MPa]	[MPa]	[MPa]	[%]
		$\mathbf{N = 2 \cdot 10^6}$		
5	177,46	165,61	11,84	7,15
50	192,97	188,46	4,51	2,39
95	215,40	214,45	0,95	0,44
CI_{90}	37,95	48,84	10,89	22,30
		$\mathbf{N = 5 \cdot 10^6}$		
5	163,10	143,07	20,03	14,00
50	176,26	164,61	11,65	7,08
95	195,17	189,40	5,78	3,05
CI_{90}	32,08	46,33	14,25	30,76

Table 4.5: Steel S690QL. PWM-Quantiles and CIs - Estimations and comparisons between the models of Weibull and Basquin. See Figure 4.7.

S1-30-S690QL-AW MLE - Quantiles and CIs				
Prob. [%]	$\mathbf{W}$ [MPa]	$\mathbf{B}$ [MPa]	$\mathbf{d_a(W,B)}$ [MPa]	$\mathbf{d_p(W,B)}$ [%]
		$\mathbf{N = 2 \cdot 10^6}$		
5	177,94	165,61	12,32	7,44
50	193,15	188,46	4,69	2,49
95	214,25	214,45	0,21	0,10
CI_{90}	36,31	48,84	12,53	25,66
		$\mathbf{N = 5 \cdot 10^6}$		
5	163,51	143,07	20,44	14,29
50	176,42	164,61	11,81	7,17
95	194,20	189,40	4,81	2,54
CI_{90}	30,70	46,33	15,63	33,74

Table 4.6: Steel S690QL. MLE-Quantiles and CIs - Estimations and comparisons between the models of Weibull and Basquin. See Figure 4.8.

In summary, in comparison with the Basquin model the results obtained from the Weibull model allow to estimate a higher fatigue life of the specimen and tigher confidence intervals for the stress range.

4.6.2 Specimens of S355J2

In this application 26 welded specimens from steel S355J2, which did not receive any post weld treatment are considered. The main properties of the specimens are described in Table 4.7 and their geometry and measurements are showed in Figure 4.9.

L1-30-S355J2-AW Properties	
Project	REFRESH
Material	S355J2
Minimum yield strength R_{eH}	355 MPa
Treatment	As welded
Thickness	30 mm
Geometry	see Figure 4.9
Nr. of samples	26

Table 4.7: Steel S355J2. Properties - Corresponding to the tested specimens.

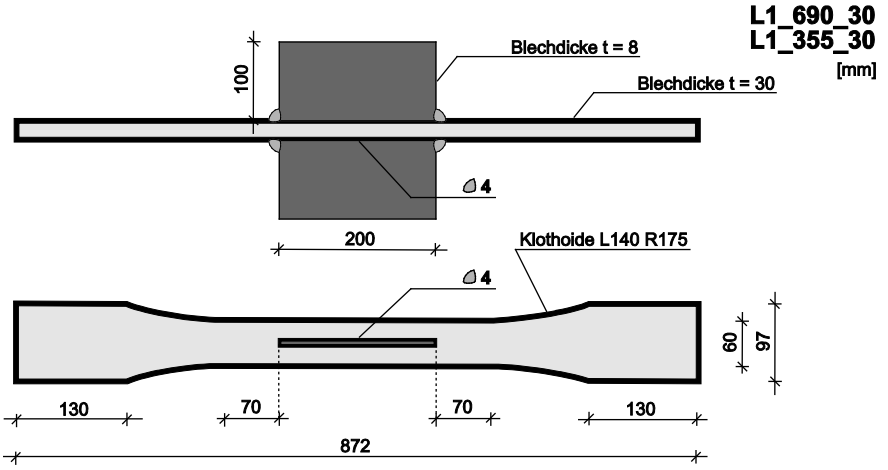

Figure 4.9: Steel S355J2. Specimens - Geometry and measurements.

During the performance of the fatigue experiments seven different stress ranges $\Delta\sigma_i$ were applied. As fatigue failure criterion a variation in the test frequency of more than 5% was set in the testing machine. This criterion was related to the presence of large cracks up to the brake-through of the specimens. Their corresponding stress ratio R and number of load cycles N are presented in Table 4.8.

L1-30-S355J2-AW $\mathbf{R = 0,1}$					
$\mathbf{\Delta\sigma}$ [MPa]	$\mathbf{N}$ [-]				
282	40 503	98 699	–	–	–
244	80 548	94 911	97 903	–	–
207	124 036	164 065	167 923	–	–
188	226 845	247 513	–	–	–
169	175 283 275 653	184 192 297 327	235 445 307 220	261 981 375 095	267 413 –
141	459 163	532 217	–	–	–
113	942 345	999 613	1 021 360	1 136 616	1 308238

Table 4.8: Steel S355J2. Fatigue data - Experimental results. All specimens failed.

Results and analysis

In this case, the estimations of the Weibull parameters a, b and c given by the PWM and MLE methods are different, see Table 4.9. However, their corresponding Wöhler curves have a similar geometry, see Figures 4.10 and 4.11. Hence, the value of the quantiles do not differ much, see Tables 4.10 and 4.11. A detailed explanation of the influence of the variation of the Weibull parameters in the geometry of the Wöhler curves is presented in the Section 3.2.

L1-30-S355J2-AW		
Parameter estimation		
Geometrical parameters		
B	5,93	
C	2,96	
N_{min} [-]	376	
$\Delta\sigma_{\infty}$ [MPa]	19,47	
m	3,13	
Weibull parameters		
	PWM	**MLE**
a	1,03	6,63
b	13,28	7,67
c	31,12	17,99

Table 4.9: Steel S355J2. Parameter estimation - Geometrical and Weibull parameters. The corresponding Wöhler curves are shown in Figures 4.10 and 4.11.

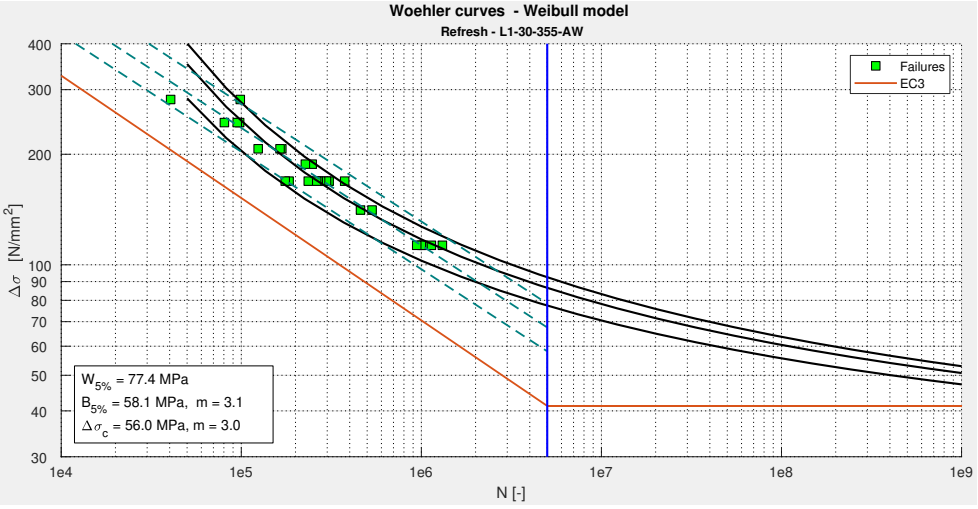

Figure 4.10: Steel S355J2. PWM-Wöhler curves - The curves represent the quantiles corresponding to a failure probability of 5, 50 and 95 percent.

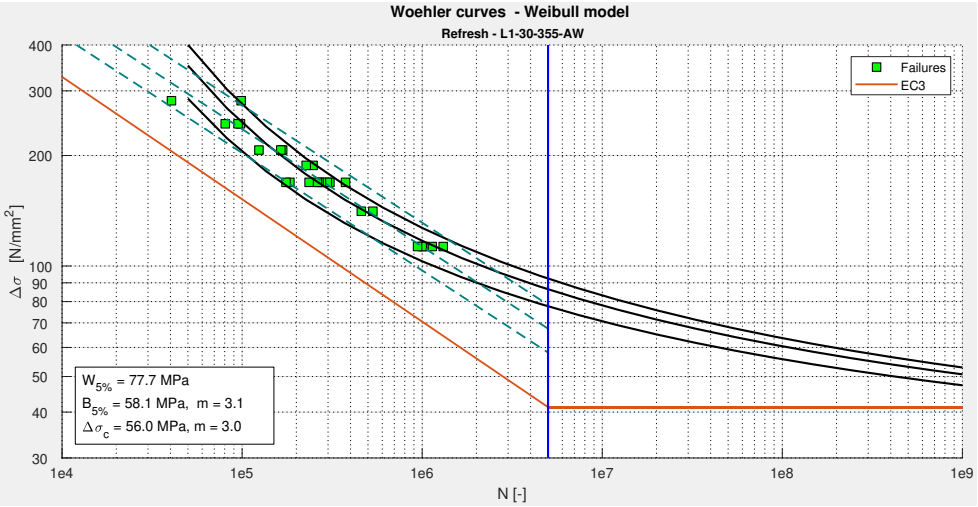

Figure 4.11: Steel S355J2. MLE-Wöhler curves - The curves represent the quantiles corresponding to a failure probability of 5, 50 and 95 percent.

L1-30-S355J2-AW PWM - Quantiles and CIs				
Prob. [%]	$\mathbf{W}$ [MPa]	$\mathbf{B}$ [MPa]	$\mathbf{d_a(W,B)}$ [MPa]	$\mathbf{d_p(W,B)}$ [%]
		$\mathbf{N = 2 \cdot 10^6}$		
5	89,7	78,9	10,8	13,7
50	101,4	90,5	10,9	12,0
95	109,2	103,8	5,4	5,2
CI_{90}	19,5	24,9	5,4	21,7
		$\mathbf{N = 5 \cdot 10^6}$		
5	77,4	58,1	19,3	33,2
50	86,5	67,5	19,0	28,2
95	92,5	78,4	14,1	17,9
CI_{90}	15,0	20,3	5,3	25,9

Table 4.10: Steel S355J2. PWM-Quantiles and CIs - Estimations and comparisons between the models of Weibull and Basquin. See Figure 4.10.

L1-30-S355J2-AW MLE - Quantiles and CIs				
Prob. [%]	$\mathbf{W}$ [MPa]	$\mathbf{B}$ [MPa]	$\mathbf{d_a}(\mathbf{W},\mathbf{B})$ [MPa]	$\mathbf{d_p}(\mathbf{W},\mathbf{B})$ [%]
		$\mathbf{N = 2 \cdot 10^6}$		
5	90,0	78,9	11,1	14,1
50	101,3	90,5	10,8	11,9
95	109,1	103,8	5,3	5,1
CI_{90}	19,1	24,9	5,8	23,3
		$\mathbf{N = 5 \cdot 10^6}$		
5	77,7	58,1	19,6	33,7
50	86,4	67,5	18,9	28,0
95	92,4	78,4	14,0	17,9
CI_{90}	14,8	20,3	5,5	27,3

Table 4.11: Steel S355J2. MLE-Quantiles and CIs - Estimations and comparisons between the models of Weibull and Basquin. See Figure 4.11.

The quantiles corresponding to the Weibull model become higher than those of the Basquin model, and the confidence intervals according to Weibull are significantly tighter than those of Basquin, see Tables 4.10 and 4.11. The 5% quantile obtained by applying the Weibull model is considerably higher than the 5% quantile obtained by applying the Basquin model. Particulary, at 2 millions load cycles, the 5% Weibull quantile is 13,7% higher than the 5% Basquin quantile according to PWM method and according to the MLE, the 5% Weibull quantile is 14,1% higher than the 5% Basquin quantile. Moreover, by applying the PWM method, the 90% confidence interval is reduced by 21,7%. By applying the MLE method, the same interval is reduced by 23,3%.

Comparing the Wöhler curves given by applying the Weibull model with those used as reference in Eurocode 3 shows that the reference curve of Eurocode 3 is more conservative. At 5 million load cycles the difference is 21,4 MPa with the PWM method and 21,7 MPa with the MLE method, see Figures 4.10 and 4.11. In this case, the constant slope $m = 3$ proposed in Eurocode 3 describes the behaviour shown by the experimental data.

The two applications presented in this section show clearly the benefits of applying the Weibull model for the statistical evaluation of fatigue data and for the modelling of the Wöhler curves. On the one hand, by applying the Weibull model, the estimation of the 5% quantile at 5 millions load cycles is higher than by applying the Basquin

model. On the other hand, the difference becomes even bigger if the reference curve given by Eurocode 3 is considered or the amount of load cycles increases.

The Wöhler curves based on the Weibull distribution show properly the asymptotic behaviour of the lifetime of the specimens. This fact allows to estimate the fatigue limit with certain probability. However, the Wöhler curves (actually straight lines) obtained from the Basquin model have to change their slope in order to describe the asymptotic behaviour near the fatigue limit. As a matter of fact, in Eurocode 3, the asymptotic behaviour is depicted with the help of two knee points at 5 and 100 millions load cycles. Moreover, the location of the first knee point is restricted to the asumption of having a straight line of slope m=3 in the finite fatigue region and to a predetermined detail category for every construction detail. Clearly, this restriction can not be applied when the slope of the regression differs too much from 3, like in the first example whose slope is m=6,77.

4.7 Fatigue tests containing failures and runouts

In this section, the considered fatigue data include both failures and runouts. Two applications are presented, and their corresponding data belong to two different kind of specimens: main girders from the Stahringer bridge built in 1895 and hourglass specimens of untempered steel type 49MnVS3. In every case, a comparison between the results obtained by considering only the failures and considering the failures and runouts together is presented.

The innovative aspect of these applications is including the runouts information into the statistical evaluation of fatigue data. This fact has been ignored in the international standards.

The main point in order to obtain the mentioned information from the runouts is estimating the number of cycles in which they would have failed if the fatigue test had not been stopped, see Section 3.5. From the statistical point of view, the runouts are considered as censored data of Type-I, see Subsection 4.2.1.

4.7.1 Stahringer bridge - 1895

As a part of a research project on antique german steel bridges several tests were conducted in order to analyse the fatigue life of these structures [134], [135], [136].

One of the considered structures was the Stahringer bridge which was built on 1895. Several components of the bridge were tested. The bridge was cut into small pieces in order to investigate the main girders, longitudinal girders, cross girders and joints individually. In this application 49 fatigue experiments performed on the main

girders with original holes and riveting are considered [125]. After the fatigue tests the main girders presented some cracks such as those shown on Figures 4.12 and 4.13. The cracks were initiated at different locations, so that it was difficult to indicate precisely where the fatigue failure began. The fatigue data, which include one runout are shown in Tables 4.12 and 4.13 .

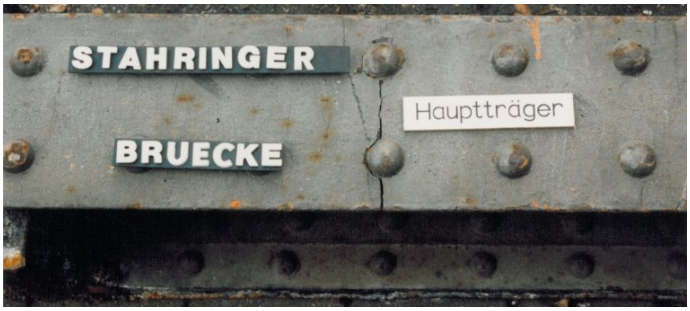

Figure 4.12: Stahringer bridge main girder - Crack after fatigue failure.

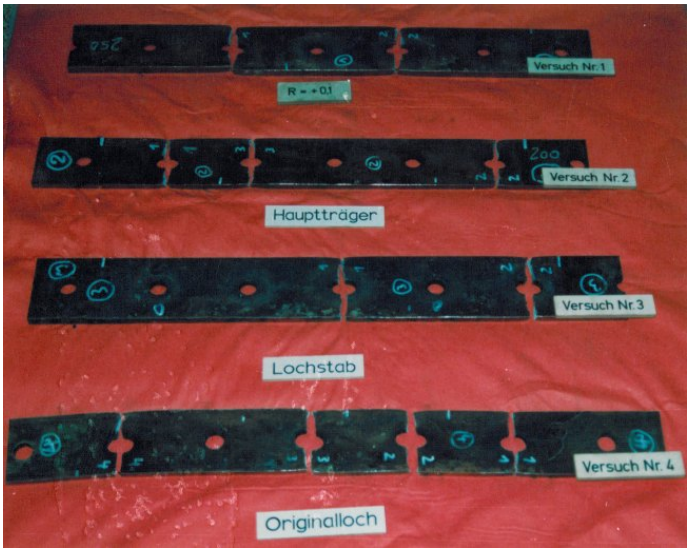

Figure 4.13: Stahringer bridge main girders - Cracks from the main girders after fatigue failure. The cracks initiated at different locations.

Stahringer bridge 1895 - Failures $\mathbf{R = -1,0}$					
$\boldsymbol{\Delta\sigma}$			$\mathbf{N}$		
[MPa]			[-]		
225	38 927	46 474	–	–	–
180	112 302	138 322	142 491	133 710	127 800
	235 782	302 732	133 500	133 840	289 800
	330 300	–	–	–	–
144	523 200	398 319	554 726	496 652	647 726
	897 183	885 600	1 200 640	661 550	683 264
	739 415	827 473	989 000	456 020	456 480
	292 680	309 570	355 100	–	–
126	1 333 748	1 904 087	1 964 597	766 126	1 236 622
	1 514 865	1 272 776	1 313 096	1 689 579	1 882 968
	775 688	1 084 235	1 334 498	1 401 002	–
108	2 980 233	3 504 216	5 484 220	–	–

Table 4.12: Stahringer bridge. Fatigue data of failures - Corresponding to the main girders with original holes and riveting.

Stahringer bridge 1895 - Runouts $\mathbf{R = 0,1}$			
		PWM	**MLE**
$\boldsymbol{\Delta\sigma}$	$\mathbf{N}$	$\mathbf{E(N)}$	$\mathbf{E(N)}$
[MPa]	[-]	[-]	[-]
108	17 804 820	20 150 546	20 396 215

Table 4.13: Stahringer bridge. Fatigue data of runouts - Experimental results of N and estimations of its lifetime $E(N_1)$. The values of $E(N_1)$ are plotted in blue on Figures 4.16 and 4.17.

Results and analysis

The results presented in the Table 4.14 show that both the PWM and the MLE methods give similar values for the estimation of the Weibull parameters a, b and c when the same type of data are considered. The same situation occurs for the estimated geometrical parameters B and C. This fact can be appreciated in the similar geometry of the Wöhler curves in the Figures 4.14 and 4.15 which consider only the failures and in the Figures 4.16 and 4.17 which consider failures and runouts.

Stahringer bridge 1895 Parameter estimation				
Parameter	**PWM**		**MLE**	
	F	F-RO	F	F-RO
Geometrical parameters				
B	3,53	2,85	3,53	2,84
C	3,37	3,35	3,37	3,35
N_{min} [-]	34	17	34	17
$\Delta\sigma_\infty$ [MPa]	29,07	28,59	29,07	28,58
m	5,90			
Weibull parameters				
a	14,07	15,62	14,27	15,60
b	1,63	1,34	1,40	1,39
c	2,47	1,84	2,16	1,96

Table 4.14: Stahringer bridge. Parameter estimation - Geometrical and Weibull parameters. The corresponding Wöhler curves are shown in Figures 4.14 to 4.17.

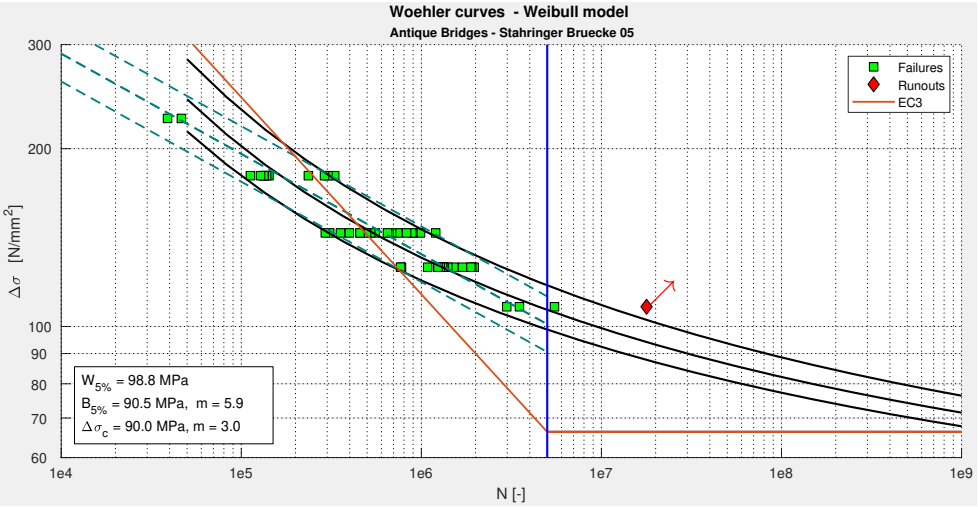

Figure 4.14: Stahringer bridge. PWM-Wöhler curves. Failures - The curves represent the quantiles corresponding to a failure probability of 5, 50 and 95 percent.

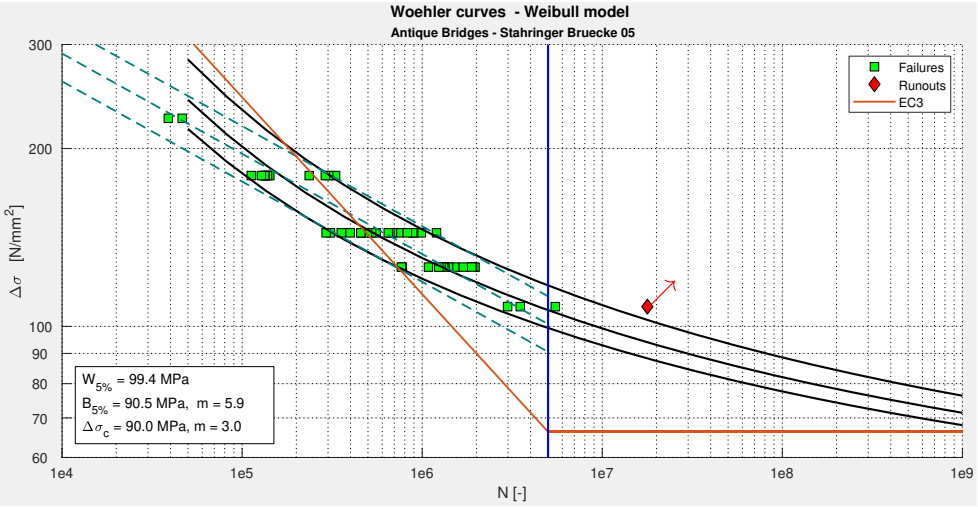

Figure 4.15: Stahringer bridge. MLE-Wöhler curves. Failures - The curves represent the quantiles corresponding to a failure probability of 5, 50 and 95 percent.

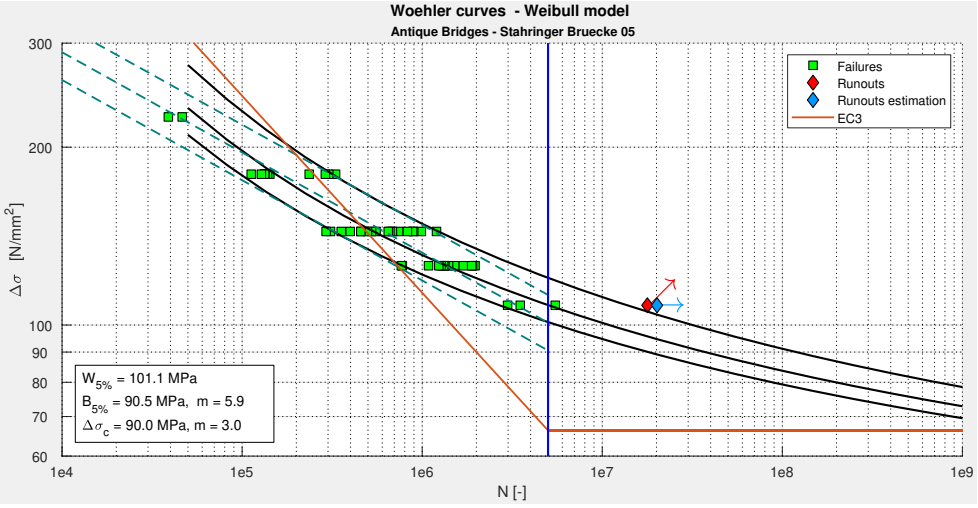

Figure 4.16: Stahringer bridge. PWM-Wöhler curves. Failures and runouts - The curves represent the quantiles corresponding to a failure probability of 5, 50 and 95 percent.

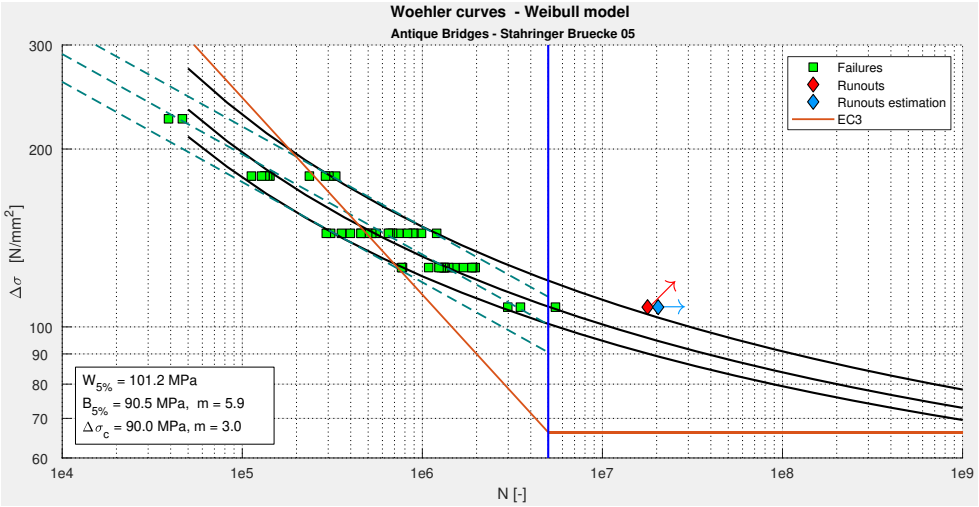

Figure 4.17: Stahringer bridge. MLE-Wöhler curves. Failures and runouts - The curves represent the quantiles corresponding to a failure probability of 5, 50 and 95 percent.

Stahringer bridge 1895				
Quantiles and CIs values				
$\mathbf{N = 1 \cdot 10^7}$ **cycles**				
	PWM		**MLE**	
Prob.	F	F-RO	F	F-RO
[%]	[MPa]	[MPa]	[MPa]	[MPa]
Weibull model				
W_5	92,37	94,68	92,87	94,71
W_{50}	99,32	100,81	99,18	100,93
W_{95}	108,70	111,48	108,62	111,11
CI_{W90}	16,34	16,81	15,75	16,40
Basquin model				
B_5	80,24	–	80,24	–
B_{50}	89,71	–	89,71	–
B_{95}	100,30	–	100,30	–
CI_{B90}	20,06	–	20,06	–

Table 4.15: Stahringer bridge. Quantiles and CIs - Estimations corresponding to the models of Weibull and Basquin by $N = 1 \cdot 10^7$. See Figures 4.14 to 4.17.

Stahringer bridge 1895 PWM - Quantiles and CIs comparisons $\mathbf{N = 1 \cdot 10^7}$ cycles				
	F		**F-RO**	
Prob. [%]	$\mathbf{d_a(W,B)}$ [MPa]	$\mathbf{d_p(W,B)}$ [%]	$\mathbf{d_a(W,B)}$ [MPa]	$\mathbf{d_p(W,B)}$ [%]
(W_5, B_5)	12,13	15,11	14,44	17,99
(W_{50}, B_{50})	9,61	10,71	11,10	12,37
(W_{95}, B_{95})	8,40	8,38	11,19	11,15
(CI_{W90}, CI_{B90})	3,72	18,56	3,25	16,20

Table 4.16: Stahringer bridge. PWM-Quantiles and CIs - Absolute and percentage differences between the models of Weibull and Basquin. See Figures 4.14 and 4.16.

Stahringer bridge 1895 MLE - Quantiles and CIs comparisons Comparison by $\mathbf{N = 1 \cdot 10^7}$ cycles				
	F		**F-RO**	
Prob. [%]	$\mathbf{d_a(W,B)}$ [MPa]	$\mathbf{d_p(W,B)}$ [%]	$\mathbf{d_a(W,B)}$ [MPa]	$\mathbf{d_p(W,B)}$ [%]
(W_5, B_5)	12,63	15,74	14,47	18,03
(W_{50}, B_{50})	9,47	10,56	11,22	12,51
(W_{95}, B_{95})	8,32	8,30	10,81	10,78
(CI_{W90}, CI_{B90})	4,30	21,46	3,65	18,22

Table 4.17: Stahringer bridge. MLE-Quantiles and CIs - Absolute and percentage differences between the models of Weibull and Basquin. See Figures 4.15 and 4.17.

Considering the influence of the runouts in the Weibull model offers a suitable alternative to analize the fatigue properties of the bridge structure. The asymptotic behaviour of the Wöhler curves in the VHCF region can be better identified if the runout is considered in the statistical analysis, see Figures 4.16 and 4.17. This fact represents an enormous advantage if the goal, is estimating the intervals of confidence from the stress range and the fatigue lifetime in the HCF or VHCF regions. Despite the fact that only one runout is available, in this application the Weibull model shows two important advantages in comparison with the Basquin model:

a) By applying the Weibull model, the estimations of the quantiles in the HCF region are considerably higher than those given by the Basquin model, see the Table 4.15. On the one hand, by applying the PWM method, the 5% quantile at 10 millions load cycles increases by 15,11% if only the failures are considered, and it increases by 17,99% if the failures and runouts are taken into account, see Table 4.16. On the other hand, with the MLE method, the same quantile

increases by 15,74% if only the failures are considered, and it increases by 18,03% if the failures and runouts are taken into account, see Table 4.17.

b) Comparing the Wöhler curves given by applying the Weibull model with those used as reference in Eurocode 3 shows that the reference curve of Eurocode 3 is more conservative. At 5 million load cycles the differences are 8,8 MPa and 11,1 MPa with the PWM method and 9,4 MPa and 11,2 MPa with the MLE method, see Figures 4.14 - 4.17. Moreover, the constant slope $m = 3$ proposed in Eurocode 3 does not describe the behaviour shown by the experimental data.

c) The confidence intervals for the stress range given by the Weibull model are considerably tighter than those given by the Basquin model, see the Table 4.15. On the one hand, by applying the PWM method, the 90% interval at 10 millions load cycles is reduced by 18,56% if only the failures are considered, and it is reduced by 16,20% if the failures and runouts are taken into account, see Table 4.16. On the other hand, with the MLE method, the same interval is reduced by 21,46% if only the failures are considered, and it is reduced by 18,22% if the failures and runouts are taken into account, see Table 4.17.

4.7.2 Specimens of 49MnVS3

In this example, the experimental fatigue data have been taken from [137] and they correspond to 20 hourglass shaped samples of radius $\phi = 6$ mm made from untempered steel 49MnSV3 with an ultimate tensile strength $R_m = 840$ MPa and a yield strength $R'_{p0.2} = 520$ MPa. Since this steel is used on the automotive industry, the experimental results cannot be compared with the criteria proposed in the Eurocode 3. The corresponding data which include 4 runouts are shown on Tables 4.18and 4.19.

49MnVS3 Untempered steel - Failures $\mathbf{R = -1,0}$	
$\mathbf{\Delta\sigma}$ [MPa]	$\mathbf{N}$ [-]
761,3	246
751,0	250
751,7	270
638,0	1 290
637,0	1 250
613,3	1 160
555,2	4 250
547,1	3 300
546,4	3 800
451,2	35 000
449,8	21 000
420,9	60 000
420,2	95 000
403,0	150 000
393,9	284 000
379,5	780 000

Table 4.18: Steel 49MnVS3. Fatigue data of failures - Experimental results.

49MnVS3 Untempered steel - Runots $\mathbf{R = -1,0}$			
		PWM	**MLE**
$\mathbf{\Delta\sigma}$ [MPa]	$\mathbf{N}$ [-]	$\mathbf{E(N)}$ [-]	$\mathbf{E(N)}$ [-]
390,1	2 209 000	2 276 268	2 817 812
387,3	11 112 700	11 190 592	11 218 783
384,9	4 136 000	4 230 689	4 242 873
379,1	5 083 600	5 236 743	5 250 698

Table 4.19: Steel 49MnVS3. Fatigue data of runouts - Experimental results and estimations of the lifetime of the runouts $E(N_1)$. The values of $E(N_1)$ are plotted in blue on Figures 4.20 and 4.21.

Results and analysis

The results presented in Table 4.20 show that both the PWM and the MLE methods give different values for the estimation of the Weibull parameters a, b and c, no matter which type of data are considered. However, the estimation of the geometrical parameters B and C is identical when the same type of data are considered. This fact can be appreciated in the similar geometry of the Wöhler curves in the Figures 4.18 and 4.19 which consider only the failures.

49MnVS3 Untempered steel Parameter estimation				
Parameter	**PWM**		**MLE**	
	F	F-RO	F	F-RO
Geometrical parameters				
B	0,00	0,63	0,00	0,63
C	5,40	5,55	5,40	5,55
N_{min} [-]	1	2	1	2
$\Delta\sigma_\infty$ [MPa]	221,46	258,00	221,46	258,01
m	10,55			
Weibull parameters				
a	5,53	4,62	6,07	4,99
b	1,82	1,01	1,27	0,50
c	6,81	2,48	5,05	0,85

Table 4.20: Steel 49MnVS3. Parameter estimation - Geometrical and Weibull parameters. The corresponding Wöhler curves are shown from Figures 4.18 to 4.21.

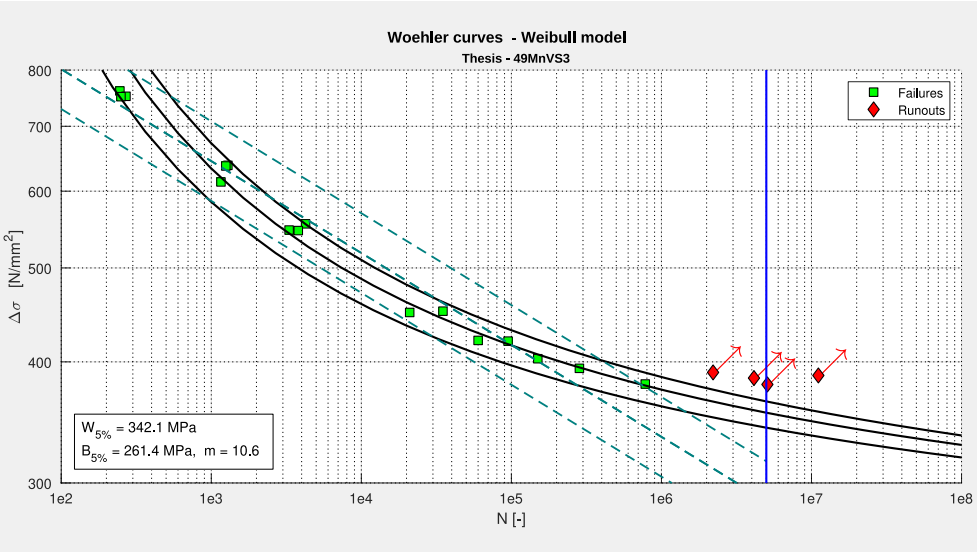

Figure 4.18: Steel 49MnVS3. PWM-Wöhler curves. Failures - The curves represent the quantiles corresponding to a failure probability of 5, 50 and 95 percent.

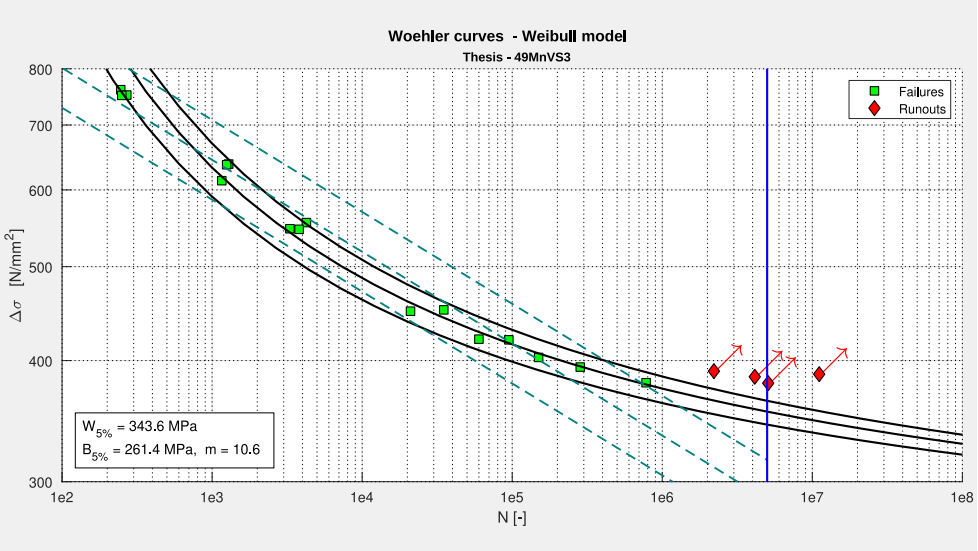

Figure 4.19: Steel 49MnVS3. MLE-Wöhler curves. Failures - The curves represent the quantiles corresponding to a failure probability of 5, 50 and 95 percent.

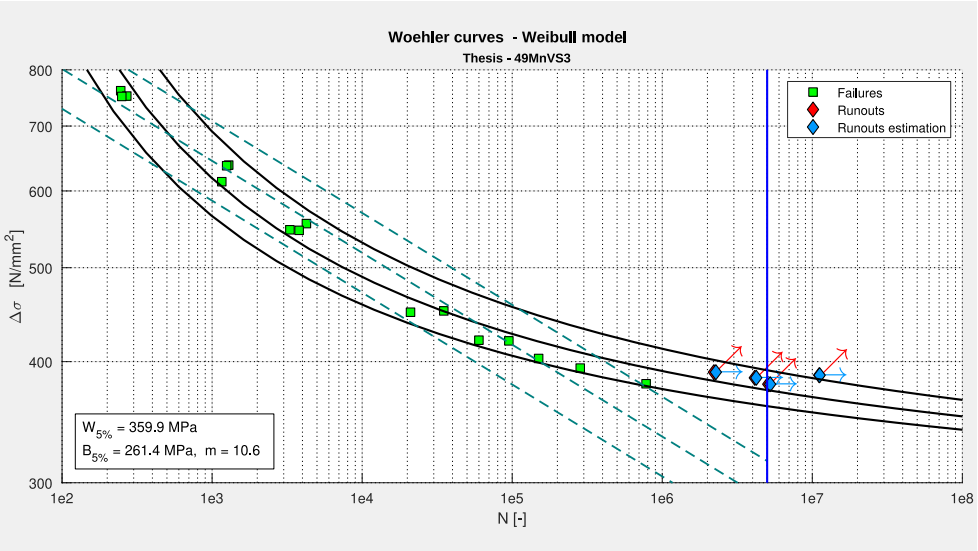

Figure 4.20: Steel 49MnVS3. PWM-Wöhler curves. Failures and runouts - The curves represent the quantiles corresponding to a failure probability of 5, 50 and 95 percent.

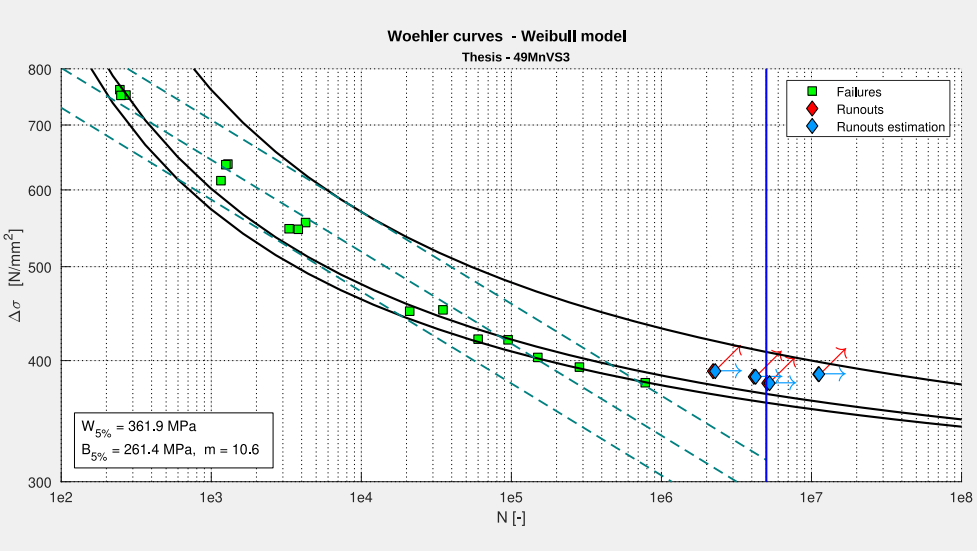

Figure 4.21: Steel 49MnVS3. MLE-Wöhler curves. Failures and runouts - The curves represent the quantiles corresponding to a failure probability of 5, 50 and 95 percent.

49MnVS3 Untempered steel Quantiles and CIs values $\mathbf{N = 5 \cdot 10^6}$ cycles				
	PWM		**MLE**	
Prob.	F	F-RO	F	F-RO
[%]	[MPa]	[MPa]	[MPa]	[MPa]
Weibull model				
W_5	342,10	359,85	343,57	361,92
W_{50}	354,49	373,83	354,32	369,53
W_{95}	364,13	391,88	363,55	408,26
CI_{W90}	22,03	32,03	19,98	46,34
Basquin model				
B_5	261,42	–	261,42	–
B_{50}	287,36	–	287,36	–
B_{95}	315,87	–	315,87	–
CI_{B90}	54,45	–	54,45	–

Table 4.21: Steel 49MnVS3. Quantiles and CIs - Estimations corresponding to the models of Weibull and Basquin. See Figures 4.18 to 4.21.

49MnVS3 Untempered steel PWM - Quantiles and CIs comparisons $\mathbf{N = 5 \cdot 10^6}$ cycles				
	F		**F-RO**	
Prob. [%]	$\mathbf{d_a(W,B)}$ [MPa]	$\mathbf{d_p(W,B)}$ [%]	$\mathbf{d_a(W,B)}$ [MPa]	$\mathbf{d_p(W,B)}$ [%]
(W_5, B_5)	80,68	30,86	98,43	37,65
(W_{50}, B_{50})	67,13	23,36	86,48	30,09
(W_{95}, B_{95})	48,26	15,28	76,00	24,06
(CI_{W90}, CI_{B90})	32,42	59,54	22,42	41,18

Table 4.22: Steel 49MnVS3. PWM-Quantiles and CIs - Absolute and percentage differences between the models of Weibull and Basquin. See Figures 4.18 and 4.20.

49MnVS3 Untempered steel MLE - Quantiles and CIs comparisons $\mathbf{N = 5 \cdot 10^6}$ cycles				
	F		**F-RO**	
Prob. [%]	$\mathbf{d_a(W,B)}$ [MPa]	$\mathbf{d_p(W,B)}$ [%]	$\mathbf{d_a(W,B)}$ [MPa]	$\mathbf{d_p(W,B)}$ [%]
$(W_5 - B_5)$	82,15	31,42	100,51	38,45
$(W_{50} - B_{50})$	66,96	23,30	82,17	28,60
$(W_{95} - B_{95})$	47,68	15,09	92,39	29,25
$(CI_{W90} - CI_{B90})$	34,47	63,30	8,12	14,91

Table 4.23: Steel 49MnVS3. MLE-Quantiles and CIs - Absolute and percentage differences between the models of Weibull and Basquin. See Figures 4.19 and 4.21.

In this application, the advantages of considering the runouts influence in the modelling of the Wöhler curves by applying the Weibull model are more evident and they can be summarized as follows:

a) The consideration of four runouts and their influence offer the opportunity to see clearly how the curves get closer to the theoretical endurance limit as far the number of cycles grows. It means the asymptotic behaviour of the Wöhler curves is better described, see Figures 4.18 to 4.21.

b) By applying the Weibull model, the estimations of the quantiles in the HCF region are considerably higher than those given by the Basquin model, see Table 4.21. On the one hand, at 5 millions load cycles by applying the PWM method the 5% quantile increases by 30,86% if only the failures are considered, and it increases by 37,65% if the failures and runouts are taken into account, see Table 4.22. On the other hand, with the MLE method, the same quantile

increases by 31,42% if only the failures are considered, and it increases by 38,45% if the failures and runouts are taken into account, see Table 4.23.

c) The confidence intervals for the stress range given by the Weibull model are much tighter than those given by the Basquin model, see Table 4.21. On the one hand, at 5 millions load cycles by applying the PWM method, the 90% interval is reduced by 59,54% if only the failures are considered, and it is reduced by 41,18% if the failures and runouts are taken into account, see Table 4.22. On the other hand, with the MLE method, the same interval is reduced by 63,30% if only the failures are considered, and it is reduced by 14,91% if the failures and runouts are taken into account, see Table 4.23.

From the engineering design point of view, these advantages allow obtaining more confidence and accuracy in the estimation of the lifetime of a structure under cyclic loading.

The two applications presented in this section prove the importance of considering the runouts in the evaluation of fatigue data and in the modelling of the Wöhler curves. In both cases, the 5% quantiles given by the Weibull model are higher than those given by the Basquin model. While the Wöhler curves obtained by applying the Basquin model need changing their slope and defining two knee points in order to describe the asymptotic behaviour of the fatigue lifetime, the curves given by the Weibull model are self asymptotic and allow to estimate the fatigue limit. Moreover, the confidence intervals given by the Weibull model are tighter than those obtained by the Basquin model.

4.8 Fatigue tests containing failures, runouts and retested runouts

Since the Weibull model was proposed, its main goal has been obtaining accurate and reliable estimations for the lifetime of a structure by taking into consideration all of the experimental information from the fatigue tests. Besides the failures, this information can be provided by the runouts and retested runouts according to the following procedures:

- Estimating the number of cycles in which a runout could have failed. This fact allows to consider its influence in the geometry of the Wöhler curves and their corresponding quantiles, see Section 3.5.

- Estimating the damage accumulation of a runout and its corresponding damage equivalence under a higher stress range. This fact allows to consider the influence of a subsequent fatigue test, see Section 3.8.

In this section two general applications of the Weibull model are presented, and their data belong to two different specimens: welded specimens of steel S690QL from the REFRESH project and specimens of steel S355J2+N from a fatigue research project which was funded by the German Research Foundation DFG[3].

4.8.1 Specimens of S690QL

In this case 12 welded specimens from steel S690QL which received an ultrasonic impact treatment (UIT) after welding are considered [125]. The specimens belong to the REFRESH project [83]. The main properties of the specimens are described in Table 4.24 and their geometry is shown in Figure 4.22.

L1-16-S690QL-KS	
Properties	
Project	REFRESH
Material	S690QL
Minimum yield strength R_{eH}	690 MPa
Treatment	Ultrasonic impact treatment (UIT)
Thickness	16 mm
Geometry	see Figure 4.22
Nr. of Samples	12

Table 4.24: Steel S690QL. Properties - Corresponding to the tested specimens.

L1-16-S690QL-KS - Failures			
$\mathbf{R = 0,1}$			
$\mathbf{\Delta\sigma}$		$\mathbf{N}$	
[MPa]		[-]	
270	83 500	–	–
198	332 000	299 300	163 500
162	842 200	496 300	455 800
126	921 700	1 085 300	1 940 500

Table 4.25: Steel S690QL. Fatigue data of failures - Experimental results.

[3] Deutsche Forschungsgemeinschaft

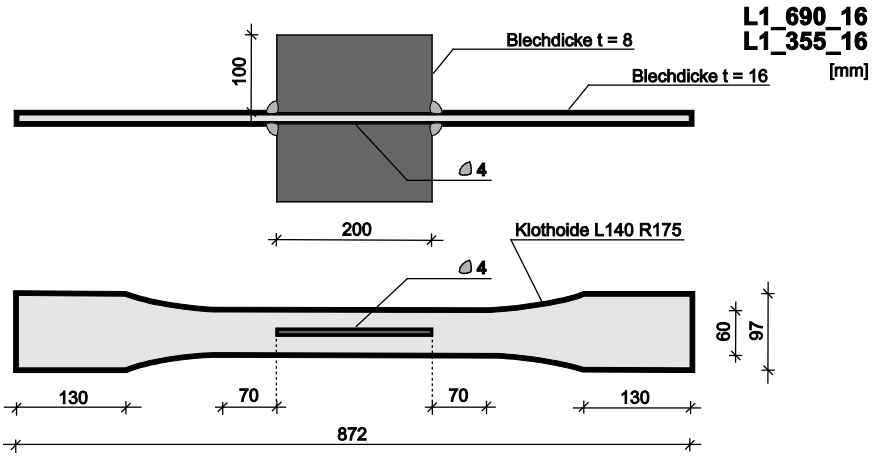

Figure 4.22: Steel S690QL. Specimens - Geometry and measurements.

L1-16-S690QL-KS - Runots $\mathbf{R = 0,1}$							
		PWM	**MLE**		**PWM**	**MLE**	
$\mathbf{\Delta\sigma_1}$	$\mathbf{N_1}$	$\mathbf{E(N_1)}$	$\mathbf{E(N_1)}$	$\mathbf{\Delta\sigma_2}$	$\mathbf{E(N_{acc})}$	$\mathbf{E(N_{acc})}$	$\mathbf{N_2}$
[MPa]	[-]	[-]	[-]	[MPa]	[-]	[-]	[-]
90	5 000 000	8 383 377	5 722 316	198	154 838	190 895	229 900
	5 000 000	12 848 154	9 404 223		154 838	190 895	163 500

Table 4.26: Steel S690QL. Fatigue data of runouts and retests - Experimental results and estimations of the lifetime of the runouts $E(N_1)$ and their damage accumulation $E(N_{acc})$. The values of $E(N_1)$ are plotted in blue and the values of $E(N_{acc}) + N_2$ are plotted in yellow, see Figures 4.25 to 4.28.

Results and analysis

Applying the Weibull model to evaluate these few fatigue data has been done in order to see how important the amount of available data is.

The estimation of the geometrical parameter B varies considerably depending on which estimation method and data are considered. The effects of B can be seen in the variation of the threshold N_{min} which is 199 cycles when the failures and runouts are considered by the PWM method and becomes 342 cycles when the failures, runouts and retested runouts are considered by the MLE method, see Table 4.27. This variation may be caused because at the higher experimental stress range of 270 MPa only one data is available.

The estimation of the geometrical parameter C does not vary too much, so that the fatigue limit $\Delta\sigma_\infty$ varies from 18,06 MPa to 22,05 MPa. This situation can be

explained by the presence of three data failures at the lowest experimental stress range and by the availability of two runouts and their retests, see Table 4.27.

The estimated Weibull parameters a, b and c vary depending on which estimation method and data are considered as well. The parameter a varies considerably in the case when the runouts are taken into account. However, when the runouts and retests are considered the value of a is very similar to that obtained only from the failures. The parameters b and c change significantly when all together, the failures, runots and retests are considered.

Regarding the geometry of the Wöhler curves, when the PWM method is applied, the geometry in the three cases concerning to the data selection does not change significantly, see Figures 4.23, 4.25 and 4.27. On the other hand, when the MLE method is applied, the 95% quantile increases when the considered data do not include the retests, see Figures 4.24 and 4.26. In this case, this behaviour may be caused because the estimated parameter a increases and combined with a probability $p = 0.95$ moves the corresponding quantile up, for a detailed explanation of this situation see Section 3.2. As it will be explained below, this affects to the size of the confidence intervals.

L1-16-S690QL-KS						
Parameter estimation						
Parameter	**PWM**			**MLE**		
	F	F-RO	F-RO-RT	F	F-RO	F-RO-RT
Geometrical parameters						
B	5,83	5,30	5,45	5,83	5,65	5,84
C	3,09	2,99	2,96	3,09	2,93	2,89
N_{min} [-]	340	199	233	340	284	342
$\Delta\sigma_\infty$ [MPa]	22,05	19,88	19,38	22,05	18,69	18,06
m	3,56					
Weibull parameters						
a	12,74	14,61	12,57	13,56	15,00	13,15
b	1,95	1,97	4,09	0,79	0,96	3,18
c	2,59	2,77	6,22	0,60	0,70	4,73

Table 4.27: Steel S690QL. Parameter estimation - Geometrical and Weibull parameters. The corresponding Wöhler curves are shown in Figures 4.23 to 4.28.

Besides the differences in the estimation of the parameters explained above, it is important to keep in mind that a single Wöhler curve based on the Weibull model is defined by six parameters: the probability of failure p, the geometrical parameters B, C and the Weibull parameters a, b and c , see Equation (3.31). For this reason, in order to understand better the estimation results, it is suggested to analyze the

values of the quantiles and the sizes of the confidence intervals which are given in Tables 4.28 to 4.30.

Comparing the results of the Weibull model with those of the Basquin model, the differences are considerable. Tables 4.29 and 4.30 show the quantiles and confidence intervals by 5 millions load cycles. The Weibull quantiles are higher than those from Basquin.

When the PWM method is applied considering only the failures, the 5% quantile is 29,78% higher than the quantile obtained by Basquin and the confidence interval is 39,18% tighter. When the MLE method is applied, the 5% quantile from Weibull is 32,55% higher than the quantile from Basquin. Since the MLE estimation of 95% quantile of Weibull W_{95} is high, the confidence interval from Weibull is 46,59% wider than the Basquin one, see Figure 4.24.

When the PWM method is applied on the failures and runouts, the 5% quantile is 31,50% higher than the quantile obtained by Basquin, and the confidence interval is 44,80% tighter than the Basquin one, see Figure 4.25. When the MLE method is applied, the 5% quantile is 27,01% higher than the quantile obtained by Basquin. The MLE estimation of the 95% quantile of Weibull W_{95} is also high, then the confidence interval from Weibull is 26,81% wider than the Basquin one, see Figure 4.26.

In the general case, when the PWM method is applied on all of the availabla data, the 5% quantile is 28,86% higher than the quantile obtained by Basquin, and the confidence interval is 42,84% tighter, see Figure 4.27. When the MLE method is applied, the 5% quantile is 24,23% higher than the quantile obtained by Basquin and the confidence interval from Weibull is 43,10% tighter, see Figure 4.28. Comparing the Wöhler curves given by applying the Weibull model with those used as reference in Eurocode 3 shows that the reference curve of Eurocode 3 is more conservative. At 5 million load cycles the differences are 32,7 MPa, 33,9 MPa and 32,1 MPa with the PWM method and 34,6 MPa, 30,8 MPa and 28,9 MPa with the MLE method, see Figures 4.23-4.28. In this case, the constant slope $m = 3$ proposed in Eurocode 3 describes the behaviour shown by the experimental data.

Despite the fact that few experimental data are available, the Wöhler curves given by the Weibull model show the expected asymptotic behaviour of the fatige lifetime. Moreover, the 5% Weibull quantiles allow to assure a higher fatigue lifetime of the specimens than the 5% Basquin quantiles.

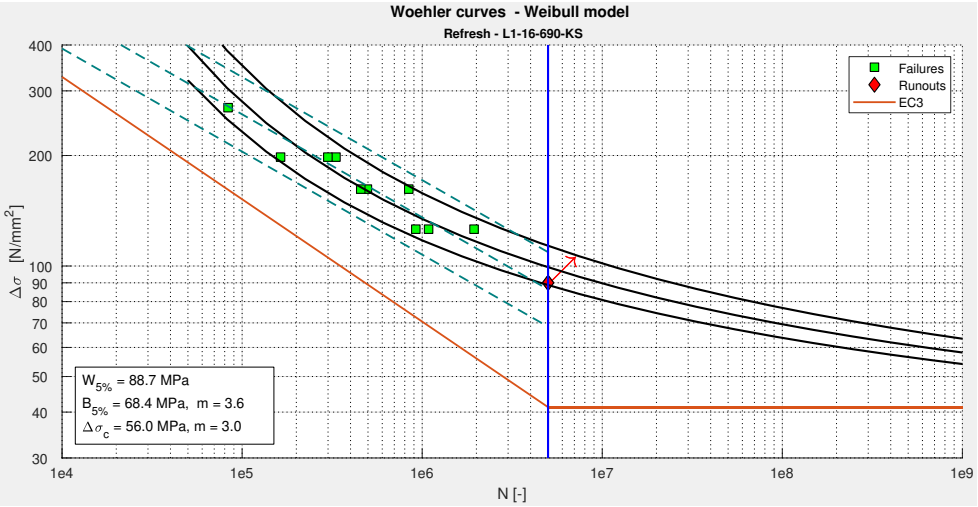

Figure 4.23: Steel S690QL. PWM-Wöhler curves. Failures - The curves represent the quantiles corresponding to a failure probability of 5, 50 and 95 percent.

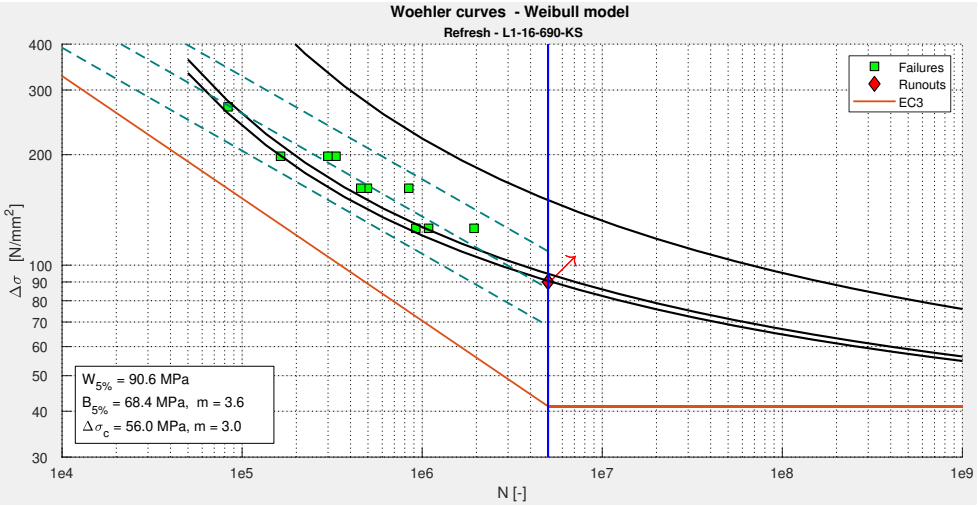

Figure 4.24: Steel S690QL. MLE-Wöhler curves. Failures - The curves represent the quantiles corresponding to a failure probability of 5, 50 and 95 percent.

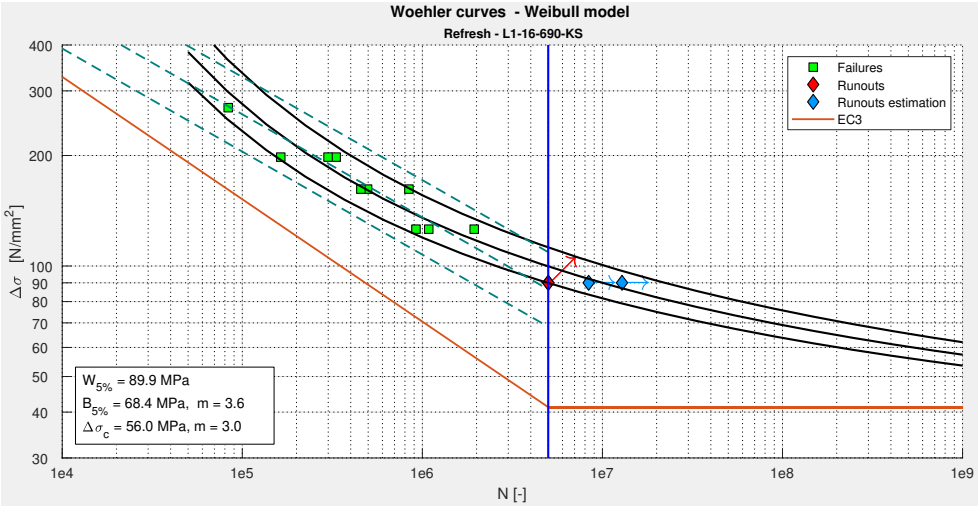

Figure 4.25: Steel S690QL. PWM-Wöhler curves. Failures and runouts - The curves represent the quantiles corresponding to a failure probability of 5, 50 and 95 percent.

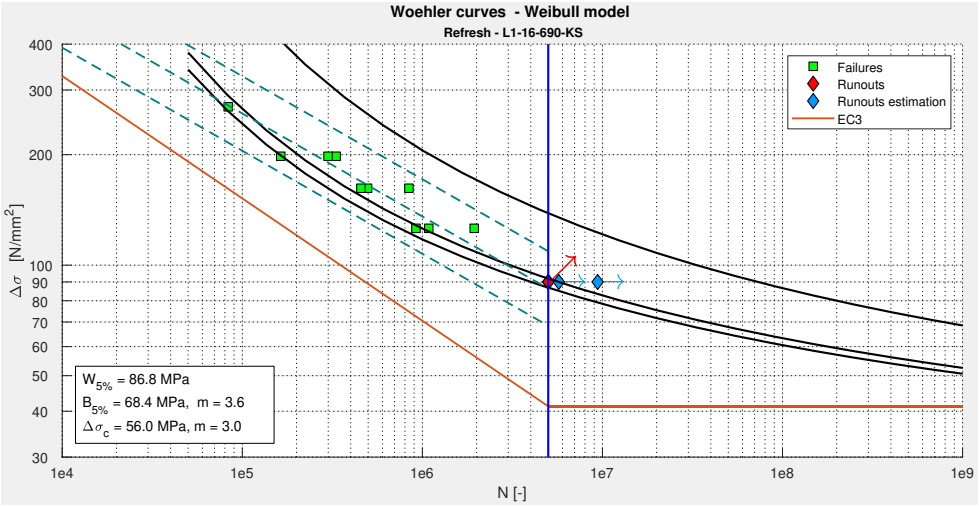

Figure 4.26: Steel S690QL. MLE-Wöhler curves. Failures and runouts - The curves represent the quantiles corresponding to a failure probability of 5, 50 and 95 percent.

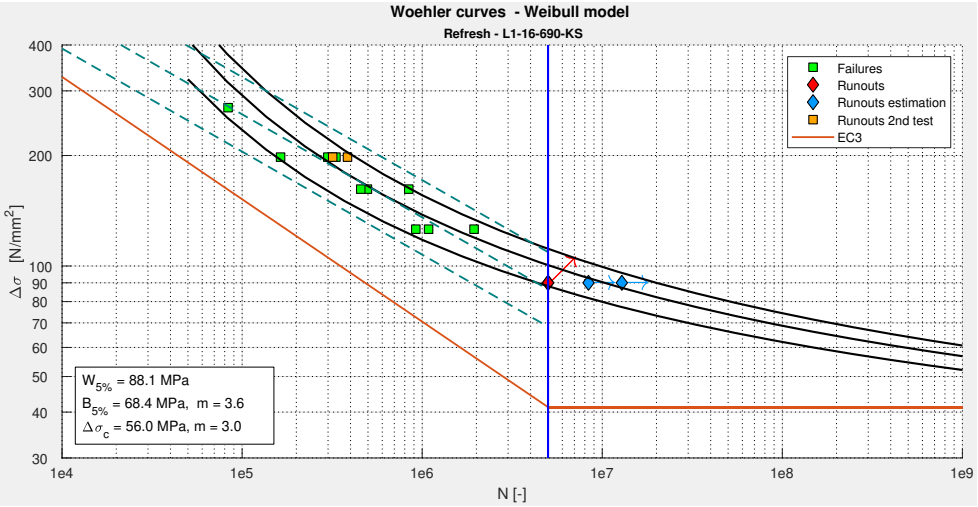

Figure 4.27: Steel S690QL. PWM-Wöhler curves. Failures, runouts and retested runouts - The curves represent the quantiles corresponding to a failure probability of 5, 50 and 95 percent.

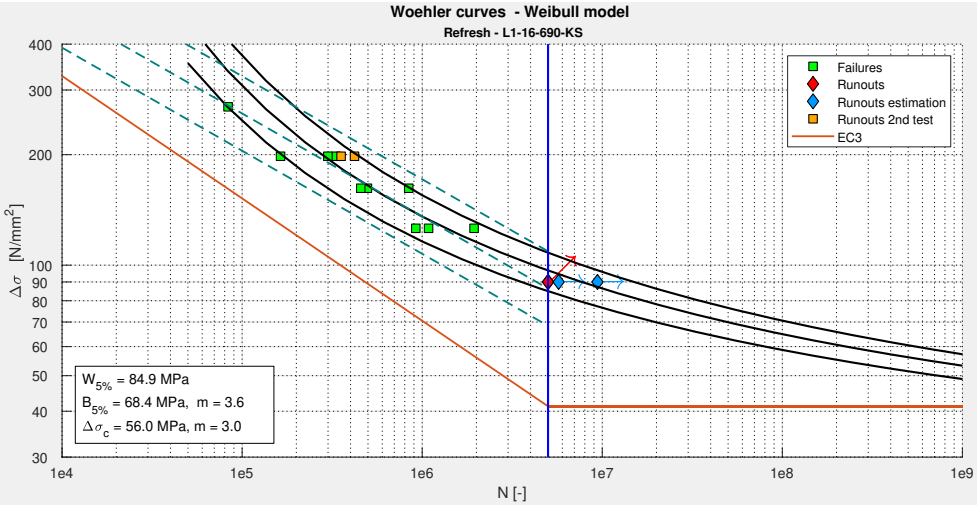

Figure 4.28: Steel S690QL. MLE-Wöhler curves. Failures, runouts and retested runouts - The curves represent the quantiles corresponding to a failure probability of 5, 50 and 95 percent.

L1-16-S690QL-KS Quantiles and CIs values $\mathbf{N = 5 \cdot 10^6}$ cycles						
	PWM			**MLE**		
Prob.	F	F-RO	F-RO-RT	F	F-RO	F-RO-RT
[%]	[MPa]	[MPa]	[MPa]	[MPa]	[MPa]	[MPa]
Weibull model						
W_5	88,72	89,89	88,08	90,61	86,82	84,92
W_{50}	99,24	99,75	100,52	94,69	91,89	96,70
W_{95}	113,49	112,37	111,36	150,32	138,47	108,09
CI_{W90}	24,77	22,48	23,28	59,71	51,65	23,17
Basquin model						
B_5	68,36	–	–	68,36	–	–
B_{50}	86,35	–	–	86,35	–	–
B_{95}	109,09	–	–	109,09	–	–
CI_{B90}	40.73	–	–	40,73	–	–

Table 4.28: Steel S690QL. Quantiles and CIs estimations - Corresponding to the models of Weibull and Basquin by $N = 5 \cdot 10^6$. See Figures 4.23 to 4.28.

L1-16-S690QL-KS PWM - Quantiles and CIs comparisons $\mathbf{N = 5 \cdot 10^6}$ cycles						
	F		**F-RO**		**F-RO-RT**	
Prob.	$\mathbf{d_a(W,B)}$	$\mathbf{d_p(W,B)}$	$\mathbf{d_a(W,B)}$	$\mathbf{d_p(W,B)}$	$\mathbf{d_a(W,B)}$	$\mathbf{d_p(W,B)}$
[%]	[MPa]	[%]	[MPa]	[%]	[MPa]	[%]
(W_5, B_5)	20,36	29,78	21,53	31,50	19,73	28,86
(W_{50}, B_{50})	12,88	14,92	13,40	15,52	14,17	16,41
(W_{95}, B_{95})	4,40	4,04	3,28	3,01	2,28	2,09
(CI_{W90}, CI_{B90})	15,96	39,18	18,25	44,80	17,45	42,84

Table 4.29: Steel S690QL. PWM-Quantiles and CIs comparisons - Absolute and percentage differences between the models of Weibull and Basquin. See Figures 4.23, 4.25 and 4.27.

L1-16-S690QL-KS MLE - Quantiles and confidence intervals Comparison by $\mathbf{N = 5 \cdot 10^6}$ cycles						
	F		**F-RO**		**F-RO-RT**	
Prob.	$\mathbf{d_a(W,B)}$	$\mathbf{d_p(W,B)}$	$\mathbf{d_a(W,B)}$	$\mathbf{d_p(W,B)}$	$\mathbf{d_a(W,B)}$	$\mathbf{d_p(W,B)}$
[%]	[MPa]	[%]	[MPa]	[%]	[MPa]	[%]
(W_5, B_5)	22,25	32,55	18,46	27,01	16,56	24,23
(W_{50}, B_{50})	8,34	9,65	5,54	6,41	10,35	11,99
(W_{95}, B_{95})	41,23	37,80	29,38	26,93	0,99	0,91
(CI_{W90}, CI_{B90})	18,98	46,59	10,92	26,81	17,56	43,10

Table 4.30: Steel S690QL. MLE-Quantiles and CIs comparisons - Absolute and percentage differences between the models of Weibull and Basquin. See Figures 4.24, 4.26 and 4.28.

4.8.2 Specimens of S355J2+N - DFG research project

The application presented in this subsection belong to a fatigue research project funded by the German Research Foundation (DFG).

For this research project sixty specimens were manufactured from steel S355J2+N by the Technik-Haus (TEC) of the KIT, see Figure 4.29.

Figure 4.29: Steel S355J2+N. Tested specimens - After fatigue testing.

The main properties of the material and the specimens are described in Table 4.31, and their geometry is shown in Figure 4.30. The inspection certificate of the steel is in the Annex A.3.

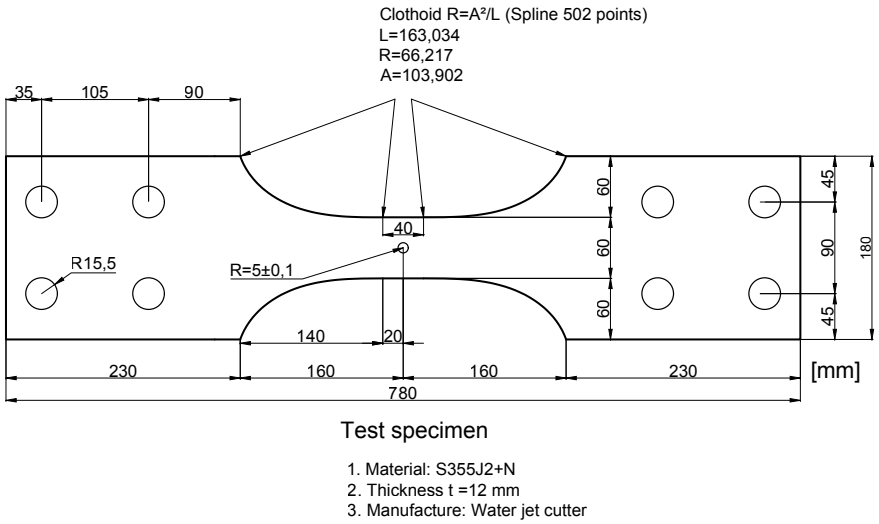

Figure 4.30: Steel S355J2+N. Specimens - Geometry and measurements.

DFG Fatigue research project **Material and specimens properties**	
Project	DFG Fatigue research
Material	S355J2+N
Minimum yield strength R_{eH}	355 MPa
Yield strength Re	440, 423, 470 MPa
Ultimate tensile strength R_m	553, 565, 557 MPa
Treatment	None
Thickness	12 mm
Geometry	Clothoid, see Figure 4.30
Cutting process	Waterjet
Nr. of Samples	60

Table 4.31: Steel S355J2+N. Properties - Corresponding to the tested specimens.

The steel specimens were axially tested under a constant stress range in a high frequency pulsator Zwick/Roell Typ HFP 5100, see Figure 4.31. The average of the frequency during the test was 105 Hz. From the sixty manufactured specimens, only fiftyone could be tested in a proper way. This situation occured because some setting and technical problems were present in the pulsator.

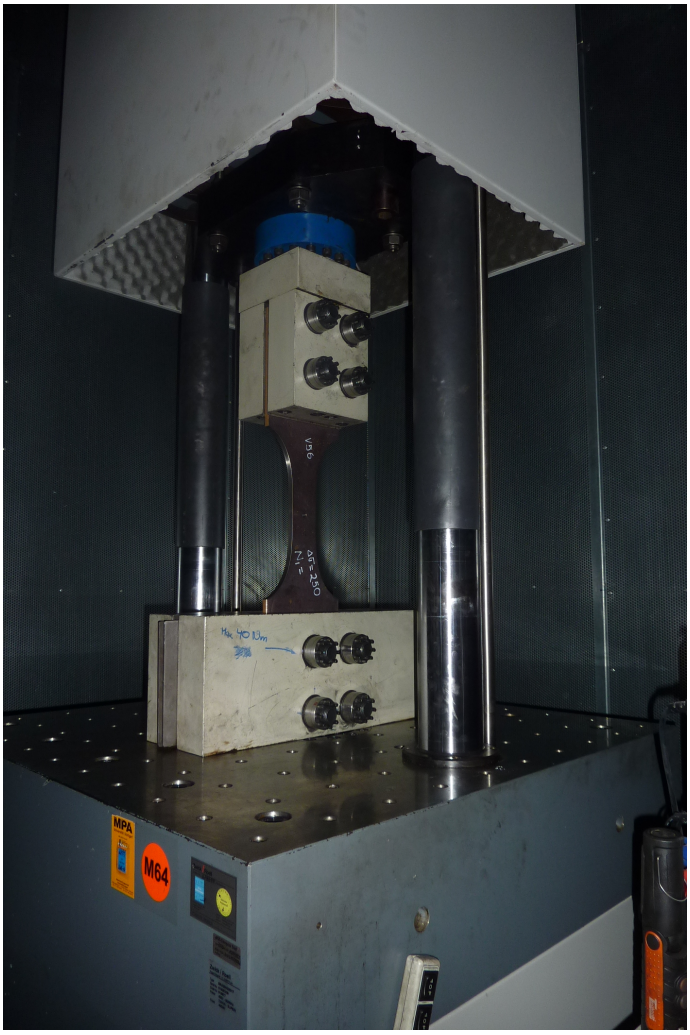

Figure 4.31: DFG research project. Fatigue test setup - High frequency pulsator Zwick/Roell Typ HFP 5100.

DFG Fatigue research project - Runots $\mathbf{R = 0,1}$							
		PWM	MLE		PWM	MLE	
$\Delta\sigma_1$ [MPa]	$\mathbf{N_1}$ [-]	$\mathbf{E(N_1)}$ [-]	$\mathbf{E(N_1)}$ [-]	$\Delta\sigma_2$ [MPa]	$\mathbf{E(N_{acc})}$ [-]	$\mathbf{E(N_{acc})}$ [-]	$\mathbf{N_2}$ [-]
250	39 644 083	51 824 154	49 139 485	265	13 128 645	12 686 384	428 667
	54 550 363	70 609 565	66 869 468	265	17 704 471	17 097 372	822 009
244	25 000 000	34 170 462	32 538 061	265	5 442 589	5 191 283	255 017
	90 000 000	119 199 655	110 916 285	250	53 782 813	52 872 201	41 902 329
240	25 000 000	30 483 974	29 662 600	250	11 180 923	10 886 468	1 170 333
	25 000 000	42 178 607	39 150 003	265	4 010 906	3 789 669	458 052
	89 296 811	118 298 671	111 877 711	250	37 605 903	36 542 574	622 427
	90 000 000	119 199 655	112 725 976	244	62 762 487	61 994 447	1 452 254
230	40 000 000	58 354 003	55 825 273	250	7 388 655	6 986 144	885 248
	60 000 000	85 406 107	81 287 551	240	23 773 699	23 018 531	1 462 162
200	5 000 004	204 476 599	660 684 595	250	93 154	81 627	604 446
	35 000 004	213 646 460	245 218 765	250	394 534	339 997	350 961
	60 000 004	214 914 387	224 461 928	250	588 470	504 790	936 489

Table 4.33: Steel S355J2+N. Fatigue data of runouts and retests - Experimental results and estimations of the lifetime of the runouts $E(N_1)$ and their damage accumulation $E(N_{acc})$. The values of $E(N_1)$ are plotted in blue and the values of $E(N_{acc}) + N_2$ are plotted in yellow, see Figures 4.40 to 4.43.

DFG Fatigue research project - Failures $\mathbf{R = 0,1}$				
$\Delta\sigma$ [MPa]	$\mathbf{N}$ [-]			
320	138 935	142 615	143 586	153 708
	161 375	172 720	–	–
300	152 436	210 540	211 394	238 157
	240 615	293 426	327 781	–
280	283 698	332 766	380 918	398 138
	449 557	451 540	621 402	–
265	385 488	430 018	496 605	509 252
	581 821	658 281	986 474	1 283 326
250	967 485	1 082 144	1 298 494	1 396 809
	1 509 958	1 699 609	1 911 722	–
244	12 018 356	20 405 452	35 951 206	–

Table 4.32: Steel S355J2+N. Fatigue data of failures - Experimental results.

Since the target of the investigation was considering the runouts and their subsequent retests on the evaluation of fatigue data, some tests were performed by applying a determined stress range that did not lead to the failure of the specimen. From the statistical point of view, the runouts are censored Type-I data, see subsection 4.2.1.
In case of one specimen did not fail up to reach a determined number of load cycles, it was tested again under a higher stress range until its failure. From the fifty one specimens tested on the pulsator, thirteen specimens became runouts. The fatigue data corresponding to the failures are shown in Table 4.32, while the data corresponding to the runouts and their retests are shown in Table 4.33. Additionaly, Table 4.33 contains the estimations of lifetime of the runouts $E(N_1)$, see Section 3.5 and the damage accumulation of the first fatigue test $E(N_{acc})$, see Section 3.8.

Results and analysis

The visualization of the experimental data shown in Figure 4.32 depicts the typical scatter of fatigue data. It means, that the scatter of the fatigue lifetime increases while decreasing the stress range. Particulary, this fact is evident in the region of normal stresses lower or equal than 250 MPa where the thirteen runouts were obtained.

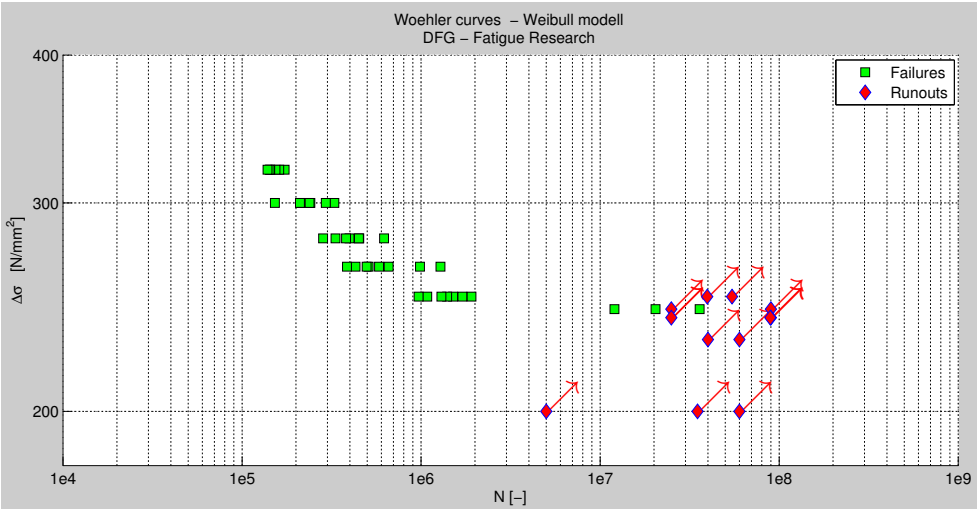

Figure 4.32: Steel S355J2+N. Experimental data. - A considerable scatter of the fatigue lifetime can be seen when the stress range is lower than 250 MPa. Precisely below this stress range the runouts were obtained.

DFG Fatigue research project Parameter estimation						
Parameter	**PWM**			**MLE**		
	F	F-RO	F-RO-RT	F	F-RO	F-RO-RT
Geometrical parameters						
B	0,99	0,00	0,00	0,99	0,00	0,00
C	4,65	4,66	4,65	4,65	4,69	4,67
N_{min} [-]	3	1	1	3	1	1
$\Delta\sigma_{\infty}$ [MPa]	104,99	105,35	104,31	104,99	108,31	107,23
m	12,01					
Weibull parameters						
a	10,99	11,84	11,61	10,89	11,51	11,26
b	0,95	1,39	2,07	1,08	1,25	2,02
c	1,49	1,20	1,55	1,72	1,04	1,65

Table 4.34: Steel S355J2+N. Parameter estimation - Geometrical and Weibull parameters. The corresponding Wöhler curves are shown in Figures 4.38 to 4.43.

The estimated parameters of the Weibull model are shown in Table 4.34.

In this application there is no significant variation in the estimation of the geometrical parameters. The geometrical parameter B is 0,99 when only the failures are considered, and when the runouts or their retests are considered its value became zero. Then, the threshold N_{min} is between 1 and 3. The geometrical parameter C kept its value around 4,6. Then, the estimation of the fatigue limit is between 104,31 MPa and 108,31 MPa.

The Weibull parameters a, b, and c vary depending on the kind of data which are considered in the applied estimation method. These variations cause differences in the geometry of the Wöhler curves, as it has been explained in the Section 3.2.
Then, in order to appreciate the differences caused by the estimation method or by the type of considered data, it is necessary to compare their corresponding Wöhler curves. In this case, the geometry of the Wöhler curves corresponding to the probability p=0,5 is compared.

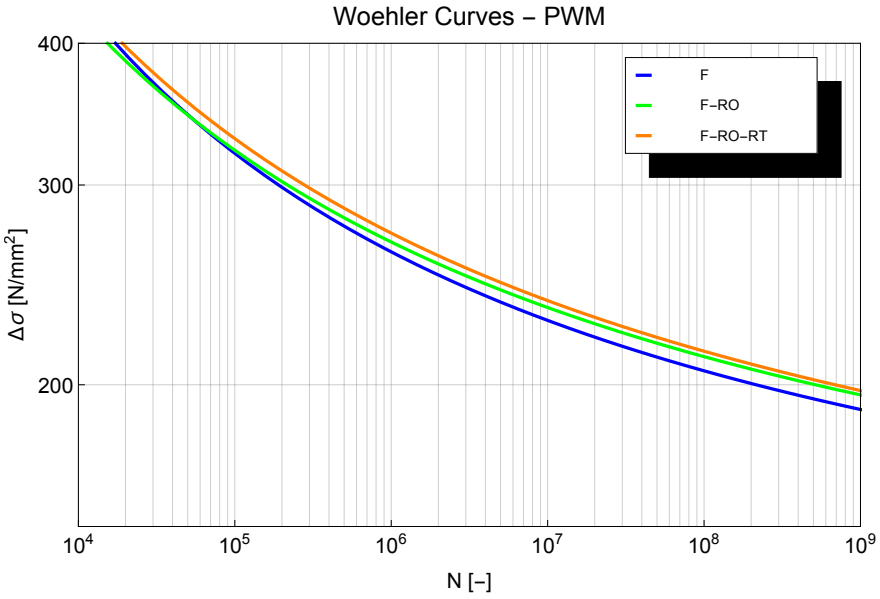

Figure 4.33: PWM Wöhler curves - Comparison depending on the considered data.

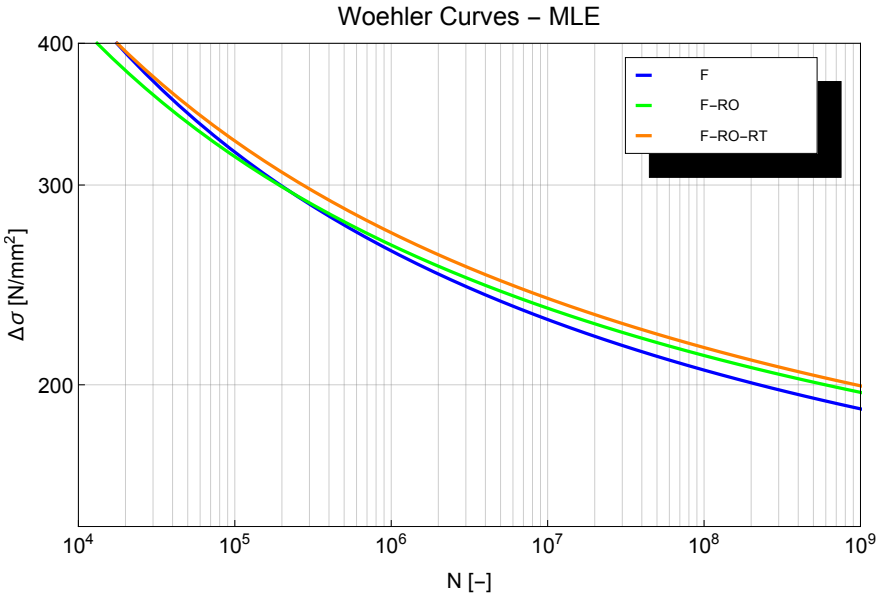

Figure 4.34: MLE Wöhler curves - Comparison depending on the considered data.

The Figures 4.33 and 4.34 show the influence of the considered data in the geometry of the Wöhler curves, according to a particular estimation method. Considering the runouts in the evaluation of fatigue data leads to higher Wöhler curves than those obtained when only the failures are taken into account. Additionally, when the retests are included in the evaluation, the Wöhler curves increase again. Hence, the estimation of the lifetime and the fatigue limit $\Delta\sigma_{\infty}$ becomes higher when the runouts and retests are considered. This fact reflects the importance and the advantage of considering the runouts and their retests on the statistical evaluation.

Besides the comparison based on the considered data, it is also possible to compare the geometry of the Wöhler curves by considering the same data but different estimation methods.

Figure 4.35 shows two Wöhler curves obtained when only the failures are considered. These curves corresponding to the PWM and MLE method are almost identical, even though the estimate Weibull parameters are slightly different, see Table 4.34.

Figure 4.36 shows the Wöhler curves corresponding to the failures and runouts. In this case, a small difference in the low cycle fatigue region can be seen. However, this difference is not relevant since the goal of the Weibull model is estimating the fatigue limit and the lifetime in the HCF and VHCF regions.

Figure 4.37 shows the Wöhler curve corresponding to the failures, runouts and retests. In this case a small difference in the extremes of the curves can be observed. This difference is not relevant either. In fact, the fatigue limit $\Delta\sigma_{\infty}$ by applying the PWM method is 104,31 MPa and for the MLE method is 107,23 MPa, see Table 4.34.

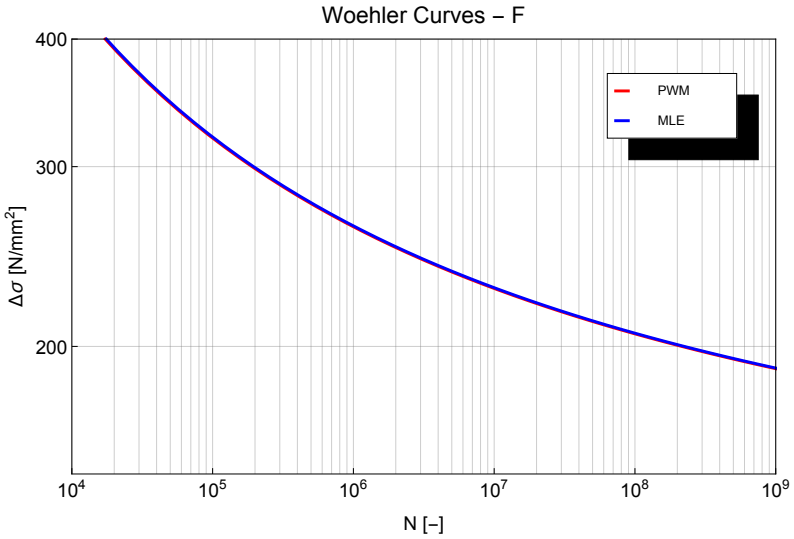

Figure 4.35: Wöhler curves geometry for fatigue failures - Comparison depending on the estimation method.

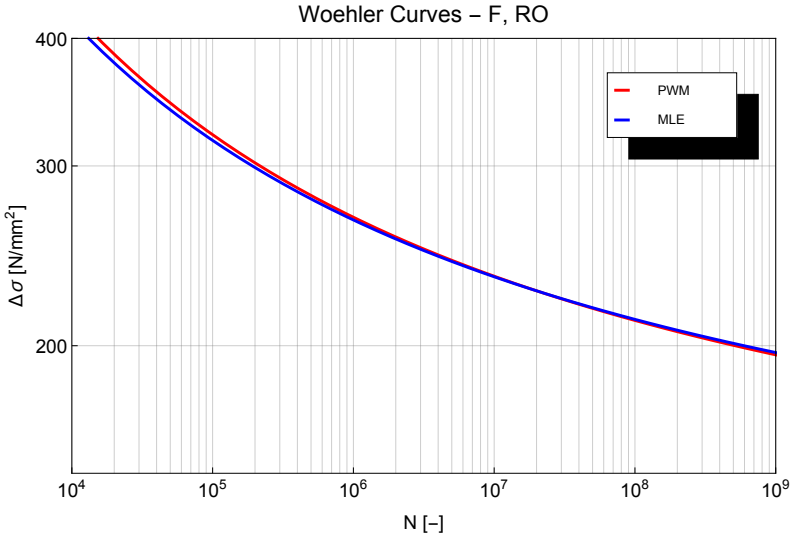

Figure 4.36: Wöhler curves geometry for fatigue failures and runouts - Comparison depending on the estimation method.

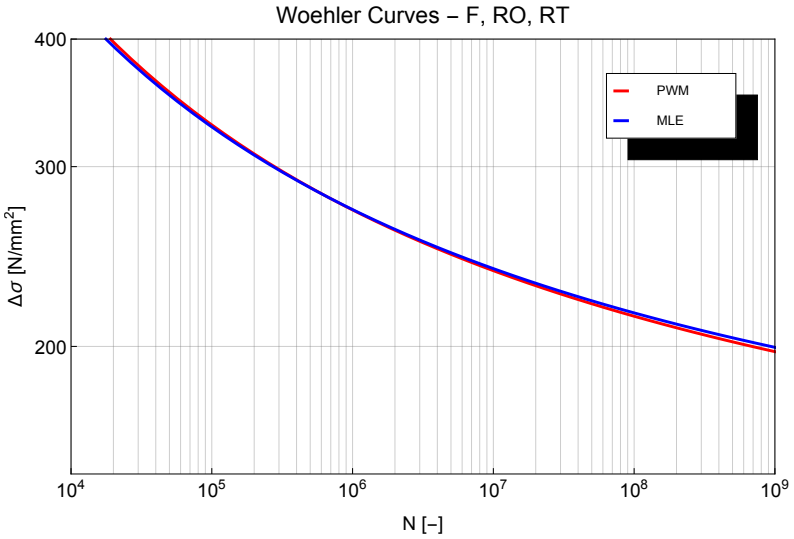

Figure 4.37: Wöhler curves geometry for fatigue failures, runouts and retests - Comparison depending on the estimation method.

These comparisons show that the geometry of Wöhler curves are quite similar independently of which statistical method is applied to estimate the model parameters.

In addition to the geometrical differences explained above, it is important to keep in mind that according to Equation (3.31) a single Wöhler curve from the Weibull model is defined by six parameters: the probability of failure p, the geometrical parameters B, C and the Weibull parameters a, b and c. For more details see Section 3.2.

For this reason, in order to evaluate the differences between the obtained Wöhler curves, it is more appropriate to analyze the values of the quantiles and the sizes of the confidence intervals. Table 4.35 shows the 5%, 50% and 95% quantiles and the 90% confidence intervals at 5 million load cycles. These values correspond to the application of the models of Weibull and Basquin.

Either by applying the PWM method or the MLE method, the quantiles corresponding to the Wöhler curves do not differ significantly. As it was mentioned before, in this case both statistical methods give similar results. The main difference between the quantiles appears when different data are considered. On the one hand, the confidence intervals are tighter when only the failures are considered. On the other hand, if the runouts and retests are considered the confidence intervals are wider. This occurs because the 95% Weibull quantile W_{95} increased when the runouts and

retests are considered, this fact is related to the scatter of the lifetime. All of these differences are depicted in the Wöhler curves in Figures 4.38 to 4.43.

Comparing the quantiles and the confidence intervals of the Weibull model with those of the Basquin model at 5 millions load cycles, gives valuable information, see Tables 4.36 and 4.37. This information allows to observe the differences and hence the advantages of applying the Weibull model in the evaluation of fatigue data.

When the PWM method is applied considering only the failures, the 5% quantile is 9,13% higher than the quantile from Basquin. When the MLE method is applied, the same quantile is 8,82% higher. The confidence interval is 39,57% tighter for both estimation methods.

When the runots and the failures are considered, the 5% quantile given by applying the PWM method is 10,05% higher than the quantile from Basquin, and the corresponding confidence interval is 8,18% wider. The MLE method gives a 5% quantile which is 10,45% higher than the quantile from Basquin and a confidence interval which is 14,73% wider.

When all of the available data are considered and the PWM method is applied, the value of the 5% quantile is 8,70% higher than the quantile from Basquin, while the MLE is applied this quantile is 9,43% higher. The confidence interval given by applying the PWM is 26,88% wider than the confidence interval from Basquin and the confidence interval obtained by applying the MLE is 16,51% wider.

Comparing the Wöhler curves given by applying the Weibull model with those used as reference in Eurocode 3 shows that the reference curve of Eurocode 3 is more conservative. At 5 million load cycles the differences are 66,7 MPa, 68,7 MPA and 65,8 MPa with the PWM method and 66,1 MPa, 69,5 MPa and 67,4 with the MLE method, see Figures 4.38-4.43. Moreover, the constant slope $m = 3$ proposed in Eurocode 3 does not describe the behaviour shown by the experimental data.

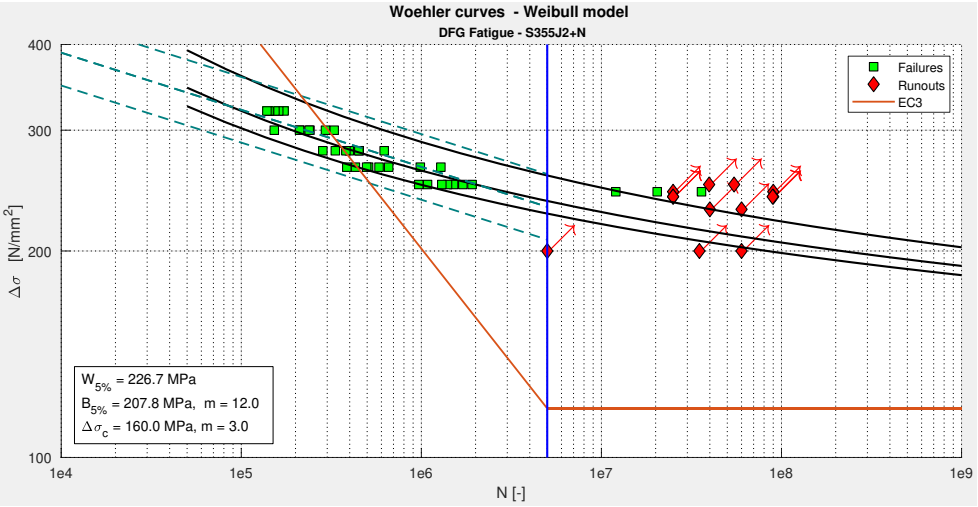

Figure 4.38: Steel S355J2+N. PWM Wöhler curves. Failures - The curves represent the quantiles corresponding to a failure probability of 5, 50 and 95 percent.

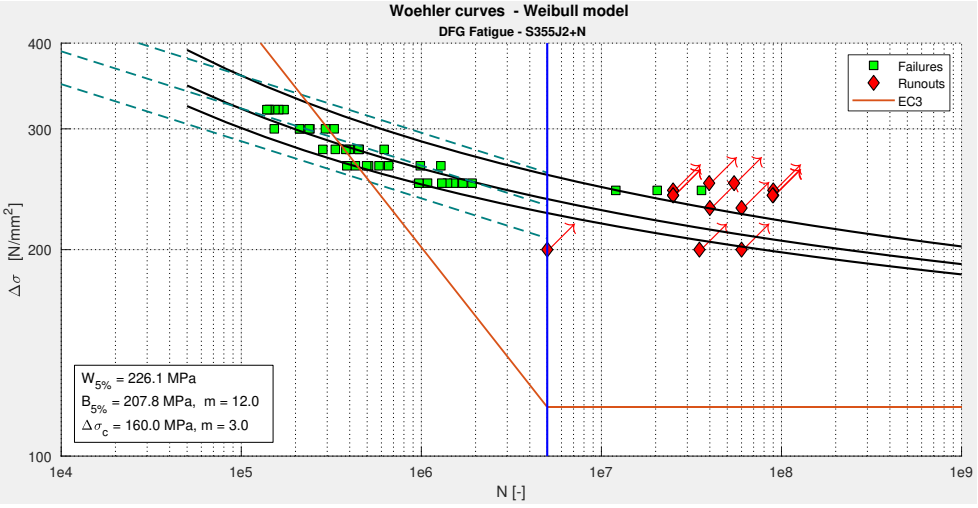

Figure 4.39: Steel S355J2+N. MLE Wöhler curves. Failures - The curves represent the quantiles corresponding to a failure probability of 5, 50 and 95 percent.

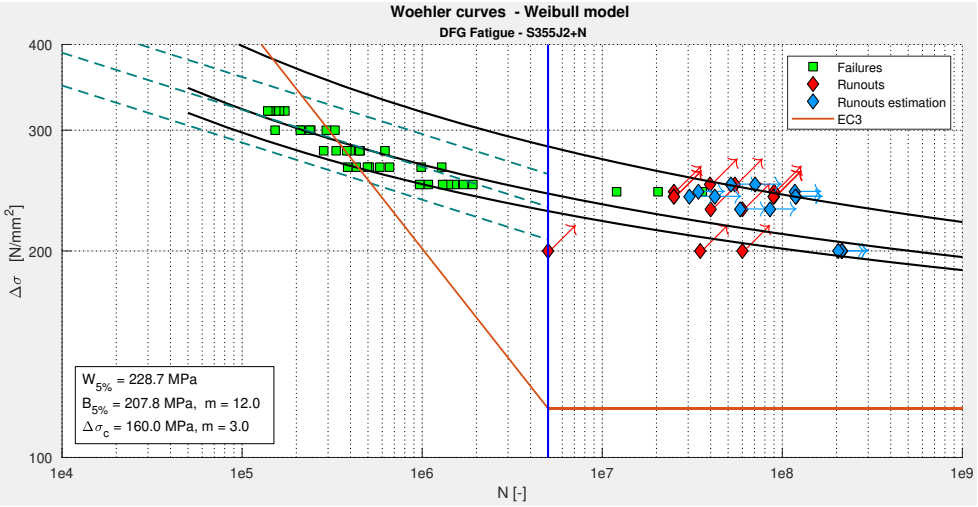

Figure 4.40: Steel S355J2+N. PWM Wöhler curves. Failures and runouts - The curves represent the quantiles corresponding to a failure probability of 5, 50 and 95 percent.

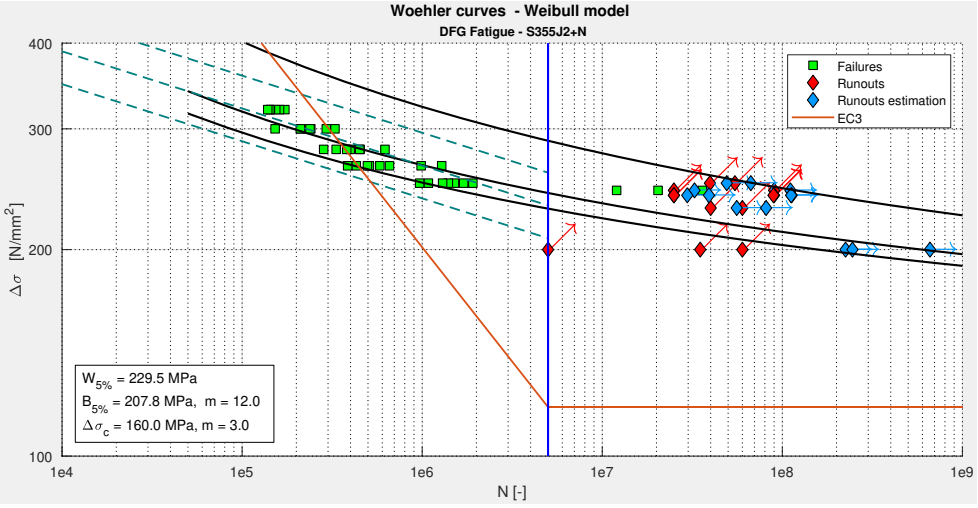

Figure 4.41: Steel S355J2+N. MLE Wöhler curves. Failures and runouts - The curves represent the quantiles corresponding to a failure probability of 5, 50 and 95 percent.

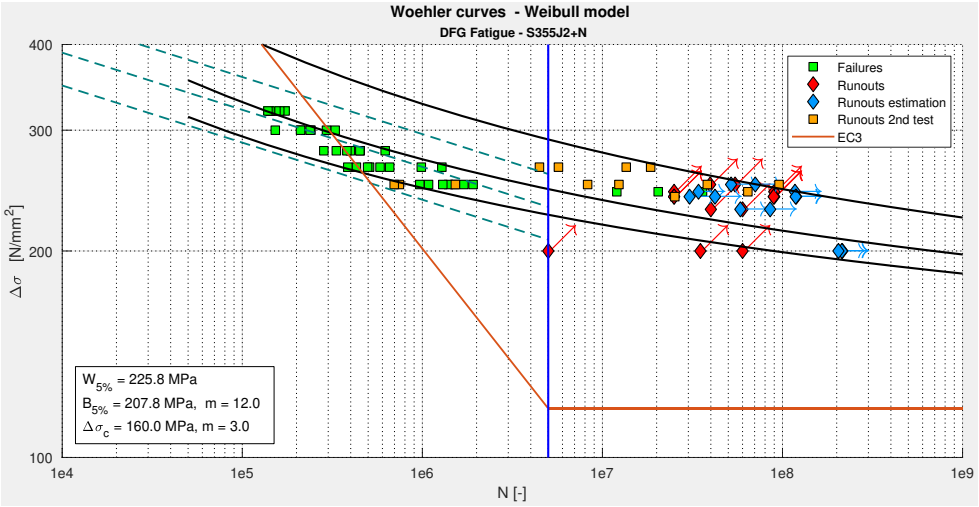

Figure 4.42: Steel S355J2+N. PWM Wöhler curves. Failures, runouts and retests - The curves represent the quantiles corresponding to a failure probability of 5, 50 and 95 percent.

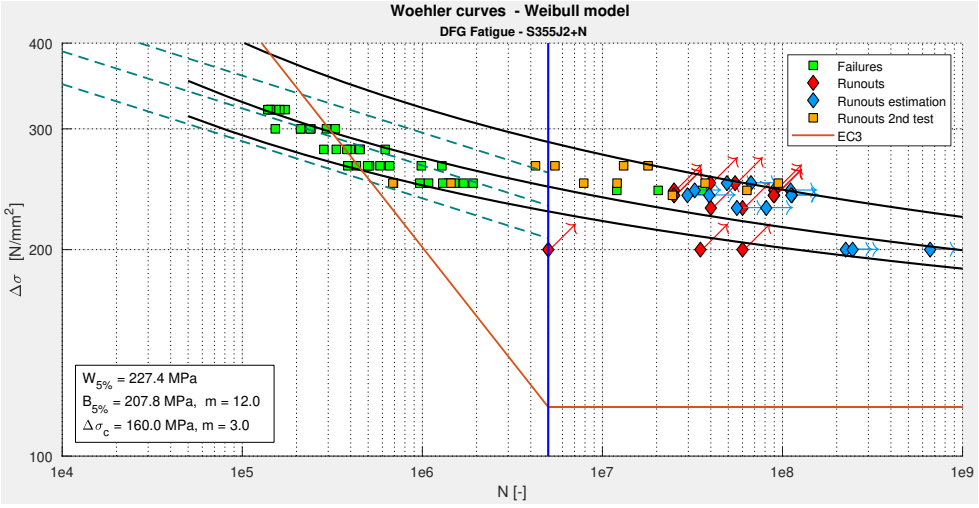

Figure 4.43: Steel S355J2+N. MLE Wöhler curves. Failures, runouts and retests - The curves represent the quantiles corresponding to a failure probability of 5, 50 and 95 percent.

DFG Fatigue research project Quantiles and CIs values $\mathbf{N = 5 \cdot 10^6}$ cycles						
	PWM			**MLE**		
Prob.	F	F-RO	F-RO-RT	F	F-RO	F-RO-RT
[%]	[MPa]	[MPa]	[MPa]	[MPa]	[MPa]	[MPa]
Weibull model						
W_5	226,74	228,65	225,85	226,11	229,48	227,37
W_{50}	236,56	242,48	246,18	237,00	241,86	247,07
W_{95}	257,67	284,03	290,80	257,04	288,21	287,02
CI_{W90}	30,94	55,38	64,95	30,94	58,73	59,64
Basquin model						
B_5	207,77	–	–	207,77	–	–
B_{50}	231,96	–	–	231,96	–	–
B_{95}	258,96	–	–	258,96	–	–
CI_{B90}	51,49	–	–	51,19	–	–

Table 4.35: Steel S355J2+N. Quantiles and CIs - Estimations corresponding to the models of Weibull and Basquin by $N = 5 \cdot 10^6$. See Figures 4.38 to 4.43.

DFG Fatigue research project PWM - Quantiles and CIs comparisons $\mathbf{N = 5 \cdot 10^6}$ cycles						
	F		**F-RO**		**F-RO-RT**	
Prob.	$\mathbf{d_a(W,B)}$	$\mathbf{d_p(W,B)}$	$\mathbf{d_a(W,B)}$	$\mathbf{d_p(W,B)}$	$\mathbf{d_a(W,B)}$	$\mathbf{d_p(W,B)}$
[%]	[MPa]	[%]	[MPa]	[%]	[MPa]	[%]
(W_5, B_5)	18,96	9,13	20,87	10,05	18,07	8,70
(W_{50}, B_{50})	4,60	1,98	10,52	4,53	14,22	6,13
(W_{95}, B_{95})	1,29	0,50	25,06	9,68	31,84	12,29
(CI_{W90}, CI_{B90})	20,26	39,57	4,19	8,18	13,76	26,88

Table 4.36: Steel S355J2+N. PWM-Quantiles and CIs comparisons - Absolute and percentage differences between the models of Weibull and Basquin. See Figures 4.38, 4.40 and 4.42.

DFG Fatigue research project MLE - Quantiles and confidence intervals Comparison by $\mathbf{N = 5 \cdot 10^6}$ cycles						
	F		**F-RO**		**F-RO-RT**	
Prob.	$\mathbf{d_a(W,B)}$	$\mathbf{d_p(W,B)}$	$\mathbf{d_a(W,B)}$	$\mathbf{d_p(W,B)}$	$\mathbf{d_a(W,B)}$	$\mathbf{d_p(W,B)}$
[%]	[MPa]	[%]	[MPa]	[%]	[MPa]	[%]
(W_5, B_5)	18,33	8,82	21,71	10,45	19,60	9,43
(W_{50}, B_{50})	5,04	2,17	9,90	4,27	15,11	6,51
(W_{95}, B_{95})	1,92	0,74	29,25	11,30	28,05	10,83
(CI_{W90}, CI_{B90})	20,25	39,57	7,54	14,73	8,45	16,51

Table 4.37: Steel S355J2+N. MLE-Quantiles and CIs comparisons - Absolute and percentage differences between the models of Weibull and Basquin. See Figures 4.39, 4.41 and 4.43.

As it has been seen, the Weibull model describes the asymptotic behaviour of the Wöhler curves in VHCF region better than the model from Basquin. This fact makes also possible to estimate the fatigue limit, situation that is not possible by applying the Basquin model without assuming the existence of two knee points. The differences between the quantiles and confidence intervals are very significant. In fact, these differences are bigger if the comparison is made in the HCF or VHCF regions.

From the engineering point of view, the results for the six applications presented in this chapter show the benefits of applying the Weibull model in the modelling of the Wöhler curves and in the evaluation of fatigue data. As a matter of fact, they allow to make more accurate and reliable estimations of the fatigue lifetime from structure.

Chapter 5

Conclusions, recommendations and subsequent research

> Es ist doch nicht genug, eine Sache zu beweisen, man muß die Menschen zu ihr auch noch verführen.
>
> *Friedrich Nietzsche*

Since its origins, between the end of the 18th century and begining of the 19th century, the industrial revolution transformed the world and the life of human beings faster and deeper than during the prior two thousand years. The unexplained failures of mechanical components drove engineers to study the reasons behind these failures. Among several brillant engineers who were researching this phenomen, August Wöhler proposed a law to describe the fatigue of steel structures and its consequences. This law was the begining of a wonderfull area of research, which today is very important in the design of steel structures and machines.

The mechanical and stochastic properties of the fatigue have made very difficult to establish a general theory to describe it. The differences between the mechanical properties concerning to the VLCF and VHCF areas have caused that the proposed models consider only one of this areas in order to define the range of their application. As it is common in engineering, the attempts to propose a model are the result of empirical knowledge and several assumptions which allow a relative simple mathematical formulation. However, sometimes these assumptions are arbitrary and in other cases these are very relaxed, so that the results offer not more than an elementary geometrical description of the experimental data.

Trying to overcome the deficiencies from previous fatigue models, Enrique Castillo and Alfonso Fernández Canteli proposed an alternative mathematical model based on the three-parameter Weibull distribution $W(a, b, c)$ to depict the Wöhler curves and to evaluate fatigue data. This model emphasizes the probabilistic nature of the fatigue more than its empirical or phenomenological characteristics.
Even though their book "A unified Statistical Methodology for Modelling Fatigue Damage" was published in 2009, their first results on this field appeared in 1985 while they worked in a project of the IABSE[1] in Zurich. The proposed methodology considers the stress-based, strain-based and the fracture mechanics approaches, from a novel and integrated point of view [35]. Besides these engineering approaches, diverse mathematical topics were also applied, such as functional equations, dimensional analysis, probability theory and statistics.

The results of this research show that the Weibull distribution is adequate to model fatigue and to analyse experimental results from the finite life region up to the HCF region. Moreover, the possibility of taking into account runouts, their accumulated damage and their subsequent tests into the data analysis represents an important achievement.
Within this dissertation only the stress-based approach is considered in order to model the Wöhler cuves. Modelling the Wöhler curves under these conditions depends on six parameters, the probability of failure p, the geometrical parameters B, C and the Weibull parameters a, b and c.

In order to depict the Wöhler curves, the first step is estimating the geometrical parameters B, C and this action can be performed by the least squares method.
Concerning to the estimation of Weibull parameters a, b and c, the probablity weighted moments PWM method and the maximum likelihood MLE method were applied. Particularly, a general formulation of the PWM for the three-parameter Weibull distribution $W(a, b, c)$ was deduced by the author.
Taking into account, the classification of the experimental data according to their status, such as failures, runouts and retested runouts has been important as well. This classification allows to describe a fatigue analysis as a function of the type of data that are considered.

In order to evaluate the adequacy and reliability of the proposed fatigue model and the choosen estimation methods, six applications were performed. The results were compared with those given by the traditional Basquin model which is applied in the international standards.
The first and second application consider only failures, the third and the fourth

[1] International Association for Bridge and Structural Engineering

consider failures and runouts, and the fifth and sixth application consider failures, runouts and retested runouts. A summary of the relevant results of these applications is given in the subsequent sections.

5.1 Considering failures

The experimental data for the first two applications come from the REFRESH project and correspond to welded specimens made of steel S690QL and S355J2.
In the first example, the estimations of the Weibull model parameters obtained by the MLE and PWM methods were very similar, see Table 4.4. The Wöhler curves given by the Weibull and Basquin Models are similar in the region limited by [200,300] MPa and $[2 \cdot 10^5, 8 \cdot 10^5]$ cycles, see Figures 4.7 and 4.8. By 5 millions load cycles, the 5% PWM quantile of Weibull is 14% higher than the Basquin's quantile, and the 5% MLE quantile is 14,29% higher, see Tables 4.5 and 4.6.
In the second example, the estimations of the Weibull parameters given by the PWM and the MLE method were different, see Table 4.9. However, the geometry of the corresponding Wöhler curves are very similar, see Figures 4.10 and 4.11. By 5 millions load cycles, the 5% PWM quantile of Weibull is 13,7% higher than the Basquin's quantile, and the 5% MLE quantile is 14,1% higher, see Tables 4.10 and 4.11.

Despite the fact that only failures were considered in these two applications, the differences between the quantiles from Weibull and Basquin show the advantage of applying the Weibull Model. This fact, allows to obtain a higher and reliable estimation of the fatigue life.

5.2 Considering failures and runouts

The next two applications consider fatigue data corresponding to failures an runouts. Considering the runouts in the modelling of the Wöhler curves is one of the most innovative properties of the Weibull model. To do this, the runouts were included in a truncated Weibull distribution, which allows to estimate the cycles when the runouts could fail.
In both applicationss, the estimation of the Weibull parameters was performed in two ways. Firstly only the failures were considered and then the failures and the runouts together were considered.

The first example considers the data coming from the main girders of the Stahringer Bridge built in 1895.

When only the failures were considered, the estimations of the Weibull parameters given by the PWM and the MLE method were similar, see Table 4.14. The geometry of the corresponding Wöhler curves are similar as well, see Figure 4.14 and 4.15. By 10 millions load cycles, the 5% PWM quantile of Weibull is 15,11% higher than the Basquin's quantile, and the 5% MLE quantile is 15,74% higher, see Tables 4.16 and 4.17.
When the failures and the runouts were considered, the estimations of the Weibull parameters and the Wöhler curves given by the PWM and the MLE method were similar as well, see Table 4.14 and Figures 4.16 and 4.17. By 10 millions load cycles the 5% PWM quantile has an increment of 17,99% in comparison to the Basquin's quantile, and the 5% MLE quantile has an increment of 18,02%, see Tables 4.16 and 4.17. Despite the fact that only one runout is available, the 5% quantile became higher when it is considered.

In the second example the fatigue data came from hourglass shaped samples made of untempered steel 49MnVS3.
When only the failures were considered, the estimations of the Weibull parameters given by the PWM and the MLE method vary, see Table 4.20. However, the geometry of the corresponding Wöhler curves are very similar, see Figures 4.18 and 4.19. By 5 millions load cycles, the 5% PWM quantile of Weibull is 30,86% higher than the Basquin's quantile, and the 5% MLE quantile is 31,42% higher, see Tables 4.22 and 4.23.
When the failures and the runouts were considered, the estimations of the Weibull parameters and the Wöhler curves given by the PWM and the MLE method were different too, see Table 4.20. The 5% and 50% Wöhler curves given by PMM and MLE method are similar, however the 95% MLE curve is higher than the PWM curve, see Figures 4.20 and 4.21. By 5 millions load cycles the 5% PWM quantile has an increment of 37,65% in comparison to the Basquin's quantile, and the 5% MLE quantile has an increment of 38,45%, see Tables 4.22 and 4.23.

The results of these applications allow to appreciate clearly the asymptotic behavior of the Wöhler curves in the HCF region up to $N = 10^8$ load cycles. Keeping in mind that one of the assumptions of the Weibull model is the existence of the fatigue limit $\Delta\sigma_\infty$, eventhough there is no agreement about this fact, it seems plausible to suggest the consideration of the estimated fatigue limit as reference in the design of steel structures.

The increments of the 5% quantiles represent a very important and enormous difference between the models of Weibull and Basquin. For these reasons, appying the Weibull model offers a reliable alternative to estimate the lifetime of a structure.

5.3 Considering failures, runouts and retests

The last two applications consider fatigue data corresponding to failures, runouts and their retests. Besides the failures and runouts, the Weibull model also allows to consider the retests of the runouts. Particularly, in order to perform a second test of a runout, it was necessary to define a damage accumulation function, which was used to estimate the load cycles that a runout could hold under a higher stress range.
In both examples, the estimation parameters of the Weibull model was performed in three ways. Firstly only the failures were considered, secondly the failures and the runouts were considered and finally the failures, the runouts and their retests were considered.

The experimental data for the first application came from the REFRESH project and correspond to welded specimens made of steel S690QL.
When only the failures were considered, the estimations of the Weibull parameters given by the PWM and the MLE method vary, see Table 4.27. The 5% Wöhler curves given by PMM and MLE method are similar, however the 95% MLE curves are higher than the PWM curves, see Figures 4.23 and 4.24. By 5 millions load cycles, the 5% PWM quantile of Weibull is 29,78% higher than the Basquin's quantile, and the 5% MLE quantile is 32,55% higher, see Tables 4.29 and 4.30.
When the failures and the runouts were considered, the estimations of the Weibull parameters and the Wöhler curves given by the PWM and the MLE method vary as well, see Table 4.27. The 5% Wöhler curves given by PWM and MLE method are similar, however the 95% MLE curves are higher than the PWM curves, see Figures 4.25 and 4.26. By 5 millions load cycles the 5% PWM quantile has an increment of 31,50% in comparison to the Basquin's quantile, and the 5% MLE quantile has an increment of 27,01%, see Tables 4.29 and 4.30.
When the failures, runouts and their retests were considered, the estimations of the Weibull parameters and the Wöhler curves given by the PWM and the MLE method vary as well, see Table 4.27. However, the Wöhler curves became similar so that their corresponding quantiles are similar as well, see Figures 4.27 and 4.28. By 5 millions load cycles the 5% PWM quantile has an increment of 28,86% in comparison to the Basquin's quantile, and the 5% MLE quantile has an increment of 24,23%, see Tables 4.29 and 4.30.

The second application concerns to specimens made from steel S355J2+N. In this case the amount of available data was adequate to assure that the obtained estimations are accurate and reliable.
When only the failures were considered, the estimations of the Weibull parameters

and their corresponding Wöhler curves given by the PWM and the MLE method were similar, see Table 4.34 and Figures 4.38 and 4.39. By 5 millions load cycles, the 5% PWM quantile of Weibull is 9,13% higher than the Basquin's quantile, and the 5% MLE quantile is 8,82% higher, see Tables 4.36 and 4.37.
When the failures and the runouts were considered, the estimations of the Weibull parameters and the Wöhler curves given by the PWM and the MLE method are similar, see Table 4.34 and Figures 4.40 and 4.41. By 5 millions load cycles the 5% PWM quantile has an increment of 10,05% in comparison to the Basquin's quantile, and the 5% MLE quantile has an increment of 10,45%, see Tables 4.36 and 4.37
When the failures, runouts and their retests were considered, the estimations of the Weibull parameters and their corresponding Wöhler curves given by the PWM and the MLE method were similar, see Table 4.34 and Figures 4.42 and 4.43. By 5 millions load cycles the 5% PWM quantile has an increment of 8,70% in comparison to the Basquin's quantile, and the 5% MLE quantile has an increment of 9,43%, see Tables 4.36 and 4.37
In this case the increment of the quantiles values is very representative and shows the robustness and suitability of the Weibull model.

The six applications presented in this research project offer promising results that support the fact that the Weibull distribution is one suitable statistical alternative to evaluate the fatigue data and to model the Wöhler curves from the finite life region up to HCF region. The asymptotic behaviour of the Wöhler curves based on the Weibull distribution allows to estimate the fatigue limit $\Delta\sigma$ without using arbitrary knee points like in the model of Basquin which is used in the actual standards. The substantial increment of the 5% quantiles represent a technical benefit of the Weibull Model and could play a relevant role in the fatigue design of structures. Moreover, from the statistical point of view, the reduction of the confidence intervals corresponding to the lifetime of the stucture allow to make more accurated estimations about it.

5.4 Recommendations

As it has been seen in the previous sections, the modelling of the Wöhler curves has been improved by applying the Weibull model from Castillo und Fernández-Canteli. Moreover, this model allows to estimate the fatigue lifetime and fatigue limit of a structure. Due the mathematical background of the Weibull model, from the statistical point of view, the accuracy and reliability of these estimations are better than those obtained by applying the Basquin model.

In order to obtain the best results from applying the Weibull model to depict the Wöhler curves and to evaluate fatigue data of steel structures, the following suggestions should be taken into account in the planning of the fatigue tests.

1. Select and keep a constant stress ratio R.
2. Prepare at least 26 specimens.
3. Perform one or two tensile experiments of the specimens in order to determine the yield strength.
4. Establish as the higher experimental stress range $\Delta\sigma_{sup}$, a value of approximately the 70% of experimental yield strength.
5. If previous technical information from fatigue tests is available, estimate the stress range in which the specimen will hold around 10 millions load cycles with a high probability. Establish this stress range as the lowest experimental stress range $\Delta\sigma_{inf}$. If no previous information is available, $\Delta\sigma_{inf}$ can be determined by the staircase method. However, this procedure demands more specimens.
6. Establish as a runout criteria at least 10 millions load cycles.
7. Define three additional -if possible equidistant- stress ranges between $\Delta\sigma_{sup}$ and $\Delta\sigma_{inf}$. See Figure 5.1.
8. Perform four fatigue tests at each of the five defined stress levels.
9. Perform 4 fatigue tests under a stress range $\Delta\sigma_{ro}$, such that $\Delta\sigma_{ro} < \Delta\sigma_{inf}$, in order to obtain runouts. Due to time planning, the corresponding fatigue tests can be a stopped at a prestablised number of load cycles for all the specimens.
10. Retest the runouts under a higher stress range.

5.5 Subsequent research

As any mathematical model, the fatigue Weibull model considered in this research can still be improved in order to increase its range of application.

From the experimental point of view, performing fatigue tests on different contructional details according to Eurocode 1993-1-9 will allow to improve the estimation of their corresponding fatigue strength, so that the classification of the details can be done with higher accuracy and more reliability.

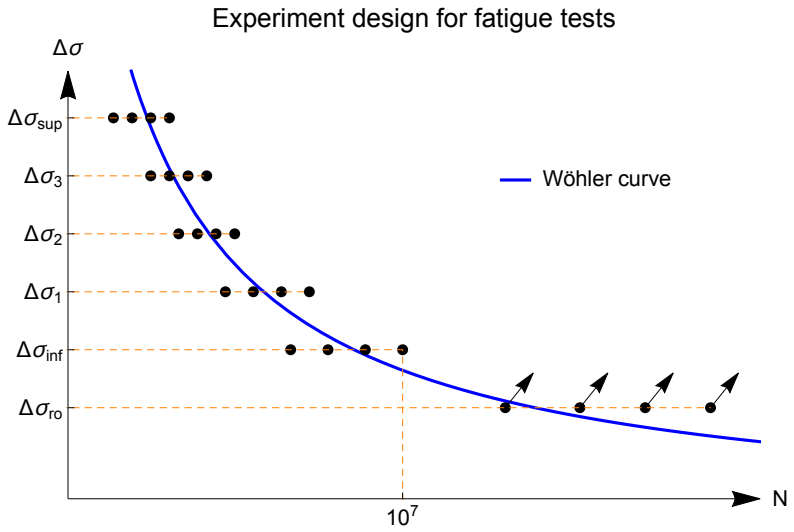

Figure 5.1: Ideal fatigue data - Determination of the experimental stress ranges.

Additionally, considering the amplitude whose role is very relevant and some additional parameters, such as the size of the specimens, the stress ratio and the frequency during the fatigue tests will allow to establish the importance of these parameters to be included in the Weibull model.

In the case of welded structures, it could be useful including in the fatigue Weibull model an analysis of variance ANOVA in order to evaluate the influence of some qualitative parameters such as the welding procedures or the post welding treatments. Moreover, the consideration of the experimental data coming from the VLCF region has to be investigated. In this area the strain plays a fundamental role, and some attempts have been done in order to include the strain in the Weibull model. These region still represent an interesting challenge for engineers and scientists.

The research presented in this dissertation, analyses the phenomen of fatigue only from a statistical point of view. It contributes to have more knowledge about this fascinating engineering topic.

The model proposed in this research does not pretend becoming a paradigm. In fact, to be accepted as a paradigm, a theory must seem better than its competitors, but it need not, and in fact never does, explain all the facts with which it can be confronted [138].

There are still a lot of questions and concerns, which have to be considered in future investigations. Therefore, investment on this research field should continue. The different engineering branches and their permanent challenges give enough motivation to continue with this work.

References

[1] Thomas Tredgold. *A Practical Essay on the Strength of Cast Iron and other Metals*. J. Taylor, 1822.

[2] W.A.J. Albert. über Treibseile am Harz. *Archive für Mineralogie Geognosie Bergbau und Hüttenkunde*, 10:215–234, 1837.

[3] W. Schütz. Zur Geschichte der Schwingfestigkeit. *Materialwissenschaft und Werkstofftechnik*, 24(6):203–232, 1993.

[4] Roland Verreet. Eine kurze Geschichte des Drahtseils. Technical report, Ingenieurbüro für Drahtseiltechnik Wire Rope Technology Aachen GmbH, 2018.

[5] John Oliver York. Account of a series of experiments on the comparative strength of solid and hollow axles. *Journal of the Franklin Institute*, 36(5):332 – 336, 1843.

[6] August Wöhler. über die Festigkeitsversuche mit Eisen and Stahl. *Zeitschrift für Bauwesen*, 20:73 – 106, 1870.

[7] Harald Zenner and Karsten Hinkelmann. Fatigue of Components August Wöhler (1819-1914). A Historical Review. Technical report, Deutscher Verband für Materialforschung und -prüfung e.V., 2017.

[8] L. Spangenberg. über das Verhalten der metalle bei wiederholten Anstrengungen (teil 1). *Zeitschrift für Bauwesen*, (24):474–495, 1874.

[9] W. Kloth and T. Stroppel. Kräfte, Beanspruchungen und Sicherheiten in den Landmaschinen. *VDI-Zeitschrift*, 80(4):85–92, Januar 1936.

[10] Andreas Martin, Karsten Hinkelmann, and Alfons Esderts. Zur Auswertung von schwingsfestigkeitsversuchen im zeitfestigkeitsbereich. *Materials Testing*, 53(9):502–512, September 2011.

[11] O. H. Basquin. The exponential law of endurance tests. *American Society for Testing and Materials Proceedings*, 10:625, 1910.

[12] Adolf F Hobbacher. The new iiw recommendations for fatigue assessment of welded joints and components - a comprehensive code recently updated. *International Journal of Fatigue*, 31(1):50–58, 2009.

[13] Tadeuz Łagoda. *Lifetime Estimation of Welded Joints*. Springer Verlag, 2008.

[14] G. Marquis, M. Huther, and A. Galtier. Guidance for the application of the best practice guide on statistical analysis of fatigue data. *IIW-WG1-132-08*, 2008.

[15] J. Schijve. *Fatigue of Structures and Materials*. Springer Verlag, 2009.

[16] Sedlacek, Hobbacher, Nussbaumer, and Stötzel. 1^{st} draft of the background document prEN 1993-1-9. *Eurocode 3: Design of steel structures*, 2005.

[17] Nils Arvid Palmgren. Die Lebensdauer von Kugellagern. *Zeitschrift des Vereins Deutscher Ingenieure*, 68(14):339 – 441, April 1924.

[18] Nils Arvid Palmgren. The service life of ball bearings. Technical report, National Aeronautics and Space Administration, March 1971. Translation of the original paper.

[19] Erwin V. Zaretsky. A. palmgren revisited - a basis for bearing life prediction. Technical Report 107440, National Aeronautics and Space Administration, May 1997.

[20] Ioannides Eustathios, Bergling Gunnar, and Gabelli Antonio. The SKF formula for rolling bearing life. *Evolution*, 1:25 – 28, February 2001.

[21] M.A. Miner. Cummulative Damage in Fatigue. *Journal of Applied Mechanics*, 12(3):A159 – A164, 1945.

[22] J. Schijve. Fatigue of structures and materials in the 20th century and the state of the art. *International Journal of Fatigue*, 25(8):679 – 702, 2003.

[23] Anke Zeidler-Finsel. Leichter, leiser, zuverlässiger. 100. Geburtstag des Leichtbaupioniers Ernst Gaßner. Technical report, Fraunhofer-Institut für Betriebsfestigkeit und Systemzuverlässigkeit LBF, 2008.

[24] Ernst Heinrich Hirschel, Horst Prem, and Gero Madelung. *Aeronautical Research in Germany. From Lilienthal until Today*. Springer Verlag, December 2003.

[25] N.N. Aerial disaster. *Sunday Times (Perth, WA : 1902 - 1954)*, page 1, Sep 1927.

[26] Ernst Gaßner. Strength investigations in aircraft construction under repeated application of the load. Technical Report 1087, National Advisory Committee for Aeronautics, Washington DC, August 1946.

[27] Ernst Gaßner. Festigkeitsversuche mit Wiederholter Beansprunchung im Flugzeugbau. *Luftwissen*, 6(2):61–64, 1939.

[28] Fritz Scholz. Weibull reliability analysis. Technical report, The Boeing Company, 2002.

[29] Herbert Eller. *Stahlbau Handbuch (Für Studium und Praxis)*, volume 1. Stahlbau-Verlags-GmbH Köln, 2 edition, 1982.

[30] Akademischer Verein Hütte. *Hütte, Taschenbuch der Werkstoffkunde (Stoffhütte)*. Wilhelm Ernst & Sohn, 1967.

[31] Adolf F. Hobbacher. New developments at the recent update of the iiw recommendations for fatigue of welded joints and components. *Steel Construction*, 3(4):231–242, 2010.

[32] C.M. Suh, R. Yuuki, and H. Kitagawa. Fatigue microcracks in a low carbon steel. *Fatigue & Fracture of Engineering Materials & Structures*, 8(2):193–203, 1985.

[33] Imaging & Microscopy. Martina Dienstleder Is the Winner of the 2011 FEI Owner Image Contest. Technical report, Imaging & Microscopy, August 2011.

[34] C. Bathias. There is no infinite fatigue life in metallic materials. *Fatigue & Fracture of Engineering Materials & Structures*, 22(7):559–565, 1999.

[35] E. Castillo and A. Fernández-Canteli. *A Unified Statistical Methodology for Modeling Fatigue Damage*. Springer Verlag, 2009.

[36] CEN Management Centre (CMC). En 1993-1-9:2005 (E) + AC:2009. *Eurocode 3: Design of steel structures*, Part 1-9: Fatigue, 2010.

[37] E. Haibach. *Betriebsfestigkeit: Verfahren und Daten zur Bauteilberechnung*. Springer Verlag, 2006.

[38] Richard J. Larsen and Morris L. Marx. *An Introduction to Mathematical Statistics and Its Applications*. Prentice Hall, Third edition, 2001.

[39] P. D. Toasa Caiza. Linear regression analysis for fatigue results and its implementation in the program "WÖHLER". Technical report, Versuchsanstalt für Stahl, Holz und Steine, Abteilung Stahl- und Leichtmetallbau. Universität Karlsruhe (TH), 2008.

[40] D. Wackerly, W. Mendenhall, and R.L. Scheaffer. *Mathematical Statistics with Applications*. Duxbury Press, 2001.

[41] J.E. Spindel and E. Haibach. The method of maximum likelihood applied to the statistical analysis of fatigue data. *International Journal of Fatigue*, 1(2):81 – 88, 1979.

[42] C.E. Stromeyer. The determination of fatigue limits under alternating stress conditions. *Proceedings of the Royal Society of London*, 90(620):411–425, 1914.

[43] F.A. Bastenaire. New method for the statistical evaluation of constant stress amplitude fatigue-test results. *Probabilistic Aspects of Fatigue*, STP(511):3–28, 1972.

[44] Fritz Stüssi. *Tragwerke aus Aluminium*. Springer Verlag, 1955.

[45] J. Kohout and S. Věchet. A new function for fatigue curves characterization and its multiple merits. *International Journal of Fatigue*, 23(2):175–183, 2001.

[46] F. Pascual and W. Meeker. Estimating fatigue curves with the random fatigue-limit model. *Technometrics*, 41(4):277–290, 1999.

[47] T. Lassen, Ph Darcis, and N. Recho. Fatigue behavior of welded joints part 1 - statistical methods for fatigue life prediction. *Welding Journal*, pages 183–187, 2005.

[48] Tom. Lassen and Naman. Recho. Proposal for a more accurate physically based S-N curve for welded steel joints. *International Journal of Fatigue*, 31(1):70–78, 2009.

[49] T. Lassen and N. Recho. Life prediction of welded steel joints - accuracy and shape of the S-N curves under constant and variable amplitude loading. *Fatigue Design 2009*, 2009.

[50] Enrique Castillo and Janos Galambos. Lifetime regression models based on a functional equation of physical nature. *Journal of Applied Probability*, 24(1):160–169, 1987.

[51] Enrique Castillo, Volker Esslinger, and Alfonso Fernández-Canteli. Statistical model for fatigue analysis of wires, strands and cables. In *IABSE Proceedings*, volume 9. IABSE, IABSE Periodica, 1985.

[52] E. Buckingham. On physically similar systems; illustrations of the use of dimensional equations. *Phys. Rev*, 4:345–376, 1914.

[53] N.L. Johnson, S. Kotz, and N. Balakrishnan. *Continuous Univariate Distributions Vol. 1*. John Wiley & Sons, 1994.

[54] N.L. Johnson, S. Kotz, and N. Balakrishnan. *Continuous Univariate Distributions Vol. 2*. John Wiley & Sons, 1995.

[55] J. Schijve. A normal distribution or a weibull distribution for fatigue lives. *Fatigue & Fracture of Engineering Materials & Structures*, 16(8):851–859, 1993.

[56] Wayne Nelson. Fitting of fatigue curves with nonconstant standard deviation to data with runouts. *Journal of Testing and Evaluation*, 12(2):69–77, 03 1984.

[57] F. Pascual and W. Meeker. Analysis of fatigue data with runouts based on a model with nonconstant standard deviation and a fatigue limit parameter. *Journal of Testing and Evaluation*, 25(3):292–301, 05 1997.

[58] S. Sarkani, T.A. Mazzuchi, D. Lewandowski, and D.P. Kihl. Runout analysis in fatigue investigation. *Engineering Fracture Mechanics*, 74(18):2971 – 2980, 2007.

[59] Hubert Bomas, Klaus Burkart, and Hans-Werner Zoch. Evaluation of s-n curves with more than one failure mode. *International Journal of Fatigue*, 33:19–22, 2011.

[60] T. Sakai, B. Lian, M. Takeda, K. Shiozawa, N. Oguma, Y. Ochi, M. NNakajima, and T. Nakamura. Statistical duplex s-n characteristics of high carbon chromium bearing steel in rotating bending in very high cycle regime. *International Journal of Fatigue*, 32(3):497–504, 2010.

[61] M. Goto. Statistical investigation of the behaviour of microcracks in carbon steels. *Fatigue & Fracture of Engineering Materials & Structures*, 14(8):833–845, 1991.

[62] M. Goto. Scatter in small crack propagation and fatigue behaviour in carbon steels. *Fatigue & Fracture of Engineering Materials & Structures*, 16(8):795–809, 1993.

[63] M. Goto. Statistical investigation of the behaviour of small cracks and fatigue life in carbon steels with different ferrite grain sizes. *Fatigue & Fracture of Engineering Materials & Structures*, 17(6):635–649, 1994.

[64] Waloddi Weibull. A statistical distribution function of wide applicability. *Trans. ASME, Journal of Applied Mechanics*, 73:293 – 297, 1951.

[65] Dietrich Stoyan. Weibull, rrsb or extreme-value theorists? *Metrika*, pages 1–7, 2011.

[66] Maurice Fréchet. Sur la loi de probabilité de l'écart maximum. *Annales de la Société Polonaise de Mathematique*, 6:93 – 116, 1927.

[67] Erich Rammler. Gesetzmäßigkeiten in der Kornverteilung zerkleinerter Stoffe. *Beihefte "Verfahrenstechnik" zur VDI-Zeitschrift*, 5:161 –168, 1937.

[68] Heinrich Schubert and Eberhard Wächtler. Erich rammler - a pioneer of particle technology. *Particle & Particle Systems Characterization*, 4(1-4):45–48, 1987.

[69] Erich Rammler. RRSB-Verteilung und Weibull Verteilung. *Neue Bergbautechnik*, 6:284 – 286, 1974.

[70] D. J. Dupuis. Parameter and quantile estimation for the generalized extreme-value distribution: a second look. *Environmetrics*, 10:119–124, 1999.

[71] Éric Gourdin, Pierre Hansen, and Brigitte Jaumard. Finding maximum likelihood estimators for the three-parameter weibull distribution. *Journal of Global Optimization*, 5:373–397, 1994.

[72] V. G. Gupta and R. C. Panchang. On the determination of three-parameter weibull mle's. *Communications in Statistics - Simulation and Computation*, 18(3):1037–1057, 1989.

[73] H. Hirose. Maximum likelihood estimation in the 3-parameter weibull distribution. a look through the generalized extreme- value distribution. *Dielectrics and Electrical Insulation, IEEE Transactions on*, 3(1):43 –55, 1996.

[74] J.R.M. Hosking, J.R. Wallis, and E.F. Wood. Estimation of the generalized extreme-value distribution by the method of probability-weighted moments. *Technometrics*, 27(3):251–261, 1985.

[75] D. Marković, D. Jukić, and M. Benšić. Nonlinear weighted least squares estimation of a three-parameter weibull density with a nonparametric start. *J. Comput. Appl. Math.*, 228(1):304–312, 2009.

[76] R. Offinger. Maximum likelihood and least squares estimation in the three-parameter weibull model with applications to river drain data. *University of Magdeburg*, 1996.

[77] H. Rinne. *The Weibull Distribution*. Crc Pr Inc, 2008.

[78] Paul Dario Toasa Caiza and Thomas Ummenhofer. General probability weighted moments for the three-parameter Weibull distribution and their application in $S - N$ curves modelling. *International Journal of Fatigue*, 33(12):1533 – 1538, 2011.

[79] S. Zanaquis and J. Kyparisis. A review of maximum likelihood estimation methods for the three-parameter weibull distribution. *Journal of Statistical Computation and Simulation*, 25:53–73, 1986.

[80] J.A. Greenwood, J.M. Landwehr, N.C. Matalas, and J.R. Wallis. Probability weighted moments: Definition and relation to parameters of several distributions expressable in inverse form. *Water Resources Research*, 15(05):1049–1054, 1979.

[81] E. Castillo and A. S. Hadi. Parameter und quantile estimation for the generalized extreme-value distribution. *Environmetrics*, 5:417–432, 1994.

[82] L.E. Zapata-Ordúz, G. Portela, and O.M. Suárez. Weibull statistical analysis of splitting tensile strength of concretes containing class f fly ash, micro/nano-sio2. *Ceramics International*, 40(5):7373 – 7388, 2014.

[83] T. Ummenhofer, S. Herion, S. Rack, I. Weich, G. Telljohann, S. Dannemeyer, H. Strohbach, H. Eslami-Chalandar, A. K. Kern, M. Smida, U. Rahlf, and B. Senk. *REFRESH - Lebensdauerverlängerung bestehender und neuer geschweißter Stahlkonstruktionen*. Number D 761 in Forschung für die Praxis. Forschungsvereinigung Stahlanwendung e.V., 2010.

[84] Stanley Corrsin. A simple geometrical proof of buckingham's π-theorem. *American Journal of Physics*, 19(3):180 – 181, 1951.

[85] Enrique Castillo and Alfonso Fernández-Canteli. A general regression model for lifetime evaluation and prediction. *International Journal of Fracture*, 107:117–137, 2001.

[86] D. G. Harlow, R. L. Smith, and H. M. Taylor. Lower tail analysis of the distribution of the strength of load-sharing systems. *Journal of Applied Probability*, 20(2):pp. 358–367, 1983.

[87] Wagner De Souza Borges. On the limiting distribution of the failure time of fibrous materials. *Advances in Applied Probability*, 15(2):pp. 331–348, 1983.

[88] I. B. Karosas. Asymptotic distribution of the failure time of a system. *Cybernetics and Systems Analysis*, 7:304–307, 1971. 10.1007/BF01071803.

[89] Anders Wormsen and Gunnar Härkegård. A statistical investigation of fatigue behaviour according to weibull's weakest-link theory. 15th European Conference on Fracture. European Structural Integrity Society, ESIS, August 2004.

[90] Enrique Castillo. Estadística de Valores Extremos. Distribuciones Asintóticas. *Estadística Española*, (116):5–34, 1988.

[91] Arjun K. Gupta, Wei-Bin Zeng, and Yanhong Wu. *Probability and Statistical Models. Foundations for Problems in Reliability and Financial Mathematics*. Birkhäuser Boston, 2010.

[92] B. Pyttel, D. Schwerdt, and C. Berger. Very high cycle fatigue – is there a fatigue limit? *International Journal of Fatigue*, 33(1):49 – 58, 2011.

[93] C.M. Sonsino. Course of sn-curves especially in the high-cycle fatigue regime with regard to component design and safety. *International Journal of Fatigue*, 29(12):2246 – 2258, 2007.

[94] Albano António Sousa. *Ultra low cycle fatigue of welded steel joints under multiaxial loading*. PhD thesis, École polytechnique fédérale de Lausanne (EPFL), 2017.

[95] Alfonso Fernández-Canteli, María Jesús Lamela, and Manuel López-Aenlle. Modelling Engineering Fatigue Problems. In *International Conference on Mathematical and Statistical Modeling in Honor of Enrique Castillo*. ICMSM 2006, June 2006.

[96] Thomas F. Coleman and Yuying Li. On the convergence of interior-reflective newton methods for nonlinear minimization subject to bounds. *Math. Program.*, 67:189–224, 1994.

[97] Thomas F. Coleman and Yuying Li. An interior trust region approach for nonlinear minimization subject to bounds. *SIAM Journal on Optimization*, 6:418–445, 1996.

[98] Enrique. Castillo, Alfonso. Fernández-Canteli, Hernán. Pinto, and Manuel. López-Aenlle. A general regression model for statistical analysis of strain-life fatigue data. *Materials Letters*, 62(21-22):3639 – 3642, 2008.

[99] J.K. Lindsey. *Applying Generalized Linear Models*. Springer Verlag, 1997.

[100] P. McCullagh and J.A. Nelder. *Generalized Linear Models*. Crc Pr Inc, 2008.

[101] A. Clifford Cohen. Progressively censored samples in life testing. *Technometrics*, 5(3):327–339, 1963.

[102] A. Clifford Cohen. Multi-censored sampling in the three parameter weibull distribution. *Technometrics*, 17(3):347 – 351, August 1965.

[103] Dallas R. Wingo. Solution of the three-parameter weibull equations by constrained modified quasilinearization (progressively censored samples). *Reliability, IEEE Transactions on*, R-22(2):96 –102, june 1973.

[104] N. Balakrishnan and M. Kateri. On the maximum likelihood estimation of parameters of weibull distribution based on complete and censored data. *Statistics & Probability Letters*, 78(17):2971–2975, 2008.

[105] H.K.T Ng, P.S Chan, and N Balakrishnan. Optimal progressive censoring plans for the weibull distribution. *Technometrics*, 46(4):470–481, 2004.

[106] U. Balasooriya and C.-K. Low. Competing causes of failure and reliability tests for weibull lifetimes under type i progressive censoring. *Reliability, IEEE Transactions on*, 53(1):29 – 36, march 2004.

[107] Shuo-Jye Wu and Coşkun Kuş. On estimation based on progressive first-failure-censored sampling. *Computational Statistics & Data Analysis*, 53(10):3659 – 3670, 2009.

[108] A. Clifford Cohen. Maximum likelihood estimation in the weibull distribution based on complete and on censored samples. *Technometrics*, 7(4):579–588, 1965.

[109] Glen H. Lemon. Maximum likelihood estimation for the three parameter weibull distribution based on censored samples. *Technometrics*, 17(2):247–254, 1975.

[110] A. Fatemi and L. Yang. Cumulative fatigue damage and life prediction theories: a survey of the state of the art for homogeneous materials. *International Journal of Fatigue*, 20(1):9 – 34, 1998.

[111] H. J. Grover. An observation concerning the cycle ratio in cumulative damage. In *Symposium on Fatigue of Aircraft Structures*, pages 120 – 124, Philadelphia, PA, 1960. American Society for Testing and Materials.

[112] B. F. Langer. Fatigue failure from stress cycles of varying amplitude. *ASME Journal of Applied Mechanics*, 59:A160 – A162, 1937.

[113] F. R. Shanley. A theory of fatigue based on unbounding during reversed slip. Technical Report P-350, The Rand Corporation, Santa Monica, 1952.

[114] S.R. Valluri. A unified engineering theory of high stress level fatigue. *Aerospace Engineering*, 20:18–19, 1961.

[115] S.R. Valluri. A theory of cumulative damage in fatigue. Technical Report ARL 182, Aerospace Research Laboratories (US), 1961.

[116] T. D. Scharton and S. H. Crandall. Fatigue failure under complex stress histories. *ASME J. Basic Eng.*, 88:247 – 250, 1966.

[117] S.S. Manson and G.R. Halford. Practical implementation of the double linear damage rule and damage curve approach for treating cumulative fatigue damage. *International Journal of Fracture*, 17(2):169–192, 1981.

[118] T. Bui Quoc, J. Dubuc, A. Bazergui, and A. Biron. Cumulative fatigue damage under stress-controlled conditions. *ASME J. Basic Eng.*, 93(4):691 – 698, 1971.

[119] O. E. Wheeler. Spectrum loading and crack growth. *ASME J. Basic Eng.*, D94(1):181 – 186, 1972.

[120] N. P. Inglis. Hysteresis and fatigue of Wöhler rotating cantilever specimen. *The Metallurgist*, pages 23 – 27, 1927.

[121] Lazar Kachanov. Rupture time under creep conditions. *International Journal of Fracture*, 97:11–18, 1999. 10.1023/A:1018671022008.

[122] G. Backhaus. Yu. n. rabotnov, creep problems in structural members. (north-holland series in applied mathematics and mechanics.) ix + 822 s. m. 255 fig. amsterdam/london 1969. north-holland publishing company. preis geb. hfl. 120. –. *ZAMM - Journal of Applied Mathematics and Mechanics / Zeitschrift für Angewandte Mathematik und Mechanik*, 51(7):575–576, 1971.

[123] Davide Leonetti, Johan Maljaars, and H.H. (Bert) Snijder. Fitting fatigue test data with a novel s-n curve using frequentist and bayesian inference. *International Journal of Fatigue*, 105:128 – 143, 2017.

[124] Luca D'Angelo and Alain Nussbaumer. Estimation of fatigue s-n curves of welded joints using advanced probabilistic approach. *International Journal of Fatigue*, 97:98 – 113, 2017.

[125] Paul Dario Toasa Caiza and Thomas Ummenhofer. Consideration of the runouts and their subsequent retests into s-n curves modelling based on a three-parameter weibull distribution. *International Journal of Fatigue*, 106(Supplement C):70 – 80, 2018.

[126] W. Weibull. *Fatigue Testisng and Analysis of Results*. Pergamon Press, 1961.

[127] Barry C. Arnold, N. Balakrishnan, and H.N. Nagaraja. *A First Course in Order Statistics*, volume 54 of *Classics in Applied Mathematics*. SIAM-Society for Industrial and Applied Mathematics, 2008.

[128] B. L. Vlcek, E. V. Zaretsky, and R. C. Hendricks. Test population selection from weibull-based, monte carlo simulations of fatigue life. In *49th AIAA/ASME/ASCE/AHS/ASC Structures, Structural Dynamics and Materials Conference*, volume 6 of *49th AIAA/ASME/ASCE/AHS/ASC Structures, Structural Dynamics and Materials Conference*, pages 3676 – 3683. American Institute for Aeronautics and Astronautics (AIAA), Curran Associates, Inc, April 2008.

[129] Nicholas Theodore. *High Cycle Fatigue: A Mechanics of Materials Perspective*. Elsevier Science, First edition, September 2006.

[130] D. Radaj. *Ermüdungsfestigkeit: Grundlagen für Ingenieure*. Springer Verlag, 2007.

[131] N. Balakrishnan and Rita Aggarwala. *Progressive Censoring. Theory, Methods, and Applications*. Statistics for industry and technology. Birkhäuser, 2000.

[132] W. J. Dixon and A. M. Mood. A method for obtaining and analyzing sensitivity data. *Journal of the American Statistical Association*, 43(241):109 – 126, march 1948.

[133] M. Prot. Fatigue tests under progressive load.a new technique f or testing materials. *Rev. Métall*, 45(12):481 – 489, 1948.

[134] Rosemarie Helmerich. Alte Stähle und Stahlkonstruktionen. Materialuntersuchungen, Ermüdungsversuche an originalen Brückenträgern und Messungen von 1990 bis 2003. Technical Report 271, Bundesanstalt für Materialforschung und -prüfung (BAM), Unter den Eichen 87. 12205 Berlin, 2005.

[135] F. Mang and O. Bucak. Remaining fatigue life of old steel bridges-theoretical and experimental investigations on railway bridges. In *Fatigue and Fracture in Steel and Concrete structures*, volume 2 of *ISFF '91 Proceedings*, pages 971–991. Structural Engineering Research Centre. Madras, India., Oxford & IBH Publishing Co.Pvt.Ltd., 1991.

[136] P. D. Toasa Caiza. Ermüdungsversuche an alten Stahlkonstruktionen. Technical Report 088006, Versuchsanstalt für Stahl, Holz und Steine, Abteilung Stahl- und Leichtmetallbau, Karlsruher Institut für Technologie (KIT), July 2008.

[137] Chr. Boller and T. Seeger. *Materials Data for Cycling Loading*, volume 42B of *Materials Science Monographs*. Elsevier, 1987.

[138] Thomas S. Kuhn. *The Structure of Scientific Revolutions*, volume 2 of *International Encyclopedia of Unified Science*. University of Chicago Press, 1962.

Appendix A

Software, simulation and certificates

A.1 Matlab graphical user interface (GUI)

In order to record and analyse the experimental fatigue data, a suitable graphical user interface (GUI) in Matlab and a database in MySQL were developed. The GUI contains the applied numerical algorithms to estimate the geometrical and the Weibull parameters from the Weibull model and the regression parameters from the Basquin model. Additionaly, the GUI performs the data acquisition from the database and display the results, see Figure A.1. The MySQL was designed in order to record all of the relevant qualitative and quantitaive information from the fatigue experiments.

The main features from the developed Matlab application are:

- Estimation of the geometrical parameters B, C from the Weibull model
- Estimation of the Weibull Parameters a, b and c by applying either the PWM or the MLE method
- Estimation of the regression parameters from the Basquin model
- Estimation of the stress range percentiles for the Weibull and Basquin models corresponding to any value of load cycles. The percentiles correspond to probabilities of 2,5%, 5%, 50%, 95% and 97,5%
- Allows considering in the statistical analysis together or separated the different fatigue data such as runouts, failures and retested runouts
- Estimation of the fatigue limit $\Delta\sigma_{\infty}$ and the threshold of the load cycles N_{min}

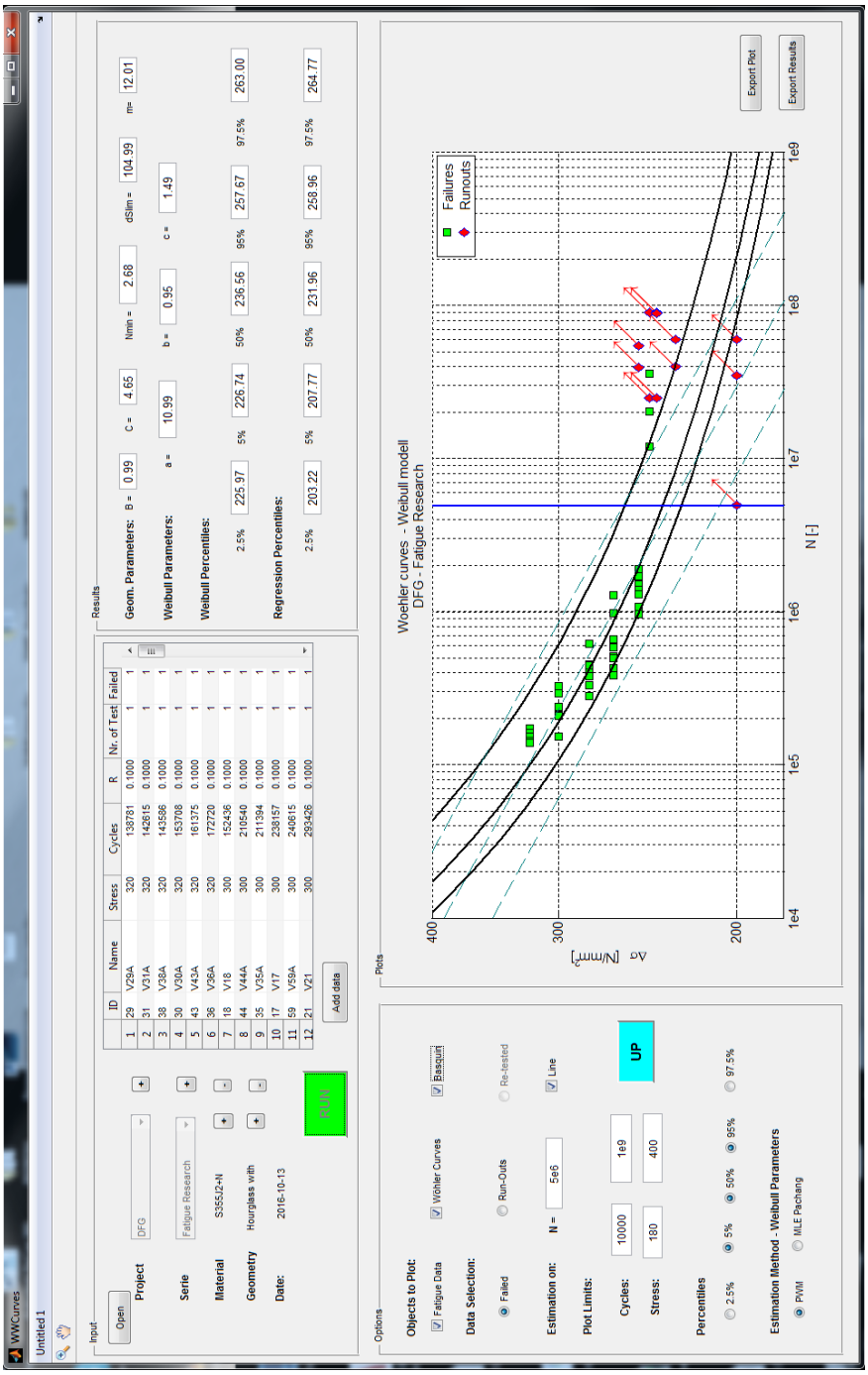

Figure A.1: Graphical User Interface - Matlab is necessary to use this interface.

- Display of the Wöhler curves according to the Weibull and Basquin models
- Exporting the figures in pdf format
- Exporting the results in a text file
- Managing the MySQL database

The font codes from the matlab GUI and the MySQL database are kept available in order to implement new algorithms or develop additional functions.

A.2 Measure of the strain and its simulation by FEM

In order to verify the functionality of the high frequency pulsator M64, the strain was measured during a fatigue test, which was performed with a stress range $\Delta\sigma = 244$ MPa. Two single strain gauges with factor $k = 2,12$ were located at both sides of the central perforation of the specimen. The Figure A.2 shows the diagram with the position of the strain gauges on the specimen, and the Figure A.3 shows where the strain gauges were placed on the real specimen before the fatigue test.

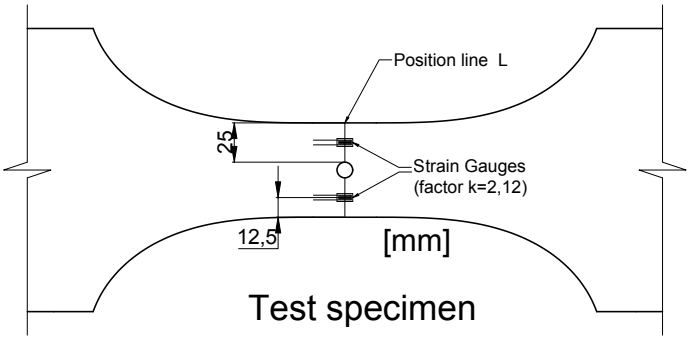

Figure A.2: Position of the strain gauges - The strain gauges were located on the middle point between the border of the perforation and the border of the specimen over the line L.

Several measures of the strain were taken with a recording frequency of 2400 Hz. Based on these measurements, the variation of the stress was determined. The Figure A.4 shows the stress variation during the begining of the fatigue test. The Figure A.5 shows closer the initial stress variation in a period of approximately 2,5 seconds. In this figure it is possible to observe how the pulsator M64 tries to estabilize the applied forces on the specimen. The Figure A.6 shows the stress variation when the pulsator has reached the stablization of the applied forces.

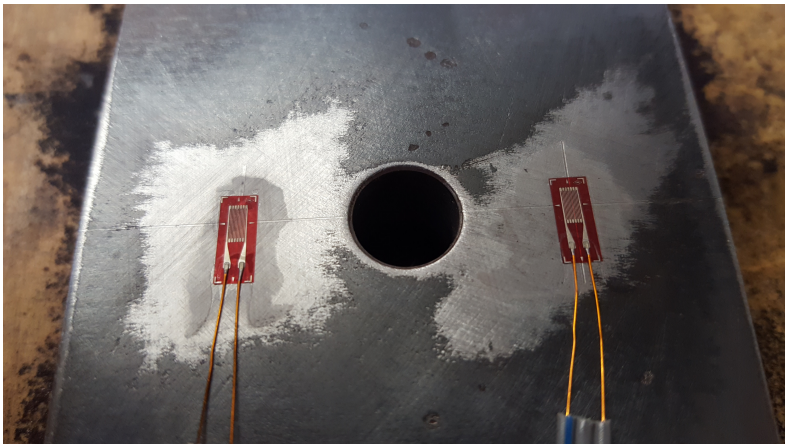

Figure A.3: Strain gauges on the specimen - Single strain gauges used to measure the strain during the fatigue test.

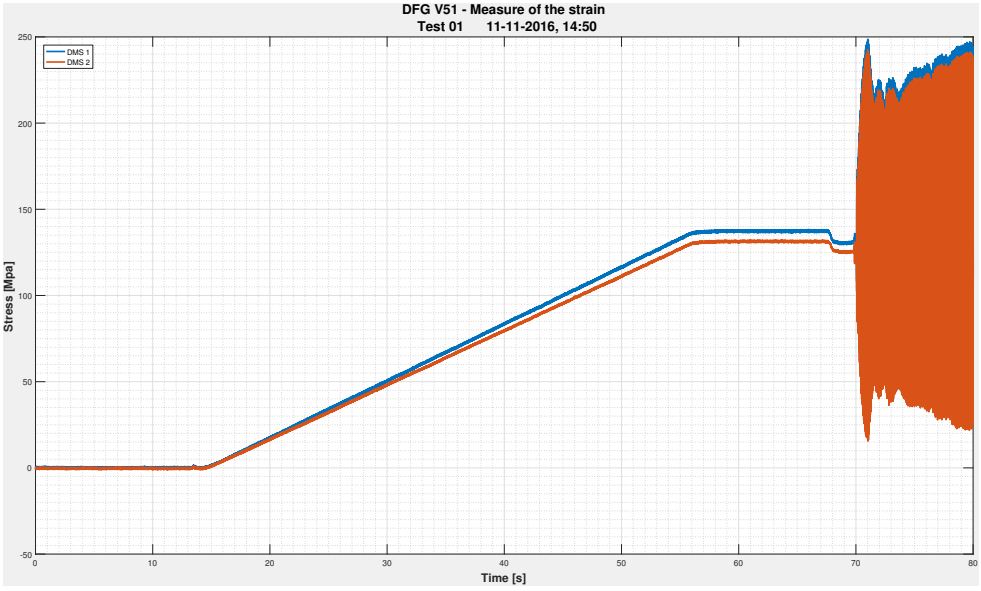

Figure A.4: Initial stress variation - Variation of the stress during the begining of the fatigue test.

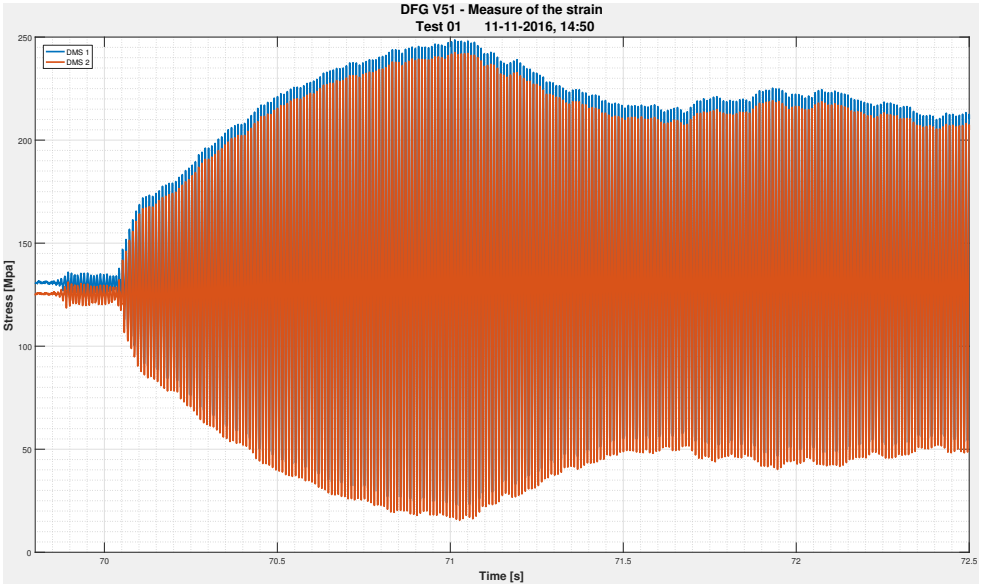

Figure A.5: Zoomed initial stress variation - Variation of the stress during the begining of the fatigue test.

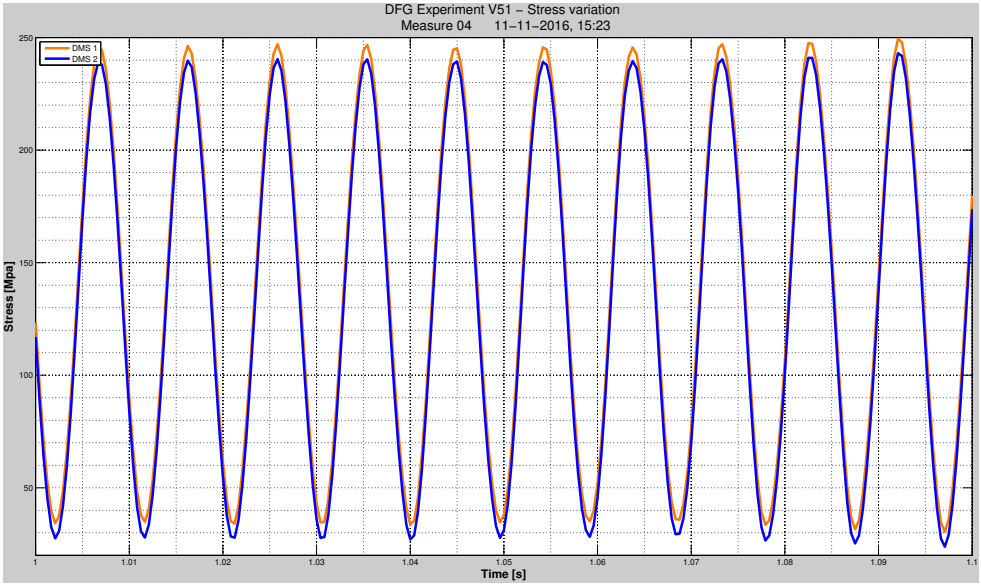

Figure A.6: Stress variation during the fatigue test - The stabilization of the applied forces has been reached and the fatigue test runs normally.

These experimental results were compared with those obtained by a FEM simulation of the stress performed with ANSYS.
The Figure A.7 shows the geometry of the specimen and its grid used on the FEM simulation. The Figure A.8 shows the FEM simulation of the stress around the region where the strain gauges were located. In order to compare the simulated results with those measured with the strain gauges, a path was defined in the FEM model. This path coincides with the position line L where the strain gauges were placed, see Figure A.2.
The Figures A.9 to A.12 show the maximum and minimum stress along the position line L. The simulated values of the stress corresponding to the position of the strain gauges are explicitly written. The simulated values of the stress do not vary considerable with those measured with the strain gauges.
The small difference between the real and the simulated values may be caused because the strain gauges are not located precisely in the position determined in the Figure A.2 . Moreover, in the FEM simulation the steel is assumed to be an homogeneous material. For these reasons, it can be concluded that the pulsator worked properly.

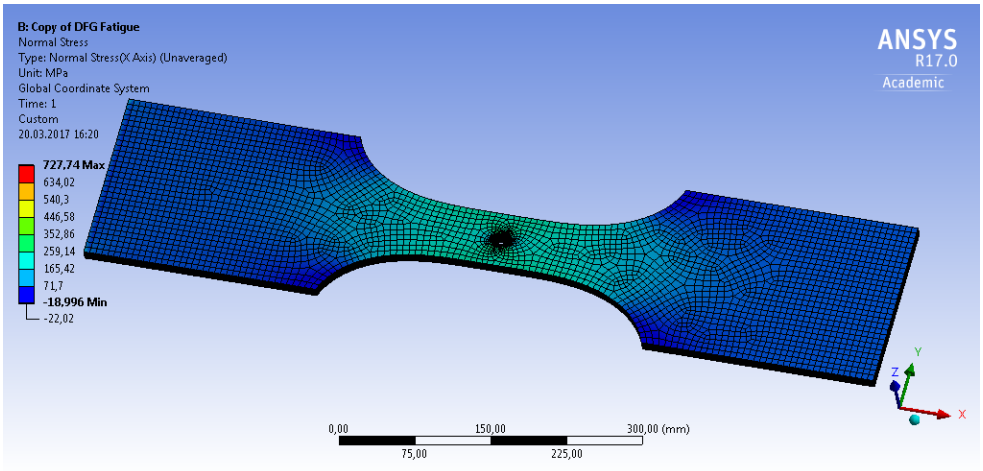

Figure A.7: Geometry and grid of the specimen - The FEM simulation was performed to simulate the stress on the strain gauges.

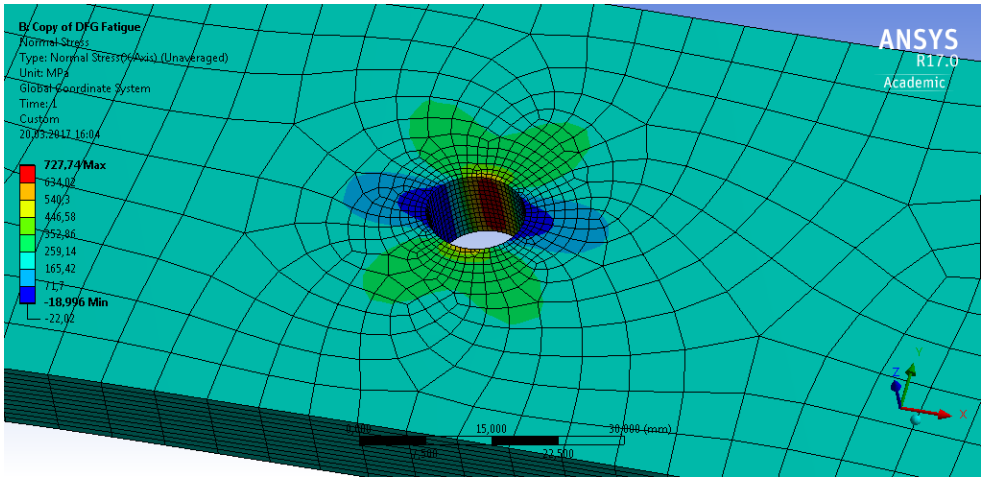

Figure A.8: FEM simulation of the stress - The FEM simulation was performed to simulate the stress on the strain gauges.

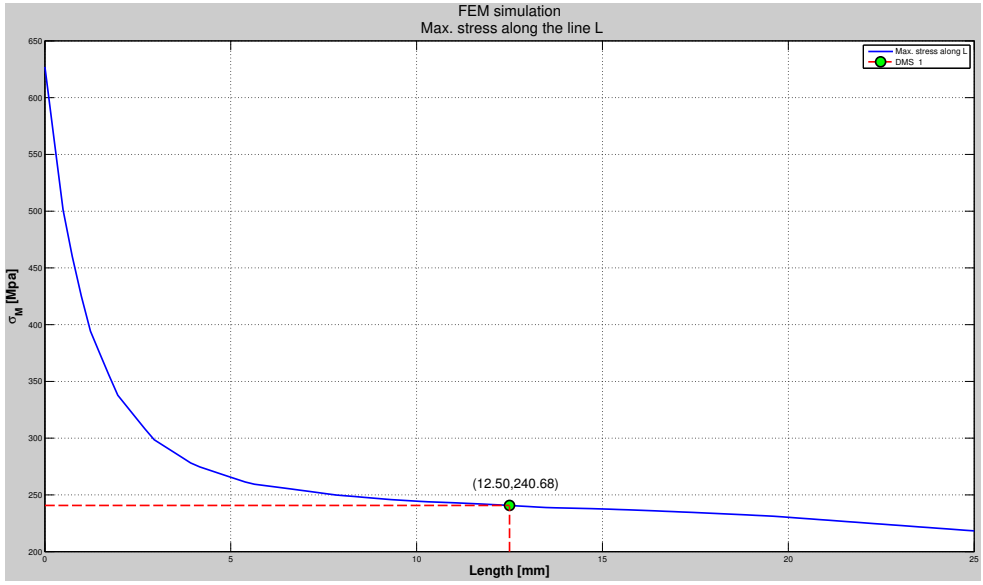

Figure A.9: FEM Maximum stress on the first strain gauge - The written values of the stress correspond to the position of the strain gauge.

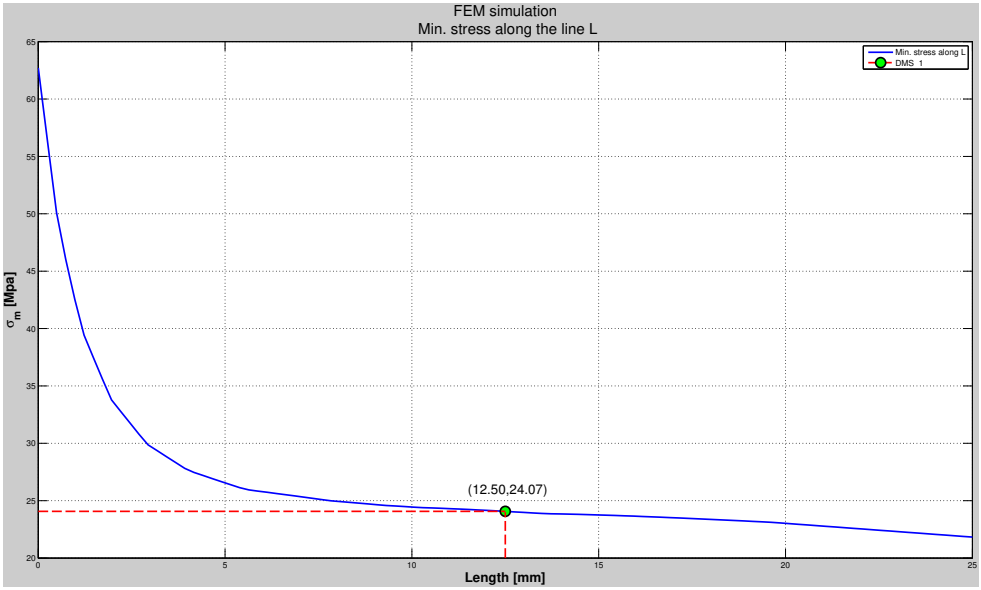

Figure A.10: FEM Minimum stress on the first strain gauge - The written values of the stress correspond to the position of the strain gauge.

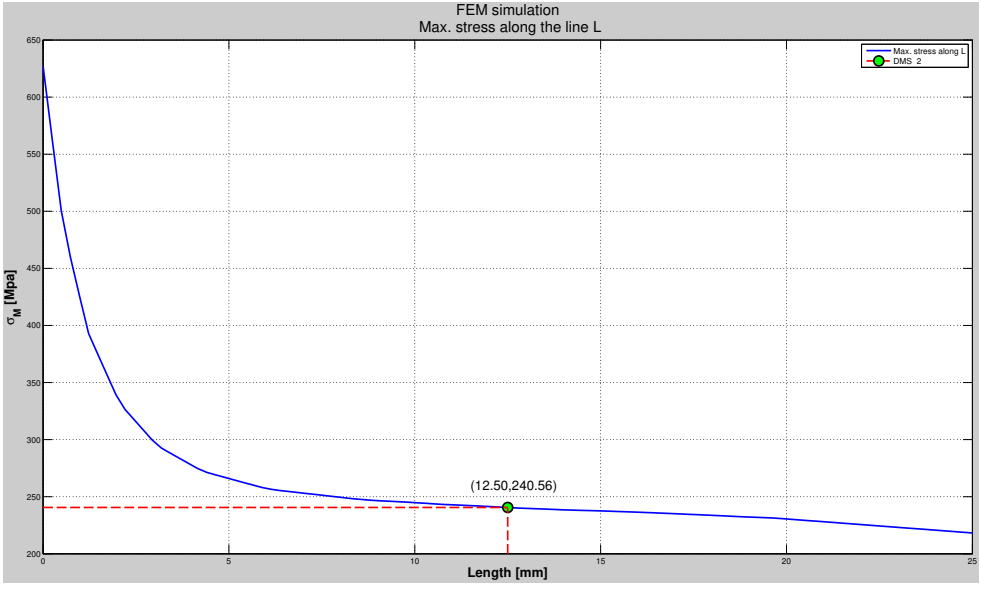

Figure A.11: FEM Maximum stress on the second strain gauge - The written values of the stress correspond to the position of the strain gauge.

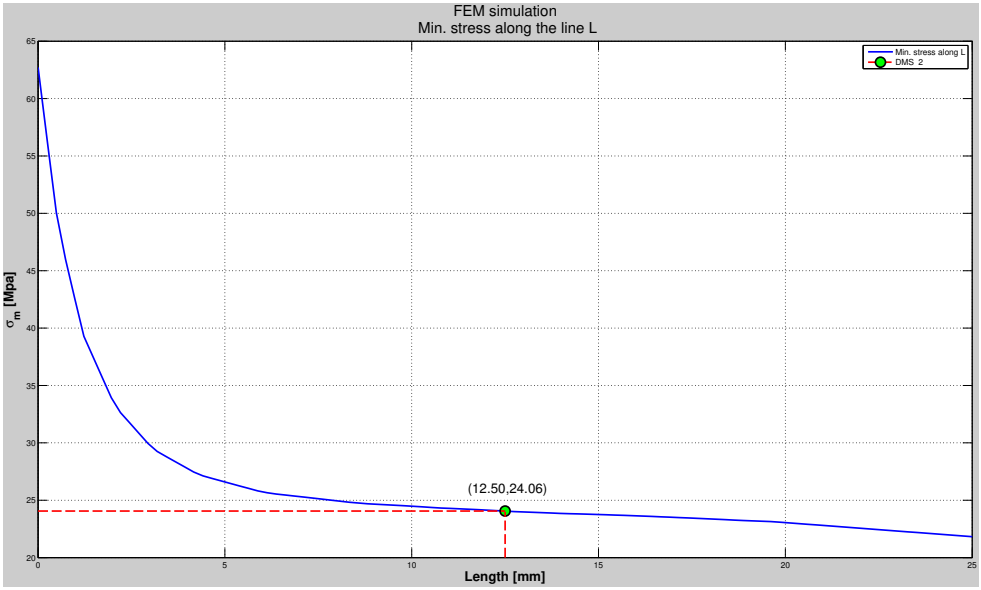

Figure A.12: FEM Minimum stress on the second strain gauge - The written values of the stress correspond to the position of the strain gauge.

A.3 Material inspection certificates

4043266

ILSENBURGER GROBBLECH
Ein Unternehmen der Salzgitter Gruppe

Abnahmeprüfzeugnis 3.1
Inspection certificate 3.1
Certificat de reception 3.1
DIN EN 10204
(A02)

Nr./No./N° (A03) **894455**
Seite/Page/Page 1/6
Datum/Date/Date 20.11.2014

Nr. (A07) 0071142613 01.10.2014
Besteller Universal
Purchaser Eisen und Stahl GmbH
Acheteur 41415 Neuss
(A06)

Nr. (A07)
Empfänger Universal
Customer Eisen und Stahl GmbH
Destinataire 41415 Neuss
(A06)

Erzeugnis Grobblech
Product Heavy plate
Produit Tôle forte
(B01)

Werksauftrags-Nr. 0000075083
Works order No.
N° de commande
(A08)

Lieferschein-Nr. 0085249570
Dispatch note No. 16.11.2014
Avis d'expédition N°

Werkstoff und Lieferbedingung S355J2+N
Steel grade and terms of delivery DIN EN 10025-2 04/05
Nuance et conditions de livraison AD 2000 W1 07/06
(B02–B03) DIN EN 10029 B 02/11
DIN EN 10163-2 Kl. A UG3 03/05

Abnahme WS
Inspection
Reception
(A05)

Kennzeichnung des Materials / Marking of the product / Marquage du produit (B06)
Herstellerzeichen/Stahlsorte/Schmelzen-Nr/
Erzeugnis-Nr./Sachverständigenstempel
Trademark/Steelgrade/Heat-No/Product-No/
inspector's stamp
Sigle de l´usine/Nuance de l´acier/N° coulée/
N° produit/Poinçon de l' expert

Materialdaten / Material data / Données des matériaux (B01–B99)

Pos. Item Poste	Anzahl Quantity Nombre (B08)	Erzeugnis-Nr. Product No. N° produit (B07)	Schmelzen-Nr. Heat No. N° Coulée (B07)	Lieferzustand Cond. of delivery Etat de livraison (B04)	Dicke x Breite x Länge Thickness x Width x Length Epaisseur x Largeur x Longueur (B09–B11) mm x mm x mm
01	1	545537 1	40296	N	12,00 x 2000,0 x 6000
01	1	545537 2	40296	N	12,00 x 2000,0 x 6000
01	1	545537 3	40296	N	12,00 x 2000,0 x 6000
01	1	545537 4	40296	N	12,00 x 2000,0 x 6000
01	1	545538 1	40296	N	12,00 x 2000,0 x 6000
01	1	545538 2	40296	N	12,00 x 2000,0 x 6000
01	1	545538 3	40296	N	12,00 x 2000,0 x 6000
01	1	545539 1	14627	N	12,00 x 2000,0 x 6000
01	1	545539 2	14627	N	12,00 x 2000,0 x 6000
01	1	545539 3	14627	N	12,00 x 2000,0 x 6000
01	1	545539 4	14627	N	12,00 x 2000,0 x 6000
01	1	545540 1	14627	N	12,00 x 2000,0 x 6000
01	1	545540 2	14627	N	12,00 x 2000,0 x 6000
01	1	545540 3	14627	N	12,00 x 2000,0 x 6000
01	1	545540 4	14627	N	12,00 x 2000,0 x 6000
02	1	545534 1	40296	N	12,00 x 2000,0 x 8000
02	1	545534 2	40296	N	12,00 x 2000,0 x 8000
02	1	545534 3	40296	N	12,00 x 2000,0 x 8000
02	1	545535 1	40296	N	12,00 x 2000,0 x 8000
02	1	545535 2	40296	N	12,00 x 2000,0 x 8000
02	1	545535 3	40296	N	12,00 x 2000,0 x 8000
02	1	545536 1	40296	N	12,00 x 2000,0 x 8000

N: normalisiert / normalized / normalisé

Es wird bestätigt, daß die Lieferung den Anforderungen der Lieferbedingung entspricht.
We hereby certify that the delivered material complies with the terms of the order.
Nous certifions que la fourniture répond aux conditions de livraison.
(Z01)
QM-System: Certification as per ISO 9001 since 28 February 1990

Herstellerzeichen
Trademark
Sigle du producteur
(A04)

Ilsenburger Grobblech GmbH
Veckenstedter Weg 10
D-38871 Ilsenburg
(A01)

Abnahmestempel
Inspection Stamp
Poinçon de l'expert
(Z03)

CE

Abnahmebeauftragter
Inspection Representative
Représentant autorisé
(Z02)

Cyron

Diese durch ein geeignetes Datenverarbeitungssystem erstellte Bescheinigung ist gemäß EN 10 204, Abschnitt 5, ohne Unterschrift gültig.
This certificate was prepared by a suitable data processing system and is valid without signature according to EN 10 204, section 5.
Ce certificat a été établi par un système adéquat de traitement de données, il est valable sans signature selon EN 10 204, section 5.

ILSENBURGER GROBBLECH
Ein Unternehmen der Salzgitter Gruppe

Abnahmeprüfzeugnis 3.1
Inspection certificate 3.1
Certificat de reception 3.1
DIN EN 10204
(A02)

Nr./No./N° (A03) 894455
Seite/Page/Page 2/6
Datum/Date/Date 20.11.2014

Nr. (A07)	0071142613	01.10.2014	Nr. (A07)
Besteller	Universal		Empfänger Universal
Purchaser	Eisen und Stahl GmbH		Customer Eisen und Stahl GmbH
Acheteur	41415 Neuss		Destinataire 41415 Neuss
(A06)			(A06)

Erzeugnis Grobblech
Product Heavy plate
Produit Tôle forte
(B01)

Werkstoff und Lieferbedingung S355J2+N
Steel grade and terms of delivery DIN EN 10025-2 04/05
Nuance et conditions de livraison AD 2000 W1 07/06
(B02–B03) DIN EN 10029 B 02/11
DIN EN 10163-2 Kl. A UG3 03/05

Werksauftrags-Nr. 0000075083
Works order No.
N° de commande
(A08)
Lieferschein-Nr. 0085249570
Dispetch note No. 16.11.2014
Avis d'expédition N°

Abnahme WS
Inspection
Reception
(A05)

Materialdaten / Material data / Données des matériaux (B01–B99)

Pos. Item Poste	Anzahl Quantity Nombre (B08)	Erzeugnis-Nr. Product No. N° produit (B07)	Schmelzen-Nr. Heat No. N° Coulée (B07)	Lieferzustand Cond. of delivery Etat de livraison (B04)	Dicke x Breite x Länge Thickness x Width x Length Epaisseur x Largeur x Longueur (B09–B11) mm x mm x mm
02	1	545536 2	40296	N	12,00 x 2000,0 x 8000
02	1	545536 3	40296	N	12,00 x 2000,0 x 8000
02	1	545693 1	40296	N	12,00 x 2000,0 x 8000
02	1	545693 2	40296	N	12,00 x 2000,0 x 8000
02	1	545693 3	40296	N	12,00 x 2000,0 x 8000
03	1	542394 1	15323	N	40,00 x 2000,0 x 6000
03	1	542394 2	15323	N	40,00 x 2000,0 x 6000

01	15	Gewicht	16.950	kg
02	12	Weight	18.084	kgs
03	2	Poids	7.536	kgs
		(B12)		
Σ	29		42.570	

N: normalisiert / normalized / normalisé

Maßprüfung und Sichtkontrolle auf äußere Beschaffenheit: ohne Beanstandung
Dimensional check and visual examination of the surface condition:
without objection
Contrôle dimensionnel et examen visuel de l'état de surface: satisfaisants

Es wird bestätigt, daß die Lieferung den Anforderungen der Lieferbedingung entspricht.
We hereby certify that the delivered material complies with the terms of the order.
Nous certifions que la fourniture répond aux conditions de livraison.
(Z01)
QM-System: Certification as per ISO 9001 since 28 February 1990

Herstellerzeichen
Trademark
Sigle du producteur
(A04)

Ilsenburger Grobblech GmbH
Veckenstedter Weg 10
D-38871 Ilsenburg
(A01)

Abnahmestempel
Inspection Stamp
Poinçon de l'expert
(Z03)

CE

Abnahmebeauftragter
Inspection Representative
Représentant autorisé
(Z02)

Cyron

Diese durch ein geeignetes Datenverarbeitungssystem erstellte Bescheinigung ist gemäß EN 10 204, Abschnitt 5, ohne Unterschrift gültig.
This certificate was prepared by a suitable data processing system and is valid without signature according to EN 10 204, section 5.
Ce certificat a été établi par un système adéquat de traitement de données, il est valable sans signature selon EN 10 204, section 5.

ILSENBURGER GROBBLECH
Ein Unternehmen der Salzgitter Gruppe

Abnahmeprüfzeugnis 3.1
Inspection certificate 3.1
Certificat de reception 3.1
DIN EN 10204
(A02)

Nr./No./N° (A03) 894455
Seite/Page/Page 3/6
Datum/Date/Date 20.11.2014

Nr. (A07) 0071142613 01.10.2014
Besteller Universal
Purchaser Eisen und Stahl GmbH
Acheteur 41415 Neuss
(A06)

Nr. (A07)
Empfänger Universal
Customer Eisen und Stahl GmbH
Destinataire 41415 Neuss
(A06)

Erzeugnis Grobblech
Product Heavy plate
Produit Tôle forte
(B01)

Werkstoff und Lieferbedingung S355J2+N
Steel grade and terms of delivery DIN EN 10025-2 04/05
Nuance et conditions de livraison AD 2000 W1 07/06
(B02-B03) DIN EN 10029 B 02/11
DIN EN 10163-2 Kl. A UG3 03/05

Werksauftrags-Nr. 0000075083
Works order No.
N° de commande
(A08)
Lieferschein-Nr. 0085249570
Dispatch note No. 16.11.2014
Avis d'expédition N°

Abnahme WS
Inspection
Reception
(A05)

Schmelzenanalyse / Ladle analysis / Analyse de coulée (C70-C99)

Herstellerangaben / Manufacturer standard / Données du fabricant

Schmelzen-Nr. Heat No. N° Coulée (B07)	C %	Si % ≤ 0,55	Mn % ≤ 1,60	P % ≤ 0,025	S % ≤ 0,025	N %	Al %	Cu % ≤ 0,55	Cr %	Ni %
14627	0,14	0,28	1,48	0,016	0,002	0,003	0,042	0,02	0,02	0,03
15323	0,15	0,35	1,57	0,013	0,001	0,004	0,042	0,01	0,03	0,03
40296	0,13	0,30	1,48	0,012	0,002	0,005	0,043	0,07	0,02	0,10

Schmelzen-Nr. Heat No. N° Coulée (B07)	Mo %	V %	Ti %	Nb %	EV1 1) % ≤ 0,43
14627	0,003	0,004	0,02	0,03	0,40
15323	0,01	0,004	0,01	0,03	0,42
40296	0,01	0,004	0,02	0,02	0,39

1) EV1 : CEV=C+Mn/6+Mo/5+Ni/15+Cr/5+V/5+Cu/15

Stahlherstellung: Sauerstoffaufblasverfahren
Steel making: Basic oxygen process
Fabrication d´acier: Procédé au convertisseur à l´oxygène
(C70)

Es wird bestätigt, daß die Lieferung den Anforderungen der Lieferbedingung entspricht.
We hereby certify that the delivered material complies with the terms of the order.
Nous certifions que la fourniture répond aux conditions de livraison.
(Z01)

QM-System: Certification as per ISO 9001 since 28 February 1990

Herstellerzeichen
Trademark
Sigle du producteur
(A04)

Ilsenburger Grobblech GmbH
Veckenstedter Weg 10
D-38871 Ilsenburg
(A01)

Abnahmestempel
Inspection Stamp
Poinçon de l'expert
(Z03)

Abnahmebeauftragter
Inspection Representative
Représentant autorisé
(Z02)

Cyron

Diese durch ein geeignetes Datenverarbeitungssystem erstellte Bescheinigung ist gemäß EN 10 204, Abschnitt 5, ohne Unterschrift gültig.
This certificate was prepared by a suitable data processing system and is valid without signature according to EN 10 204, section 5.
Ce certificat a été établi par un système adéquat de traitement de données, il est valable sans signature selon EN 10 204, section 5.

ILSENBURGER GROBBLECH
Ein Unternehmen der Salzgitter Gruppe

Abnahmeprüfzeugnis 3.1
Inspection certificate 3.1
Certificat de reception 3.1
DIN EN 10204
(A02)

Nr./No./N° (A03) 894455
Seite/Page/Page 4/6
Datum/Date/Date 20.11.2014

Nr. (A07) 0071142613 01.10.2014
Besteller Universal
Purchaser Eisen und Stahl GmbH
Acheteur 41415 Neuss
(A06)

Nr. (A07)
Empfänger Universal
Customer Eisen und Stahl GmbH
Destinataire 41415 Neuss
(A06)

Erzeugnis Grobblech
Product Heavy plate
Produit Tôle forte
(B01)

Werkstoff und Lieferbedingung S355J2+N
Steel grade and terms of delivery DIN EN 10025-2 04/05
Nuance et conditions de livraison AD 2000 W1 07/06
(B02–B03) DIN EN 10029 B 02/11
DIN EN 10163-2 Kl. A UG3 03/05

Werksauftrags-Nr. 0000075083
Works order No.
N° de commande
(A08)
Lieferschein-Nr. 0085249570
Dispatch note No. 16.11.2014
Avis d'expédition N°

Abnahme WS
Inspection
Reception
(A05)

Zugversuch / Tensile test / Essai de traction (C10–C29)

Proben-Nr. Specimen No. N° éprouvette (C00)	Schmelzen-Nr. Heat No. N° Coulée (B07)	Ort Location Lieu (C01) 1) 2) 3)	Richt. Direct. Orient. (C02) 4)	Zustand Cond. Cond. (B05) 5)	Form Type Type (C10) 6)	Streckgrenze Yield point Limite d'élasticité (C11) ReH N/mm2	Zugfestigkeit Tensile strength Résistance (C12) Rm N/mm2	ReH/Rm ReH/Rm ReH/Rm	Bruchdehnung Elongation Allongement (C13) A5 %	
							470 - 630		7) ≥ 20	
534320 *)	14627	K4G	Q	N	P	440	553	0,80	31	
542395 *)	15323	K4G	Q	N	P	423	565	0,75	27	
545536	40296	K4G	Q	N	P	470	557	0,84	29	

1) K: Kopf / Top / Tête
2) 4: 1/4 Breite / 1/4 Width / 1/4 Largeur
3) G: Erzeugnisdicke / Thickness of product / Epaisseur du produit
4) Q: quer / transversal / transversal
5) N: normalisiert / normalized / normalisé
6) P: prismatisch / prismatic / prismatique
7) A5: Lo=5,65 √So
*) Das Probestück ist nicht Bestandteil der Lieferung / The sample product is not part of the delivery / Le produit-échantillon ne fait pas partie de la livraison

Kerbschlagbiegeversuch / Impact test / Essai de résilience (C40–C49)

Proben-Nr. Specimen No. N° éprouvette (C00)	Schmelzen-Nr. Heat No. N° Coulée (B07)	Ort Location Lieu (C01) 1) 2) 3)	Richt. Direct. Orient. (C02) 4)	Zustand Cond. Cond. (B05) 5)	Probenform Type of specimen Type d'éprouvette (C40–C41)	Temperatur Temperature Température (C03) °C	Schlagarbeit Impact energy Energie de rupture (C42–C43) 1 J ≥ 19	2	3	MW 6) J ≥ 27
534320 *)	14627	K4O	L	N	KV450	-020	275	219	284	259
542395 *)	15323	K4O	L	N	KV450	-020	249	254	242	248

1) K: Kopf / Top / Tête
2) 4: 1/4 Breite / 1/4 Width / 1/4 Largeur
3) O: oberflächennah / near surface / près de la peau
4) L: längs / longitudinal / longitudinal
5) N: normalisiert / normalized / normalisé
6) MW: Mittelwert / Average / Moyenne
*) Das Probestück ist nicht Bestandteil der Lieferung / The sample product is not part of the delivery / Le produit-échantillon ne fait pas partie de la livraison

Es wird bestätigt, daß die Lieferung den Anforderungen der Lieferbedingung entspricht.
We hereby certify that the delivered material complies with the terms of the order.
Nous certifions que la fourniture répond aux conditions de livraison.
(Z01)

QM-System: Certification as per ISO 9001 since 28 February 1990

Herstellerzeichen
Trademark
Sigle du producteur
(A04)

Ilsenburger Grobblech GmbH
Veckenstedter Weg 10
D-38871 Ilsenburg
(A01)

Abnahmestempel
Inspection Stamp
Poinçon de l'expert
(Z03)

CE

Abnahmebeauftragter
Inspection Representative
Représentant autorisé
(Z02)

Cyron

Diese durch ein geeignetes Datenverarbeitungssystem erstellte Bescheinigung ist gemäß EN 10 204, Abschnitt 5, ohne Unterschrift gültig.
This certificate was prepared by a suitable data processing system and is valid without signature according to EN 10 204, section 5.
Ce certificat a été établi par un système adéquat de traitement de données, il est valable sans signature selon EN 10 204, section 5.

ILSENBURGER GROBBLECH
Ein Unternehmen der Salzgitter Gruppe

Abnahmeprüfzeugnis 3.1
Inspection certificate 3.1
Certificat de reception 3.1
DIN EN 10204
(A02)

Nr./No./N° (A03) 894455
Seite/Page/Page 5/6
Datum/Date/Date 20.11.2014

Nr. (A07) 0071142613 01.10.2014
Besteller Universal
Purchaser Eisen und Stahl GmbH
Acheteur 41415 Neuss
(A06)

Nr. (A07)
Empfänger Universal
Customer Eisen und Stahl GmbH
Destinataire 41415 Neuss
(A06)

Erzeugnis Grobblech
Product Heavy plate
Produit Tôle forte
(B01)

Werksauftrags-Nr. 0000075083
Works order No.
N° de commande
(A08)
Lieferschein-Nr. 0085249570
Dispatch note No. 16.11.2014
Avis d'expédition N°

Werkstoff und Lieferbedingung S355J2+N
Steel grade and terms of delivery DIN EN 10025-2 04/05
Nuance et conditions de livraison AD 2000 W1 07/06
(B02–B03) DIN EN 10029 B 02/11
DIN EN 10163-2 Kl. A UG3 03/05

Abnahme WS
Inspection
Reception
(A05)

Kerbschlagbiegeversuch / Impact test / Essai de résilience (C40–C49)

Proben-Nr. Specimen No. N° éprouvette (C00)	Schmelzen-Nr. Heat No. N° Coulée (B07)	Ort Location Lieu (C01) 1) 2) 3)	Richt. Direct. Orient. (C02) 4)	Zustand Cond. Cond. (B05) 5)	Probenform Type of specimen Type d'éprouvette (C40–C41)	Temperatur Temperature Température (C03) °C	Schlagarbeit Impact energy Energie de rupture (C42–C43) 1 J ≥ 19	2	3	MW 6) J ≥ 27
545536	40296	K4O	L	N	KV450	-020	260	192	315	256

1) K: Kopf / Top / Tête
2) 4: 1/4 Breite / 1/4 Width / 1/4 Largeur
3) O: oberflächennah / near surface / près de la peau
4) L: längs / longitudinal / longitudinal
5) N: normalisiert / normalized / normalisé
6) MW: Mittelwert / Average / Moyenne
*) Das Probestück ist nicht Bestandteil der Lieferung / The sample product is not part of the delivery / Le produit-échantillon ne fait pas partie de la livraison

Unsere Produkte sind frei von radioaktiven Stoffen.
Der Freigabegrenzwert von 100 Bq/kg, der die Einhaltung der Grenzwerte der Strahlenschutzverordnung (StrlSchV) für die uneingeschränkte Freigabe von festen Stoffen (StrlSchV Anlage III, Spalte 5) für eisenverwandte Nuklide gewährleistet, wird nicht überschritten.

Our products are free of radioactive substances and do not exceed the clearing limit value of 100 Bq/kg, which guarantees the compliance with limit values given in the Radiation Protection Ordinance (StrlSchV) for the unrestricted clearance of solid material (StrlSchV Annex III, Section 5) for ferrous nuclides.

Es wird bestätigt, daß die Lieferung den Anforderungen der Lieferbedingung entspricht.
We hereby certify that the delivered material complies with the terms of the order.
Nous certifions que la fourniture répond aux conditions de livraison.
(Z01)
QM-System: Certification as per ISO 9001 since 28 February 1990

Herstellerzeichen
Trademark
Sigle du producteur
(A04)

Ilsenburger Grobblech GmbH
Veckenstedter Weg 10
D-38871 Ilsenburg
(A01)

Abnahmestempel
Inspection Stamp
Poinçon de l'expert
(Z03)

CE

Abnahmebeauftragter
Inspection Representative
Représentant autorisé
(Z02)

Cyron

Diese durch ein geeignetes Datenverarbeitungssystem erstellte Bescheinigung ist gemäß EN 10 204, Abschnitt 5, ohne Unterschrift gültig.
This certificate was prepared by a suitable data processing system and is valid without signature according to EN 10 204, section 5.
Ce certificat a été établi par un système adéquat de traitement de données, il est valable sans signature selon EN 10 204, section 5.

ILSENBURGER GROBBLECH
Ein Unternehmen der Salzgitter Gruppe

Abnahmeprüfzeugnis 3.1
Inspection certificate 3.1
Certificat de reception 3.1
DIN EN 10204
(A02)

Nr./No./N° (A03) **894455**
Seite/Page/Page 6/6
Datum/Date/Date 20.11.2014

CE

0045

Ilsenburger Grobblech GmbH
Veckenstedter Weg 10
D-38871 Ilsenburg

13

0045-CPR-0673

EN 10025-1

Warmgewalzte Baustahlprodukte
Hot rolled structural steel products
Produits en acier de construction laminé à chaud

Vorgesehene Verwendungen: Intended uses: Usages prévus:	Hochbauten und Ingenieurbauwerke Building constructions or civil engineering Construction de bâtiments ou génie civil
Grenzabmaße und Formtoleranzen: Tolerances on dimensions and shape: Tolérances sur les dimensions et la forme:	Warmgewalztes Grobblech Hot rolled heavy plates Tôles fortes refendues laminées à chaud: EN 10029
Dehnung / Elongation / Élongation: Zugfestigkeit / Tensile strength / Résistance à la traction: Streckgrenze / Yield strenght / Limite d'élasticité: Kerbschlagarbeit / Impact strenght / Résistance au choc: Schweißeignung / Weldability / Soudabilité:	S355J2+N DIN EN 10025-2 04/05
Dauerhaftigkeit: Durability: Durabilité:	Keine Leistung festgestellt No performance determined Aucune performance déterminée
Regulierter Stoff: Regulated substance: Substance Réglementée:	Keine Leistung festgestellt No performance determined Aucune performance déterminée

Die Leistungserklärung (DoP) gemäß EU-Verordnung 305/2011, Anhang III kann unter
www.ilsenburger-grobblech.de/de/Produkte/Qualitaetsphilosophie_IMS_/Zertifikate gerufen werden.

The Declaration of Performance (DoP) in acc. with EU-Regulation 305/2011, Annex III is available under
www.ilsenburger-grobblech.de/en/Produkte/Qualitaetsphilosophie_IMS_/Zertifikate

BERICHTE ZUM STAHL- UND LEICHTBAU

Versuchsanstalt für Stahl, Holz und Steine, Stahl- und Leichtbau
Karlsruher Institut für Technologie (KIT) | ISSN 2198-7912

Eine Übersicht der Berichte der Versuchsanstalt für Stahl, Holz und Steine ab dem Jahr 1963 finden Sie unter folgender URL: http://stahl.vaka.kit.edu/berichte.php

Band 1 OLIVER FLEISCHER
Axial beanspruchte K-Knoten aus dünnwandigen Rechteckhohlprofilen. 2014
ISBN 978-3-7315-0190-9

Band 2 THOMAS REINKE
Tragverhalten von biegebeanspruchten Stahlmasten mit polygonalen Querschnitten. 2015
ISBN 978-3-7315-0398-9

Band 3 ROBIN MARC PLUM
Fatigue crack detection on structural steel members by using ultrasound excited thermography. Erkennung von Ermüdungsrissen in Stahlbauteilen durch ultraschallangeregte Thermografie. 2015
ISBN 978-3-7315-0417-7

Band 4 TIM ZINKE
Nachhaltigkeit von Infrastrukturbauwerken – Ganzheitliche Bewertung von Autobahnbrücken unter besonderer Berücksichtigung externer Effekte. 2016
ISBN 978-3-7315-0509-9

Band 5 MAX JONAS SPANNAUS
Bemessung von Erzeugnissen aus Stahlguss unter vorwiegend ruhender Beanspruchung. 2016
ISBN 978-3-7315-0560-0

Band 6 MATTHIAS FRIEDRICH ALBIEZ
Zur statischen Tragfähigkeit geklebter Kreishohlprofilverbindungen im Stahlbau. 2016
ISBN 978-3-7315-0561-7

Band 7 ANDREAS LIPP
Kreishohlprofil-X-Knoten aus nichtrostenden Stählen unter Axialbeanspruchung. 2016
ISBN 978-3-7315-0569-3

Band 8 PAUL DARIO TOASA CAIZA
Consideration of runouts by the evaluation of fatigue experiments. 2019
ISBN 978-3-7315-0900-4

Die Bände sind unter www.ksp.kit.edu als PDF frei verfügbar oder als Druckausgabe bestellbar.

VERSUCHSANSTALT FÜR STAHL, HOLZ UND STEINE
BERICHTE ZUM STAHL– UND LEICHTBAU
8

According to the Eurocode EC3, the estimation of the fatigue life from a welded structure subjected to a cyclic loading is determined by considering its corresponding detail category. The details categories have been made from Wöhler curves which have been obtained by applying the Basquin model in order to evaluate the data of fatigue experiments. Unfortunately, from the statistical point of view this model does not allow to extrapolate the Wöhler curves in the High Cycle Fatigue (HCF) region. Moreover, the runouts, which are the most expensive experimental tests are not considered into the evaluation of fatigue data. These deficiencies affect the estimation of the fatigue lifetime and the design of a steel structure subjected to a high amount of cyclic loads. In order to overcome these deficiencies, a new methodology has been proposed by Castillo and Fernández–Canteli. Based on a Weibull distribution, this methodology allows estimating the fatigue life of a steel structure in the HCF region. Moreover, it allows considering the runouts and their subsequent retests into the modeling of the Wöhler curves.

ISBN 978-3-7315-0900-4
9 783731 509004 >

ISSN 2198-7912 | ISBN 978-3-7315-0900-4

Gedruckt auf FSC-zertifiziertem Papier